BioMed Research International

Recent Advances in Biofilmology and Antibiofilm Measures

Guest Editors: Nithyanand Paramasivam, Shunmugiah K. Pandian, Ariel Kushmaro, Supayang Voravuthikunchai, and Aruni Wilson

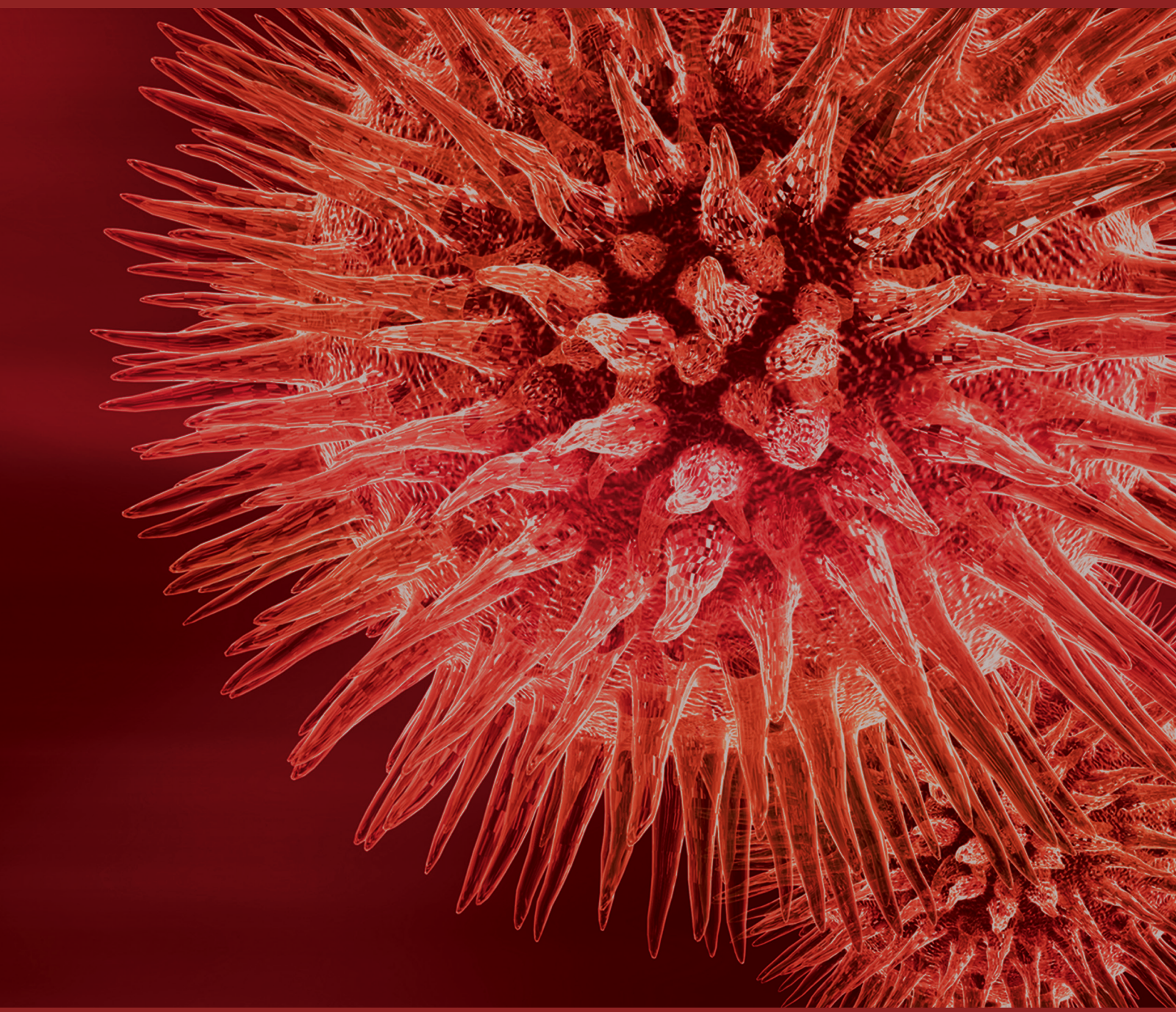

Recent Advances in Biofilmology and Antibiofilm Measures

BioMed Research International

Recent Advances in Biofilmology and Antibiofilm Measures

Guest Editors: Nithyanand Paramasivam, Shunmugiah K. Pandian, Ariel Kushmaro, Supayang Voravuthikunchai, and Aruni Wilson

Copyright © 2017 Hindawi Publishing Corporation. All rights reserved.

This is a special issue published in "BioMed Research International." All articles are open access articles distributed under the Creative Commons Attribution License, which permits unrestricted use, distribution, and reproduction in any medium, provided the original work is properly cited.

Contents

Hindawi
BioMed Research International
Volume 2017, Article ID 5409325, 2 pages
http://dx.doi.org/10.1155/2017/5409325

Editorial

Recent Advances in Biofilmology and Antibiofilm Measures

Nithyanand Paramasivam,[1] Shunmugiah Karutha Pandian,[2] Ariel Kushmaro,[3] Supayang Voravuthikunchai,[4] and Aruni Wilson[5]

[1]*Biofilm Biology Laboratory, Anusandhan Kendra II, School of Chemical and Biotechnology, SASTRA University, Tirumalaisamudram, Thanjavur, Tamil Nadu 613 401, India*
[2]*Department of Biotechnology, Alagappa University, Science Campus, Karaikudi, Tamil Nadu 630 003, India*
[3]*Department of Biotechnology Engineering, Ben-Gurion University of the Negev, 84105 Beer-Sheva, Israel*
[4]*Department of Microbiology, Faculty of Science, Prince of Songkla University, Hat-Yai, Songkhla 90112, Thailand*
[5]*Division of Microbiology and Molecular Genetics, School of Medicine, Loma Linda University, Loma Linda, CA, USA*

Correspondence should be addressed to Nithyanand Paramasivam; pnithyanand@gmail.com

Received 26 January 2017; Accepted 29 January 2017; Published 15 March 2017

Copyright © 2017 Nithyanand Paramasivam et al. This is an open access article distributed under the Creative Commons Attribution License, which permits unrestricted use, distribution, and reproduction in any medium, provided the original work is properly cited.

Biofilms have now been recognized as a predominant life style of several bacteria and fungi, wherein single-cell organisms assume a temporary multicellular lifestyle. A hallmark of biofilms is the formation of an extracellular matrix or EPS (extracellular polymeric substances) that forms a thick layer encasing the microbial cells, thereby protecting them from antimicrobials and from the host immune response. Hence, the treatment of biofilm infections has become a challenge and has attracted significant scientific attention. To address this important issue we therefore present a number of reviews and research papers focusing on the control of biofilms in a special issue of this journal.

One of the papers in the special issue points out that siderophore molecules such as transferrin have a major impact on *Bacillus thuringiensis* biofilms. This is important, as it is well known that members of the genus *Bacillus* survive even in adverse conditions. The study showed for the first time that the molecule transferrin helps *B. thuringiensis* to be established and sustained as biofilms and provides important information regarding the mechanism of biofilm establishment of this bacterium. Another paper reports on the development of a novel antibiofilm dressing technology using carboxymethylcellulose silver-containing dressing and tests its efficacy on several biofilm models. Results showed that this wound dressing was also more effective than the available standard silver dressings in reducing the EPS layer, the protective biofilm component.

Another paper provides a detailed review about the recently developed nanotechnology-based biomaterials to prevent biofilms and discusses various strategies used to make antibiofilm surfaces. The review pointed out that some interesting compounds such as dendrimers have antibiofilm activity and concludes that preparation of cost-efficient nanobiomaterials is the "need of the hour." An additional review article in this special issue deals with oral biofilm models. Since bacterial species present in the oral cavity predominantly live in a biofilm life style, oral biofilm models have become important to study as to how these bacteria form biofilms or to understand the functioning of oral microcosm in a biofilm. The review gives a detailed account on the pros and cons of the currently existing oral biofilm models and finally advocates that the right model should be chosen based on the rationale to be addressed.

S. Gowrishankar et al. report a very interesting observation about the presence of biofilm forming methicillin-resistant *Staphylococcus aureus* (MRSA) strains from pharyngitis patients. The coexistence of MRSA along with Group A Streptococcus (GAS), the causative agent of pharyngitis, stresses the need for a broad-spectrum antibiofilm agent that acts on both the biofilm inhabiting species. Since biofilms

formed by food borne pathogens or food spoilage bacteria on food processing equipment are the main cause for food contamination, two papers address this burgeoning problem in this issue. Till date, it is thought that disinfection of food processing plants by sanitizers is the most feasible option for food industries. L. Cincarova et al. show that usages of sublethal concentrations of disinfectants are not effective in removing biofilms of *S. aureus* isolated from meat processing plants. This study emphasizes the need for optimizing the exact dosage and duration of disinfectants in food industries. An additional common problem encountered in food industries is biofilm formation by *Asaia* sp. on production lines of soft drink plants which eventually contaminates soft drinks even in the presence of preservatives. H. Antolak et al. show that that polyphenolics present in bilberry and blackcurrant juices prevented the adhesive property of *Asaia* sp. The authors further state that bilberry and blackcurrant juices which can prove to be interesting alternatives to artificial additives to keep the microbial stability of final products. Drug resistance by biofilm forming pathogens has reached alarming proportions worldwide. This necessitates the need of new antimicrobial agents, either synthetic or natural products, to treat these recalcitrant infections. The final paper of this issue addresses this important problem wherein B. Fu et al. show that a Chinese medical herb *Herba Patriniae* inhibited the mature biofilms of *Pseudomonas aeruginosa* and also decreased the exopolysaccharide (EPS) production.

Nithyanand Paramasivam
Shunmugiah Karutha Pandian
Ariel Kushmaro
Supayang Voravuthikunchai
Aruni Wilson

Hindawi
BioMed Research International
Volume 2017, Article ID 9584703, 10 pages
http://dx.doi.org/10.1155/2017/9584703

Research Article

Inhibition of *Pseudomonas aeruginosa* Biofilm Formation by Traditional Chinese Medicinal Herb *Herba patriniae*

Bo Fu,[1] Qiaolian Wu,[1] Minyan Dang,[1] Dangdang Bai,[1] Qiao Guo,[1] Lixin Shen,[1] and Kangmin Duan[1,2]

[1]*Key Laboratory of Resources Biology and Biotechnology in Western China, Ministry of Education, College of Life Sciences, Northwest University, Xi'an, Shaanxi 710069, China*
[2]*Department of Oral Biology & Medical Microbiology, Rady Faculty of Health Sciences, University of Manitoba, 780 Bannatyne Ave., Winnipeg, MB, Canada R3E 0W2*

Correspondence should be addressed to Lixin Shen; shenlx@nwu.edu.cn and Kangmin Duan; kangmin.duan@umanitoba.ca

Received 16 August 2016; Accepted 5 January 2017; Published 9 March 2017

Academic Editor: P. Nithyanand

Copyright © 2017 Bo Fu et al. This is an open access article distributed under the Creative Commons Attribution License, which permits unrestricted use, distribution, and reproduction in any medium, provided the original work is properly cited.

New antimicrobial agents are urgently needed to treat infections caused by drug-resistant pathogens and by pathogens capable of persisting in biofilms. The aim of this study was to identify traditional Chinese herbs that could inhibit biofilm formation of *Pseudomonas aeruginosa*, an important human pathogen that causes serious and difficult-to-treat infections in humans. A *luxCDABE*-based reporter system was constructed to monitor the expression of six key biofilm-associated genes in *P. aeruginosa*. The reporters were used to screen a library of 36 herb extracts for inhibitory properties against these genes. The results obtained indicated that the extract of *Herba patriniae* displayed significant inhibitory effect on almost all of these biofilm-associated genes. Quantitative analysis showed that *H. patriniae* extract was able to significantly reduce the biofilm formation and dramatically altered the structure of the mature biofilms of *P. aeruginosa*. Further studies showed *H. patriniae* extract decreased exopolysaccharide production by *P. aeruginosa* and promoted its swarming motility, two features disparately associated with biofilm formation. These results provided a potential mechanism for the use of *H. patriniae* to treat bacterial infections by traditional Chinese medicines and revealed a promising candidate for exploration of new drugs against *P. aeruginosa* biofilm-associated infections.

1. Introduction

Pseudomonas aeruginosa is a remarkably adaptive bacterial pathogen which can cause persistent infections in burn patients, immune-compromised patients, and individuals with the genetic disease cystic fibrosis. It is one of the most prevalent nosocomial pathogens, and the infections caused by *P. aeruginosa* can be very serious and life-threatening [1].

Biofilm formation is a major characteristic of *P. aeruginosa* chronic infections [2, 3]. *P. aeruginosa* cells in biofilms are surrounded by exopolysaccharides and form a structured aggregates, and these cells exhibit increased resistance to antibiotics and other adversary agents [3–6]. Infections caused by biofilm-forming *P. aeruginosa,* such as those in cystic fibrosis lung, are almost impossible to eradicate [7]. There is an urgent need to find novel antimicrobial agents to control such infections [8, 9].

Traditional Chinese medicines (TCMs) have been widely used to treat infectious diseases for more than a thousand years in China. Many components constituents of TCMs have been found to be very effective in treating bacterial infections such as gastritis, stomatitis, dermatitis, and bacterial pneumonia [10]. However, the mechanisms of these herbs in treatment infectious diseases are mostly unknown.

Herba patriniae is a perennial herbal of TCM, which contains various beneficial ingredients such as amino acids, vitamins, minerals, alkaloids, tannins, and saponins. It has been reported to have functions of antioxidant, antibacterial, antiviral, blood-activating and stasis-eliminating, promoting regeneration of liver cells, and anxiety-alleviating. The boiling water extracts of *H. patriniae* had been identified having anticyanobacteria activity against *Microcystis aeruginosa* [11].

In this study, 36 extracts of 18 Chinese herbs that are commonly used for treating infection-like symptoms were

Table 1: Bacterial strains used in this study.

Strains/plasmids	Description	Source
E. coli DH10B	F-mcrA(mrr-hsdRMS-mcrBC)80dlacZ ΔM15ΔlacX74 deoR recA1 endA1 araD139 Δ(ara leu)7697 galU galKλ-rpsl nupG	Invitrogen
P. aeruginosa PAO1	Wild type	This lab
pMS402	Expression reporter plasmid carrying the promoterless *luxCDABE*; Kan^r, Tmp^r	This lab
pKD-*pslM*	pMS402 containing *pslM* promoter region; Kan^r, Tmp^r	This study
pKD-*pelA*	pMS402 containing *pelA* promoter region; Kan^r, Tmp^r	This study
pKD-*algU*	pMS402 containing *algU* promoter region; Kan^r, Tmp^r	This study
pKD-*ppyR*	pMS402 containing *ppyR* promoter region; Kan^r, Tmp^r	This study
pKD-*algA*	pMS402 containing *algA* promoter region; Kan^r, Tmp^r	This study
pKD-*bdlA*	pMS402 containing *bdlA* promoter region; Kan^r, Tmp^r	This study

Table 2: Reporter genes and primer sequences used.

PA number	Gene	Function	Primer	Sequence ($5' \rightarrow 3'$)
PA0762	*algU*	RNA polymerase sigma factor	pKD-*algU*-S	GCACTCGAGAGGATGCCTGAAGACCTC
			pKD-*algU*-A	GTAGGATCCGATGGCGATCCGATACAG
PA2243	*pslM*	Succinate dehydrogenase; fumarate reductase flavoprotein	pKD-*pslM*-S	ATCCTCGAGCGGTGCGCAAGAAGACC
			pKD-*pslM*-A	GTTGGATCCCGTAACGCTCGCCCAGTT
PA3064	*pelA*	Glycoside hydrolase; deacetylase	pKD-*pelA*-S	CGTCTCGAGCTTTCCACTTTGCCACAG
			pKD-*pelA*-A	TACGGATCCTACCAGAACGCCACGCT
PA3551	*algA*	Phosphomannose isomerase; guanosine 5′-diphospho-D-mannose pyrophosphorylase	pKD-*algA*-S	TGACTCGAGTGAAGGCGGACTGAGAC
			pKD-*algA*-A	TATGGATCCGCGACCAGTTTCATC
PA2663	*ppyR*	psl and pyoverdine operon regulator	pKD-*ppyR*-S	GCACTCGAGCACTTCTTCTGCTACAGC
			pKD-*ppyR*-A	GTAGGATCCAGCACTTGCACAGCAGAC
PA1423	*bdlA*	Biofilm dispersion locus A	pKD-*bdlA*-S	GCACTCGAGCGTCATATTTCCGACGAA
			pKD-*bdlA*-A	TCAGGATCCGTAGTCTTCCGATTGCG

screened for inhibitory effect against *P. aeruginosa* biofilms. We found that the extract of the Chinese herb *H. patriniae* significantly inhibited the expression of the genes associated with biofilm formation in *P. aeruginosa* PAO1. It reduced exopolysaccharide production and biofilm formation and then altered the structure of the mature biofilms.

2. Materials and Methods

2.1. Bacterial Strains and Culture Conditions. Bacterial strains used in this study are listed in Table 1. All the strains were cultured in LB (Luria Bertani) broth at 37°C with orbital shaking at 200 rpm or on LB agar plates supplemented with antibiotic of kanamycin (Kan, 50 μg/mL) or trimethoprim (Tmp, 300 μg/mL) where appropriate.

2.2. Traditional Chinese Medicine Extraction. Traditional Chinese medicinal herbs were selected according to their efficacy in treatment of infection-like symptoms in Chinese medicine. They were obtained from local pharmacy (Yikang Pharm chain store, China). The pulverized herb was firstly immerged in 75% ethanol or deionized water, respectively, for 2 h and then boiled for 2 h additionally (weight to solvent volume was 1 : 5). The extracts were filtered by filter paper and were evaporated under vacuum at 35°C using a rotary evaporator (Buchi, Switzerland). The concentrated extracts were then freeze-dried using a lyophilizer and stored at −80°C. The water extracts were redissolved in deionized water and ethanol extracts were redissolved in methanol and then sterilized immediately with 0.22 μm Iwaki filter before use.

2.3. Gene Expression Assay. Key genes *algU* [12], *pslM* [13, 14], *pelA* [15], *algA* [16], *ppyR* [17], and *bdlA* [18] that are known to be involved in biofilm formation in *P. aeruginosa* were selected to construct *luxCDABE*-based promoter-reporter fusions (Table 2). The reporters were constructed as previously described [19, 20] and were subsequently transformed into PAO1. Using *luxCDABE*-based reporters, gene expression in liquid cultures was measured by light luminescence (in counts per second) in a Victor^3 multilabel plate reader

(Perkin-Elmer). Strains containing different reporters were cultivated overnight in LB broth supplemented with Tmp (300 μg/mL) and then diluted to an optical density at 600 nm of 0.2. The diluted cultures were used as inoculants. After additional 2 h incubation, 5 μL cultures were inoculated into parallel wells on a 96-well black plate containing 93 μL medium and 2 μL herbal extract in different concentrations. 50 μL mineral oil was added to the wells to prevent evaporation. Promoter activities were measured every 30 min for 24 h in a Victor multilabel plate reader and bacterial growth was monitored by measuring OD_{600} at the same time.

2.4. Gene Expression Measurement by Real-Time Quantitative PCR (RT-qPCR). Bacterial RNA was extracted using RNAprep Pure Cell/Bacteria Kit (TIANGEN). 1 μg of RNA sample was reverse transcribed to cDNA using 1st Strand cDNA Synthesis Kit (Takara). Real-time qPCR was performed using SuperReal PerMix Plus (SYBR Green/probe) (TIANGEN) and primers specific for *algU* (Forward: 5′-AACACCGCGAAGAACCACCT-3′, Reverse: 5′-ATCTCATCCCGCAACATCGCG-3′), *algA* (Forward: 5′-AGAACTGAAGAAGCACGACG-3′, Reverse: 5′-TTCTCCATCACCGCGTAGT-3′), *pelA* (Forward: 5′-ATGGCTGAAGGTATGGCTG-3′, Reverse: 5′-AGGTGCTGGAGGACTTCATC-3′), and *pslM* (Forward: 5′-CTATGACGCACGGCAACTGG-3′, reverse: 5′-CGCCATTGACCAGGTGCAT-3′). The values obtained were normalized to the housekeeping gene *proC* (Forward: 5′-CAGGCCGGGCAGTTGCTGTC-3′, reverse: 5′-GGTCAGGCGCGAGGCTGTCT -3′).

2.5. Quantification of the Biofilm Formation. Biofilm formation was measured in 96-well polystyrene microtiter plate as described previously with minor modifications [21]. 10 μL of overnight cultures of PAO1 was added to 90 μL fresh LB broth containing 160 μg *H. patriniae* water extract. Same volume of deionized water was used as control. After being cultured with shaking at 200 rpm for 1 h the plates were kept at stationary state at 37°C for 3 days and 7 days with a medium replacement at every 24 h interval. Then wells were washed twice with deionized water gently to remove the planktonic cells. The sedentary cells were stained with 1% (v/v) crystal violet solution for 15 min. Unbound dye in the wells were washed off by deionized water before 200 μL of 95% ethanol was added to dissolve the crystal violet stains. The absorbance of the solutions was then measured at 570 nm [7, 22].

2.6. Biofilm Imaging by Silver Staining Method. To examine the biofilm structure, silver staining method was used as described previously with some modifications [23, 24]. Similar to the above described biofilm assay, biofilms were grown on cover slip (8 mm diameter) placed at bottom of the wells of 24-well plates. 200 μL of fresh bacterial culture was inoculated to 1.8 mL TSB supplemented with 3.2 mg *H. patriniae*. The plates were incubated at 37°C with TSB medium replaced every 24 h. After 3 days or 7 days of cultivation, the cover slip was taken out and washed three times with saline water to remove the planktonic cells. The cover slip was immersed in 2.5% glutaraldehyde for 1 h for the cells fixation and rinsed with distilled water for 1 min. Then the cover slip was immersed in saturated calcium chloride solution for 15 min and rinsed with distilled water for 5 min. The biofilms on the cover slip were then stained with 5% silver nitrate for 15 min, followed by 1% hydroquinone colour-rendering for 2 min and then rinsed with distilled water for 1 min. Fixation was treated with 5% sodium thiosulfate for 1 min, followed by a final water rinse. The cover slip was placed on an inverted optical microscope for biofilm structure observation.

2.7. Swarming Motility Assay. Swarming assay was carried out as previously reported [25]. The medium used for swarming motility assay consists of nutrient broth (0.8%), glucose (0.5%), and agar (0.5%). The plates were dried at room temperature overnight before being used. 2 μL of *P. aeruginosa* PAO1 culture (OD600 = 0.5) mixed with 106.67 μg of *H. patriniae* water extract was spotted onto the swarming plate and the one with deionized water was used as blank control. Plates were incubated at 37°C for 24 h before the swarming diameter was measured.

2.8. Measurement of Exopolysaccharide Production. Overnight culture of PAO1 (OD600 = 0.005) was spotted onto Congo red plates (1% Tryptone, 1% agar, 4% Congo red, and 2% Coomassie blue) with or without *H. patriniae* water extract. The amount of *H. patriniae* water extract was 64 μg. The colony morphology and staining were observed after 3 days of incubation at 37°C [22].

3. Results and Discussion

3.1. Screening for Herbs with Inhibitory Effect on P. aeruginosa Biofilm-Associated Genes. Eighteen traditional Chinese medicinal herbs were selected because of their common usage for infection-like symptoms. Both boiling water extracts and ethanol extracts were obtained and used to screen for antibiofilm activities. Since *P. aeruginosa* biofilm formation is directly associated with the activity of several known genes, we constructed *luxCDABE*-based reporters to examine the effect of herb extracts on these genes. The effects of the crude extracts on the expression of these biofilm-associated genes (*algU*, *pslM*, *pelA*, *algA*, *ppyR*, and *bdlA*) are presented in Table 3. The results indicate that different herbal extracts exhibited various degrees of inhibitory effects on these genes. The water extract of *H. patriniae* showed the most significant effect on the expression of *algU*, *algA*, *pslM*, and *bdlA*. Examples of the gene expression profiles in the presence of *H. patriniae* are shown in Figure 1.

To confirm the results obtained from the *lux*-based reporter assay, real-time qPCR was carried out using bacterial RNA samples isolated in the presence and absence of *H. patriniae*. The results are shown in Table 4. In agreement with the results from the reporter assay, the mRNA levels of *algU*, *algA*, *pslM*, and *bdlA* in PAO1 were all significantly decreased in the presence of *H. patriniae* extract (at 1.6 mg/mL) compared with those in the absence of *H. patriniae* extract. It is noted that the inhibition of *algU* and *algA* was more pronounced in the qPCR assay.

Table 3: Effect of water and ethanolic herb extracts on biofilm-associated genes expression.

The English name of herbs	Water extract						The English name of herbs	Ethanolic extract					
	algU	*pslM*	*pelA*	*algA*	*ppyR*	*bdlA*		*algU*	*pslM*	*pelA*	*algA*	*ppyR*	*bdlA*
Atractylodes lancea	+1.5	0	−2.5	0	0	0	*Atractylodes lancea*	0	0	0	0	0	0
Cortex fraxini	0	−3	−1.5	−1	0	0	*Cortex fraxini*	−1.8	−2.5	−0.5	−1.5	0	0
Cyrtomium fortunei	0	−1.5	−2	−1	0	0	*Cyrtomium fortunei*	0	0	0	0	0	0
Erodium stephanianum Willd.	a	a	a	a	a	a	*Erodium stephanianum willd*	a	a	a	a	a	a
Folium artemisiae Argyi	−2	0	−2	0	−1.5	0	*Folium artemisiae argyi*	0	0	−2	0	−1.5	0
Fructus quisqualis	a	a	a	a	a	a	*Fructus quisqualis*	a	a	a	a	a	a
Herba agrimoniae	a	a	a	a	a	a	*Herba agrimoniae*	a	a	a	a	a	a
Herba patriniae	−2	−2.5	−0.5	−2.5	0	−2	*Herba patriniae*	0	0	0	0	−1.5	−1
Herba scutellariae barbatae	0	0	0	−1	0	0	*Herba scutellariae barbatae*	0	0	0	0	0	−1.5
Pomegranate rind	−1.5	−1.2	0	−1	0	0	*Pomegranate rind*	−1.5	−1	−1	−0.5	0	0
Portulacae herba	+1	0	0	+1.5	0	0	*Portulacae herba*	0	0	0	0	0	0
Radix paeoniae	−0.5	−0.5	0	0	−1	0	*Radix paeoniae*	0	0	0	0	0	0
Radix sanguisorbae	−1.5	−1	−1.5	−1	−0.5	0	*Radix sanguisorbae*	−1.6	−1.5	0	0	−0.5	0
Radix lithospermi	0	−1.2	−2	0	−1	0	*Radix lithospermi*	0	0	0	0	0	0
Scrophulariae	−2	+1.5	0	0	0	0	*Scrophulariae*	−0.5	0	−1	0	0	0
Smoked plum	a	a	a	a	a	a	*Smoked plum*	a	a	a	a	a	a
Taraxacum mongolicum	0	0	0	0	0	0	*Taraxacum mongolicum*	0	+2	0	0	0	0
Tripterygium	−1.5	0	−2.5	0	0	0	*Tripterygium*	0	0	−2	0	−2.5	0

Note: herbal extracts were used at 1.6 mg/mL. The values shown represent maximal inhibition (fold changes between experiments with and without herb extract). "+" represents induction of gene expression by herb extracts; "−" represents inhibition of biofilm gene expression by herb extracts; "0" represents no effect of biofilm gene expression by herb extracts; "a" represents inhibition of the growth of bacteria. Numbers represent fold changes at the time points where maximal expression was reached in the absence of herbal extract.

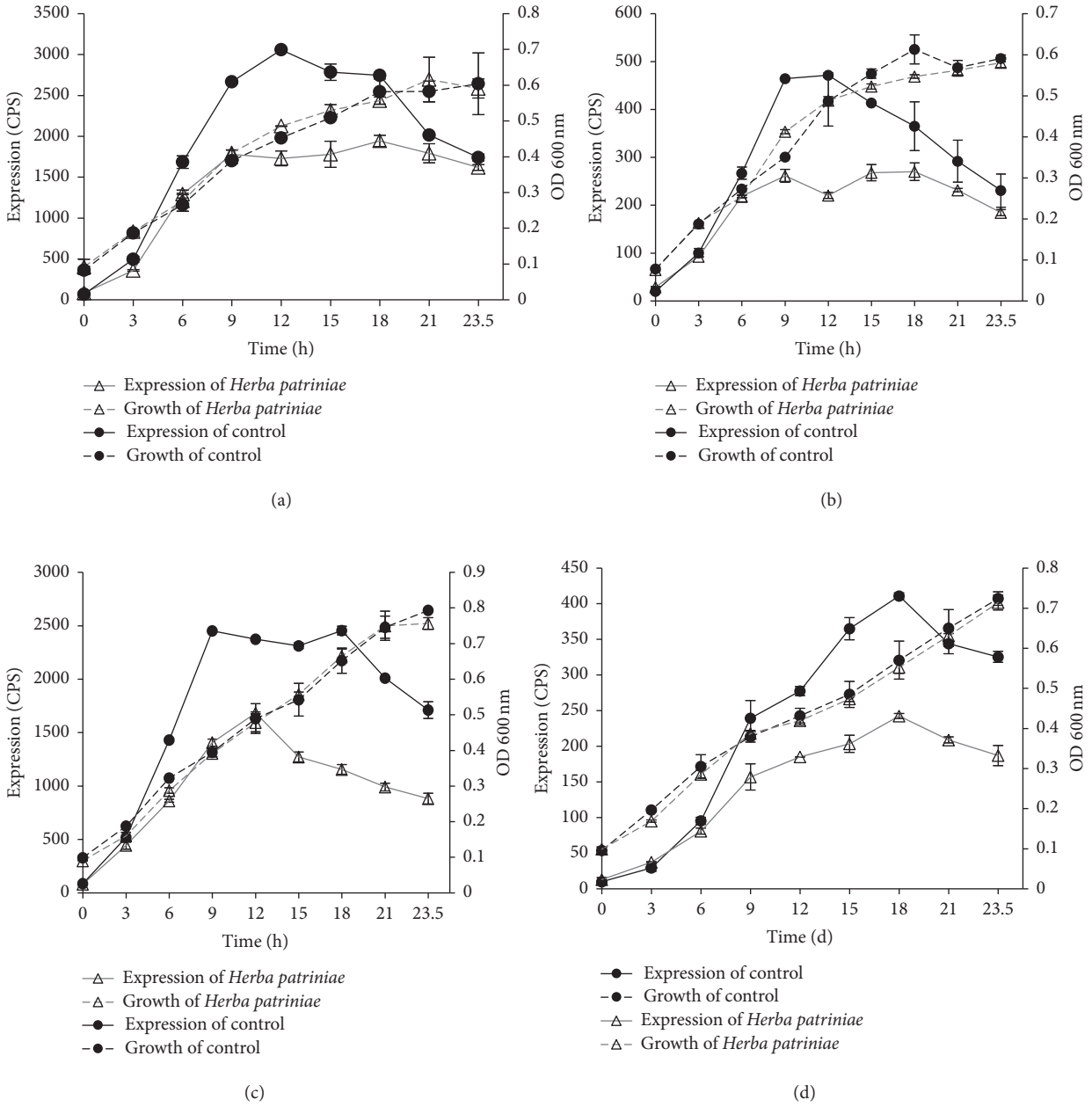

Figure 1: Expressions of *algU*, *algA*, *pslM*, and *bdlA* in medium with water extract of *Herba patriniae*. Expressions of *algU* (a), *algA* (b), *pslM* (c), and *bdlA* (d) in medium (total volume of 100 μL) with 160 μg *H. patriniae* extract and the controls were the ones without herbal extract.

The results indicate that many of these herbs have an inhibitory effect on the genes associated with biofilm formation in *P. aeruginosa*. This is somewhat not surprising because they all have been used for treatment of chronic bacterial infections in traditional Chinese medicine.

The effect from the water extract of *H. patriniae* was remarkable as it inhibited five genes tested. It has been reported that the herb had antibacterial and antiviral activity. However, it was noted that the water extract did not inhibit the growth of *P. aeruginosa* (Figure 1). Even though conventional antibiotic compounds may exist in *H. patriniae* against other bacteria, this result indicates no such component was present against *P. aeruginosa*, at least not at the concentrations used in our experiments.

Lacking of bacterial killing or growth inhibition activity, however, may not be a weakness of such herbs in treating infectious diseases. As discussed in previous reports [26–29], a promising new class of antipathogenic drugs that target virulence factors and/or biofilm formation instead of killing the pathogens has many advantages in clinical use. First, these antipathogenic drugs theoretically are less likely to render drug resistance in the pathogens because they do not assert

Table 4: The transcriptional levels of selected genes in PAO1 and PAO1 treated with *H. patriniae*.

Gene	Relative mRNA level determined by ΔCt calculation		
	Without *H. patriniae*	With *H. patriniae*	*P* value
algU	1.00	0.192	0.014
algA	1.00	0.090	0.011
pslM	1.00	0.695	0.043
bdlA	1.00	0.412	0.036

Note: the mRNA level of each gene was normalized to that of *proC*. The values shown represent the mean of three different tests.

a selective pressure on the pathogen's survival. Second, such therapeutics would unlikely affect other nonpathogenic or beneficial bacteria, that is, the microbiome in the host.

3.2. Extract of H. patriniae Inhibits P. aeruginosa Biofilm Formation. From the gene expression results, the extract of *H. patriniae* presumably would inhibit the biofilm formation of *P. aeruginosa*. To verify such an effect, *P. aeruginosa* biofilm formation was compared in the presence and absence of *H. patriniae* extract. As shown in Figure 2(a), significantly less biofilm was formed in the presence of the herb extract than that without the extract at the irreversible attachment stage (1 d) and mature stage (3 d and 7 d) after inoculation. The result is in agreement with the gene expression data, suggesting the *H. patriniae* extract could reduce biofilm formation through inhibiting the genes associated with biofilm formation.

Importantly, the addition of the *H. patriniae* also dramatically altered the structure of the biofilms (Figure 2(b)). It appears that the herb extract prevented the formation of mature biofilms, only allowing *P. aeruginosa* to form smaller cell clusters. These results indicate that the water extract of *H. patriniae* indeed was able to inhibit *P. aeruginosa* biofilm formation.

3.3. Water Extract of H. patriniae Inhibited P. aeruginosa Exopolysaccharide Production. The exopolysaccharide (EPS) matrix is an important component of biofilm structure [30]. We compared the exopolysaccharide production in the presence of *H. patriniae* extract to those without *H. patriniae* extract. As shown in Figure 3, *P. aeruginosa* PAO1 cells produced more EPS shown in red by Congo red staining than the cells with *H. patriniae* extract. This result indicates that *H. patriniae* inhibited *P. aeruginosa* exopolysaccharide production and hence affected biofilm formation.

3.4. H. patriniae Water Extract Promoted PAO1 Swarming Motility. Upon encountering a surface, the surface-associated behaviors of *P. aeruginosa,* such as biofilm formation and swarming, are often coregulated [31]. In *P. aeruginosa*, swarming motility is reversely correlated with biofilm formation. Examination of the swarming motility of PAO1 in the presence and absence of the water extract of *H. patriniae* showed that *H. patriniae* promoted *P. aeruginosa* swarming motility (Figure 4(a)). The diameter of PAO1 grown with 106.67 μg *H. patriniae* was almost 5.60 cm, while the control was less than 2.0 cm (Figure 4(b)). Considering the reverse relationship between swarming motility and biofilm formation, the enhanced swarming motility by *H. patriniae* extract could have contributed the inhibition of biofilm formation.

Taken together, the extract of *H. patriniae* clearly inhibited the biofilm formation of *P. aeruginosa*. It inhibited several key genes *algU*, *pslM*, *pelA*, *algA*, and *bdlA* that are involved in biofilm formation. *H. patriniae* reduced exopolysaccharide production and promoted swarming motility. Increased motility may reduce adhesion and enable bacteria to actively escape the biofilm matrix to become planktonic bacteria [13, 31, 32]. As depicted in Figure 5, multiple factors/pathways probably have contributed to the reduction of biofilm formation and the altered biofilm structure in the presence of *H. patriniae*.

In a time of resistance to multiple antimicrobial agents in pathogenic bacteria being spread, there is an urgent need to develop new antibacterial agents [1, 32]. Drugs against infections that involve biofilms are particularly required. Pathogens in biofilm formation are more resistant to conventional antibiotics and other adversary conditions such as nutritional stress. Biofilms also protect bacterial cells from the activity of host immune response [33, 34].

Traditional Chinese medicines are a valuable source for novel antibacterial agents [35–37]. The inhibitory effect of the water extract of *H. patriniae* against *P. aeruginosa* biofilms and biofilm-related phenotypes signifies that *H. patriniae* is a promising candidate for treatment of infections caused by *P. aeruginosa* biofilms. It could be used in the way of traditional Chinese medicine or it can be explored for active compounds.

4. Conclusions

Our results indicate *H. patriniae* extract could significantly inhibit the expression of *P. aeruginosa* genes associated with biofilm formation, alter the structure, and prevent the formation of mature biofilms. It also decreased exopolysaccharide production and promoted swarming motility. These results provided a potential underlying mechanism for the use of *H. patriniae* to treat bacterial infections in traditional Chinese medicine and revealed a promising candidate for exploration of new drugs against *P. aeruginosa* biofilm-associated infections.

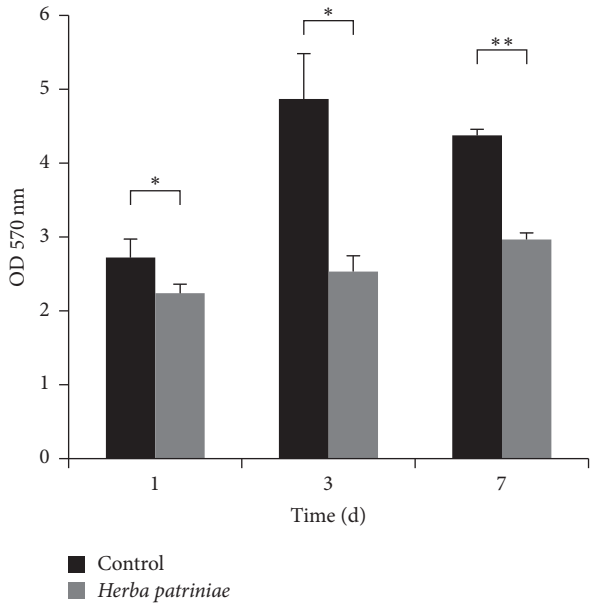

(a)

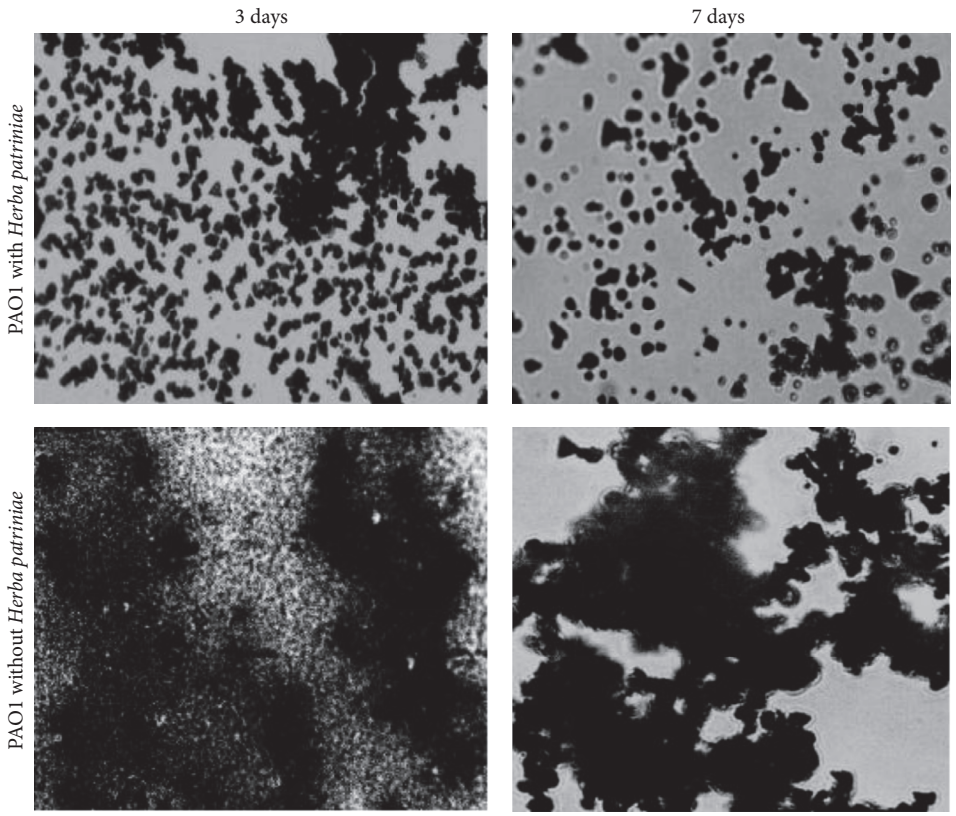

(b)

Figure 2: (a) Inhibition of biofilm production of PAO1 by *H. patriniae* extract. The control did not contain any herb extract. "$*$" indicates significant difference between the herb group and the control group ($P < 0.05$). "$**$" indicates very significant difference ($P < 0.01$). (b) Micrographs of biofilms formed with and without *H. patriniae*. Top row, PAO1 silver stained biofilms in the presence of extract of *H. patriniae* after 3 days and 7 days of incubation. Bottom row, PAO1 silver stained biofilms without *H. patriniae*.

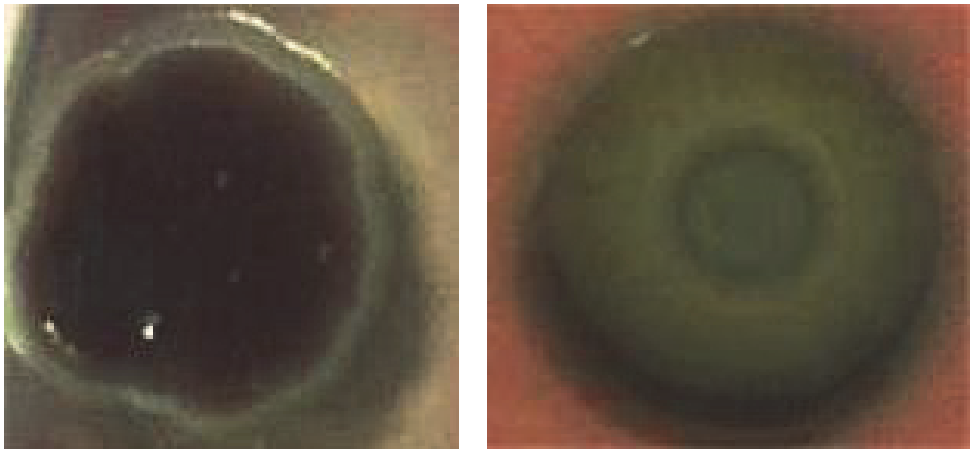

(a) (b)

Figure 3: Photograph of exopolysaccharide production on Congo red plates. (a) Without *H. patriniae*. (b) With *H. patriniae*. The colony morphology and staining were observed after 3 days of incubation at 37°C.

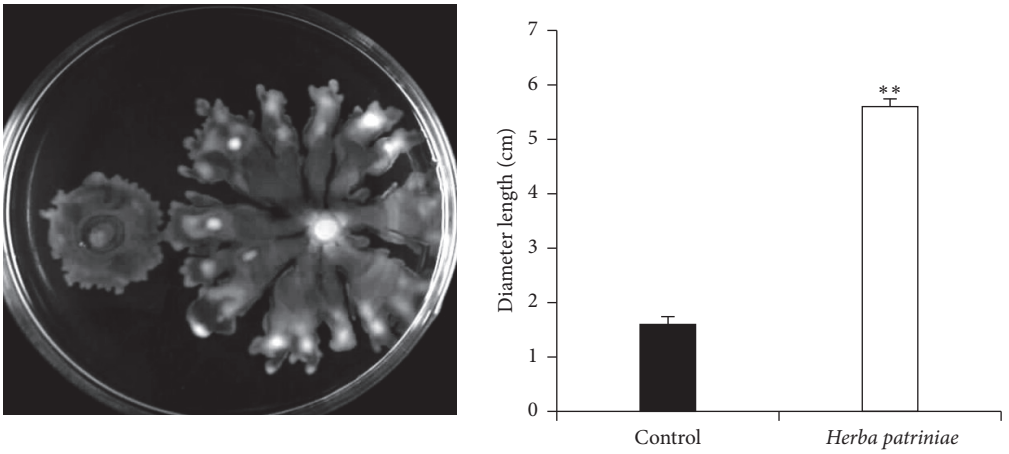

(a) (b)

Figure 4: Swarming motility of PAO1. (a) PAO1 grown with *H. patriniae* was at right; the one without herb was at left. (b) The swarming diameter of PAO1 with *H. patriniae*, the control was the one without herb. "$**$" indicates significant difference ($P < 0.01$).

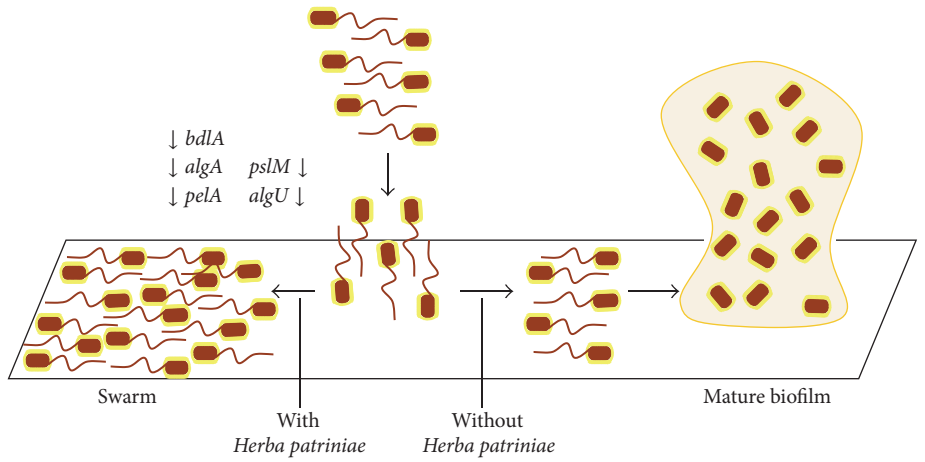

Figure 5: *P. aeruginosa* biofilm formation and swarming motility in the influence of *H. patriniae*.

Competing Interests

The authors declare that they have no competing interests regarding the publication of this paper.

Acknowledgments

This work was supported by grants from the NSFC (31570131), NSERC (402943-2011 RGPIN), CPSF (2014M562444), and PCSIRT (IRT 15R55).

References

[1] H. M. Zowawi, P. N. A. Harris, M. J. Roberts et al., "The emerging threat of multidrug-resistant Gram-negative bacteria in urology," *Nature Reviews Urology*, vol. 12, no. 10, pp. 570–584, 2015.

[2] T. Bjarnsholt, "The role of bacterial biofilms in chronic infections," *APMIS. Supplementum*, no. 136, pp. 1–51, 2013.

[3] M. Rybtke, L. D. Hultqvist, M. Givskov, and T. Tolker-Nielsen, "Pseudomonas aeruginosa biofilm infections: community structure, antimicrobial tolerance and immune response," *Journal of Molecular Biology*, vol. 427, no. 23, pp. 3628–3645, 2015.

[4] N. E. Head and H. Yu, "Cross-sectional analysis of clinical and environmental isolates of *Pseudomonas aeruginosa*: biofilm formation, virulence, and genome diversity," *Infection and Immunity*, vol. 72, no. 1, pp. 133–144, 2004.

[5] T.-F. Mah, B. Pitts, B. Pellock, G. C. Walker, P. S. Stewart, and G. A. O'Toole, "A genetic basis for Pseudomonas aeruginosa biofilm antibiotic resistance," *Nature*, vol. 426, no. 6964, pp. 306–310, 2003.

[6] M. Whiteley, M. G. Bangera, R. E. Bumgarner et al., "Gene expression in *Pseudomonas aeruginosa* biofilms," *Nature*, vol. 413, no. 6858, pp. 860–864, 2001.

[7] Q. Guo, W. Kong, S. Jin, L. Chen, Y. Xu, and K. Duan, "PqsR-dependent and PqsR-independent regulation of motility and biofilm formation by PQS in Pseudomonas aeruginosa PAO1," *Journal of Basic Microbiology*, vol. 54, no. 7, pp. 633–643, 2014.

[8] T. Rasamiravaka, Q. Labtani, P. Duez, and M. El Jaziri, "The formation of biofilms by pseudomonas aeruginosa: a review of the natural and synthetic compounds interfering with control mechanisms," *BioMed Research International*, vol. 2015, Article ID 759348, 17 pages, 2015.

[9] G. H. Talbot, J. Bradley, J. E. Edwards Jr., D. Gilbert, M. Scheid, and J. G. Bartlett, "Bad bugs need drugs: an update on the development pipeline from the antimicrobial availability task force of the infectious diseases society of America," *Clinical Infectious Diseases*, vol. 42, no. 5, pp. 657–668, 2006.

[10] Q. Guo, S. Jin, J. Xiao, D. Zhang, L. Shen, and K. Duan, "Inhibition of quorum sensing-associated virulence factors in Pseudomonas aeruginosa PAO1 by Folium artemisiae argyi extract," *Journal of Pure and Applied Microbiology*, vol. 7, no. 1, pp. 261–270, 2013.

[11] J.-D. Yang, L.-B. Hu, W. Zhou, Y.-F. Yin, J. Chen, and Z.-Q. Shi, "Lysis of Microcystis aeruginosa with extracts from chinese medicinal herbs," *International Journal of Molecular Sciences*, vol. 10, no. 9, pp. 4157–4167, 2009.

[12] A. Bazire, K. Shioya, E. Soum-Soutéra et al., "The sigma factor AlgU plays a key role in formation of robust biofilms by nonmucoid *Pseudomonas aeruginosa*," *Journal of Bacteriology*, vol. 192, no. 12, pp. 3001–3010, 2010.

[13] K. D. Jackson, M. Starkey, S. Kremer, M. R. Parsek, and D. J. Wozniak, "Identification of psl, a locus encoding a potential exopolysaccharide that is essential for *Pseudomonas aeruginosa* PAO1 biofilm formation," *Journal of Bacteriology*, vol. 186, no. 14, pp. 4466–4475, 2004.

[14] L. Ma, M. Conover, H. Lu, M. R. Parsek, K. Bayles, and D. J. Wozniak, "Assembly and development of the Pseudomonas aeruginosa biofilm matrix," *PLoS Pathogens*, vol. 5, no. 3, 2009.

[15] L. Friedman and R. Kolter, "Genes involved in matrix formation in Pseudomonas aeruginosa PA14 biofilms," *Molecular Microbiology*, vol. 51, no. 3, pp. 675–690, 2004.

[16] U. Remminghorst and B. H. A. Rehm, "In vitro alginate polymerization and the functional role of Alg8 in alginate production by Pseudomonas aeruginosa," *Applied and Environmental Microbiology*, vol. 72, no. 1, pp. 298–305, 2006.

[17] C. Attila, A. Ueda, and T. K. Wood, "PA2663 (PpyR) increases biofilm formation in Pseudomonas aeruginosa PAO1 through the psl operon and stimulates virulence and quorum-sensing phenotypes," *Applied Microbiology and Biotechnology*, vol. 78, no. 2, pp. 293–307, 2008.

[18] R. Morgan, S. Kohn, S.-H. Hwang, D. J. Hassett, and K. Sauer, "BdlA, a chemotaxis regulator essential for biofilm dispersion in *Pseudomonas aeruginosa*," *Journal of Bacteriology*, vol. 188, no. 21, pp. 7335–7343, 2006.

[19] K. Duan, C. Dammel, J. Stein, H. Rabin, and M. G. Surette, "Modulation of *Pseudomonas aeruginosa* gene expression by host microflora through interspecies communication," *Molecular Microbiology*, vol. 50, no. 5, pp. 1477–1491, 2003.

[20] H. Liang, N. Li, Z. Dong, M. G. Surette, and K. Duan, "The YebC family protein PA0964 negatively regulates the Pseudomonas aeruginosa quinolone signal system and pyocyanin production," *Journal of Bacteriology*, vol. 190, no. 18, pp. 6217–6227, 2008.

[21] G. A. O'Toole and R. Kolter, "Initiation of biofilm formation in Pseudomonas fluorescens WCS365 proceeds via multiple, convergent signalling pathways: a genetic analysis," *Molecular Microbiology*, vol. 28, no. 3, pp. 449–461, 1998.

[22] W. Kong, L. Chen, J. Zhao et al., "Hybrid sensor kinase PA1611 in Pseudomonas aeruginosa regulates transitions between acute and chronic infection through direct interaction with RetS," *Molecular Microbiology*, vol. 88, no. 4, pp. 784–797, 2013.

[23] C. Passariello, F. Berlutti, L. Selan, M. C. Thaller, and R. Pezzi, "A rapid staining procedure to demonstrate glycocalyx production and bacterial biofilms," *New Microbiology*, vol. 17, no. 3, pp. 225–230, 1994.

[24] J. Zhao, H. Jiang, W. Cheng et al., "The role of quorum sensing system in antimicrobial induced *ampC* expression in *Pseudomonas aeruginosa* biofilm," *Journal of Basic Microbiology*, vol. 55, no. 5, pp. 671–678, 2015.

[25] H. Liang, J. Duan, C. D. Sibley, M. G. Surette, and K. Duan, "Identification of mutants with altered phenazine production in Pseudomonas aeruginosa," *Journal of Medical Microbiology*, vol. 60, no. 1, pp. 22–34, 2011.

[26] S. Yang, Q. Guo, and K. Duan, "Perspectives on antibacterial activities of traditional Chinese medicine and its potential mechanisms," *Chinese Journal of Biochemical and Pharmaceutics*, vol. 36, no. 4, pp. 15–20, 2016.

[27] M. Otto, "Quorum-sensing control in Staphylococci—a target for antimicrobial drug therapy?" *FEMS Microbiology Letters*, vol. 241, no. 2, pp. 135–141, 2004.

[28] A. R. Hauser, J. Mecsas, and D. T. Moir, "Beyond antibiotics: new therapeutic approaches for bacterial infections," *Clinical Infectious Diseases*, vol. 63, no. 1, pp. 89–95, 2016.

[29] S. Wagner, R. Sommer, S. Hinsberger et al., "Novel strategies for the treatment of *Pseudomonas aeruginosa* infections," *Journal of Medicinal Chemistry*, vol. 59, no. 13, pp. 5929–5969, 2016.

[30] D. G. Davies, M. R. Parsek, J. P. Pearson, B. H. Iglewski, J. W. Costerton, and E. P. Greenberg, "The involvement of cell-to-cell signals in the development of a bacterial biofilm," *Science*, vol. 280, no. 5361, pp. 295–298, 1998.

[31] N. C. Caiazza, J. H. Merritt, K. M. Brothers, and G. A. O'Toole, "Inverse regulation of biofilm formation and swarming motility by Pseudomonas aeruginosa PA14," *Journal of Bacteriology*, vol. 189, no. 9, pp. 3603–3612, 2007.

[32] Y.-M. Zhou, L. Shao, J.-A. Li et al., "An efficient and novel screening model for assessing the bioactivity of extracts against multidrug-resistant pseudomonas aeruginosa using caenorhabditis elegans," *Bioscience, Biotechnology and Biochemistry*, vol. 75, no. 9, pp. 1746–1751, 2011.

[33] S. A. Ochoa, A. Cruz-Córdova, G. E. Rodea et al., "Phenotypic characterization of multidrug-resistant Pseudomonas aeruginosa strains isolated from pediatric patients associated to biofilm formation," *Microbiological Research*, vol. 172, pp. 68–78, 2015.

[34] M. Bala, S. Gupte, P. Aggarwal, M. Kaur, and A. Manhas, "Biofilm producing multidrug resistant Acinetobacter species from a tertiary care hospital: a therapeutic challenge," *International Journal of Research in Medical Sciences*, vol. 4, no. 7, pp. 3024–3026, 2016.

[35] K. Anani, Y. Adjrah, Y. Ameyapoh et al., "Effects of hydroethanolic extracts of *Balanites aegyptiaca* (L.) Delile (Balanitaceae) on some resistant pathogens bacteria isolated from wounds," *Journal of Ethnopharmacology*, vol. 164, pp. 16–21, 2015.

[36] B. P. Marasini, P. Baral, P. Aryal et al., "Evaluation of antibacterial activity of some traditionally used medicinal plants against human pathogenic bacteria," *BioMed Research International*, vol. 2015, Article ID 265425, 6 pages, 2015.

[37] G. Y. Zuo, G. C. Wang, Y. B. Zhao et al., "Screening of Chinese medicinal plants for inhibition against clinical isolates of methicillin-resistant Staphylococcus aureus (MRSA)," *Journal of Ethnopharmacology*, vol. 120, no. 2, pp. 287–290, 2008.

Hindawi Publishing Corporation
BioMed Research International
Volume 2016, Article ID 3628268, 7 pages
http://dx.doi.org/10.1155/2016/3628268

Research Article

Transferrin Impacts *Bacillus thuringiensis* Biofilm Levels

Bianca Garner,[1] Elrica Brown,[1] Martha Taplin,[1,2] Angel Garcia,[1] and Baracka Williams-Mapp[1]

[1] *Tougaloo College, 500 West County Line Road, Tougaloo, MS, USA*
[2] *Jackson State University, 1400 John R. Lynch Street, Jackson, MS, USA*

Correspondence should be addressed to Bianca Garner; bgarner@tougaloo.edu

Received 15 July 2016; Revised 7 November 2016; Accepted 8 November 2016

Academic Editor: Aruni Wilson

Copyright © 2016 Bianca Garner et al. This is an open access article distributed under the Creative Commons Attribution License, which permits unrestricted use, distribution, and reproduction in any medium, provided the original work is properly cited.

The present study examined the impact of transferrin on *Bacillus thuringiensis* biofilms. Three commercial strains, an environmental strain (33679), the type strain (10792), and an isolate from a diseased insect (700872), were cultured in iron restricted minimal medium. All strains produced biofilm when grown in vinyl plates at 30°C. *B. thuringiensis* 33679 had a biofilm biomass more than twice the concentration exhibited by the other strains. The addition of transferrin resulted in slightly increased growth yields for 2 of the 3 strains tested, including 33679. In contrast, the addition of 50 μg/mL of transferrin resulted in an 80% decrease in biofilm levels for strain 33679. When the growth temperature was increased to 37°C, the addition of 50 μg/mL of transferrin increased culture turbidity for only strain 33679. Biofilm levels were again decreased in strain 33679 at 37°C. Growth of *B. thuringiensis* cultures in polystyrene resulted in a decrease in overall growth yields at 30°C, with biofilm levels significantly decreased for 33679 in the presence of transferrin. These findings demonstrate that transferrin impacts biofilm formation in select strains of *B. thuringiensis*. Identification of these differences in biofilm regulation may be beneficial in elucidating potential virulence mechanisms among the differing strains.

1. Introduction

Bacillus thuringiensis is a ubiquitous Gram-positive, spore forming microbe. Because it is employed as a biological pesticide, *B. thuringiensis* is routinely isolated from agricultural commodities [1–5]. This microbe produces insecticidal toxins that target select hosts [6, 7]. Taxonomically, *B. thuringiensis* falls within the *Bacillus cereus sensu lato* group of microbes, which include the human opportunistic pathogen *B. cereus* and the zoonotic pathogen *Bacillus anthracis* [8]. Although a high degree of genetic similarity is found among the three strains, *B. thuringiensis* is considered a distinct species based on the physiological variations, including virulence factors [9].

Biofilm development is one of the many physiological processes that differ within the *B. cereus sensu lato* group microbes. The ability to form biofilms is not aligned with a particular species in the group and can fluctuate from strain to strain [10]. Biofilm formation is also not correlated with cell surface moieties or pathogenicity [10, 11]. In *B. cereus* clinical strains, microbes recovered from certain niches, like the oral cavity, are less likely to produce biofilms in cultures. This phenomenon has not been recorded in *B. thuringiensis* [10, 12]. What is evident is that the ability of *B. cereus* to form biofilms is contingent on environmental conditions, including nutrient accessibility [13].

Required in low levels for normal cellular functions, iron has been verified to regulate biofilm formation in countless microbes, including *Haemophilus influenzae, Klebsiella pneumonia*, and *Escherichia coli* [14–16]. Iron is required for biofilm development in *Staphylococcus aureus, Pseudomonas aeruginosa*, and *Mycobacterium smegmatis* [17–19]. The iron impact cannot be attributed to growth unaided, as the increase is more dramatic in biofilms than in planktonic cells [20]. In *B. cereus*, the impact of iron on biofilm formation is highly variable. Only two (2) *B. cereus* strains demonstrated an increase in biofilm when iron was restricted, versus nine (9) strains that had a decrease in biofilm when iron was limited [21]. In the nine (9) strains that required iron for biofilm growth, biofilm biomass directly correlated to the

specific iron source utilized for growth. For example, only two (2) strains exhibited biofilm concentrations higher in the presence of transferrin than in the iron restricted samples [21]. These findings are in direct opposition to reports that transferrin increases *B. cereus sensu lato* microbial growth under iron restriction [22–24].

The present study sought to investigate the impact of transferrin on *B. thuringiensis* biofilm physiology. Commercial strains originally isolated from different sources were assayed for biofilm formation in minimal medium. Turbidity was monitored in microtiter plates to ascertain whether the addition of transferrin impacted culture growth. Biofilm levels were quantified to classify the impact of transferrin on biofilm biomass of the three different strains.

2. Materials and Methods

2.1. Microbiological Conditions. *B. thuringiensis* strains were purchased from the American Type Culture Collection (ATCC). Strains were randomly selected but included the type strain (laboratory) and an environmental strain. Strains were maintained as spores on sporulation agar (23 g nutrient agar, 0.5 g yeast extract, 6.0 mg $MnCl_2$, 95.0 mg $MgCl_2$, and 78.0 mg $CaCl_2$ per liter) at 4°C. Growth assays were carried out in a defined minimal medium consisting of MM9 salts (3 g KH_2PO_4, 5 g NaCl, and 10 g NH_4Cl per liter), glucose (0.2%), and casamino acids (0.3%). This medium was treated with Chelex-100 (Bio-Rad) to remove excess iron and filter sterilized. Metals were added to this sterile medium base at the following concentrations: 830 μM Mg, 36 μM Mn, and 0.32 μM Zn. This defined medium is referred to hereafter as CTM for Chelex-treated medium. Holo-transferrin (Sigma) was purchased in powder form and solubilized in water. Transferrin was filter sterilized and added to the cultures in the indicated amounts.

2.2. Biofilm Measurement. Quantification of biofilm biomass was performed with the microtiter plate assay as previously described with some modifications [21]. Brain-heart infusion agar (Fisher Scientific) slants were inoculated for overnight incubation at 37°C. Overnight cultures were then used to inoculate CTM at final turbidity (OD_{600}) of 0.02 in 96-well microtiter plates (200 μL). Samples were incubated overnight, without shaking. After incubation, growth was measured via the turbidity (A_{620}) with the BioTek Synergy 2 plate reader. After measuring the turbidity, the plates were inverted to remove unattached cells. Adherent cells were stained with crystal violet (200 μL) and samples were incubated for at least 1 minute. Plates were then inverted to remove excess dye and washed thrice with phosphate buffered saline. Plates were inverted a final time and remained inverted for 5 minutes. Gram stain alcohol decolorizer (200 μL) was added to each well to solubilize the crystal violet bound to the adherent cells. The optical densities of these samples are the biofilm biomass and were measured spectrophotometrically at A_{540} with the BioTek Synergy 2. Biofilm level was calculated as the biomass of the sample divided by the biomass of the sample without transferrin. Biofilm level indicates either an increase in biofilm (>1.0) or a decrease in biofilm (<1.0) as compared to the transferrin-free samples.

2.3. Statistical Analysis. Experiments were repeated 3 times. Data is the average of the measurements and error bars, where indicated, are the standard deviation. A standard t-test was performed on data and significance established with $p < 0.05$.

3. Results and Discussions

Production of biofilms has been well documented in Gram-positive microbes, including the *Bacillus* species. Elucidation of the mechanisms that govern biofilm formation in *B. cereus* group microbes has implications both in the environment, where they are frequent contaminants, and in medicine, where nosocomial infections are linked to various species [12]. Iron availability has been linked to biofilm formation in numerous microbes and has emerged as an area of interest in *B. cereus sensu lato* group because of its implications in microbial virulence [24].

Biofilm formation is altered by transferrin in some *B. cereus* laboratory and environmental strains [21]. Although *B. anthracis, B. cereus*, and *B. thuringiensis* share many genetic similarities, the regulatory patterns that govern physiology vary among the microbes. Thus, while some *B. cereus* strains may require iron for optimal biofilm conditions, it is unclear how iron or any of the potential iron sources will impact biofilm formation in *B. thuringiensis*. This member of the *B. cereus sensu lato* group has traditionally not been viewed as pathogenic, as many of the toxin genes target insects, as opposed to humans. There are cases, however, of human infections by *B. thuringiensis* in the immunocompromised, with some infections characterized by biofilm development [25–27]. The basis for the present study was to determine whether transferrin would impact *B. thuringiensis* biofilm levels similar to the process observed in *B. cereus*.

Commercially available *B. thuringiensis* strains were purchased from the American Type Culture Collection (ATCC) to examine the potential role of transferrin in biofilm development under iron limiting conditions [28]. ATCC strain 33679, serotype H3:3a,3b, is a commonly used strain that encodes the insecticidal toxins and was originally isolated from a diseased insect larva. ATCC strain 700872, serovar israelensis, is an environmental strain isolated from soil. ATCC strain 10792 is the type strain originally isolated from animal tissue. Thus, the three strains selected represent differing origins of isolation. While this has not been demonstrated to be a determining factor in the ability of *B. thuringiensis* to form biofilms, it does provide a comparison of how isolates might respond to transferrin when cultured in defined, minimal medium.

CTM containing MM9 was selected as the medium for biofilm assays. *B. cereus* demonstrates an iron restrictive phenotype when cultured in MM9 alone [22]. MM9 supplemented with additional nutrients are more effective for the growth of *B. anthracis* [29]. CTM in the present study contains MM9, glucose, and casamino acids. This minimal

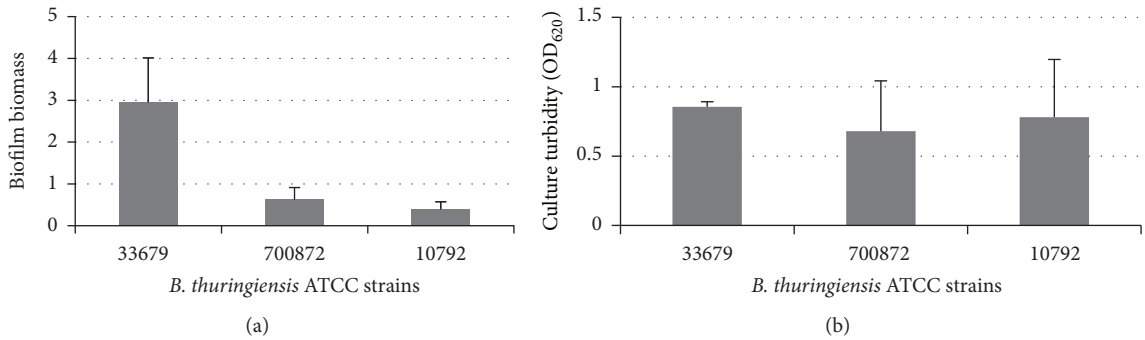

Figure 1: (a) *B. thuringiensis* strains form biofilms in iron restrictive medium. CTM was inoculated to an OD_{600} of 0.02 in vinyl plates and incubated for 24 hours at 30°C. Microtiter plates were inverted to remove unattached cells. Samples were stained with crystal violet and washed with PBS. Biofilm biomass was detected by the addition of alcohol decolorizer, which was measured at A_{540}. Data are presented as the average, with error bars indicating the standard deviation. (b) *B. thuringiensis* strains grow in iron restrictive medium. CTM was inoculated to an OD_{600} of 0.02 in vinyl plates and incubated for 24 hours at 30°C. Culture turbidity was measured at OD_{620}. Samples are presented as the average, with error bars indicating the standard deviation.

medium was then Chelex-treated to remove all metal contamination, which allows for control of the metal composition in the medium. Although there might be some internal carryover iron from the overnight growth, *B. thuringiensis* cells grown in CTM for 24 hours are iron restricted based on molecular and biochemical analyses of cultures [30].

Biofilm biomass was measured in strains cultured in vinyl plates at 30°C for 24 hours in CTM. All three strains produced biofilm under the conditions tested. Biofilm formation was the highest in strain 33679 and the lowest in strain 10792 (Figure 1(a)). Biofilm biomass in strain 33679 was more than three (3) times higher than in strain 10792 and two (2) times higher than in strain 700872. These results are consistent with studies which indicate that biofilm concentration varies within a given species and demonstrate *B. thuringiensis* biofilm formation in minimal medium [31].

Microbial growth was measured spectrophotometrically in the vinyl plates to identify whether differences in biofilm could be correlated with differences in culture growth. All strains grew to similar levels in CTM, with optical densities above 0.5 (Figure 1(b)). Strain 33679 demonstrated the highest growth yields, but there was no significant difference in final growth yields between the three strains. Thus, differences observed in biofilm biomass between the three strains cannot be attributed solely to culture growth levels.

While iron is an abundant metal required in only small quantities for normal cellular processes, microbes cannot readily access iron during an infection. Transferrin is one of several host iron binding proteins utilized for growth by a variety of microbes [32]. In *B. cereus,* the addition of transferrin to iron restrictive medium results in an increase in growth [22]. Growth yields and biofilm levels were measured for the three strains cultured in the presence of transferrin for 24 hours in vinyl plates at 30°C to observe whether the compound altered *B. thuringiensis* physiology.

The addition of transferrin resulted in increased growth yields for 2 of the 3 *B. thuringiensis* strains when compared to the no transferrin cultures. A statistically significant dose-dependent increase in growth was observed for strain 10792 with transferrin (Figure 2(a)). An increase in growth was observed for 33679, but the values were not statistically significant when compared to the no transferrin samples. Only strain 700872 demonstrated a decrease in growth with 50 μg/mL of transferrin, but only by approximately 3%. Thus, as in *B. cereus*, transferrin can increase growth of some, but not all, *B. thuringiensis* strains.

The vast differences in biofilm biomass concentrations made comparison between the three strains difficult, as the levels for 2 of the strains were considerably lower in the minimal medium (Figure 1(a)). Thus, the change in biofilm concentration was measured as a ratio of the biofilm level. This allowed for a comparison of the impacts of transferrin on biofilm development between the strains. For this analysis, the samples without transferrin were designated the baseline. Biofilm biomass of the transferrin containing cultures was measured spectrophotometrically. Each biomass was then divided by the baseline. Thus, biofilm levels indicate either a decrease (below 1.0) or an increase (above 1.0) in concentration relative to the baseline.

While the addition of transferrin resulted in slight increases in growth for 2 of the 3 strains, transferrin had the opposite impact on biofilm levels. Transferrin resulted in a decrease in biofilm formation for 2 strains cultured in vinyl plates at 30°C for 24 hours. A statistically significant dose-dependent decrease in biofilm level was observed in strain 33679 (Figure 2(b)). Biofilm levels decreased by more than 50% when strain 33679 was cultured with 10 μg/mL of transferrin and 80% with 50 μg/mL of transferrin as compared to the baseline (Figure 2(b)). Strain 700872 had an 8% decrease in biofilm level with 10 μg/mL of transferrin and a significant 20% decrease when cells were cultured with 50 μg/mL of transferrin. Although a slight decrease in biofilm level occurred for strain 10792 with 10 μg/mL of transferrin, no overall transferrin trend was measured. These studies suggest that while *B. thuringiensis* culture growth is increased with transferrin for some strains, the biofilm levels may not be regulated in a similar manner. Because environmental factors

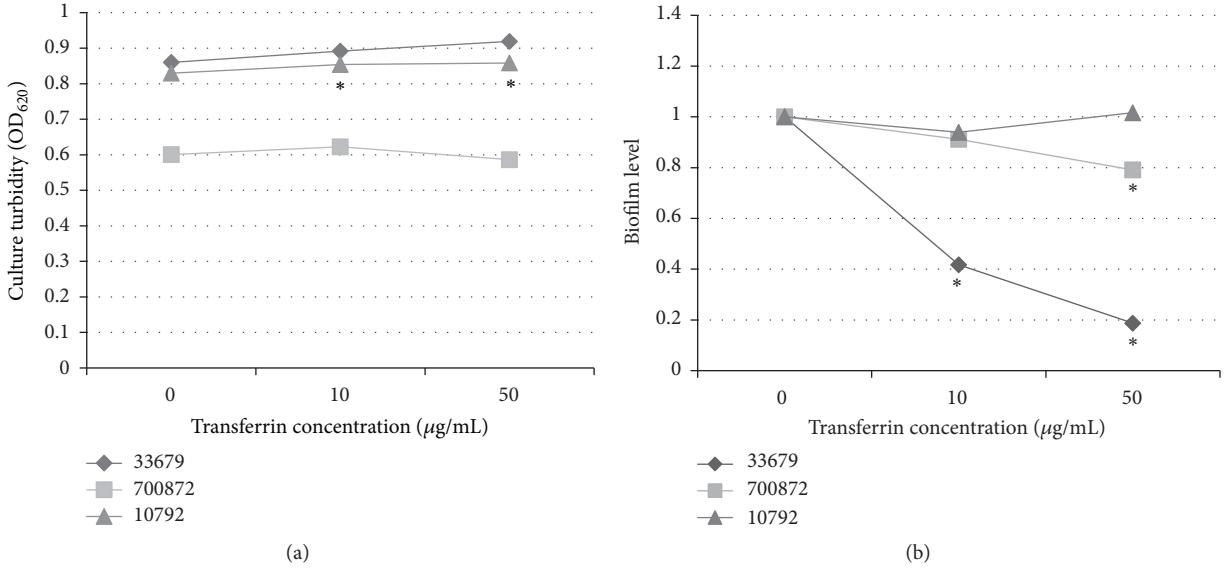

Figure 2: (a) *B. thuringiensis* strains grew in the presence of transferrin. CTM with varying concentrations of transferrin was inoculated to an OD_{600} of 0.02 in vinyl plates and incubated for 24 hours at 30°C. Culture turbidity was measured in a plate reader at OD_{620}. Samples are presented as the average. Asterisks indicate a statistically significant ($p < 0.05$) change as compared to the no transferrin samples. (b) Transferrin decreases biofilm formation in *B. thuringiensis* strains. CTM with varying concentrations of transferrin was inoculated to an OD_{600} of 0.02 in vinyl plates and incubated for 24 hours at 30°C. Samples were analyzed for biofilm biomass as described. Biofilm levels indicate a change in biomass relative to the baseline. Asterisks indicate a statistically significant ($p < 0.05$) change as compared to the no transferrin samples.

can alter biofilm biomass, it was postulated that the impact of transferrin on biofilm levels is dependent on additional factors.

Like many microbes, *Bacillus* species alter their physiology to adapt to the changing environment, allowing them to survive diverse conditions. Temperature is a critical environmental regulator of *B. cereus sensu lato* physiology [33]. While 37°C is the preferable temperature for *B. cereus* and *B. anthracis* virulence, lower temperatures are important in the pathogenicity for the insect pathogen *B. thuringiensis* [33, 34]. Although the optimal growth temperature for *B. thuringiensis* is indicated to be 30°C, the organism has been isolated from human infections and, thus, can grow at higher temperatures.

To ascertain whether temperature is important in the transferrin impact on biofilm formation, *B. thuringiensis* strains were cultured in vinyl plates at 37°C for 24 hours and assayed as described above. Growth was measured first to determine whether the change in temperature altered growth. Strain 33679 had the highest yields, similar to the values observed at 30°C (Figure 3(a)). In contrast, growth for strains 700872 and 10792 at 37°C was less than growth observed at 30°C. The addition of 50 μg/mL of transferrin resulted in increased growth for 33679 and decreased growth for both 700872 and 10792 as compared to the no transferrin samples, but the results were not statistically significant.

Biofilm was evident in all *B. thuringiensis* strains cultured at 37°C in vinyl plates. The addition of 10 μg/mL of transferrin resulted in a slight decrease in biofilm levels for all strains (Figure 3(b)). The increase of transferrin to 50 μg/mL resulted in additional decreases for strains 33679 and 700872. The decrease in biofilm levels for strain 33679 was more than 80% and more than 20% for 700872. These responses were similar to biofilm levels observed at 30°C, indicating that transferrin impacts biofilm development in vinyl plates, regardless of the temperature for some *B. thuringiensis* strains.

Temperature is one environmental factor that may play a role in biofilm formation. In *B. cereus,* strains demonstrated a higher affinity to form biofilms based on the growth substrate. The iron regulation of biofilm formation was more evident when these microbes were cultured in polystyrene plates versus other substrates [21]. To examine whether polystyrene was an effective surface for biofilm formation, *B. thuringiensis* strains were cultured as described above in noncoated polystyrene microtiter plates for 24 hours at 30°C.

Growth was decreased for all strains in polystyrene plates when compared to growth in vinyl plates without the added transferrin. No culture turbidity average was over 0.5, with all three strains exhibiting growth between optical densities of 0.3 to 0.4 (Figure 4(a)). It is unclear what role polystyrene had in growth, as levels were more than 50% decreased when compared to growth in vinyl plates at the same temperature. A dose-dependent statistically significant decrease in growth was observed for strain 33679 in the presence of transferrin (Figure 4(a)). The addition of 50 μg/mL of transferrin resulted in a statistically significant decrease in growth for all three strains.

Regardless of the low growth levels, biofilm was detected in all three strains cultured at 30°C in polystyrene. The addition of transferrin to *B. thuringiensis* 33679 resulted in a statistically significant decrease in biofilm levels similar

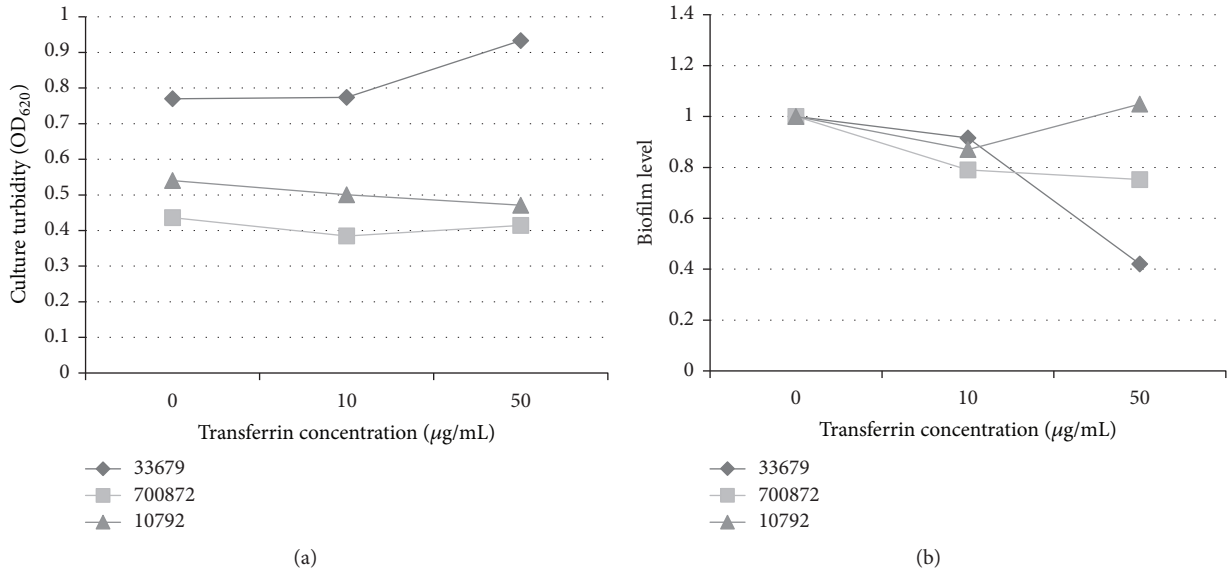

Figure 3: (a) *B. thuringiensis* strains grow in vinyl plates at 37°C. CTM was inoculated to an OD_{600} of 0.02 and incubated for 24 hours at 37°C. Culture turbidity was measured in a plate reader at OD_{620}. Samples are presented as the average. (b) Transferrin decreases biofilm formation in certain *B. thuringiensis* strains in vinyl plates at 37°C. CTM was inoculated to an OD_{600} of 0.02 and incubated for 24 hours at 37°C. Samples were analyzed for biofilm biomass as described. Biofilm biomass was detected by the addition of alcohol decolorizer. Biofilm levels indicate a change in biomass relative to the baseline. Samples are presented as the average.

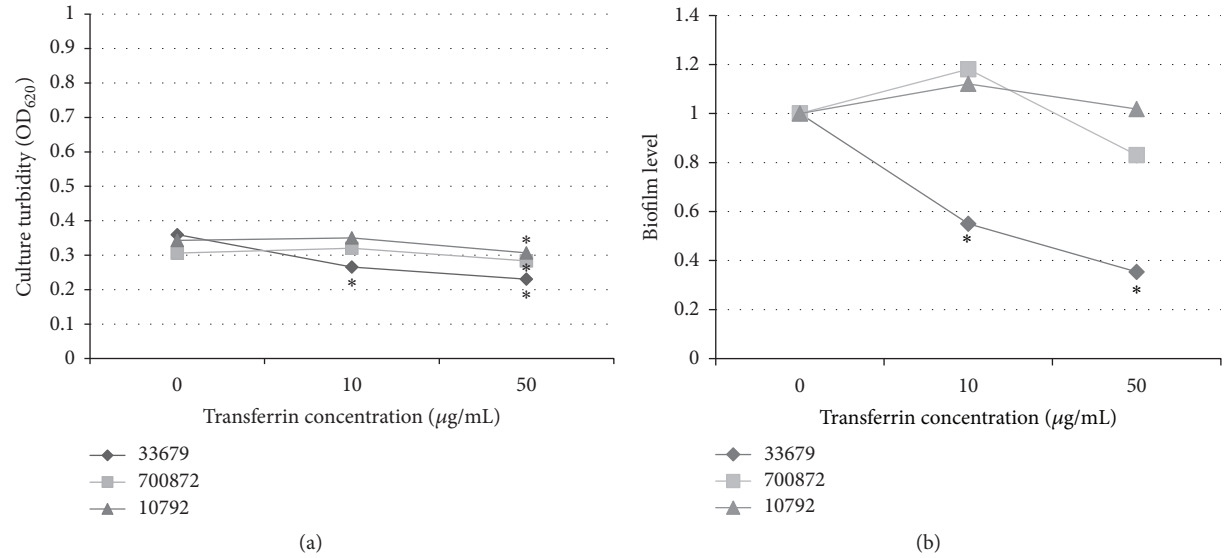

Figure 4: (a) *B. thuringiensis* strains form biofilms in polystyrene plates. CTM was inoculated to an OD_{600} of 0.02 and incubated in CTM for 24 hours at 30°C. Culture turbidity was measured in a plate reader at OD_{620}. Samples are presented as the average. Asterisks indicate a statistically significant ($p < 0.05$) change as compared to the no transferrin samples. (b) Transferrin decreases biofilm formation in certain *B. thuringiensis* strains in polystyrene plates. CTM was inoculated to an OD_{600} of 0.02 and incubated for 24 hours at 30°C. Samples were analyzed for biofilm biomass as described. Biofilm levels indicate a change in biomass relative to the baseline. Asterisks indicate a statistically significant ($p < 0.05$) change as compared to the no transferrin samples.

to those observed in the vinyl cultures (Figure 1 and Figure 4(b)). Transferrin increased biofilm levels in strains 700872 and 10792 at 10 μg/mL, but the addition of 50 μg/mL resulted in a decrease of biofilm levels back to or below the baseline. Thus, the transferrin impact on *B. thuringiensis* 33679 is consistent at 30°C, regardless of the growth substrate.

Biofilms are environmentally important niches that allow *B. cereus* microbes to survive under diverse and harsh conditions. These microbes must use a variety of cues to regulate the production of the various factors that help to establish and sustain biofilms. Once established, biofilms represent an important physiological state where increased

microbial survival occurs. These are the first studies to demonstrate a potential role for transferrin in *B. thuringiensis* biofilm development. Within the *B. cereus sensu lato* group, *B. thuringiensis* has traditionally not been viewed as pathogenic, as many of the identified *B. thuringiensis* toxin genes target insects. There are cases, however, of human infections by *B. thuringiensis* generally from nosocomial infections [32–34]. Thus, it is important to identify factors that facilitate biofilm formation in this strain that is a potential health hazard.

The present study highlights the complex regulatory mechanism that governs biofilm levels in *B. thuringiensis*. Biofilm formation is determined by the physiological state of the microbe, which is dependent on many environmental variables. The ability of transferrin to impact biofilm formation was highly variable and dependent on multiple factors. Additional comparative biochemical and molecular studies must be performed to identify the regulatory pathways that govern biofilm formation within the species. The discovery of these processes may potentially lead to the identification of additional virulence factors within the *B. cereus* group.

4. Conclusions

Transferrin can impact biofilm levels in some *B. thuringiensis* strains cultured under minimal conditions. This process may be altered, however, by growth temperature and growth substrate.

Competing Interests

The authors have no competing interests to declare.

Acknowledgments

This work was supported by the National Science Foundation (1412858), the Howard Hughes Biomedical Institute (UGRAD 52007562), and the National Institutes of Health Jackson Heart Study (HHSN268201300048C).

References

[1] U. Hariram and R. Labbé, "Spore prevalence and toxigenicity of *Bacillus cereus* and *Bacillus thuringiensis* isolates from U.S. retail spices," *Journal of Food Protection*, vol. 78, no. 3, pp. 590–596, 2015.

[2] B. Kim, J. Bang, H. Kim et al., "*Bacillus cereus* and *Bacillus thuringiensis* spores in Korean rice: prevalence and toxin production as affected by production area and degree of milling," *Food Microbiology*, vol. 42, pp. 89–94, 2014.

[3] K. Frederiksen, H. Rosenquist, K. Jørgensen, and A. Wilcks, "Occurrence of natural *Bacillus thuringiensis* contaminants and residues of *Bacillus thuringiensis*-based insecticides on fresh fruits and vegetables," *Applied and Environmental Microbiology*, vol. 72, no. 5, pp. 3435–3440, 2006.

[4] G. Zhou, H. Liu, J. He, Y. Yuan, and Z. Yuan, "The occurrence of *Bacillus cereus*, *B. thuringiensis* and *B. mycoides* in Chinese pasteurized full fat milk," *International Journal of Food Microbiology*, vol. 121, no. 2, pp. 195–200, 2008.

[5] M. Bartoszewicz, B. M. Hansen, and I. Swiecicka, "The members of the Bacillus cereus group are commonly present contaminants of fresh and heat-treated milk," *Food Microbiology*, vol. 25, no. 4, pp. 588–596, 2008.

[6] L. Palma, D. Muñoz, C. Berry, J. Murillo, P. Caballero, and P. Caballero, "*Bacillus thuringiensis* toxins: an overview of their biocidal activity," *Toxins*, vol. 6, no. 12, pp. 3296–3325, 2014.

[7] F. Celandroni, S. Salvetti, S. Senesi, and E. Ghelardi, "*Bacillus thuringiensis* membrane-damaging toxins acting on mammalian cells," *FEMS Microbiology Letters*, vol. 361, no. 2, pp. 95–103, 2014.

[8] T. D. Read, S. N. Peterson, N. Tourasse et al., "The genome sequence of *Bacillus anthracis* Ames and comparison to closely related bacteria," *Nature*, vol. 423, no. 6935, pp. 81–86, 2003.

[9] R. T. Okinaka and P. Keim, "The phylogeny of *Bacillus cereus sensu* lato," *Microbiology Spectrum*, vol. 4, no. 1, 2016.

[10] S. Auger, N. Ramarao, C. Faille, A. Fouet, S. Aymerich, and M. Gohar, "Biofilm formation and cell surface properties among pathogenic and nonpathogenic strains of the *Bacillus cereus* group," *Applied and Environmental Microbiology*, vol. 75, no. 20, pp. 6616–6618, 2009.

[11] K. García, J. E. Ibarra, A. Bravo et al., "Variability of *Bacillus thuringiensis* strains by ERIC-PCR and biofilm formation," *Current Microbiology*, vol. 70, no. 1, pp. 10–18, 2015.

[12] R. Kuroki, K. Kawakami, L. Qin et al., "Nosocomial bacteremia caused by biofilm-forming *Bacillus cereus* and *Bacillus thuringiensis*," *Internal Medicine*, vol. 48, no. 10, pp. 791–796, 2009.

[13] H. Hayrapetyan, L. Muller, M. Tempelaars, T. Abee, and M. Nierop Groot, "Comparative analysis of biofilm formation by *Bacillus cereus* reference strains and undomesticated food isolates and the effect of free iron," *International Journal of Food Microbiology*, vol. 200, pp. 72–79, 2015.

[14] S. Chhibber, D. Nag, and S. Bansal, "Inhibiting biofilm formation by *Klebsiella pneumoniae* B5055 using an iron antagonizing molecule and a bacteriophage," *BMC Microbiology*, vol. 13, no. 1, article 174, 2013.

[15] W. H. DePas, D. A. Hufnagel, J. S. Lee et al., "Iron induces bimodal population development by *Escherichia coli*," *Proceedings of the National Academy of Sciences of the United States of America*, vol. 110, no. 7, pp. 2629–2634, 2013.

[16] B. R. Szelestey, D. R. Heimlich, F. K. Raffel, S. S. Justice, and K. M. Mason, "*Haemophilus* responses to nutritional immunity: epigenetic and morphological contribution to biofilm architecture, invasion, persistence and disease severity," *PLoS Pathogens*, vol. 9, no. 10, Article ID e1003709, 2013.

[17] E. Banin, M. L. Vasil, and E. P. Greenberg, "Iron and *Pseudomonas aeruginosa* biofilm formation," *Proceedings of the National Academy of Sciences of the United States of America*, vol. 102, no. 31, pp. 11076–11081, 2005.

[18] A. Ojha and G. F. Hatfull, "The role of iron in *Mycobacterium smegmatis* biofilm formation: the exochelin siderophore is essential in limiting iron conditions for biofilm formation but not for planktonic growth," *Molecular Microbiology*, vol. 66, no. 2, pp. 468–483, 2007.

[19] M.-H. Lin, J.-C. Shu, H.-Y. Huang, and Y.-C. Cheng, "Involvement of iron in biofilm formation by *Staphylococcus aureus*," *PLoS ONE*, vol. 7, no. 3, article e34388, 2012.

[20] G. M. Patriquin, E. Banin, C. Gilmour, R. Tuchman, E. P. Greenberg, and K. Poole, "Influence of quorum sensing and iron on twitching motility and biofilm formation in *Pseudomonas*

aeruginosa," *Journal of Bacteriology*, vol. 190, no. 2, pp. 662–671, 2008.

[21] H. Hayrapetyan, R. Siezen, T. Abee, and M. Nierop Groot, "Comparative genomics of iron-transporting systems in *Bacillus cereus* strains and impact of iron sources on growth and biofilm formation," *Frontiers in Microbiology*, vol. 7, article 842, 2016.

[22] R.-Y. Park, M.-H. Choi, H.-Y. Sun, and S.-H. Shin, "Production of catechol-siderophore and utilization of transferrin-bound iron in *Bacillus cereus*," *Biological and Pharmaceutical Bulletin*, vol. 28, no. 6, pp. 1132–1135, 2005.

[23] B. L. Garner, J. E. L. Arceneaux, and B. R. Byers, "Temperature control of a 3,4-dihydroxybenzoate (protocatechuate)-based siderophore in Bacillus anthracis," *Current Microbiology*, vol. 49, no. 2, pp. 89–94, 2004.

[24] S. H. M. Rooijakkers, S. L. Rasmussen, S. M. McGillivray et al., "Human transferrin confers serum resistance against Bacillus anthracis," *Journal of Biological Chemistry*, vol. 285, no. 36, pp. 27609–27613, 2010.

[25] M. C. Callegan, D. C. Cochran, S. T. Kane et al., "Virulence factor profiles and antimicrobial susceptibilities of ocular *Bacillus* isolates," *Current Eye Research*, vol. 31, no. 9, pp. 693–702, 2006.

[26] E. Ghelardi, F. Celandroni, S. Salvetti, E. Fiscarelli, and S. Senesi, "*Bacillus thuringiensis* pulmonary infection: critical role for bacterial membrane-damaging toxins and host neutrophils," *Microbes and Infection*, vol. 9, no. 5, pp. 591–598, 2007.

[27] E. Peker, E. Cagan, M. Dogan, A. Kilic, H. Caksen, and O. Yesilmen, "Periorbital cellulitis caused by *Bacillus thuringiensis*," *European Journal of Ophthalmology*, vol. 20, no. 1, pp. 243–245, 2010.

[28] American Type Culture Collection, http://www.atcc.org.

[29] M. K. Wilson, R. J. Abergel, J. E. L. Arceneaux, K. N. Raymond, and B. R. Byers, "Temporal production of the two *Bacillus anthracis* siderophores, petrobactin and bacillibactin," *BioMetals*, vol. 23, no. 1, pp. 129–134, 2010.

[30] K. M. Williams, W. E. Martin, J. Smith, B. S. Williams, and B. L. Garner, "Production of protocatechuic acid in *Bacillus thuringiensis* ATCC33679," *International Journal of Molecular Sciences*, vol. 13, no. 3, pp. 3765–3772, 2012.

[31] K. García, J. E. Ibarra, A. Bravo et al., "Variability of *Bacillus thuringiensis* strains by ERIC-PCR and biofilm formation," *Current Microbiology*, vol. 70, no. 1, pp. 10–18, 2014.

[32] A. Morgenthau, A. Pogoutse, P. Adamiak, T. F. Moraes, and A. B. Schryvers, "Bacterial receptors for host transferrin and lactoferrin: molecular mechanisms and role in host-microbe interactions," *Future Microbiology*, vol. 8, no. 12, pp. 1575–1585, 2013.

[33] T. M. Koehler, "*Bacillus anthracis* genetics and virulence gene regulation," *Current Topics in Microbiology and Immunology*, vol. 271, pp. 143–164, 2002.

[34] T. J. Lysyk and L. B. Selinger, "Effects of temperature on mortality of larval stable fly (Diptera: Muscidae) caused by five isolates of *Bacillus thuringiensis*," *Journal of Economic Entomology*, vol. 105, no. 2, pp. 732–737, 2012.

Hindawi Publishing Corporation
BioMed Research International
Volume 2016, Article ID 7616471, 14 pages
http://dx.doi.org/10.1155/2016/7616471

Research Article

Enhanced Performance and Mode of Action of a Novel Antibiofilm Hydrofiber® Wound Dressing

David Parsons,[1] Kate Meredith,[2] Victoria J. Rowlands,[2] Darryl Short,[3] Daniel G. Metcalf,[1] and Philip G. Bowler[1]

[1]*Science & Technology, ConvaTec GDC, First Avenue, Deeside Industrial Park, Flintshire CH5 2NU, UK*
[2]*Microbiology Services, Research & Development, ConvaTec GDC, First Avenue, Deeside Industrial Park, Flintshire CH5 2NU, UK*
[3]*Analytical Services, Research & Development, ConvaTec GDC, First Avenue, Deeside Industrial Park, Flintshire CH5 2NU, UK*

Correspondence should be addressed to Daniel G. Metcalf; daniel.metcalf@convatec.com

Received 15 July 2016; Revised 9 October 2016; Accepted 12 October 2016

Academic Editor: P. Nithyanand

Copyright © 2016 David Parsons et al. This is an open access article distributed under the Creative Commons Attribution License, which permits unrestricted use, distribution, and reproduction in any medium, provided the original work is properly cited.

Biofilm development in wounds is now acknowledged to be a precursor to infection and a cause of delayed healing. A next-generation antibiofilm carboxymethylcellulose silver-containing wound dressing (NGAD) has been developed to disrupt and kill biofilm microorganisms. This *in vitro* study aimed to compare its effectiveness against various existing wound dressings and examine its mode of action. A number of biofilm models of increasing complexity were used to culture biofilms of wound-relevant pathogens, before exposure to test dressings. Confocal microscopy, staining, and imaging of biofilm constituents, total viable counting, and elemental analysis were conducted to assess dressing antibiofilm performance. Live/dead staining and viable counting of biofilms demonstrated that the NGAD was more effective at killing biofilm bacteria than two other standard silver dressings. Staining of biofilm polysaccharides showed that the NGAD was also more effective at reducing this protective biofilm component than standard silver dressings, and image analyses confirmed the superior biofilm killing and removal performance of the NGAD. The biofilm-disruptive and silver-enhancing modes of action of the NGAD were supported by significant differences ($p < 0.05$) in biofilm elemental markers and silver donation. This *in vitro* study improves our understanding of how antibiofilm dressing technology can be effective against the challenge of biofilm.

1. Introduction

Antibiotics and topical antiseptics are commonly used in wound care to control wound microbial bioburden and hence facilitate healing. In order for any antibiotic or antiseptic to be effective, it needs to directly contact the microbial cell in order to induce static or "cidal" effects. However, local factors within a wound environment often impede the effectiveness of such antimicrobial agents. If a wound is poorly perfused and is harbouring antibiotic-resistant microorganisms, then the effectiveness of a systemically administered antibiotic is likely to be uncertain [1]. If an antiseptic is delivered via a wound dressing, then the dressing must be able to make the antiseptic available to microbial cells; otherwise its effectiveness will be suboptimal [2]. The variability in the availability of silver from a variety of wound dressings has previously been demonstrated *in vitro* [2].

Another potential barrier to both antiseptics and antibiotics in wounds is biofilm. Biofilm is a self-expressed extracellular matrix produced by microorganisms that protects them from environmental hostilities such as antimicrobial agents and immune cells [3]. The prevalence of biofilm in nonhealing wounds is increasingly recognised [4, 5], and the persistence and recurrence of infections are most likely attributed to the biofilm effect and consequent tolerance to antimicrobial agents [6]. With this in mind, there is a clear clinical need to facilitate antimicrobial effectiveness (both antibiotics and antiseptics) by introducing antibiofilm substances that are able to break down biofilm in wounds and expose associated microorganisms to antimicrobial attack.

A next-generation antimicrobial Hydrofiber dressing (NGAD; AQUACEL® Ag+ Extra™) has recently been developed and was designed to disperse wound biofilm and

enhance the antimicrobial action of ionic silver [7]. In this study, *in vitro* biofilm models and microscopic, microbiological, and analytical chemistry methods were developed to examine the effectiveness of the NGAD at killing biofilm-associated bacteria, including antibiotic-resistant bacteria, and its ability to remove dispersed biofilm compared to standard antimicrobial dressings. Further, this work also aimed to investigate the mode of action of the NGAD and the ability of this antibiofilm dressing to disrupt biofilm and enhance silver penetration into biofilm.

2. Materials and Methods

2.1. Biofilm Preparation. Individual strains of challenge microorganisms (Table 1) were grown to log-phase in Tryptone Soy Broth (TSB) and then diluted with the appropriate biofilm growth medium (BGM, Table 1) to approximately 1×10^5 cfu/mL. 7 mL aliquots of BGM were dispensed into each well of deep 6-well plates (BD Biosciences). Anodisc filters (25 mm dia., 0.2 μm pore size; Whatman) were carefully placed onto the support ribs within each well such that the BGM was only in contact with the downward-facing surface. Aliquots of microbial suspensions (0.1 mL aliquots of 1×10^5 cfu/mL suspension for single-species models; 45 μL of *S. aureus* and 5 μL of *K. pneumoniae* 1×10^5 cfu/mL suspensions for the polymicrobial model, Table 1) were pipetted onto the centre of the upper surface of each filter disc. The plate lid was replaced and the plate incubated at 35 ± 3°C. After 24 hours (Figure 1(a)) filter discs were removed and rinsed by moving the filter backwards and forwards 10 times with forceps in 30 mL of 0.85% w/v saline to remove planktonic microorganisms and unattached matter. The filter disc-supported biofilms were then used immediately in either a simple biofilm model or a simulated wound polymicrobial biofilm model, to test various dressings and analyse their effects using multiple methodologies (Table 1).

2.2. Dressing Applications. Dressings tested are described in Table 2. Note that for analysis of K^+, Mg^{2+}, Ca^{2+}, and Zn^{2+} ions in residual biofilm it was only possible to reliably test the CMC-containing dressings, which have a proprietary elemental composition known to the authors. The K^+, Mg^{2+}, Ca^{2+}, and Zn^{2+} contents of the NCSC and SNAD dressings are unknown.

2.3. Simple Biofilm Model. Filter disc-supported biofilms were placed biofilm uppermost into individual 55 mm Petri dishes. 24 mm diameter circles of the test dressings were applied (Figure 1(b)) as stated in the respective manufacturer's instructions for use, hydrating with sterile water or saline as indicated (e.g., for CMC, SCMC, and the NGAD, this was 0.7 mL aliquots of sterile saline). Dressings were left in contact with the biofilm for 24 or 48 hours (Table 1) at 35±3°C in the closed Petri dishes, following which the dressings were gently removed by gripping one edge with forceps and rolling back the dressing. The exposed residual biofilm-containing filter disc was analysed immediately. A minimum of six replicates were performed for each test dressing and no-dressing control.

2.4. Simulated Wound Polymicrobial Biofilm Model. In a more complex model, simulated wound set-ups were created by covering Perspex plates with bovine leather (simulating periwound skin) and cutting out a circular hole into which a 55 mm Tryptone Soy Agar (TSA) contact plate (simulating a moist wound bed containing a reservoir of isotonic nutrients) could be tightly fitted [7, 9]. 24-hour, filter disc-supported, *S. aureus-K. pneumoniae* biofilms were centrally placed on the plate, biofilm uppermost (Figure 2(a)). Test dressings were applied and hydrated with the relevant amount of simulated wound fluid (50% foetal calf serum and 50% maximal recovery diluent) using manufacturer's instructions as a guide (Figure 2(b)). The hydrated test dressing was then covered with an appropriate secondary dressing (AQUACEL Foam dressing) (Figure 2(c)). The assembled test models were incubated for 48 hours at 35 ± 3°C before the dressings were removed as in the simple biofilm model (Figure 2(d)).

2.5. Biofilm Analyses

2.5.1. Staining. A staining procedure was undertaken to determine the viability of biofilm bacteria prior to and after exposure to the test dressings. Using both the simple biofilm and the simulated wound polymicrobial biofilm models, biofilm controls (at the start and end of each experiment) and residual biofilm samples (after dressing removal) were exposed to *Live/Dead® BacLight* stain (Molecular Probes, Invitrogen) for 10 minutes at room temperature in darkness prior to analysis. Calcofluor White (Fluka® Analytical) staining at room temperature in darkness was used to establish the effect of the dressings on the biofilm extracellular polymeric substances (EPS). In the case of the simulated wound polymicrobial biofilm model, peptide nucleic acid fluorescence *in situ* hybridisation (PNA FISH, AdvanDx Inc.) was used to differentiate the two organisms (*S. aureus* and *K. pneumoniae*) using fluorescent labels to enable visualisation of the polymicrobial biofilm population. PNA FISH was conducted according to the manufacturer's instructions, with the exception of a 90-minute hybridisation step at 55 ± 1°C, and omission of a water rinse step. Stained samples were examined immediately using confocal laser scanning microscopy (CLSM; Leica TCS SP2, Leica Microsystems) and images were captured for later analysis.

2.5.2. Image Analysis. Image analysis was undertaken to determine the viability of bacteria throughout the depth of each biofilm of antibiotic-resistant *P. aeruginosa* from the simple biofilm model after exposure to silver dressings. The CLSM uses a highly focused laser beam to illuminate the test sample at right-angles to the direction of observation. The width of the beam is very narrow and its position (distance from the observer) can be closely controlled; therefore thin layers at different depths within the sample can be observed sequentially. By using selective stains which have specific emission wavelengths (colours) and coloured filters,

Table 1: Testing matrix.

Challenge microorganism	Biofilm growth medium (BGM)	Model	Test methodology	Dressings tested (Table 2)
Antibiotic-resistant *Pseudomonas aeruginosa* NCTC 13437 Community-acquired Methicillin-resistant *Staphylococcus aureus* (CA-MRSA) USA300 *Candida albicans* NCPF 3179	Foetal calf serum (FCS)	Simple biofilm model	Elemental analysis (K^+, Mg^{2+}, Ca^{2+}, Zn^{2+}, Ag^+) of residual biofilm after dressing being applied for 24 hours (a simple and chemically consistent model to investigate formulation effects) ($n = 6$)	CMC SCMC NGAD
Antibiotic-resistant *P. aeruginosa* NCTC 8506			Elemental analysis (Ag^+) and quantitative live/dead staining after dressing being applied for 48 hours (a more challenging strain and longer dressing exposure time selected to challenge the silver-containing dressings) ($n = 9$)	NGAD NCSD SNAD
S. aureus (clinical wound isolate, CI72) and *Klebsiella pneumoniae* (clinical isolate, CI45)	TSB : FCS (50 : 50)	Simulated wound polymicrobial biofilm model	Quantitative microbiology (total viable counts), PNA FISH, live/dead and Calcofluor White staining after dressing application for 48 hours (a more complex inoculum and longer dressing exposure time selected to challenge the silver dressings) ($n = 5$)	NGAD NCSD SNAD

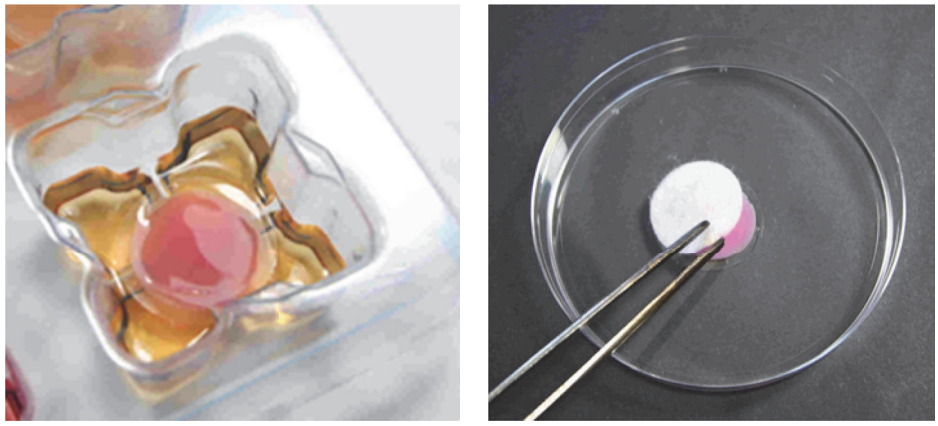

(a) (b)

Figure 1: (a) 24-hour *S. aureus* biofilm supported on a 25 mm filter disc in contact with BGM in a deep 6-well plate (biofilm is stained pink for clarity). (b) Test dressing application to biofilm (biofilm is stained pink for clarity).

individual components of the sample can be differentiated. Images (each approximately 100 × 100 μm in area) were captured at intervals of 0.5 μm vertically apart throughout the full thickness (depth) of the residual biofilm, down to the supporting filter. Qualitative and semiquantitative data were obtained by recombining each series of layers to provide a three-dimension reconstruction of the sample using *Image-Pro Premier* 3D software. Quantitative image analysis was performed on live/dead stain images of a selected range of dressings using *Image-Pro Plus*® version 7.0 software. For each image the number of objects (cells) of area greater than 10 pixels (determined by observation to be the approximate minimum size of an individual bacterium) was counted for the green (live) and red (dead) coloured series. A minimum threshold of 10 counted items per layer was set as the criteria for the confirmed presence of biofilm and to be valid for use in any further calculation. Objects that were much greater in area than bacterial cells and were clearly not of bacterial origin were excluded. Three separately treated biofilms were analysed for each of the selected dressings, observing each

Table 2: Test dressings. †Formulation proprietary to ConvaTec Ltd.

Commercial name	Physical and chemical composition	Coding
AQUACEL Extra	Two layers of a needle-punched nonwoven fleece of sodium carboxymethylcellulose (CMC) fibres	CMC
AQUACEL Ag Extra	Two layers of a needle-punched nonwoven fleece of sodium silver CMC fibres (approximately 1.2% w/w or 0.17 mg/cm^2 silver) [2]	SCMC
AQUACEL Ag+ Extra	Two layers of a needle-punched nonwoven fleece of sodium silver CMC fibres enhanced with disodium ethylenediaminetetraacetate and benzethonium chloride†, stitched with a high purity cellulose thread (approximately 1.2% w/w or 0.17 mg/cm^2 silver)	NGAD
Acticoat™ 7	Three layers of a metallic (nano) crystalline silver-encrusted high-density polyethylene (HDPE) mesh alternating with two layers of a rayon polyester nonwoven fabric, bonded at intervals by ultrasonic welding of the HDPE (approximately 8.4% w/w or 1.48 mg/cm^2 silver)	NCSD
Silvercel™ Non-Adherent	A nonwoven fabric comprised of a blend of metallic silver-coated nylon fibres and calcium alginate/CMC fibres between two apertured sheets of ethylene methyl acrylate (EMA) (approximately 4% w/w or 1.11 mg/cm^2 silver [8])	SNAD

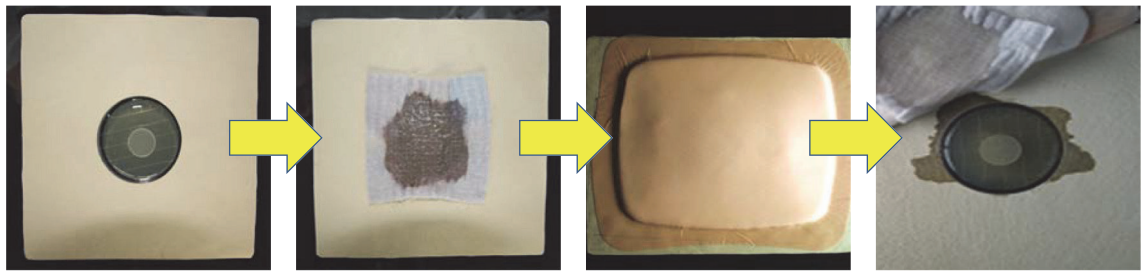

(a) TSA contact plate inserted into centre of model; biofilm-colonised filter applied to create simulated biofilm-colonised wound bed

(b) Application of dressing onto the simulated biofilm-colonised wound bed; hydrated with simulated wound fluid

(c) Addition of secondary dressing

(d) Removal of dressings

Figure 2: Simulated wound polymicrobial biofilm model with the NGAD and AQUACEL Foam secondary dressing application within the wound assembly.

biofilm at multiple sites across the sample. The only exclusion criteria were if image quality was inadequate (i.e., poor focus or interfering image artifact) or if there was an incomplete data set (i.e., no upper and/or lower boundary of the biofilm could be identified).

2.5.3. Quantitative Microbiology. In the case of the simulated wound polymicrobial biofilm model, total viable counts were performed in triplicate on the polymicrobial biofilms to allow comparison with PNA FISH microscopy data.

2.5.4. Elemental Analysis. After 24 or 48 hours of incubation with the test dressings, the filter disc-supported single-species biofilms were placed separately into individual plastic sample tubes containing 10 mL of 1.2 M aqueous hydrochloric acid. Tubes were agitated for 10 minutes or until all of the residual biofilm had visibly dissolved. The resultant solutions were filtered through 0.45 μm membrane filters (Whatman) to remove any bacteria or dressing fibres and then assayed for solubilized potassium (K^+), magnesium (Mg^{2+}), calcium (Ca^{2+}), zinc (Zn^{2+}), and silver (Ag^+) ions by inductively coupled plasma mass spectrometry (ICP-MS, Agilent Technologies 7700 Series).

2.5.5. Statistical Analysis. Student's 2-sample t-tests and one-way analysis of variance (ANOVA) (Minitab® software) were performed, where possible, to determine any statistically significant differences ($p < 0.05$) between dressing performances.

3. Results

3.1. Biofilm Models. Table 3 illustrates the reproducibility of the various biofilm models used in this *in vitro* study. Irrespective of the model, bacterial strain, duration, analytical method, or sample size, the relatively low standard deviation of the data from different biofilm characteristics indicates good reproducibility.

3.2. Dressing Effectiveness. Live/Dead BacLight selectively stains bacteria (viable cells appear green whereas nonviable (dead) cells appear red). Confocal images demonstrated that all three silver test dressings significantly reduced polymicrobial biofilm thickness (μm) compared to the control (initial biofilm $T_{24\,\text{hours}}$) ($p = 0.000$ for all dressings) (Table 4). Following ANOVA, simultaneous confidence interval comparisons demonstrated that there were statistically significant

Table 3: Reproducibility of the biofilm models utilised, as analysed by different analytical, imaging, and microbiological assays.

Model	Strain	Analysis method	n	Average	Std Dev
Simple biofilm model	Antibiotic-resistant *P. aeruginosa* NCTC 8506	Elemental analysis (values minus blank filter disc elemental analysis)	24	26.8 μM Mg^{2+}	3.2 μM
				36.2 μM K^{+}	7.1 μM
				171.9 μM Ca^{2+}	27.0 μM
	Antibiotic-resistant *P. aeruginosa* NCTC 13437	Live/dead image analysis by pixilation	19	25.6 μm thick	8.2 μm
Simulated wound polymicrobial biofilm model	*S. aureus*, *K. pneumoniae*, 24-hour control	Confocal imaging of maximum depth	15	9.74 μm thick	2.37 μm
		Total viable counts	3	9.4×10^8 cfu *S. aureus*	2.0×10^8 cfu
				7.7×10^9 cfu *K. pneumoniae*	3.2×10^9 cfu

Table 4: Depths (μm) of polymicrobial biofilm (as indicated by the presence of bacterial cells) after exposure to silver dressings for 48 hours. Dressings were tested in triplicate and five images were captured for each dressing ($n = 15$). $^{*}p < 0.000$ compared to initial biofilm. $^{\dagger}p < 0.000$ compared to NCSD and SNAD.

Sample	Maximum depth (μm) [mean ± standard deviation]
Initial biofilm $T_{24\,\text{hours}}$	9.75 ± 2.37
NCSD	$6.22 \pm 5.93^{*}$
SNAD	$4.77 \pm 1.91^{*}$
NGAD	$1.99 \pm 1.22^{*\dagger}$

differences between silver dressings. The NGAD resulted in significantly thinner residual biofilms than NCSD and SNAD ($p = 0.000$ in both instances), while there was no significant difference in biofilm thickness reduction between NCSD and SNAD exposure ($p = 0.065$). Confocal images also illustrate these differences in biofilm thickness (Figures 3(b)–3(d)) and that there were consistently more dead cells under the NGAD (Figure 3(d)) and less cells overall, compared to the other two dressings (Figures 3(b) and 3(c)). Following dressing application, the volume of green Syto®9 stain (indicative of remaining viable biofilm bacteria) was 7.8% beneath the NGAD, compared to 51.5% under NCSD and 44.1% under SNAD, for the images shown in Figures 3(b)–3(d).

3.2.1. Extracellular Polymeric Substance (EPS) Staining. Calcofluor White stains the β-1,2 and β-1,3 polysaccharides present in the biofilm EPS [10]. The NGAD was the only dressing that was able to significantly reduce biofilm mass compared to the control biofilm ($p = 0.000$) (Figure 4) as indicated by this staining method. Neither NCSD (Figure 5(b)) nor SNAD (Figure 5(c)) dressings resulted in any bulk EPS reduction compared to the control biofilm (Figure 5(a)), while bulk EPS reduction by the NGAD was evident (Figure 5(d)).

3.2.2. Total Viable Counts. Total viable counts of *S. aureus* and *K. pneumoniae* biofilm cells after 48 hours of exposure to the silver test dressings are shown in Figure 6. Initial biofilms were predominantly comprised of *K. pneumoniae* cells despite its lower starting inoculum (see Materials and Methods), which may be attributable to the avid biofilm-forming capacity of this nosocomial pathogen [11]. In all instances, *K. pneumoniae* biofilm cells were more difficult to kill. Student's 2-sample t-tests showed that each silver dressing reduced viable biofilm cells of both species compared to the no-dressing control (NCSD: $p = 0.017$; SNAD: $p = 0.015$; NGAD: $p = 0.000$). Following ANOVA, simultaneous confidence interval comparisons demonstrated that there were statistically significant differences between silver dressings. The NGAD was significantly more effective than NCSD and SNAD at killing *S. aureus* biofilm cells ($p = 0.000$). The NGAD was also more effective than NCSD and SNAD at killing *K. pneumoniae* biofilm cells ($p = 0.000$). SNAD was significantly more effective than NCSD at killing *S. aureus* biofilm cells ($p = 0.027$), but there were no significant differences between the effects of NCSD and SNAD on *K. pneumoniae* biofilm cells ($p = 0.098$).

3.2.3. PNA FISH. The confocal PNA FISH images in Figure 7 generally correlate with the total viable count data (Figure 6). The representative images of the biofilms exposed to NCSD (Figure 7(b)) and SNAD (Figure 7(c)) showed a high frequency of both green and yellow objects, indicating high concentrations of *S. aureus* and *K. pneumoniae* cells, respectively. In contrast, the image for the NGAD shows fewer yellow objects, representative of the significantly lower *K. pneumoniae* counts, and feint green areas which are likely to be cell debris rather than viable *S. aureus* cells (Figure 7(d)). The individual yellow objects appear brighter because the amount of stain added to each sample was constant; therefore a greater amount of stain was available per cell present in the NGAD treated sample.

3.2.4. Image Analysis. Live/Dead BacLight staining enables differentiation of live cells (green), mixed live and dead or dying cells (yellow/orange), and dead cells (red) in composite images as shown in Figure 8. These images are examples of sections found midway through the thickness of each sample. The control was predominantly living cells but there was some death due to natural turnover. As a general observation the

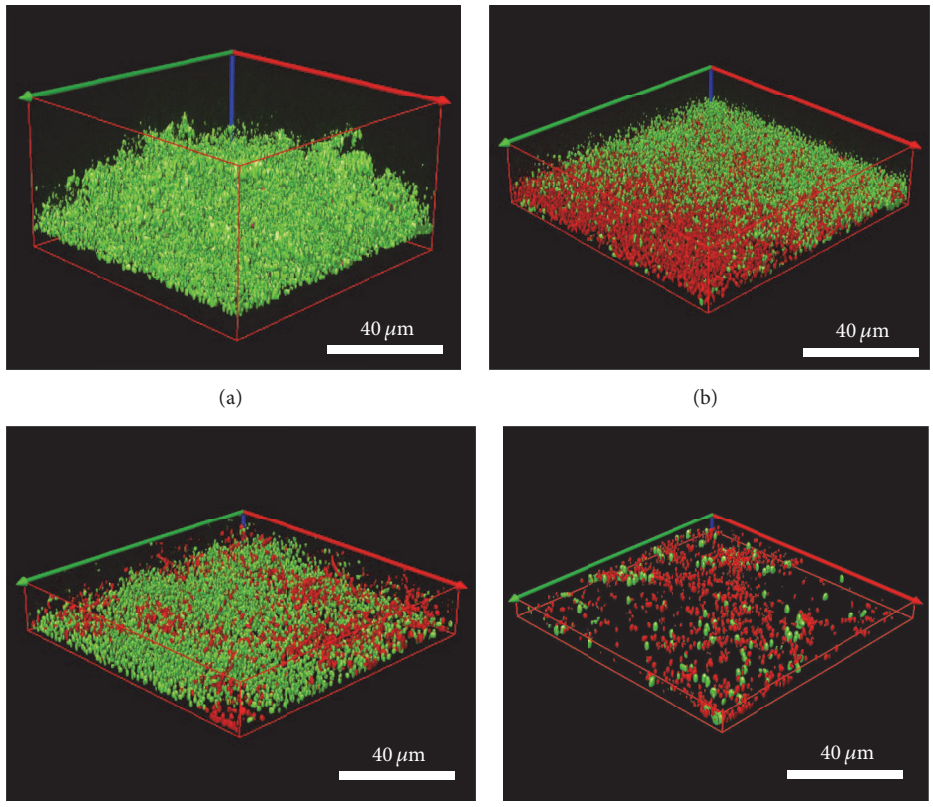

Figure 3: Representative isosurface 3D imaging, performed using the *Image-Pro Premier*® 3D software of the CLSM images biofilms stained with *BacLight*® (green = viable bacteria; red = nonviable bacteria). (a) Initial biofilm $T_{24\,\text{hours}}$. (b) NCSD after 48 hours of exposure. (c) SNAD after 48 hours of exposure. (d) NGAD after 48 hours of exposure.

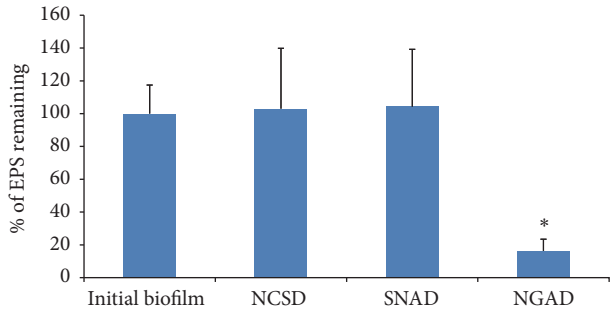

Figure 4: Percentage of EPS still remaining after exposure to the silver test dressings for 48 hours. $^{*}p = 0.000$.

apparent order of *in vitro* antimicrobial effectiveness of the dressings was NGAD > NCSD > SNAD.

However, as predicted in the 3D reconstructions in Figure 3, there were different and distinctive changes in the green-to-red ratio through the thickness of the biofilm. Figure 9 is a colour-coded representation of how this ratio changes for the different silver dressings tested. The scale extends from green (where there were more than two green cells for every red cell) through yellow (where there were approximately two red cells for every green cell) to red (where there were at least four red cells for every green cell). Control biofilms were observed to be of varying thickness (between 10 and 48 μm as indicated by the presence of stained cells) and predominantly viable (Figure 9(a)). Although NCSD showed a wide zone of bactericidal action at the point where the dressing contacted the biofilm, the thickness of the residual biofilm appeared unchanged and there was a biofilm survival zone approximately 10 μm thick at the filter surface (Figure 9(b)). This indicates the inability of ionic silver alone to kill bacteria in deeper parts of the biofilm and may explain the recurrent nature of biofilm infections, as has also been observed with antibiotics [12]. Biofilm exposed to SNAD appeared to be of reduced thickness with zones of death near the filter surface, but there were areas of viable biofilm cells nearer the upper surface that would have been in contact with the dressing (Figure 9(c)). Many of the viewed sites for the NGAD appeared to have no residual biofilm (data not shown in Figure 9(d)), but where biofilm could be observed it was of much reduced thickness and was less integral in that it contained voids (regions in the depth of the sample that contained no cells), and in regions that did contain cells these were largely devoid of green cells (surviving bacteria) (Figure 9(d)). Green objects were observed in a few samples relatively close to the filter surface but this was

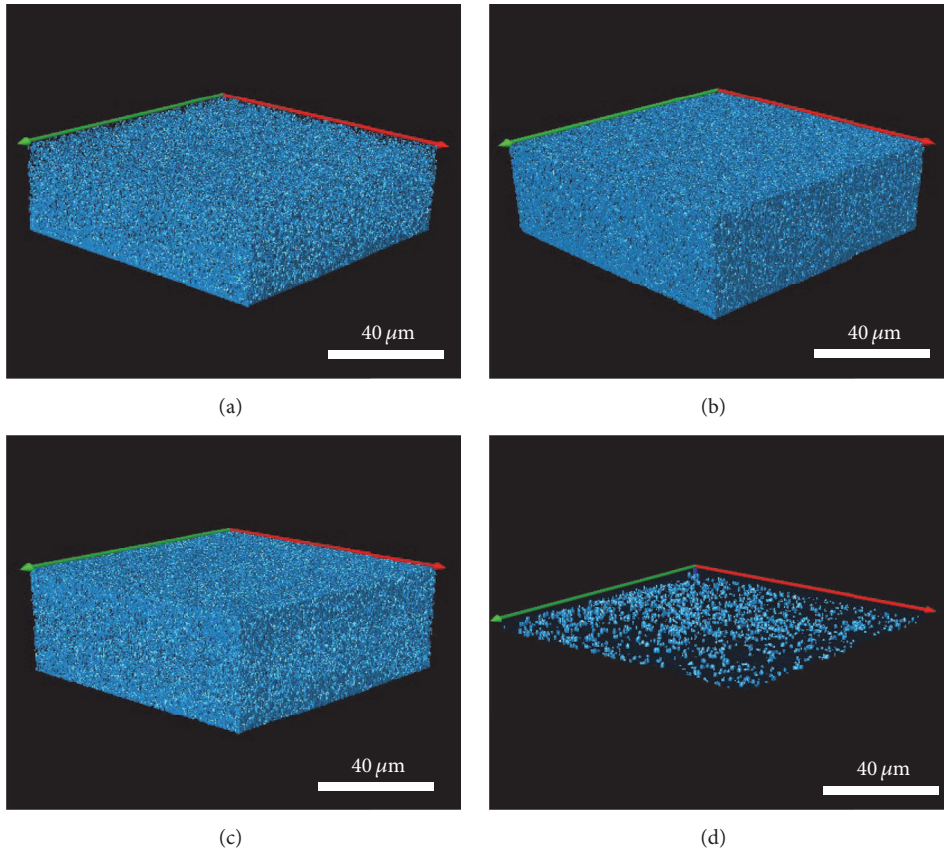

Figure 5: Representative isosurface 3D imaging, performed using the *Image-Pro Premier* 3D software, of the CLSM images biofilm EPS stained with Calcofluor White. (a) Initial biofilm $T_{24\,\text{hours}}$. (b) NCSD after 48 hours of exposure. (c) SNAD after 48 hours of exposure. (d) NGAD after 48 hours of exposure.

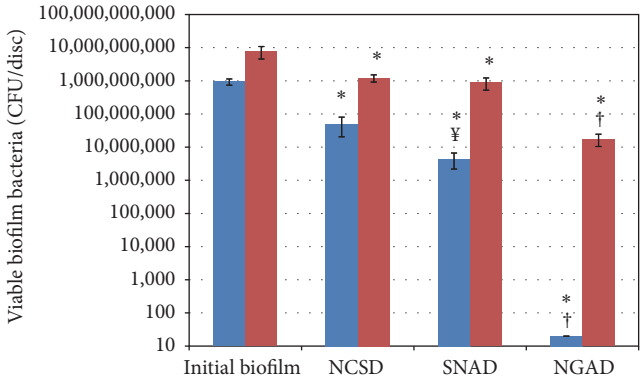

Figure 6: Total viable counts of (blue colour) *S. aureus* and (red colour) *K. pneumoniae* biofilm cells after 48 hours of exposure to silver dressings ($n = 5$). Initial biofilm = $T_{24\,\text{hours}}$. $^{*}p < 0.05$ compared to initial biofilm. $^{\dagger}p = 0.000$ compared to NCSD and SNAD. $^{¥}p = 0.027$ compared to NCSD.

the area in which image artefacts were most prevalent (e.g., deformations in the filter surface causing reflection).

3.2.5. Elemental Composition of Biofilms. Divalent metal cations such as magnesium (Mg^{2+}), calcium (Ca^{2+}), and zinc (Zn^{2+}) play an important role in the formation, adhesion, and cohesion of biofilm [13, 14] and are tightly bound into its structure. Therefore, measuring the sum of these divalent ions will give an indication of the relative amount and strength of biofilm and of the effect of the test dressings on biofilm disruption. Small monovalent cations such as sodium (Na^{+}) and potassium (K^{+}) are constant components in isotonic fluids and are not tightly bound to either biofilm, tissue, or dressings, so they can be used as an approximate measure of total mass present. The NGAD contains Na^{+} and SNAD contains Na^{+} and Ca^{2+} while NCSD contains neither; therefore comparison by following these ions was not possible. However, the elemental composition of CMC, SCMC, and the NGAD is very similar as they are all based on the same fibre; therefore these can be directly compared. Because Na^{+} was present in both biofilm and the test dressings, this could not be used to differentiate between residual biofilm and residual dressing; however K^{+} and divalent cations are absent from CMC, SCMC, the NGAD, and the filter disc; therefore any present would be indicative of biofilm only. The amount of silver (Ag^{+}) detected and ratio to K^{+} and/or the total divalent metals ($Metal^{2+}$ = the sum of Mg^{2+}, Ca^{2+}, and Zn^{2+}) will be indicative of the effectiveness of antimicrobial action. The low concentration of these metal ions required the use of a trace elemental technique such as ICP-MS.

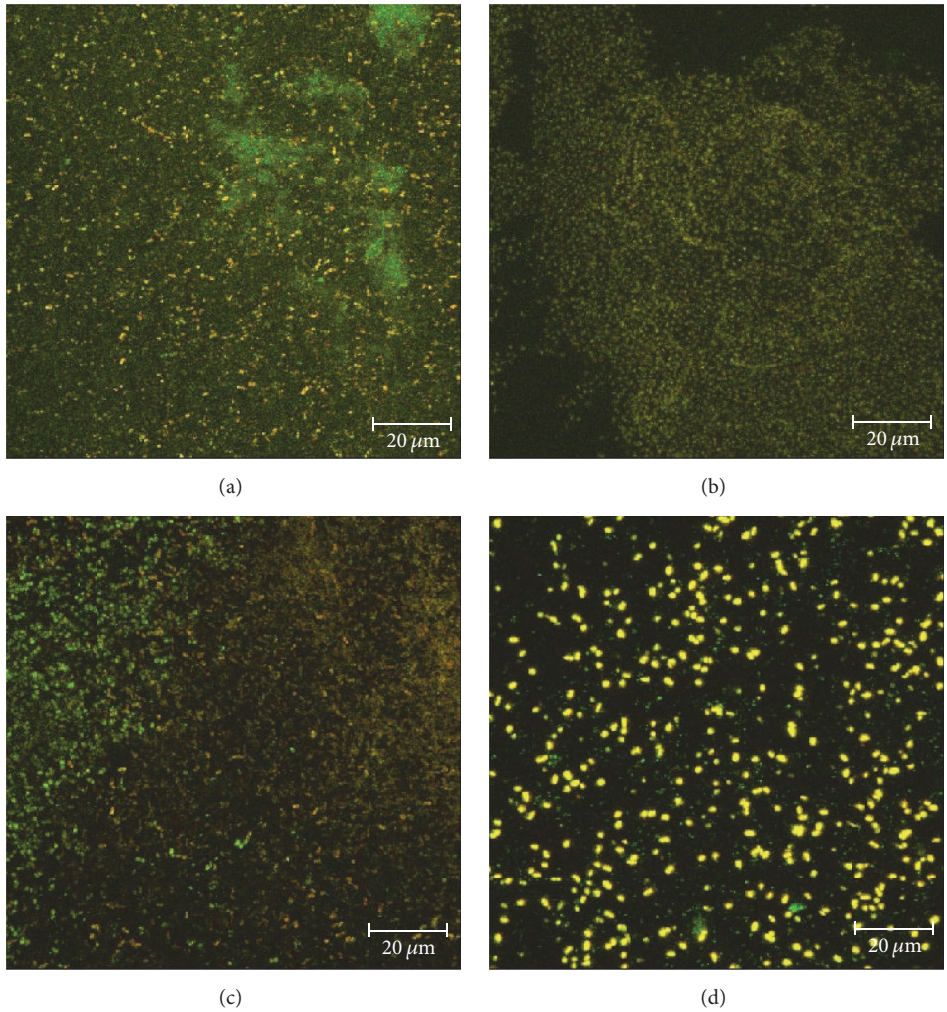

Figure 7: Representative CLSM images of polymicrobial biofilm where bacteria have been fluorescently tagged (green = *S. aureus*; yellow = *K. pneumoniae*). (a) Initial biofilm $T_{24\,\text{hours}}$; (b) NSCD after 48 hours; (c) SNAD after 48 hours; (d) NGAD after 48 hours.

3.2.6. Comparison of Carboxymethylcellulose-Based Fibre Dressings. The entire biofilm remaining on the filter disc after 24 hours of contact with hydrated dressings was analysed using a standardised sample preparation method. The comparative amount of each analyte determined is shown in Table 5. The absolute amount of K^+ and $Metal^{2+}$ in the biofilm control and the amount of Ag^+ in SCMC are designated as 100%.

With the exception of K^+ for *C. albicans* biofilm, the trends in assays of K^+ and $Metal^{2+}$ were in general agreement showing that the base CMC dressing had the ability to significantly reduce biofilm mass in each biofilm type ($p < 0.05$; mean relative reduction across the biofilm types compared to the no-dressing control of 67% and 69% for K^+ and $Metal^{2+}$, resp.). A similar biofilm mass reduction was also observed for SCMC (average for all types of biofilm of 75% (K^+) and 68% ($Metal^{2+}$)) with a statistically significant increased reduction in CA-MRSA biofilm for SCMC compared to CMC. The NGAD formulation further increased the mean reduction in K^+ and $Metal^{2+}$ (to 82% and 76%, resp.), with the NGAD being significantly more effective than SCMC at reducing both biofilm markers in *P. aeruginosa* biofilm (K^+ $p = 0.035$; $Metal^{2+}$ $p = 0.014$) and $Metal^{2+}$ in *C. albicans* biofilm ($p = 0.010$).

The NGAD dressing induced a statistically significant greater silver uptake in all biofilm types compared to the SCMC dressing (which contained the same amount, type, and form of silver), on average 134% more. Although the *C. albicans* biofilm appeared to be the most difficult biofilm to manage, being reduced in mass the least (~70% by the NGAD), the amount of silver within the residual biofilm was approximately 42% higher for the NGAD compared to the SCMC dressing ($p = 0.014$). For the *P. aeruginosa* biofilm the silver content was 81% higher after management with the NGAD than SCMC ($p = 0.006$) and the CA-MRSA biofilm seemed the most susceptible to the effects of the NGAD with approximately three times more silver (278%; $p = 0.000$) than SCMC.

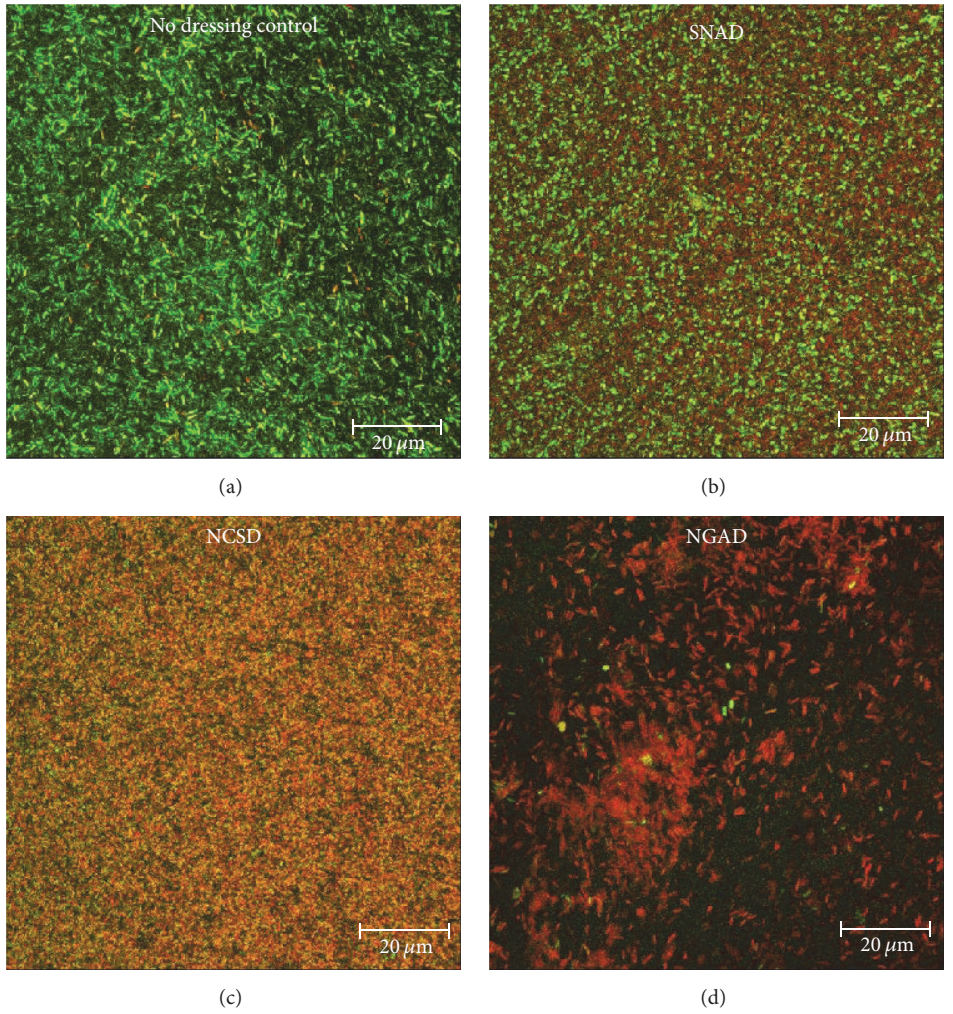

Figure 8: Composite (full thickness) images of antibiotic-resistant *P. aeruginosa* biofilm stained with *BacLight* after 48 hours of contact with the test dressings (green = viable bacteria; red = nonviable bacteria). (a) No-dressing control. (b) SNAD. (c) NCSD. (d) NGAD.

Table 5: Metal assay results, average of $n = 6$. Statistical comparisons of NGAD to $^{*}p = 0.000$ compared to no-dressing control. $^{a}p = 0.018$ compared to no-dressing control. $^{b}p = 0.007$ compared to no-dressing control. $^{c}p = 0.016$ compared to CMC. $^{d}p = 0.035$ compared to SCMC. $^{e}p = 0.006$ compared to SCMC. $^{f}p = 0.001$ compared to CMC. $^{g}p = 0.014$ compared to SCMC. $^{h}p = 0.013$ compared to no-dressing control. $^{i}p = 0.009$ compared to no-dressing control. $^{j}p = 0.010$ compared to no-dressing control. $^{k}p = 0.027$ compared to CMC. $^{l}p = 0.004$ compared to CMC. $^{m}p = 0.038$ compared to CMC. $^{n}p = 0.000$ compared to SCMC. $^{o}p = 0.017$ compared to no-dressing control. $^{q}p = 0.015$ compared to no-dressing control. $^{r}p = 0.010$ compared to SCMC. $^{s}p = 0.014$ compared to SCMC.

Sample	*P. aeruginosa*			CA-MRSA			*C. albicans*		
	K^+	$Metal^{2+}$	Ag^+	K^+	$Metal^{2+}$	Ag^+	K^+	$Metal^{2+}$	Ag^+
No-dressing control	100%	100%	0%	100%	100%	1%	100%	100%	0%
CMC	32%[a]	36%[*]	0%	17%[h]	20%[*]	0%	50%	37%[*]	0%
SCMC	33%[a]	35%[*]	100%	9%[il]	17%[*]	100%	34%[o]	44%[*]	100%
NGAD	12%[bcd]	24%[*fg]	181%[e]	10%[jk]	15%[*m]	378%[n]	31%[q]	33%[*r]	142%[s]

3.2.7. Comparison of Different Forms of Silver-Containing Dressings. Due to compositional interferences it was not possible to chemically compare the effects of different silver-containing dressing types on the weakening and removal of biofilm mass. However, it was possible to directly compare the donation of silver into residual antibiotic-resistant *P. aeruginosa* biofilm after 48 hours of exposure to the test dressings. These same samples were also subjected to live/dead staining and image analysis which enabled biofilm thickness to be estimated based on the presence of bacterial cells in image

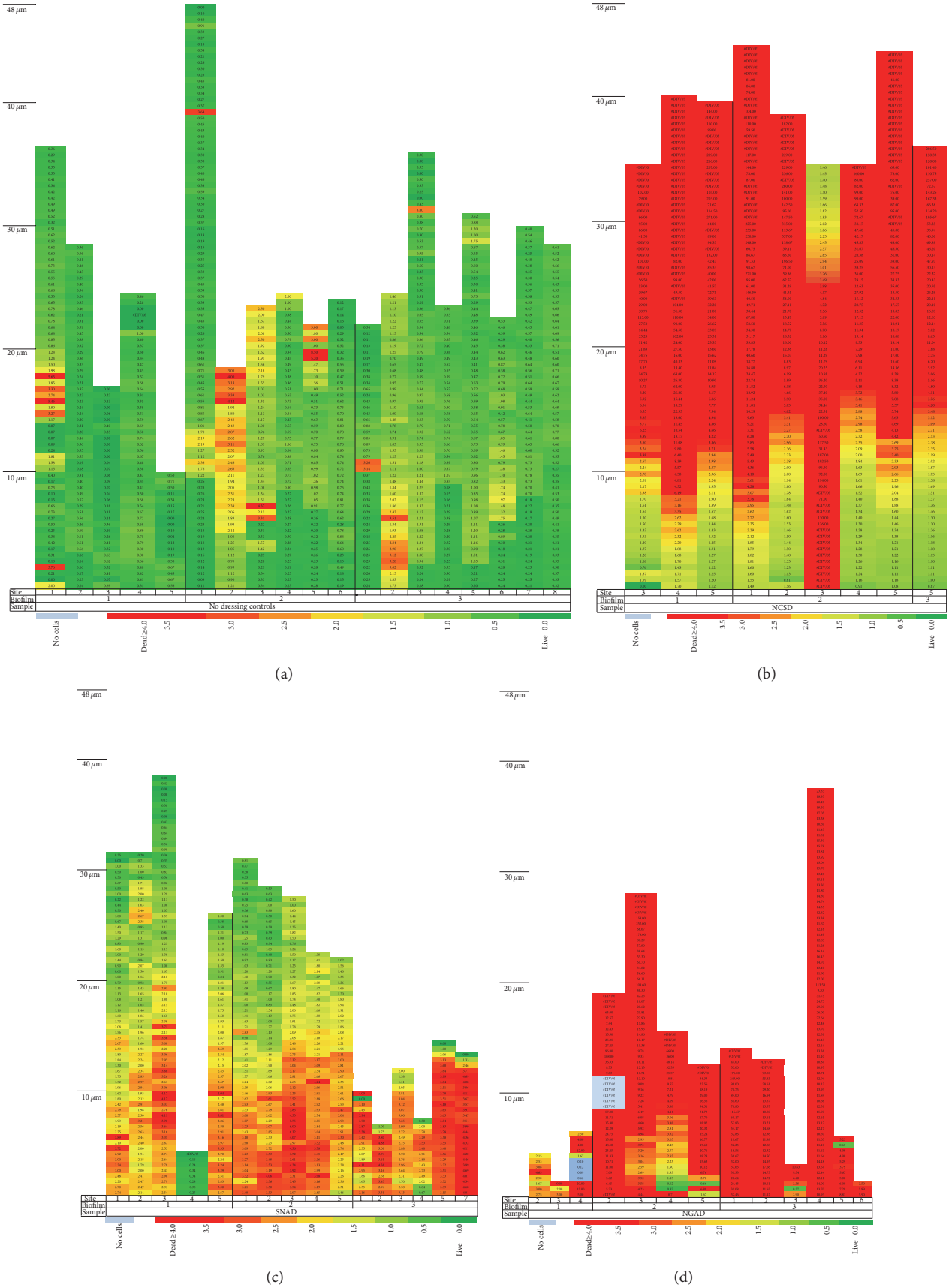

FIGURE 9: Colour-coded bacterial viability within biofilm layers as a function of distance from the filter surface for an antibiotic-resistant *P. aeruginosa* biofilm after 48 hours of contact with the test dressings (green = viable bacteria; red = nonviable bacteria). (a) No-dressing control. (b) NCSD. (c) SNAD. (d) NGAD.

Table 6: Biofilm thickness, amounts, and concentrations of silver in residual biofilm after 48 hours of dressing exposure and concentration of silver in the original applied dressings. $n = 6$ for silver assays and $n = 9$ or greater for mean biofilm thickness data. $^{*}p = 0.000$ compared to SCSD and SNAD. $^{\dagger}p = 0.009$ compared to SNAD.

	No dressing	NCSD	SNAD	NGAD
Mean biofilm thickness (μm)	25.6	37.8	20.0	12.1
Amount of silver in residual biofilm (μg)	0.0	14.1†	4.5	79.1*
Concentration of silver in residual biofilm (μg/μm)	0.0	0.4	0.2	6.5*
Concentration of silver in applied dressing (mg/cm^2)	0.0	1.48	1.11	0.17

stacks. Table 6 summarises this data as averages (statistical analysis has been performed for individual assays), and it also calculates the mass of silver per unit thickness of the residual biofilm, comparing this to the silver per unit area of dressing initially applied.

The residual biofilm after management with the NGAD contained 5-times the absolute amount of silver and more than 16-times the concentration of silver per unit biofilm thickness compared to that observed for NCSD managed biofilm ($p = 0.000$); this was despite the NGAD only containing approximately one-ninth of the silver in NCSD on a weight per dressing area basis. The residual biofilm managed with the NGAD contained 17-times the amount of silver ($p = 0.000$) and more than 30-times the concentration of silver per unit biofilm thickness compared to SNAD ($p = 0.000$), with the NGAD containing less than one-sixth of the amount of silver on a weight per area basis. Residual biofilm after management with NCSD contained significantly more silver than SNAD on an absolute amount basis ($p = 0.009$) but not on a concentration per thickness basis ($p = 0.063$).

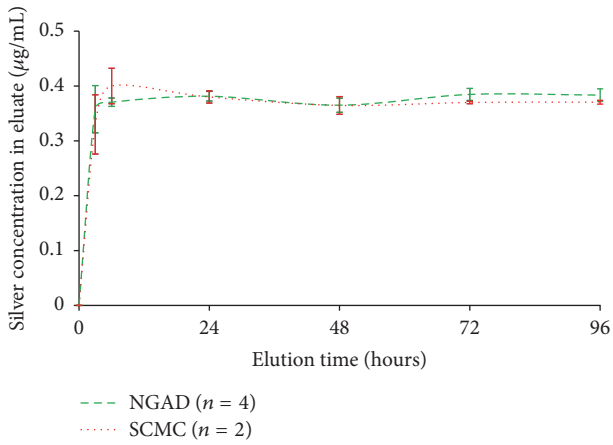

Figure 10: Comparison of elution of silver ions from the NGAD and SCMC into a constantly stirred excess of isotonic media (0.9% w/v $NaCl_{(aq)}$, 8 mL per cm^2 dressing at 37 ± 3°C) as determined by ICP-MS.

4. Discussion

Chronic wounds are invariably associated with poor healing and susceptibility to recurrent infections, and this is characteristic of a biofilm-induced chronic condition. Consequently, in order to minimise the opportunity for wound infection and encourage healing, there is a need to manage biofilm effectively. Uses of standard antibiotics and antiseptics are not necessarily the immediate solution because biofilm is notoriously tolerant to these antimicrobial agents [15]. Consequently new strategies are required to eliminate biofilm and expose associated microorganisms to make them more vulnerable to antimicrobial agents. While wound bed preparation, involving debridement and cleansing, is an ideal way to physically reduce bioburden and help expose microorganisms before dressing the wound [16, 17], it is unlikely to entirely eradicate biofilm and debridement methodologies and effective wound cleansers are not always available to all wound care practitioners in all settings. The most efficient way to provide longer-term antimicrobial action to a wound is therefore via antimicrobial dressings, and the recognition of biofilm as a key barrier to wound healing within the last decade [4, 5] has provided a new challenge to developers of therapeutic dressings.

The NGAD described in this *in vitro* study is a proprietary, highly innovative wound dressing designed to help the antimicrobial silver component work most effectively by disrupting the protective components of biofilm. Namely, this involved the careful selection of a synergistic combination of safe antibiofilm excipients [9], 0.39% disodium ethylenediaminetetraacetate (a metal chelator), 0.135% benzethonium chloride (a surfactant), and close pH control (5.0 to 6.0), to add to the formulation of a widely used silver Hydrofiber dressing (SCMC) [2]. The SCMC dressing was formulated prior to 2002, before the realisation of the significance of biofilm in wound care. Its purpose was to assist in the prevention and management of infection; therefore it was targeted at planktonic bacteria against which it is proven to be highly effective *in vitro* [1]. The NGAD has the same base formulation as SCMC (sodium silver CMC fibres containing 1.2% silver ions) and has been shown to have the same physical performance *in vitro* [7, 9], biocompatibility, and an equivalent clinical safety profile [18, 19]. In elution studies into isotonic media the silver ion release profiles of the NGAD and SCMC have also been shown to be equivalent (Figure 10). NGAD dressings prepared without silver have been shown to have no antimicrobial activity in standard log-reduction models against planktonic pathogenic wound bacteria *in vitro* (data not shown).

The *in vitro* study described here was designed to assess the antibiofilm and antimicrobial characteristics of the NGAD compared with other silver-containing dressings and further elucidate its mode(s) of action. In a program of increasingly complex and challenging biofilm models,

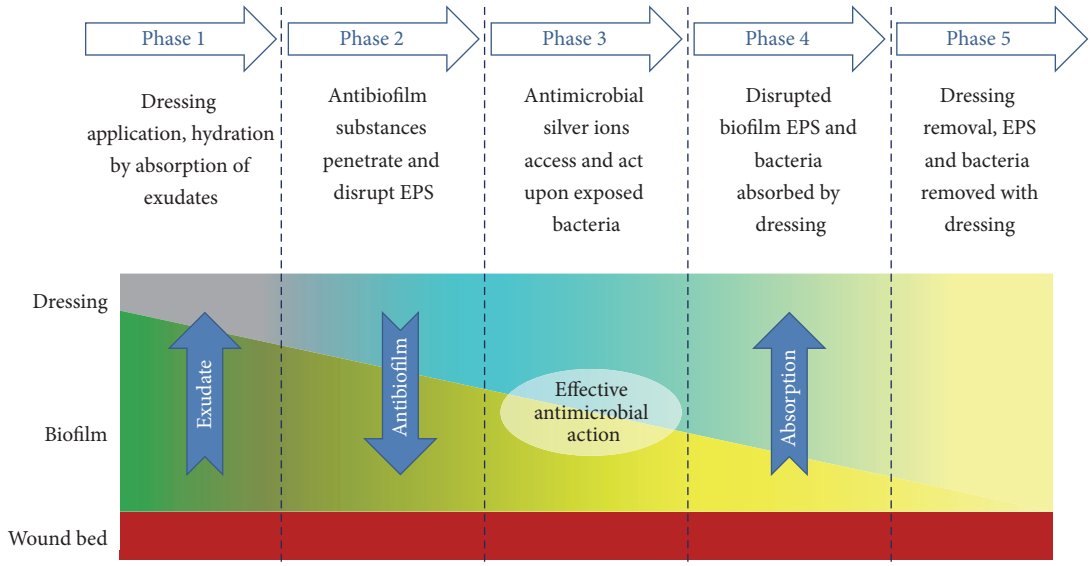

Figure 11: Functionality of the NGAD.

this study compared the antibiofilm activity of this next generation dressing to existing silver dressings. The dressing characteristics examined were the following.

(1) The Ability of the Dressings to Disrupt Biofilm. The biofilm-disrupting effect of the NGAD formulation appears to act synergistically with the inherent biofilm removal capability of Hydrofiber technology. This was demonstrated by elemental analysis in reductions in biofilm-associated ions (K^+ and $Metal^{2+}$), and the NGAD resulted in some significantly greater ($p < 0.05$) biofilm-disruptive effects than the base CMC and the silver-containing SCMC, depending on biofilm type. The Hydrofiber technology used in the NGAD has previously been shown to sequester cells *in vitro* [20], and it is therefore likely that EPS loosened or broken up by the additional components of the NGAD were also sequestered into the dressing, as supported by the EPS reduction via Calcofluor White staining.

(2) The Ability of the Dressings to Absorb Biofilm and Reduce Biomass. In addition to the EPS reduction effected by the NGAD, the reduction in the number of biofilm cells and biofilm thickness was demonstrated by live/dead staining and colorimetric image analysis, further supporting the synergy between the antibiofilm action of the formulation and the physical sequestration capability of Hydrofiber technology.

(3) Ability of the Dressings to Donate Antimicrobial Silver to Biofilm Cells. Elemental analysis showed that the NGAD donated significantly more ($p < 0.05$) silver ions to biofilm than the standard silver-containing Hydrofiber dressing and the other commercial silver-containing dressings tested (despite this latter group of dressings containing more silver). It is apparent that simply adding more silver to wound dressings is unlikely to be the most effective way of killing biofilm microorganisms. The elution rate of ionic silver into isotonic media is the same for SCMC and the NGAD, so the enhanced silver donation by the NGAD can only be attributed to the antibiofilm formulation, disodium ethylenediaminetetraacetate, benzethonium chloride, and pH control, removing the EPS barrier and enhancing the efficiency of transfer of the antimicrobial agent into the biofilm cells.

(4) The Ability of the Dressings to Kill Biofilm-Associated Microorganisms. As may be expected due to the enhanced biofilm penetration of silver ions, the biofilm viable count data was aligned with colorimetric image analysis and live/dead staining. Despite the NGAD containing notably lower concentrations of ionic silver, the NGAD significantly outperformed ($p = 0.000$) the other silver dressings in killing biofilm cells in a challenging polymicrobial biofilm model.

Irrespective of the microscopic, analytical, or microbiological method used to analyse the antibiofilm effects, the NGAD was shown to reduce biofilm thickness and reduce biofilm cell viability compared to standard silver wound dressings, despite these containing notably higher silver concentrations. This observation supports recently reported clinical observations, where static or deteriorating chronic wounds that had been unsuccessfully managed with, amongst others, standard silver dressings were dramatically improved following a switch to the NGAD in otherwise standard care protocols [18]. The enhanced antibiofilm and antimicrobial action observed in this study helps to explain the encouraging early *in vitro* [7, 9, 21], *in vivo* [22], and clinical results [18, 19, 23] observed for this next generation dressing technology and sheds further light on its modes of action. Based on the *in vitro* data generated in this study, the functionality of the NGAD can be described in five phases (Figure 11).

Phase 1. The applied NGAD dressing hydrates and gels on contact with wound fluids, contacting intimately [2] the wound bed and surface biofilm.

Phase 2. Biofilm is loosened and dispersed due to the synergistic action of the disodium ethylenediaminetetraacetate and benzethonium chloride in combination with sodium silver CMC fibres [9].

Phase 3. Exposed microorganisms become highly susceptible to killing by the action of ionic silver.

Phase 4. Residual biofilm and cells are immobilised within the gelled dressing.

Phase 5. Biofilm biomass is reduced by dressing removal.

5. Conclusions

This *in vitro* study offers new insight into the antimicrobial and antibiofilm behaviour of dressings against clinically relevant microbial forms (biofilm) and how those microorganisms respond to dressing technology. An antimicrobial dressing technology (formulation and physical properties) influences its ability to expose bacteria to the antimicrobial agent. The NGAD, with its specifically designed biofilm-disrupting formulation, ionic silver and Hydrofiber base was the most effective dressing at disrupting, killing, and removing biofilm and donating the greatest amount of silver into the residual biofilm, despite the dressing containing the least silver of the dressings tested. Antimicrobial efficacy against biofilm cannot be predicted by silver type or form, silver content, or silver elution data. This *in vitro* study improves our understanding of how this new dressing technology is effective, both in the laboratory and in the clinic.

Disclosure

The authors are all employees of ConvaTec Ltd.

Competing Interests

The authors declare that they have no competing interests.

Acknowledgments

Samantha Jones, Associate Director, Development Laboratories, was acknowledged for the development of the simulated wound polymicrobial biofilm model.

References

[1] P. G. Bowler, S. Welsby, V. Towers et al., "Multidrug-resistant organisms, wounds and topical antimicrobial protection," *International Wound Journal*, vol. 9, no. 4, pp. 387–396, 2012.

[2] P. Bowler, S. Jones, V. Towers, R. Booth, D. Parsons, and M. Walker, "Dressing conformability and silver-containing wound dressings," *Wounds UK*, vol. 6, no. 2, pp. 14–20, 2010.

[3] H.-C. Flemming and J. Wingender, "The biofilm matrix," *Nature Reviews Microbiology*, vol. 8, no. 9, pp. 623–633, 2010.

[4] G. A. James, E. Swogger, R. Wolcott et al., "Biofilms in chronic wounds," *Wound Repair and Regeneration*, vol. 16, no. 1, pp. 37–44, 2008.

[5] K. Kirketerp-Møller, P. Ø. Jensen, M. Fazli et al., "Distribution, organization, and ecology of bacteria in chronic wounds," *Journal of Clinical Microbiology*, vol. 46, no. 8, pp. 2717–2722, 2008.

[6] D. Lebeaux, J.-M. Ghigo, and C. Beloin, "Biofilm-related infections: bridging the gap between clinical management and fundamental aspects of recalcitrance toward antibiotics," *Microbiology and Molecular Biology Reviews*, vol. 78, no. 3, pp. 510–543, 2014.

[7] D. Parsons, "Designing a dressing to address local barriers to wound healing," in *Next-Generation Antimicrobial Dressings: AQUACEL™ Ag+ Extra™ and Ribbon*, Wounds International, London, UK, 2014, http://www.woundsinternational.com.

[8] S. Lindsay, "Silver white paper: everything you ever wanted to know about the use of silver in wound therapy," Systagenix 2011:22, 2011.

[9] P. G. Bowler and D. Parsons, "Combatting wound biofilm and recalcitrance with a novel anti-biofilm Hydrofiber® wound dressing," *Wound Medicine*, vol. 14, pp. 6–11, 2016.

[10] M.-Y. Chen, D.-J. Lee, J.-H. Tay, and K.-Y. Show, "Staining of extracellular polymeric substances and cells in bioaggregates," *Applied Microbiology and Biotechnology*, vol. 75, no. 2, pp. 467–474, 2007.

[11] C. Vuotto, F. Longo, M. Balice, G. Donelli, and P. Varaldo, "Antibiotic resistance related to biofilm formation in *Klebsiella pneumoniae*," *Pathogens*, vol. 3, no. 3, pp. 743–758, 2014.

[12] J. W. Costerton, P. S. Stewart, and E. P. Greenberg, "Bacterial biofilms: a common cause of persistent infections," *Science*, vol. 284, no. 5418, pp. 1318–1322, 1999.

[13] E. J. Robertson, J. M. Wolf, and A. Casadevall, "EDTA inhibits biofilm formation, extracellular vesicular secretion, and shedding of the capsular polysaccharide glucuronoxylomannan by *Cryptococcus neoformans*," *Applied and Environmental Microbiology*, vol. 78, no. 22, pp. 7977–7984, 2012.

[14] D. G. Conrady, C. C. Brescia, K. Horii, A. A. Weiss, D. J. Hassett, and A. B. Herr, "A zinc-dependent adhesion module is responsible for intercellular adhesion in staphylococcal biofilms," *Proceedings of the National Academy of Sciences of the United States of America*, vol. 105, no. 49, pp. 19456–19461, 2008.

[15] H. Ceri, M. E. Olson, C. Stremick, R. R. Read, D. Morck, and A. Buret, "The Calgary Biofilm Device: new technology for rapid determination of antibiotic susceptibilities of bacterial biofilms," *Journal of Clinical Microbiology*, vol. 37, no. 6, pp. 1771–1776, 1999.

[16] R. D. Wolcott, J. P. Kennedy, and S. E. Dowd, "Regular debridement is the main tool for maintaining a healthy wound bed in most chronic wounds," *Journal of Wound Care*, vol. 18, no. 2, pp. 54–56, 2009.

[17] R. D. Wolcott, K. P. Rumbaugh, G. James et al., "Biofilm maturity studies indicate sharp debridement opens a timedependent therapeutic window," *Journal of Wound Care*, vol. 19, no. 8, pp. 320–328, 2010.

[18] D. G. Metcalf, D. Parsons, and P. G. Bowler, "Clinical safety and effectiveness evaluation of a new antimicrobial wound dressing designed to manage exudate, infection and biofilm," *International Wound Journal*, 2016.

[19] K. G. Harding, M. Szczepkowski, J. Mikosiński et al., "Safety and performance evaluation of a next-generation antimicrobial dressing in patients with chronic venous leg ulcers," *International Wound Journal*, vol. 13, no. 4, pp. 442–448, 2016.

[20] M. Tachi, S. Hirabayashi, Y. Yonehara, Y. Suzuki, and P. Bowler, "Comparison of bacteria-retaining ability of absorbent wound

dressings," *International Wound Journal*, vol. 1, no. 3, pp. 177–181, 2004.

[21] J. Said, M. Walker, D. Parsons, P. Stapleton, A. E. Beezer, and S. Gaisford, "An *in vitro* test of the efficacy of an anti-biofilm wound dressing," *International Journal of Pharmaceutics*, vol. 474, no. 1-2, pp. 177–181, 2014.

[22] A. K. Seth, A. Zhong, K. T. Nguyen et al., "Impact of a novel, antimicrobial dressing on *in vivo, Pseudomonas aeruginosa* wound biofilm: quantitative comparative analysis using a rabbit ear model," *Wound Repair and Regeneration*, vol. 22, no. 6, pp. 712–719, 2014.

[23] K. Woo, "AQUACEL Ag+ dressings in practice," in *Next-Generation Antimicrobial Dressings: AQUACEL™ Ag+ Extra™ and Ribbon*, Wounds International, 2014, http://www.wounds-international.com.

Hindawi Publishing Corporation
BioMed Research International
Volume 2016, Article ID 1851242, 17 pages
http://dx.doi.org/10.1155/2016/1851242

Review Article

Recent Nanotechnology Approaches for Prevention and Treatment of Biofilm-Associated Infections on Medical Devices

Mohankandhasamy Ramasamy and Jintae Lee

School of Chemical Engineering, Yeungnam University, Gyeongsan 38541, Republic of Korea

Correspondence should be addressed to Jintae Lee; jtlee@ynu.ac.kr

Received 5 July 2016; Accepted 13 October 2016

Academic Editor: Ariel Kushmaro

Copyright © 2016 M. Ramasamy and J. Lee. This is an open access article distributed under the Creative Commons Attribution License, which permits unrestricted use, distribution, and reproduction in any medium, provided the original work is properly cited.

Bacterial colonization in the form of biofilms on surfaces causes persistent infections and is an issue of considerable concern to healthcare providers. There is an urgent need for novel antimicrobial or antibiofilm surfaces and biomedical devices that provide protection against biofilm formation and planktonic pathogens, including antibiotic resistant strains. In this context, recent developments in the material science and engineering fields and steady progress in the nanotechnology field have created opportunities to design new biomaterials and surfaces with anti-infective, antifouling, bactericidal, and antibiofilm properties. Here we review a number of the recently developed nanotechnology-based biomaterials and explain underlying strategies used to make antibiofilm surfaces.

1. Introduction

Biofilms are organized colonies of bacteria, fungi, or yeasts that form heterogeneous entities on biotic or abiotic surfaces by secreting extracellular polymeric substances (EPS). These substances protect individual cells from hostile factors, such as immunologic defense systems, nutrient limitations, and antibacterial agents [1]. The genotypic and phenotypic characteristics of cells in biofilms differ from those of their free-floating counterparts, and these differences make them strongly resistant to antibiotics. This resistance has been attributed to the failure of antibiotics to penetrate biofilms, the induction of multidrug efflux pumps of biofilm-specific phenotypes, and the presence of persisters [2, 3]. Basically, microbes have the ability to adhere to surfaces, including those of inert materials, synthetic polymers, and indwelling medical devices, and this leads to colonization and mature biofilm development. Furthermore, cell detachment from mature biofilms leads to infection dissemination and transmission [4, 5]. In fact, clinical infections caused by biofilms are a more challenging healthcare issue than those caused by planktonic cells, and microbial infections caused by bacterial biofilms on biomedical surfaces are a leading cause of death worldwide [6, 7]. As a result, there is an urgent clinical need to develop long-lasting biomedical materials or devices with antibacterial and antibiofilm surfaces.

Nanometer scale materials have been adopted for many biomedical applications due to the greater reactivities conferred by their large surface to volume ratios and ability to control their physicochemical properties. In fact, applications of nanotechnology in medicine resulted in a new field called "nanomedicine" which has already provided novel treatments against a wide range of diseases. Nanomaterial development is now viewed as a promise strategy for controlling or treating pathogenic biofilms on indwelling medical devices and implants. Most of the nanoparticles examined have been metals (e.g., copper, silver, iron, zinc, titanium, magnesium, or gold), metal oxides, polymers (e.g., nanoporous polymers), metal-based polymeric composites, peptides, or combinations of these, or liposomes, antibiotic encapsulated nanoparticles, or responsive smart nanomaterials that have antimicrobial effects but cause minimal damage to the host. Drug loaded nanoparticles could overcome the limitations of conventional antibiotic treatments associated with toxicity, improper delivery, or enzymatic degradation. In addition, hydroxyapatite, chitosan, collagen, silica, and titanium dioxide have been used as nanomatrices to incorporate antimicrobials because of their bioactivities,

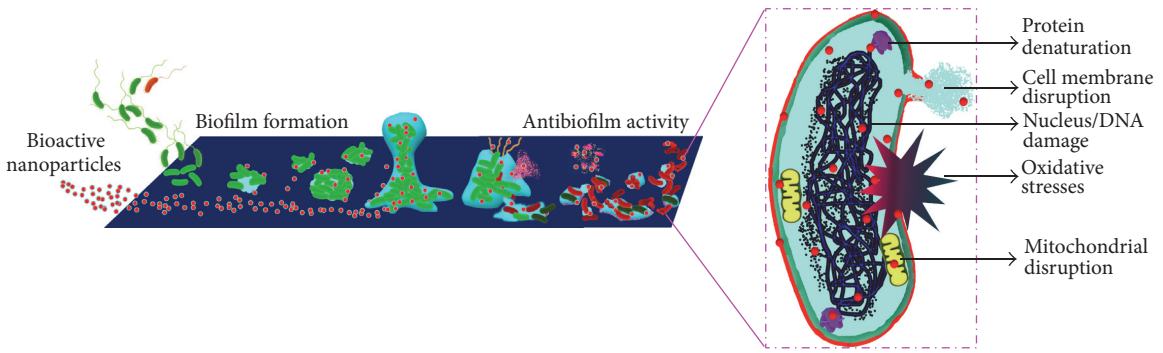

Figure 1: Schematic illustration of biofilm development and mechanisms responsible for the antimicrobial and antibiofilm effects of nanoparticles.

biocompatibilities, low toxicities, and noninflammatory and nonimmunogenic characteristics [8, 9]. Recently, novel physical approaches like near-infra red light (NIR) or alternating magnetic fields (AMFs) have been utilized with nanoparticles to cause irreversible thermal damage to cell surfaces and bacterial biofilm eradication [10, 11]. These promising developments could possibly be adapted to treat wound biofilm infections in a noninvasive, on-demand manner.

This review highlights current strategies of nanotechnology-based approaches designed to control or eradicate biofilm related infections with special emphasis on nanoparticle embedded biomedical materials.

2. Bacterial Biofilms: Formation to Dissemination

It is now realized that most bacterially derived sessile communities are capable of forming irreversible biofilms on surfaces and interfaces by embedding themselves deep in a self-generated polymeric matrix [43]. Furthermore, most of the fungal species that form biofilms do so in a similar manner; *Candida* and *Aspergillus* are fungal species of particular interest [44]. The mechanism of biofilm formation depends on environmental stimuli and a series of genetic and phenotypic changes in planktonic cells. To date, five different stages [45] have been suggested during biofilm development (Figure 1), namely, (i) reversible-irreversible adherence, (ii) microcolony formation, (iii) 3D biofilm formation, (iv) maturation, and (v) dissemination [46]. In the earliest stage, biofilm development involves surface preconditioning and the adsorption of macromolecules, followed within seconds of surface exposure, by the formation of a conditioning layer. During the second stage, microorganism adhesion and coadhesion are strengthened by strong chemical attachments to the matrix polymer, and the unfolding of cell surface structures results in the exudation of a polysaccharide slime that attracts cells and debris. During the third stage, the nutrient rich biofilm environment promotes rapid microorganism growth that ultimately results in biofilm development in a 3D manner that substantially increases biofilm thickness. As film thickness increases, the forth maturation stage is reached, which is associated with antibiotic resistance. In the final stage, due to dynamic flux of the biofilm matrix, microorganisms detach, either actively or passively, and enter the surrounding environment as planktonic cells on a regular basis. Detached cells can also disseminate to fresh surfaces in the forms of detached biofilm clumps or fluid-driven cell clusters. Furthermore, bacteria originating from biofilm communities colonize new areas to produce new sessile populations.

3. Biofilm Formation and Biofouling

Biofouling (Figure 1) is defined as the accumulation of unwanted proteins and other analytes or microorganisms on the surfaces of host materials. Microbial contamination and associated infections can have serious consequences in a number of environments, including hospitals and the food industry and in community-related settings [47]. Fouling caused by marine organisms is also an issue of concern for industry and boating. After attaching to a surface, biofouling organisms can form a conditioning layer that provides an active platform for diatoms and algae, which results in increased operational and maintenance costs and the accelerated degradation of abiotic materials. Likewise, membrane fouling hampers pressure-driven membrane processes, such as reverse osmosis, microfiltration, ultrafiltration, and nanofiltration, used for water treatment and desalinization. Membrane biofouling is caused by *Aeromonas*, *Arthrobacter*, *Bacillus*, *Corynebacterium*, *Flavobacterium*, and *Pseudomonas* sp. and to a lesser extent by other microorganisms, like, fungi [48].

In vivo, nonspecific protein adsorption facilitates bacterial attachment to surfaces and leads to colonization, subsequent biofilm formation (Figure 1), and infectious disease. Protein fouling followed by microbial attachment with biofilm development is a dormant factor of the failure of biomedical devices and implants. Furthermore, microbial attachment reduces the sensitivities and efficacies of devices, including those of *in vitro* diagnostic equipment, such as those required for immunological assays, and thus has therapeutic impacts [49].

Biofilms infections of teeth, lungs, skin, heart, and the urinary tract are always detrimental [50, 51]. Wounds and implants are susceptible to *Staphylococcus aureus* and

Staphylococcus epidermidis infections [52, 53]. *Staphylococcus* is responsible for most hospital acquired pneumonia cases and *Pseudomonas aeruginosa* also forms biofilms in lungs [54, 55]. In addition, multidrug resistant Gram-negative bacterial species, such as, *Escherichia coli*, *Klebsiella pneumoniae*, and *P. aeruginosa*, causes widespread biofilm-based infections in acute care facilities in hospitals [56, 57]. Dental plaques are tooth biofilms that lead to dental cavities and gum inflammation and infect dental implants.

Nosocomial infections are contracted in medical environments or after direct contact with healthcare settings [59]. Contact with contaminated surfaces or infection by air-borne bacteria or fungal spores places surgical patients at risk [60, 61]. In fact, more than 60% of hospital related complications and up to 80% of infection associated deaths are attributable to biofilm infections [62, 63], and nearly 80% of known pathogenic bacteria have been implicated in device-related infections [64, 65], such as intravenous and urinary catheters [66], joint prostheses [67, 68], penile prostheses [69], contact lenses [70], fracture fixation devices [71, 72], breast implants [73, 74], pacemakers [75], endoscopes [76], cardiovascular and biliary stents [77], and coherent implants [78, 79]. Biofilms on these devices transmit bacteria and act as source of infection. Currently, removal of the affected device offers the only permanent means of eradicating infection [80]. Below list describes the device-related biofilm infections.

3.1. Catheter Biofilm Infections

3.1.1. Central Venous Catheters. Hematogenous spread of infections from colonized central intravenous catheters or central lines is a long-recognized problem with infection rates of 2 and 6.8 per 1000 days, respectively [81, 82]. Vascular catheters placed for more than 30 days evidenced luminal colonization and biofilm formation which is predominant compared to central venous catheters. Therefore, bone marrow transplant patients that require a long term vascular catheter for intravenous access are at greater risk of biofilm infections [83, 84]. In clinical practice, vascular catheters are replaced regularly to reduce infection risk, but this practice substantially increases healthcare costs.

3.1.2. Urinary Catheters. Urinary catheterization is routinely used to collect urine during surgery, measure urine output, and prevent urine retention in intensive care unit patients. Periurethral skin colonization is a cause of bacterial contamination as it can result in bladder migration and the establishment of biofilms on catheters [85]. Urease producing bacteria, such as, *Proteus*, *Psuedomonas*, and *Klebsiella*, increase urinary pH by creating an alkaline environment, which promotes the formation of struvite biofilms within catheters [45]. These crystalline biofilms can form deposits on the outer surfaces, tips, and balloons of catheters and led to severe complications, such as injury to the urinary bladder. Furthermore, biofilm debris may be shed after deflating a catheter balloon, which can block urine flow [86]. The main strategies used to prevent urinary catheter-associated infections are to use catheters only when necessary, to avoid long term catheterization, and to replace catheters regularly. However, frequent replacement and the disruption caused can lead to severe complications, in particular, the spread of bacteria to uncontaminated sites due to biofilm shedding [87–89].

3.2. Endotracheal Tubes. Numerous microorganisms have been reported to colonize and form biofilms in endotracheal tubes. These organisms include methicillin-resistant *S. aureus* (MRSA) and Gram-negative bacilli, such as *E. coli*, *K. pneumoniae*, *P. aeruginosa* and *Acinetobacter spp*., which are key factors of ventilator-associated pneumonia development [90]. Reports indicate diverse microorganisms, from orally associated microflora to clinically specific isolates, can form biofilms in endotracheal tubes [91, 92].

3.3. Prosthetic Joints. Increasing evidence indicates underlying biofilm infections are a primary cause of aseptic loosening of joint prostheses. Device-associated infections in prosthetic joints by *S. epidermidis* or *Propionibacterium acnes* can induce severe complications and significant mortality after joint replacement surgery [93, 94].

3.4. Pacemakers and Heart Valves. In the US, more than 100,000 cardiovascular devices are implanted annually and heart valve infections account for 30% of implant associated mortalities. *S. aureus*, *S. epidermidis*, *P. aeruginosa*, *Acinetobacter baumannii*, *Klebsiella pneumonia*, *E. coli*, and *P. acnes* are reportedly the most common causative agents of cardiac implant infections [75] on pacemakers, prosthetic valves, defibrillators, and coronary artery bypass grafts, which incidentally grow thicker biofilms *in vivo* than *in vitro* [75, 78, 95]. Other microbes, such as *Enterococcus* and yeasts, also form biofilms on cardiovascular devices [96]. Heart valves have been reported to be targeted by *Mycobacterium fortuitum*, which causes systemic biofilm infection without causing vegetation. Heart valve biofilms reduce blood flow, cause hematogenous spread, and infect and cause emboli development in other organs. Basically, heart valves are infected by clot formation after injury, because blood clots afford an ideal surface for bacterial adhesion [97].

3.5. Contact Lenses. Although different types of polymeric contact lens materials have been developed in the attempt to prevent biofilm formation, these efforts have been uniformly unsuccessful. Biofilms of certain species, including *Candida*, *P. aeruginosa*, and *Fusarium*, are resistant to the biocides in standard contact lens solutions but are susceptible to hydrogen peroxide [98]. However, contact lenses made from hydrogels that release ceragenin are reportedly capable of resisting colonization by *P. aeruginosa* and *S. aureus* for two and four weeks, respectively [99].

3.6. Orthopedic Implants. Up to 15% of infection-associated hip implant failures required for implant replacement revision surgery are due to bacterial biofilm formation [100], which causes inflammation and tissue destruction around

implants much more rapidly than the damage caused by gingivitis [101]. Nevertheless, altering implant surface textures by sintering [102], sand blasting [103], or plasma spraying [104] can improve the biofilm resistance of orthopedic implants.

3.7. Breast Implants. Burkhardt et al. proposed that subclinical infections caused capsular contractions around breast implants [105]. Numerous bacteria in breast ducts and tissue result in biofilm formation on breast implants, which had been shown to be the leading cause of contracture [106–108]. One study showed *S. epidermis* adhered and produced biofilms on the breast implant surfaces regardless of surface textures [73].

4. Approaches to Biofilm Control

Biological response to a biomedical device depends on the structure and surface functionality of the material used, and most device-associated infections are likely to originate from material surface contamination at time of implantation. Thus, the compositions or surface functionalizations of biomaterials are tailored to achieve desired results. Surface engineering of materials can enhance device biocompatibility and functionality and material properties and surfaces can be modified to reduce microbial contamination and prevent biofilm infections. The different methodologies used include

(1) antifouling coatings [47],

(2) antiadhesive surface modifications [109],

(3) addition of antimicrobials to the surfaces of medical devices [110–112],

(4) coating devices with polymer products [113],

(5) surface engineering with chemical moieties [57, 114–116],

(6) coating, lamination, adsorption, or immobilization of biomolecules [117–119].

Microbial attachment to a surface is usually initiated by the formation of an adsorbed protein layer. Immobilizing poly(ethylene glycol) (PEG) or oligo(ethylene glycol) or a zwitterionic species on surfaces is commonly used to produce antifouling surfaces [120–122]. The introduction of sulfonate units, presence of longer brushes, and high molecular weight of poly ethylene molecules strongly resisted *E. coli*, *S. epidermidis*, *P. aeruginosa*, *Candida tropicalis*, and *C. albicans* attachment [123, 124]. Bacterial adhesion to surfaces is a complex process that is not completely understood, but it appears to be governed by the physical characteristics of bacteria and surfaces, such as surface roughness, hydrophobicity, and charge. Lotus leaves and shark skins have exceptional antifouling properties as their unique microtopographic features make these surfaces super hydrophobic and self-cleaning [125], and many researchers have mimicked this technique [126, 127]. For example, 95% bacterial resistance was recorded for a particle-layered polythiophene films by altered surface wettability [128]. A photolithography technique to create the topography of shark skin on polydimethysiloxane (PDMS) resulted in the composite significantly inhibited biofilm colonization by *S. aureus*. Furthermore, different microtopographic structures on PDMS showed 86% resistance to colonization by the sea weed *Ulva* [129, 130]. The inclusion of natural bioactive agents, including antimicrobials, into polymers has been widely applied and utilized in the textile and food industries, for drug delivery and for treating the surfaces of surgical implants and biomedical devices. Natural antimicrobials have also been incorporated into paper [131], thermoset plastics, and thermoplastics [132] and tested against pathogenic *E. coli*, *Listeria monocytogenes*, and spoilage organisms, including molds [133]. Additionally, coating glass slides with poly(4-vinyl-N-alkylpyridinium bromide) was found to kill airborne bacteria [134].

Antibiotic coatings efficiently provide surface antimicrobial activity because bacteria directly bind with antibiotics and are lysed before biofilm establishment. This strategy has been applied to bone cements [135] used in orthopedic and orthodontic applications [136, 137]. The surface active biomolecules examined include lactoferrin [138], biosurfactants [139], bacterial adhesion inhibitors [140], antibody-releasing surfaces [141], nonpathogenic bacteria [142], and quorum sensing (QS) inhibitors [143], and all have been utilized to inhibit and eradicate pathogenic bacterial biofilm development on different biomedical surfaces [144].

Quaternary ammonium compound on different surfaces was disruptive to bacterial colonization and biofilm formation [134, 145]. However, high concentrations of quaternary ammonium compounds and their cationic natures are harmful to human cells [146, 147], and thus, additional development is needed to make these materials safer; for example, embedding a cationic compound in a peptide containing MAXI hydrogel provided broad antibacterial activity without harming red blood cells or fibroblasts [148]. Accordingly, designs incorporating combinations of suitable materials that do not harm the host environment provide a key to the successful application of antibiofilm coatings [149].

Although antiadhesive coatings may provide benefits for single functionality devices like urinary catheters, voice prostheses, and contact lenses, they are not sufficient for permanent indwelling devices like heart valves, surgical meshes, hip and knee prostheses, or vascular grafts. Effective implant materials must have multifunctional surfaces that provide extended antimicrobial activity and tissue integration and disinfect surrounding tissues after implant revision surgery, but on the other hand they must not alter host immune responses to microorganisms [150]. Current research is focused on more sophisticated surface modification methods to prevent microbial adherence, inhibit microbial growth, and disrupt biofilm formation.

5. Nanotechnology Based Strategies for Biofilm Control and Treatment

It is believed nanotechnology-based approaches will provide promising advancements to prevent drug-resistant biofilm infections of medical devices and biomaterials. A small

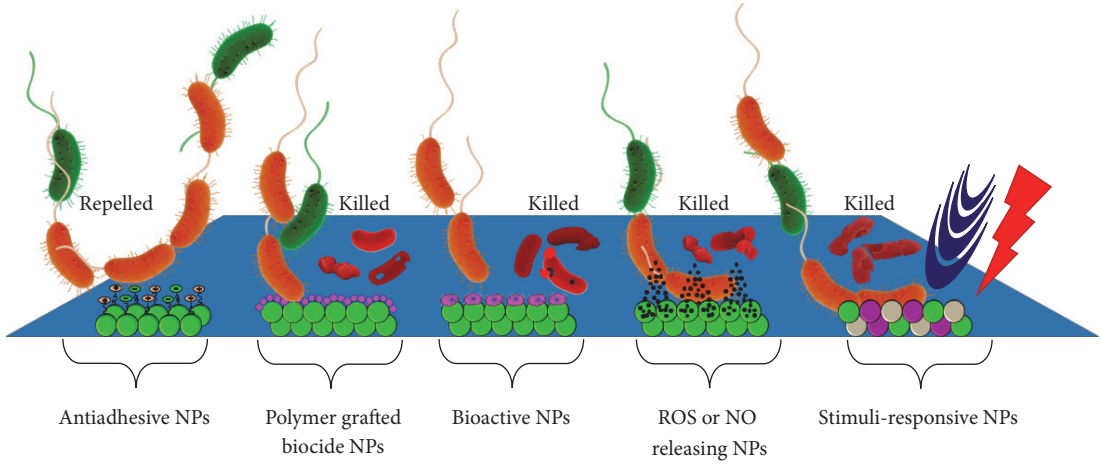

Figure 2: Schematic of biofilm inhibition showing the effects of surface-engineered nanomaterials with diverse antimicrobial properties.

number of studies have reported the use of nanoparticle (NP) coated surfaces as biofilm inhibiting agents [151]. At the nanometer scale materials exhibit unique physicochemical and biological properties and sometimes phenomena, such as quantum effects, not exhibited by their bulk counterparts. Nanomaterials have much greater surface area to volume ratios, which enhances chemical reactivities and bioactivities, and their sizes are of the same order as biomolecules. Furthermore, NPs are small enough to penetrate microbial cell walls and even biofilm layers that can cause irreversible damage to cell membranes and DNA. In addition, they have long plasma half-lives and their high surface to volume ratios facilitate the loading of drugs and targeting entities [152].

5.1. Nanoparticles in Antibiofilm Therapy. Recent advances in nanotechnology have identified new and promising opportunities for effective biofilm control and treatment. Summary of different surface-engineered NPs including metal NPs, polymer NPs, metal-polymer composites, biologically active NPs, ROS or NO releasing NPs, and stimuli-responsive smart NPs that are considered to offer the possibility of either preventing or controlling biofilm related infections on medical devices with their respective mechanisms of actions is illustrated in Figure 2.

5.2. Antibacterial Metals. Copper, gold, silver, titanium, and zinc are known to have antibacterial and antibiofilm properties, which offer alternatives to antibiotics without significantly increasing the risk of resistance development. It has been established that metal-based NPs have much better antimicrobial activities than their micro-sized counterparts [153, 154]. The surface textures of metal coated biomaterials are dependent on coating technique, for example, sintering, plasma spraying, sand blasting, anodization, or electron beam evaporation. Furthermore, devices produced using these techniques exhibit quite different bacterial adhesions, protein adsorptions, and tissue integration characteristics [155–157].

5.2.1. Inorganic Nanoparticles. Several inorganic metal NPs, such as, gold, copper, silver, zinc, and titanium NPs, exhibit antibiofilm activity. Silver nanomaterials have received considerable attraction because of their superior antimicrobial activities. Silver in ionic or NP form has an oligodynamic effect with broad spectrum antibacterial activity and is especially effective against microbial colonizations associated with biomedical infections. The antibacterial mechanism of silver NPs (Ag NPs) is probably due to interactions between silver ions with bacterial wall sulfhydryl groups that interfere with and disrupt bacterial cell membranes [158], enzyme activities [159], respiratory chains [160], and cell proliferation [161]. Ag NPs have also been shown to disrupt biofilm matrices by perturbing intermolecular forces. In one study, 24 h of treatment with Ag NPs inhibited biofilm formation by *P. aeruginosa* and *S. epidermidis* by more than 95% and biofilm formation by clinically isolated strains of MRSA and methicillin-resistant *S. epidermidis* (MRSE) [162]. Silver impregnated hydroxyapatite and silver-titania matrices reduced bacterial adhesion and prevented biofilm generation by Gram-positive and Gram-negative bacteria (Table 1), and the TiO_2 acted as a better supporting matrix and prevented the aggregation of silver and allowed the controlled release of silver ions [163]. Nevertheless, continuous exposure to silver NPs may result in reduced effectiveness with developed silver resistance on MRSA [158], and high doses of silver NPs can delay wound recovery due to toxic effects on skin cells [164].

The antibacterial activities of metal oxide NPs have also been studied; examples include zinc oxide (ZnO), copper oxide (CuO), titanium dioxide (TiO_2), iron oxide (Fe_2O_3), cerium oxide (CeO), magnesium oxide (MgO), and aluminum oxide (Al_2O_3). ZnO NPs have been found to have better antibacterial activities and low toxicities in mammalian cells and to be more effective at inhibiting biofilm formation and the growth of *E. faecalis*, *S. aureus*, *S. epidermidis*, *B. subtilis*, and *E. coli* than the NPs of other metal oxides [154, 165]. ZnO NPs in combination with β-chitin dressings were found to treat skin wound infections effectively in rat models and to reduce biofilm formation. Furthermore, nanotextured

Table 1: Nanoparticle-based solutions for prevention and treatment of biofilm associated-medical device infections.

Material	Nanomaterial description	Antibiofilm devices	Antimicrobial mechanism of NPs
Inorganic NPs	Silver NPs [12–15] Surface engineered gold NPs [16]	Urethral catheters, central venous catheters Ventricular drain catheters	Released silver ion interacts with sulfhydryl groups of bacteria and interferes with cell membrane integrity, enzyme activities, respiratory chains, and cell proliferations [17]. Highly positive surface charge disrupts the network of EPS.
Organic NPs	Quaternary ammonium chitosan NPs [18] PEG stabilized lipid NPs [19]	Bone and dental cements	Long cationic polymer chains penetrate the cell membrane and can induce ion exchange to disrupt biofilm
Metallic/metal-polymer nanocomposites	Ag-Ti composites [20] Silver or antibiotic conjugated NPs [21, 22] Silver conjugated silicone NPs [23] Diamond like carbon-metal nanocomposites [24] Silicone containing antibiotic loaded liposome [25] Polymeric silver NPs [26] Silver nanoparticle coated surfaces [27] Polycationic NPs [28]	Face masks Heart valve Catheter against fungi Pedicle screws	Highly positive surface charge disrupts the network of EPS Silver ions bound with deoxyribonucleic acid and interfere with electron transport, injuring bacterial enzymes and causing biofilm disruption
Metallic/metal-polymer nanocomposites	ZnO NP incorporated titanium implants [29] TiO_2 nanotube arrays [30] Ag NP conjugated poly(ethylene glycol diacrylate)-co-acrylic acid (PEGDA-AA) hydrogel coatings on a Ti substrate Quaternary ammonium salts (QAS) loaded TiO_2 nanotubes [31] Ciprofloxacin-loaded nanochitosan coated Ti implants [32] Polymeric NP based photodynamic therapy [33]	Orthopedic implants	ZnO alter protein adsorptions and intracellular mechanisms Positive surface of QAS disintegrates the negatively charged bacteria Released ciprofloxacin inhibits enzymes including DNA gyrase, and topoisomerase causes bacterial disruption Free radicals interact with endogenous molecular oxygen to produce ROS, superoxide hydroxyl radicals, and hydrogen peroxide damages bacteria membrane integrity and causes irreparable bacteria lysis
Metallic/metal-polymer nanocomposites	Ti implant surfaces with ZnO NPs [34] Nanostructured titania coating with Ag NPs [35] Antibiotic incorporated silk fibroin NPs coated titanium surface [36] Nanosilver-endodontic filling and dental adhesives [37, 38]	Oral implants Endodontic filling and dental adhesives	Direct contact, ZnO release, ROS generation Irreversible binding of gentamycin disrupts bacteria

Table 1: Continued.

Material	Nanomaterial description	Antibiofilm devices	Antimicrobial mechanism of NPs
Metallic/metal-polymer nanocomposites	Silica NPs [39] Hydrogel containing Ag NPs [40] Zn-CuO nanocoating on contact lenses [41] Quaternized chitosan loaded Ag NPs and antifungal agent conjugated graphene oxide [42]	Contact lenses	Released Ag ions disintegrate the bacteria and inhibit biofilm development Voriconazole inhibits ergosterol synthesis by inhibiting 14-alpha sterol demethylase which produced antifungal activity.

ZnO have been reported to have greater bacteriostatic and bacteria-resistant properties than titania nanophase [153]. However, *P. aeruginosa* and *Proteus* have been reported to exhibit zinc resistance [166, 167].

Nanosized TiO_2 is also considered as nontoxic antibacterial material due to its inert nature as compared with other metal oxides. Usually, it considered a photocatalyst and is used for various environmentally related applications, such as self-cleaning and antifogging effects. Numerous reports have been issued on photocatalytic biofilm inhibition by TiO_2 NPs. In addition, these NPs have shown promising antifungal biofilm activity on the surfaces of biomedical devices, especially against *C. albicans* [168]. The mechanism behind the antimicrobial effect of TiO_2 NPs involves the production of ROS in microbial cells, oxidation of internal enzymes, and lipid peroxidation, which reduces respiratory activity and leads to cell death (Table 1) [169]. It has also been reported that mesoporous TiO_2 NPs facilitate sustained release of attached bioactive materials and thus provide long-term antibiofilm activity [170].

CuO NPs exhibit effective antimicrobial activity against various bacteria, but they have less antibacterial activity than silver or zinc NPs, and hence higher concentrations are required to achieve desired antimicrobial effects, and at these concentrations CuO NPs could be toxic to mammalian cells [171–173]. Although CuO NPs have excellent antibacterial effects, their antibiofilm effects are limited by a narrow antibacterial window [174]. However, in combination they exhibit considerable activity; for example, CuO with ZnO NPs showed significant biofilm inhibitory activity in a NP coated tooth model [175].

Iron NPs are generally considered MRI contrast agents, but at 8 nm iron NPs eliminated *S. epidermis* infection on orthopedic implants [176]. Furthermore, antibiotic conjugated magnetic iron NPs showed higher antibacterial activity against *E. faecalis* in both its planktonic and biofilm forms than unconjugated magnetic iron NPs [177]. Catheters coated with 5 nm core-shell iron NPs showed biofilm resistance against *S. aureus* and *P. aeruginosa*, and these NPs were reported to be nontoxic and suggested for *in vivo* applications [178].

Gold NPs alone have little or no antibacterial activity [179]. Nevertheless, gold NPs bound to antibiotics [180], active compounds, or biomolecules [181] show considerable bactericidal and biofilm inhibitory activities against a variety of pathogens, including multidrug resistant strains [182]. Since gold NPs are nontoxic to cells, they have been conjugated with targeting molecules to achieve specific antibiofilm activities (Table 1) [183].

5.3. Organic Nanoparticles. Polymeric NPs and polymer based devices are engineered to provide antibacterial properties by releasing antibiotics, antimicrobial agents, or bacteriostatic peptides or by modifying their surfaces with alkyl pyrimidines or quaternary ammonium compounds to cause contact-killing (Table 1). The polycationic groups responsible for antimicrobial activity cause cell damage perhaps via an ion exchange interaction between bacteria and charged polymer surfaces resulting in the disruption of cellular membranes [184]. The polysaccharides of EPS interact with SO_4^- groups of functionalized polystyrene NPs by hydrophobic complexation, which disrupts bacterial biofilm formation [185]. A nanoporous polymer matrix composed of sodium dodecyl sulfate was found to have significant antibiofilm activity against *E. coli*. Likewise, vitamin E-conjugated cationic polymer crosslinked biodegradable hydrogels exhibit bactericidal and antifungal effects [118, 185, 186]. Levofloxacin (an antibiotic,) conjugated poly(lactic-co-glycolic acid) NPs coated with phosphatidyl choline nanohybrids exhibited enhanced antibiofilm activity against *E. coli* [187], and interestingly, a silicone functionalized PDMS surface (called the brush design) was highly effective against the bacterial and fungal biofilms of *E. coli*, *S. aureus*, and *C. albicans* without causing mammalian toxicity [188]. In addition, physicochemical surface modifications of titanium using polymers, such as polymethacrylic acid [189], polyurethane acetate [190], polyethylene oxide [191], or poly ethylene glycol (PEG) [192], prevented protein absorption and inhibited bacterial adherence [193, 194]. Nitric oxide (NO) releasing silica NPs [195] have been utilized for their bactericidal effects on planktonic *P. aeruginosa* cells and used to treat biofilm-related wound infections *in vivo* in murine models and reduced bacterial loads of MRSA [196], *A. baumannii* [197], and *C. albicans* [198].

5.4. Metal-Polymer Nanocomposites. The mechanical properties of organic polymers are inadequate for device-related

applications (Table 1), but they can be coated on metal surfaces by spin coating, dip coating, or layer-by-layer plasma polymerization [146]. Metal-polymer composites of silicone-TiO_2 NPs reduced the adhesion of *S. aureus* by 93% versus untreated silicone [199], and gallium and zinc NPs incorporated in a polyether urethane mixed PEG scaffold reduced *P. aeruginosa* infection in mice via the controlled release of gallium NPs where zinc NPs were less effective [200].

5.5. Dendrimers. Dendrimers are three-dimensional structures with the ability to encapsulate hydrophilic and hydrophobic entities into the void spaces of their highly branched structures [201]. Synthesized low molecular weight peptide dendrimers showed antimicrobial activity against *E. coli* and *S. aureus* without additional antibiotics [202], and other studies demonstrated the disruption of *P. aeruginosa* attachment and prevention of its biofilm formation were due to the attachment of fucose-specific lectins (LecB) to fucose-peptide dendrimer ligands [203].

5.6. Cyclodextrins. Cyclodextrins (CDs) are cyclic organic compounds comprised of glucopyranose units and are used to solubilize hydrophobic compounds in aqueous media. It has been reported that CDs surface functionalized with polyethylene or polypropylene loaded with miconazole reduced *C. albicans* biofilm formation by 96% *in vitro*. Furthermore, gold surface functionalized CD grafted anidulafungin and thymol reduced the surface adherence of yeast and demonstrated fungicidal activity against *C. albicans* biofilms [204, 205]. Furthermore, at enhanced drug loading and retention, ciprofloxacin loaded CD-agar hydrogels showed broad antibacterial activity against *S. aureus*, *S. epidermidis*, *P. aeruginosa*, and *E. coli* and controlled drug release [206].

5.7. Lipid-Based NPs and Microemulsions. Since liposomes resemble biological cell membrane they have been utilized in many pharmaceutical applications, including biofilm-related therapies. Various drug loaded liposomes showed effective biofilm inhibition and quorum sensing disruption *in vitro* [207] and on clinical isolates [208] of *E. coli*, *Acinetobacter lwoffii*, *A. baumannii*, *Bordetella bronchiseptica*, *Klebsiella pneumoniae*, and *P. aeruginosa*, in which they reduced the productions of lipase, protease, and chitinase [209].

Solid lipid nanoparticle (SLN) formulations containing antimicrobial agents have been used to eradicate biofilm-forming microorganisms. A SLN formulation containing PVA hydrogenated castor oil loaded with tilmicosin was used to treat *S. aureus* induced mastitis in a murine model [210] and a SLN formulation containing eugenol showed antifungal activity in a rat model oral candidiasis [211].

Microemulsions exhibited considerable antibiofilm activity against *P. aeruginosa* [212] and *C. albicans* [213] by disrupting cytoplasmic membranes, coagulating cytoplasm, and altering intracellular metabolism.

5.8. Responsive Smart Nanoparticles. A combination of external energy and energy absorbing NPs has been used as a therapeutic means of addressing antimicrobial infections (Table 1). The basic principle involves causing irreversible damage in pathogenic cells by activating metal NPs or polymer-based systems using external energy sources, such as visible light [214], temperature [215], near-infrared (NIR) radiation [216], or high frequency alternating magnetic fields (AMF) [217]. Gold, iron oxide, and graphene NPs have been utilized as photothermal agents that absorb NIR light and convert this into heat energy. Gold NPs of various shapes have been widely studied due to their excellent reactivity to NIR light, though this reactivity depends on particle size. Gram-positive, Gram-negative, and mixed species of bacteria were inactivated thermally by exposing gold [218] or graphene NPs [219] to NIR. The temperature of NP-bacterial suspensions was found to be increased beyond the physiological limits of bacteria [220].

Nanoscale carriers have also been used for photodynamic therapy (PDT) to eradicate pathogens using light and photosensitizers. Exposure of photosensitizer-NP complexes to light causes the generation of cytotoxic ROS, which then trigger bacterial cell lysis in planktonic and biofilm forms. Conjugating photosensitizers on NPs were studied for their efficient PDT in terms of destroying targeted pathogens or biofilms [221]. NPs functionalized with porphyrin, methylene blue, or rose bengal significantly inactivated MRSA [222], *C. albicans* [223], and multispecies bacterial [224] biofilms. Although PDT has potential applications for the treatment of wound infections, several factors, such as the physicochemical properties of photosensitizers, the dosages delivered, light dosimetry, and control of drug release, currently limit its clinical applications.

Magnetic nanoparticles (MNPs) absorb electromagnetic radiation from high frequency AMF and efficiently transmit it in the form of localized heat, and the hyperthermia produced by MNPs has been used to destroy *in vitro* biofilms of *S. aureus* and *P. aeruginosa* [225]. In a recent study, it was demonstrated MNP hyperthermia efficiently disrupted *S. aureus* biofilms *in vitro* and in an *in vivo* mouse model of cutaneous wound infection [226].

6. Antimicrobial and Antibiofilm Mechanisms of Nanoparticles

The mechanisms underlying the antimicrobial effects of NPs are not completely understood and vary from the productions of oxidative and/or free radical formation stressors to DNA damage (Figure 1). Table 1 summarizes published findings on the antibacterial and antibiofilm properties of nanostructured materials, ranging from metals, polymers, and their composites. Mechanisms responsible for the antibacterial activity of NPs might involve particle size [227], shape [228], surface charge [229], or composition,and are believed to involve [159, 230–232], cell membrane alterations [233, 234], loss of respiratory activity [235], lipid peroxidation [236], ROS generation [237, 238], DNA unwinding [239], nitrosation of protein thiols [240], or disruptions of metabolic pathways [241, 242].

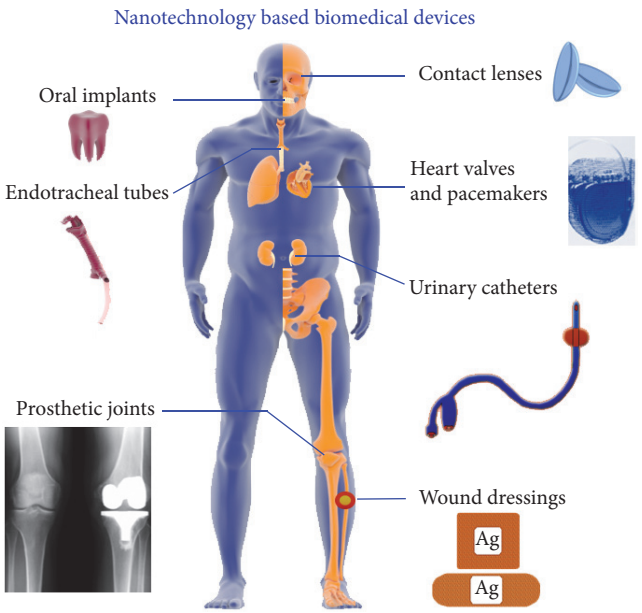

Figure 3: Summary of nanomaterial incorporating medical devices. Prosthetic joint image was reprinted with permission [58].

7. Nanoparticle-Based Antibiofilm Devices

Advances in the nanotechnology have resulted in the developments of high-performance, multifunctional, bioactive materials for biomedical devices. Given base materials with appropriate mechanical (e.g., hardness, stress, and Young's modulus) and tribological properties (e.g., wear resistance, adhesion, and friction), it would appear nanomaterial coatings are likely to result in novel multifunctional and biocompatible materials.

Various nanotools are being incorporated into the surfaces of biomedical devices to combat infections; Figure 3 and Table 1 provide more detail of the antimicrobial mechanisms involved (Figure 1).

8. Future Perspectives

Despite the advances made in the development of novel antibiofilm agents, devised biofilm treatment strategies are limited by their high costs and complexities, which means urgent development is required to identify cost-efficient alternatives. As is made clear by this review, recent developments in nanotechnology-based approaches aimed at preventing, controlling, and treating bacterial biofilm infections, especially of biomedical devices, are worthy of serious consideration. Different nanoparticle types and composites with demonstrated potential bactericidal and fungicidal properties have been shown to be efficient alternatives to antibiotics in terms of wound care and related biomedical issues. Nanomaterials are used as constituents of coatings, biomedical agents, and drug-delivery vehicles and of implant materials and research remains active in these areas. However, key issues like NP resistance and surface interactions between NPs, biofilms, and hosts need to be resolved to ensure successful clinical applications.

Nanomaterial impregnations of antibiofilm devices are believed to provide extended antimicrobial effects and to be minimally toxic as compared with small molecule antimicrobials, which exhibit short term activities and are environmentally toxic. We hope that this review of the literature persuades the reader that nanomaterials and nanomaterial-based biomedical devices with broad spectrum antibiofilm activities will be produced such that they are potent, nontoxic, biocompatible, and cost-effective, and that these novel materials will establish new standards for the treatment and prevention of pathogenic biofilms.

Competing Interests

The authors report no conflict of interests regarding the publication of this paper.

Acknowledgments

This research was supported by National Research Foundation of Korea (NRF) grant funded by the Korea government (MSIP) (no. 2015R1A2A2A01004542 to Jintae Lee) and by the Priority Research Centers Program of the NRF funded by the Ministry of Education (no. 2014R1A6A1031189).

References

[1] C. B. Whitchurch, T. Tolker-Nielsen, P. C. Ragas, and J. S. Mattick, "Extracellular DNA required for bacterial biofilm formation," *Science*, vol. 295, no. 5559, p. 1487, 2002.

[2] K. Lewis, "Persister cells and the riddle of biofilm survival," *Biochemistry*, vol. 70, no. 2, pp. 267–274, 2005.

[3] T.-F. C. Mah and G. A. O'Toole, "Mechanisms of biofilm resistance to antimicrobial agents," *Trends in Microbiology*, vol. 9, no. 1, pp. 34–39, 2001.

[4] A. Dongari-Bagtzoglou, "Pathogenesis of mucosal biofilm infections: challenges and progress," *Expert Review of Anti-Infective Therapy*, vol. 6, no. 2, pp. 201–208, 2008.

[5] Y. A. Nikolaev and V. K. Plakunov, "Biofilm-'city of microbes' or an analogue of multicellular organisms?" *Microbiology*, vol. 76, no. 2, pp. 125–138, 2007.

[6] B. Allegranzi, S. B. Nejad, C. Combescure et al., "Burden of endemic health-care-associated infection in developing countries: systematic review and meta-analysis," *The Lancet*, vol. 377, no. 9761, pp. 228–241, 2011.

[7] P. Zarb, B. Coignard, J. Griskeviciene et al., "The European Centre for Disease Prevention and Control (ECDC) pilot point prevalence survey of healthcare-associated infections and antimicrobial use," *Euro Surveillance*, vol. 17, no. 46, article 2, 2012.

[8] R. Torrecillas, M. Díaz, F. Barba, M. Miranda, F. Guitián, and J. S. Moya, "Synthesis and antimicrobial activity of a silver-hydroxyapatite nanocomposite," *Journal of Nanomaterials*, vol. 2009, Article ID 498505, 6 pages, 2009.

[9] V. Stanić, D. Janaćković, S. Dimitrijević et al., "Synthesis of antimicrobial monophase silver-doped hydroxyapatite nanopowders for bone tissue engineering," *Applied Surface Science*, vol. 257, no. 9, pp. 4510–4518, 2011.

[10] V. P. Pattani and J. W. Tunnell, "Nanoparticle-mediated photothermal therapy: a comparative study of heating for different particle types," *Lasers in Surgery and Medicine*, vol. 44, no. 8, pp. 675–684, 2012.

[11] G. Vallejo-Fernandez, O. Whear, A. G. Roca et al., "Mechanisms of hyperthermia in magnetic nanoparticles," *Journal of Physics D: Applied Physics*, vol. 46, no. 31, Article ID 312001, 2013.

[12] C. G. Kumar and P. Sujitha, "Green synthesis of Kocuran-functionalized silver glyconanoparticles for use as antibiofilm coatings on silicone urethral catheters," *Nanotechnology*, vol. 25, no. 32, Article ID 325101, 2014.

[13] P. Lackner, R. Beer, G. Broessner et al., "Efficacy of silver nanoparticles-impregnated external ventricular drain catheters in patients with acute occlusive hydrocephalus," *Neurocritical Care*, vol. 8, no. 3, pp. 360–365, 2008.

[14] K. Wu, Y. Yang, Y. Zhang, J. Deng, and C. Lin, "A ntimicrobial activity and cytocompatibility of silver nanoparticles coated catheters via a biomimetic surface functionalization strategy," *International Journal of Nanomedicine*, vol. 10, pp. 7241–7252, 2015.

[15] L. E. Fisher, A. L. Hook, W. Ashraf et al., "Biomaterial modification of urinary catheters with antimicrobials to give long-term broadspectrum antibiofilm activity," *Journal of Controlled Release*, vol. 202, pp. 57–64, 2015.

[16] K. Giri, L. R. Yepes, B. Duncan et al., "Targeting bacterial biofilms via surface engineering of gold nanoparticles," *RSC Advances*, vol. 5, no. 128, pp. 105551–105559, 2015.

[17] S. Taheri, K. Vasilev, and P. Majewski, "Silver nanoparticles: synthesis, antimicrobial coatings, and applications for medical devices," *Recent Patents on Materials Science*, vol. 8, no. 2, pp. 166–175, 2015.

[18] Z. Shi, K. G. Neoh, E. T. Kang, and W. Wang, "Antibacterial and mechanical properties of bone cement impregnated with chitosan nanoparticles," *Biomaterials*, vol. 27, no. 11, pp. 2440–2449, 2006.

[19] L.-M. Sun, C.-L. Zhang, and P. Li, "Characterization, antibiofilm, and mechanism of action of novel PEG-stabilized lipid nanoparticles loaded with terpinen-4-ol," *Journal of Agricultural and Food Chemistry*, vol. 60, no. 24, pp. 6150–6156, 2012.

[20] Y. Li, P. Leung, L. Yao, Q. W. Song, and E. Newton, "Antimicrobial effect of surgical masks coated with nanoparticles," *Journal of Hospital Infection*, vol. 62, no. 1, pp. 58–63, 2006.

[21] L. Zhang, S. Keogh, and C. M. Rickard, "Reducing the risk of infection associated with vascular access devices through nanotechnology: a perspective," *International Journal of Nanomedicine*, vol. 8, pp. 4453–4466, 2013.

[22] J. T. T. Angelina, S. Ganesan, T. M. R. Panicker, R. Narayani, M. Paul Korath, and K. Jagadeesan, "Pulsed laser deposition of silver nanoparticles on prosthetic heart valve material to prevent bacterial infection," *Materials Technology*, 2016.

[23] G. L. Grunkemeier, R. Jin, and A. Starr, "Prosthetic heart valves: objective performance criteria versus randomized clinical trial," *The Annals of Thoracic Surgery*, vol. 82, no. 3, pp. 776–780, 2006.

[24] M. Andara, A. Agarwal, D. Scholvin et al., "Hemocompatibility of diamondlike carbon-metal composite thin films," *Diamond and Related Materials*, vol. 15, no. 11-12, pp. 1941–1948, 2006.

[25] C. J. Walraven and S. A. Lee, "Antifungal lock therapy," *Antimicrobial Agents and Chemotherapy*, vol. 57, no. 1, pp. 1–8, 2013.

[26] C. H. Ho, E. K. Odermatt, I. Berndt, and J. C. Tiller, "Long-term active antimicrobial coatings for surgical sutures based on silver nanoparticles and hyperbranched polylysine," *Journal of Biomaterials Science, Polymer Edition*, vol. 24, no. 13, pp. 1589–1600, 2013.

[27] D. B. Hazer, M. Sakar, Y. Dere, G. Altinkanat, M. I. Ziyal, and B. Hazer, "Polymer-based silver nanoparticle coated pedicle screws inhibits biofilm formation—a novel experimental model in rabbits," *Global Spine Journal*, vol. 6, no. 1, supplement, p. GO226, 2016.

[28] L. Atar-Froyman, A. Sharon, E. I. Weiss et al., "Anti-biofilm properties of wound dressing incorporating nonrelease polycationic antimicrobials," *Biomaterials*, vol. 46, pp. 141–148, 2015.

[29] E. Elizabeth, G. Baranwal, A. G. Krishnan, D. Menon, and M. Nair, "ZnO nanoparticle incorporated nanostructured metallic titanium for increased mesenchymal stem cell response and antibacterial activity," *Nanotechnology*, vol. 25, no. 11, Article ID 115101, 2014.

[30] Z. Peng, J. Ni, K. Zheng et al., "Dual effects and mechanism of TiO_2 nanotube arrays in reducing bacterial colonization and enhancing C3H10T1/2 cell adhesion," *International Journal of Nanomedicine*, vol. 8, pp. 3093–3105, 2013.

[31] X. Chen, K. Cai, J. Fang et al., "Dual action antibacterial TiO_2 nanotubes incorporated with silver nanoparticles and coated with a quaternary ammonium salt (QAS)," *Surface and Coatings Technology*, vol. 216, pp. 158–165, 2013.

[32] E. De Giglio, A. Trapani, D. Cafagna et al., "Ciprofloxacin-loaded chitosan nanoparticles as titanium coatings: a valuable strategy to prevent implant-associated infections," *Nano Biomedicine and Engineering*, vol. 4, no. 4, pp. 163–169, 2012.

[33] L. de Freitas, G. Calixto, M. Chorilli et al., "Polymeric nanoparticle-based photodynamic therapy for chronic periodontitis in vivo," *International Journal of Molecular Sciences*, vol. 17, no. 5, p. 769, 2016.

[34] E. H. Abdulkareem, K. Memarzadeh, R. P. Allaker, J. Huang, J. Pratten, and D. Spratt, "Anti-biofilm activity of zinc oxide and hydroxyapatite nanoparticles as dental implant coating materials," *Journal of Dentistry*, vol. 43, no. 12, pp. 1462–1469, 2015.

[35] L. Zhao, H. Wang, K. Huo et al., "Antibacterial nano-structured titania coating incorporated with silver nanoparticles," *Biomaterials*, vol. 32, no. 24, pp. 5706–5716, 2011.

[36] S. Sharma, S. Bano, A. S. Ghosh et al., "Silk fibroin nanoparticles support *in vitro* sustained antibiotic release and osteogenesis on titanium surface," *Nanomedicine: Nanotechnology, Biology and Medicine*, vol. 12, no. 5, pp. 1193–1204, 2016.

[37] A. P. R. Magalhães, L. B. Santos, L. G. Lopes et al., "Nanosilver application in dental cements," *ISRN Nanotechnology*, vol. 2012, Article ID 365438, 6 pages, 2012.

[38] S.-J. Ahn, S.-J. Lee, J.-K. Kook, and B.-S. Lim, "Experimental antimicrobial orthodontic adhesives using nanofillers and silver nanoparticles," *Dental Materials*, vol. 25, no. 2, pp. 206–213, 2009.

[39] W. Qu, J. M. M. Hooymans, J. Qiu et al., "Nonadhesive, silica nanoparticles-based brush-coated contact lens cases—compromising between ease of cleaning and microbial transmission to contact lenses," *Journal of Biomedical Materials Research Part B: Applied Biomaterials*, vol. 101, no. 4, pp. 640–647, 2013.

[40] B. S. F. Bazzaz, B. Khameneh, M.-M. Jalili-Behabadi, B. Malaekeh-Nikouei, and S. A. Mohajeri, "Preparation, characterization and antimicrobial study of a hydrogel (soft contact lens) material impregnated with silver nanoparticles," *Contact Lens and Anterior Eye*, vol. 37, no. 3, pp. 149–152, 2014.

[41] R. Tuby, S. Gutfreund, I. Perelshtein et al., "Fabrication of a stable and efficient antibacterial nanocoating of Zn-CuO on contact lenses," *ChemNanoMat*, vol. 2, no. 6, pp. 547–551, 2016.

[42] J.-F. Huang, J. Zhong, G.-P. Chen et al., "A hydrogel-based hybrid theranostic contact lens for fungal keratitis," *ACS Nano*, vol. 10, no. 7, pp. 6464–6473, 2016.

[43] J. W. Costerton, Z. Lewandowski, D. E. Caldwell, D. R. Korber, and H. M. Lappin-Scott, "Microbial biofilms," *Annual Review of Microbiology*, vol. 49, no. 1, pp. 711–745, 1995.

[44] D. Estivill, A. Arias, A. Torres-Lana, A. J. Carrillo-Muñoz, and M. P. Arévalo, "Biofilm formation by five species of *Candida* on three clinical materials," *Journal of Microbiological Methods*, vol. 86, no. 2, pp. 238–242, 2011.

[45] S. Neethirajan, M. A. Clond, and A. Vogt, "Medical biofilms—nanotechnology approaches," *Journal of Biomedical Nanotechnology*, vol. 10, no. 10, pp. 2806–2827, 2014.

[46] M. Kostakioti, M. Hadjifrangiskou, and S. J. Hultgren, "Bacterial biofilms: development, dispersal, and therapeutic strategies in the dawn of the postantibiotic era," *Cold Spring Harbor Perspectives in Medicine*, vol. 3, no. 4, article a010306, 2013.

[47] I. Banerjee, R. C. Pangule, and R. S. Kane, "Antifouling coatings: recent developments in the design of surfaces that prevent fouling by proteins, bacteria, and marine organisms," *Advanced Materials*, vol. 23, no. 6, pp. 690–718, 2011.

[48] V. Kochkodan and N. Hilal, "A comprehensive review on surface modified polymer membranes for biofouling mitigation," *Desalination*, vol. 356, pp. 187–207, 2015.

[49] H. Zhang and M. Chiao, "Anti-fouling coatings of poly (dimethylsiloxane) devices for biological and biomedical applications," *Journal of Medical and Biological Engineering*, vol. 35, no. 2, pp. 143–155, 2015.

[50] C.-J. Jung, C.-Y. Yeh, C.-T. Shun et al., "Platelets enhance biofilm formation and resistance of endocarditis-inducing *streptococci* on the injured heart valve," *Journal of Infectious Diseases*, vol. 205, no. 7, pp. 1066–1075, 2012.

[51] L. Hall-Stoodley, J. W. Costerton, and P. Stoodley, "Bacterial biofilms: from the natural environment to infectious diseases," *Nature Reviews Microbiology*, vol. 2, no. 2, pp. 95–108, 2004.

[52] F. Götz, "*Staphylococcus* and biofilms," *Molecular Microbiology*, vol. 43, no. 6, pp. 1367–1378, 2002.

[53] C. Vuong, S. Kocianova, Y. Yao, A. B. Carmody, and M. Otto, "Increased colonization of indwelling medical devices by quorum-sensing mutants of *Staphylococcus epidermidis* in vivo," *Journal of Infectious Diseases*, vol. 190, no. 8, pp. 1498–1505, 2004.

[54] A. L. Spoering and K. Lewis, "Biofilms and planktonic cells of *Pseudomonas aeruginosa* have similar resistance to killing by antimicrobials," *Journal of Bacteriology*, vol. 183, no. 23, pp. 6746–6751, 2001.

[55] C. Von Eiff, C. Heilmann, and G. Peters, "New aspects in the molecular basis of polymer-associated infections due to *staphylococci*," *European Journal of Clinical Microbiology and Infectious Diseases*, vol. 18, no. 12, pp. 843–846, 1999.

[56] S. Niveditha, S. Pramodhini, S. Umadevi, S. Kumar, and S. Stephen, "The isolation and the biofilm formation of uropathogens in the patients with catheter associated urinary tract infections (UTIs)," *Journal of Clinical and Diagnostic Research*, vol. 6, no. 9, pp. 1478–1482, 2012.

[57] V. Antoci Jr., C. S. Adams, J. Parvizi et al., "The inhibition of *Staphylococcus epidermidis* biofilm formation by vancomycin-modified titanium alloy and implications for the treatment of periprosthetic infection," *Biomaterials*, vol. 29, no. 35, pp. 4684–4690, 2008.

[58] E. McPherson, M. Dipane, and S. Sherif, "Dissolvable antibiotic beads in treatment of periprosthetic joint infection and revision arthroplasty—The Use of Synthetic Pure Calcium Sulfate (Stimulan®) impregnated with vancomycin & tobramycin," *Reconstructive Review*, vol. 3, no. 1, 2013.

[59] S. N. Hocevar, J. R. Edwards, T. C. Horan, G. C. Morrell, M. Iwamoto, and F. C. Lessa, "Device-associated infections among neonatal intensive care unit patients: Incidence and associated pathogens reported to the national healthcare Safety Network, 2006–2008," *Infection Control and Hospital Epidemiology*, vol. 33, no. 12, pp. 1200–1206, 2012.

[60] S. Hopkins, K. Shaw, and L. Simpson, *English National Point Prevalence Survey on Healthcare-Associated Infections and Antimicrobial Use*, Health Protection Agency, London, UK, 2011.

[61] S. Saint, C. P. Kowalski, S. R. Kaufman et al., "Preventing hospital-acquired urinary tract infection in the United States: A National Study," *Clinical Infectious Diseases*, vol. 46, no. 2, pp. 243–250, 2008.

[62] E. van Kleef, J. V. Robotham, M. Jit, S. R. Deeny, and W. J. Edmunds, "Modelling the transmission of healthcare associated infections: a systematic review," *BMC Infectious Diseases*, vol. 13, article 294, 2013.

[63] R. D. Scott, *The Direct Medical Costs of Healthcare-Associated Infections in US Hospitals and the Benefits of Prevention*, Division of Healthcare Quality Promotion National Center for Preparedness, Detection, and Control of Infectious Diseases, Centers for Disease Control and Prevention, 2009.

[64] K. Ruellan, J. H. M. Frijns, G. V. Bloemberg et al., "Detection of bacterial biofilm on cochlear implants removed because of device failure, without evidence of infection," *Otology and Neurotology*, vol. 31, no. 8, pp. 1320–1324, 2010.

[65] J. A. T. Sandoe, I. R. Witherden, J. H. Cove, J. Heritage, and M. H. Wilcox, "Correlation between enterococcal biofilm formation in vitro and medical-device-related infection potential in vivo," *Journal of Medical Microbiology*, vol. 52, no. 7, pp. 547–550, 2003.

[66] J. Rogers, D. I. Norkett, P. Bracegirdle et al., "Examination of biofilm formation and risk of infection associated with the use of urinary catheters with leg bags," *Journal of Hospital Infection*, vol. 32, no. 2, pp. 105–115, 1996.

[67] P. Stoodley, S. Kathju, F. Z. Hu et al., "Molecular and imaging techniques for bacterial biofilms in joint arthroplasty infections," *Clinical Orthopaedics and Related Research*, no. 437, pp. 31–40, 2005.

[68] F. Gemmel, H. Van Den Wyngaert, C. Love, M. M. Welling, P. Gemmel, and C. J. Palestro, "Prosthetic joint infections: radionuclide state-of-the-art imaging," *European Journal of Nuclear Medicine and Molecular Imaging*, vol. 39, no. 5, pp. 892–909, 2012.

[69] C. L. Parsons, P. C. Stein, M. K. Dobke, C. P. Virden, and D. H. Frank, "Diagnosis and therapy of subclinically infected prostheses," *Journal of the American College of Surgeon*, vol. 177, no. 5, pp. 504–506, 1993.

[70] M. J. Elder, F. Stapleton, E. Evans, and J. K. G. Dart, "Biofilm-related infections in ophthalmology," *Eye*, vol. 9, no. 1, pp. 102–109, 1995.

[71] T. F. Moriarty, U. Schlegel, S. Perren, and R. G. Richards, "Infection in fracture fixation: can we influence infection rates through implant design?" *Journal of Materials Science: Materials in Medicine*, vol. 21, no. 3, pp. 1031–1035, 2010.

[72] D. G. Hargreaves, A. Pajkos, A. K. Deva, K. Vickery, S. L. Filan, and M. A. Tonkin, "The re-attachment of tendon and ligament avulsions," *Journal of Hand Surgery*, vol. 27, no. 4, pp. 337–341, 2002.

[73] A. Pajkos, A. K. Deva, K. Vickery, C. Cope, L. Chang, and Y. E. Cossart, "Detection of subclinical infection in significant breast implant capsules," *Plastic and Reconstructive Surgery*, vol. 111, no. 5, pp. 1605–1611, 2003.

[74] C. P. Virden, M. K. Dobke, P. Stein, C. L. Parsons, and D. H. Frank, "Subclinical infection of the silicone breast implant surface as a possible cause of capsular contracture," *Aesthetic Plastic Surgery*, vol. 16, no. 2, pp. 173–179, 1992.

[75] G. M. Viola and R. O. Darouiche, "Cardiovascular implantable device infections," *Current Infectious Disease Reports*, vol. 13, no. 4, pp. 333–342, 2011.

[76] A. Pajkos, K. Vickery, and Y. Cossart, "Is biofilm accumulation on endoscope tubing a contributor to the failure of cleaning and decontamination?" *Journal of Hospital Infection*, vol. 58, no. 3, pp. 224–229, 2004.

[77] J. J. Y. Sung, "Bacterial biofilm and clogging of biliary stents," *Journal of Industrial Microbiology*, vol. 15, no. 3, pp. 152–155, 1995.

[78] R. O. Darouiche, "Treatment of infections associated with surgical implants," *The New England Journal of Medicine*, vol. 350, no. 14, pp. 1422–1429, 2004.

[79] K. H. Ward, M. E. Olson, K. Lam, and J. W. Costerton, "Mechanism of persistent infection associated with peritoneal implants," *Journal of Medical Microbiology*, vol. 36, no. 6, pp. 406–413, 1992.

[80] H. W. Boucher, G. H. Talbot, J. S. Bradley et al., "Bad bugs, no drugs: no ESKAPE! An update from the Infectious Diseases Society of America," *Clinical Infectious Diseases*, vol. 48, no. 1, pp. 1–12, 2009.

[81] V. D. Rosenthal, D. G. Maki, S. Jamulitrat et al., "International Nosocomial Infection Control Consortium (INICC) report, data summary for 2003–2008, issued June 2009," *American Journal of Infection Control*, vol. 38, no. 2, pp. 95.e2–104.e2, 2010.

[82] N. P. O'Grady, "Review: paired quantitative blood cultures most accurately detect intravascular device-related bloodstream infection," *ACP Journal Club*, vol. 143, no. 3, p. 77, 2005.

[83] R. M. Donlan, R. Murga, M. Bell et al., "Protocol for detection of biofilms on needleless connectors attached to central venous catheters," *Journal of Clinical Microbiology*, vol. 39, no. 2, pp. 750–753, 2001.

[84] I. Raad, W. Costerton, U. Sabharwal, M. Sacilowski, E. Anaissie, and G. P. Bodey, "Ultrastructural analysis of indwelling vascular catheters: a quantitative relationship between luminal colonization and duration of placement," *Journal of Infectious Diseases*, vol. 168, no. 2, pp. 400–407, 1993.

[85] D. J. Stickler, "Bacterial biofilms in patients with indwelling urinary catheters," *Nature Clinical Practice Urology*, vol. 5, no. 11, pp. 598–608, 2008.

[86] S. L. Percival, N. A. Sabbuba, P. Kite, and D. J. Stickler, "The effect of EDTA instillations on the rate of development of encrustation and biofilms in Foley catheters," *Urological Research*, vol. 37, no. 4, pp. 205–209, 2009.

[87] D. Kaye and M. Hessen, "Infections associated with foreign bodies in the urinary tract," in *Infections Associated with Indwelling Medical Devices*, pp. 291–307, American Society for Microbiology, Washington, DC, USA, 1994.

[88] D. J. Stickler and S. D. Morgan, "Observations on the development of the crystalline bacterial biofilms that encrust and block Foley catheters," *Journal of Hospital Infection*, vol. 69, no. 4, pp. 350–360, 2008.

[89] S. S. Talsma, "Biofilms on medical devices," *Home Healthcare Nurse*, vol. 25, no. 9, pp. 589–594, 2007.

[90] T. T. Bauer, A. Torres, R. Ferrer, C. M. Heyer, G. Schultze-Werninghaus, and K. Rasche, "Biofilm formation in endotracheal tubes. Association between pneumonia and the persistence of pathogens," *Monaldi Archives for Chest Disease—Pulmonary Series*, vol. 57, no. 1, pp. 84–87, 2002.

[91] I. Vandecandelaere and T. Coenye, "Microbial composition and antibiotic resistance of biofilms recovered from endotracheal tubes of mechanically ventilated patients," in *Biofilm-Based Healthcare-Associated Infections*, pp. 137–155, Springer, 2015.

[92] I. Vandecandelaere, N. Matthijs, F. van Nieuwerburgh et al., "Assessment of microbial diversity in biofilms recovered from endotracheal tubes using culture dependent and independent approaches," *PLoS ONE*, vol. 7, no. 6, article e38401, 2012.

[93] D. J. McMinn, K. I. Snell, J. Daniel, R. B. Treacy, P. B. Pynsent, and R. D. Riley, "Mortality and implant revision rates of hip arthroplasty in patients with osteoarthritis: registry based cohort study," *British Medical Journal*, vol. 344, Article ID e3319, 2012.

[94] J. L. Del Pozo and R. Patel, "Infection associated with prosthetic joints," *The New England Journal of Medicine*, vol. 361, no. 8, pp. 787–794, 2009.

[95] W. Vongpatanasin, L. D. Hillis, and R. A. Lange, "Prosthetic heart valves," *The New England Journal of Medicine*, vol. 335, no. 6, pp. 407–416, 1996.

[96] M. C. Chifiriuc, O. Banu, C. Bleotu, V. Lazar, and V. Lazăr, "Interaction of bacteria isolated from clinical biofilms with cardiovascular prosthetic devices and eukaryotic cells," *Anaerobe*, vol. 17, no. 6, pp. 419–421, 2011.

[97] S. Bosio, S. Leekha, S. I. Gamb, A. J. Wright, C. L. Terrell, and D. V. Miller, "Mycobacterium fortuitum prosthetic valve endocarditis: a case for the pathogenetic role of biofilms," *Cardiovascular Pathology*, vol. 21, no. 4, pp. 361–364, 2012.

[98] L. B. Szczotka-Flynn, Y. Imamura, J. Chandra et al., "Increased resistance of contact lens-related bacterial biofilms to antimicrobial activity of soft contact lens care solutions," *Cornea*, vol. 28, no. 8, pp. 918–926, 2009.

[99] X. Gu, J. D. Jennings, J. Snarr, V. Chaudhary, J. E. Pollard, and P. B. Savage, "Optimization of ceragenins for prevention of bacterial colonization of hydrogel contact lenses," *Investigative Ophthalmology and Visual Science*, vol. 54, no. 9, pp. 6217–6223, 2013.

[100] K. J. Bozic, S. M. Kurtz, E. Lau, K. Ong, D. T. P. Vail, and D. J. Berry, "The epidemiology of revision total hip arthroplasty in the United States," *The Journal of Bone & Joint Surgery—American Volume*, vol. 91, no. 1, pp. 128–133, 2009.

[101] G. N. Belibasakis, "Microbiological and immuno-pathological aspects of peri-implant diseases," *Archives of Oral Biology*, vol. 59, no. 1, pp. 66–72, 2014.

[102] M. Gahlert, T. Gudehus, S. Eichhorn, E. Steinhauser, H. Kniha, and W. Erhardt, "Biomechanical and histomorphometric comparison between zirconia implants with varying surface textures and a titanium implant in the maxilla of miniature pigs," *Clinical Oral Implants Research*, vol. 18, no. 5, pp. 662–668, 2007.

[103] S. Grassi, A. Piattelli, D. S. Ferrari et al., "Histologic evaluation of human bone integration on machined and sandblasted acid-etched titanium surfaces in type IV bone," *Journal of Oral Implantology*, vol. 33, no. 1, pp. 8–12, 2007.

[104] C. Mangano, A. De Rosa, V. Desiderio et al., "The osteoblastic differentiation of dental pulp stem cells and bone formation on different titanium surface textures," *Biomaterials*, vol. 31, no. 13, pp. 3543–3551, 2010.

[105] B. R. Burkhardt, M. Fried, P. L. Schnur, and J. J. Tofield, "Capsules, infection, and intraluminal antibiotics," *Plastic & Reconstructive Surgery*, vol. 68, no. 1, pp. 43–47, 1981.

[106] S. Bartsich, J. A. Ascherman, S. Whittier, C. A. Yao, and C. Rohde, "The breast: a clean-contaminated surgical site," *Aesthetic Surgery Journal*, vol. 31, no. 7, pp. 802–806, 2011.

[107] E. H. Courtiss, R. M. Goldwyn, and G. W. Anastasi, "The fate of breast implants with infections around them," *Plastic and Reconstructive Surgery*, vol. 63, no. 6, pp. 812–816, 1979.

[108] J. W. Thornton, L. C. Argenta, K. D. McClatchey, and M. W. Marks, "Studies on the endogenous flora of the human breast," *Annals of Plastic Surgery*, vol. 20, no. 1, pp. 39–42, 1988.

[109] K. G. Neoh and E. T. Kang, "Combating bacterial colonization on metals via polymer coatings: relevance to marine and medical applications," *ACS Applied Materials and Interfaces*, vol. 3, no. 8, pp. 2808–2819, 2011.

[110] H. Shintani, "Modification of medical device surface to attain anti-infection," *Trends in Biomaterials and Artificial Organs*, vol. 18, no. 1, pp. 1–8, 2004.

[111] C. S. Kwok, T. A. Horbett, and B. D. Ratner, "Design of infection-resistant antibiotic-releasing polymers: II. Controlled release of antibiotics through a plasma-deposited thin film barrier," *Journal of Controlled Release*, vol. 62, no. 3, pp. 301–311, 1999.

[112] R. N. S. Sodhi, V. P. Sahi, and M. W. Mittelman, "Application of electron spectroscopy and surface modification techniques in the development of anti-microbial coatings for medical devices," *Journal of Electron Spectroscopy and Related Phenomena*, vol. 121, no. 1–3, pp. 249–264, 2001.

[113] L. Li, S. Molin, L. Yang, and S. Ndoni, "Sodium dodecyl sulfate (SDS)-loaded nanoporous polymer as anti-biofilm surface coating material," *International Journal of Molecular Sciences*, vol. 14, no. 2, pp. 3050–3064, 2013.

[114] B. Gottenbos, H. C. van der Mei, F. Klatter, P. Nieuwenhuis, and H. J. Busscher, "In vitro and in vivo antimicrobial activity of covalently coupled quaternary ammonium silane coatings on silicone rubber," *Biomaterials*, vol. 23, no. 6, pp. 1417–1423, 2002.

[115] E. B. H. Hume, J. Baveja, B. Muir et al., "The control of *Staphylococcus epidermidis* biofilm formation and in vivo infection rates by covalently bound furanones," *Biomaterials*, vol. 25, no. 20, pp. 5023–5030, 2004.

[116] S. V. Pavlukhina, J. B. Kaplan, L. Xu et al., "Noneluting enzymatic antibiofilm coatings," *ACS Applied Materials and Interfaces*, vol. 4, no. 9, pp. 4708–4716, 2012.

[117] X. Khoo, P. Hamilton, G. A. O'Toole, B. D. Snyder, D. J. Kenan, and M. W. Grinstaff, "Directed assembly of PEGylated-peptide coatings for infection-resistant titanium metal," *Journal of the American Chemical Society*, vol. 131, no. 31, pp. 10992–10997, 2009.

[118] A. L. Z. Lee, V. W. L. Ng, W. Wang, J. L. Hedrick, and Y. Y. Yang, "Block copolymer mixtures as antimicrobial hydrogels for biofilm eradication," *Biomaterials*, vol. 34, no. 38, pp. 10278–10286, 2013.

[119] C. R. Arciola, D. Campoccia, P. Speziale, L. Montanaro, and J. W. Costerton, "Biofilm formation in *Staphylococcus* implant infections. A review of molecular mechanisms and implications for biofilm-resistant materials," *Biomaterials*, vol. 33, no. 26, pp. 5967–5982, 2012.

[120] J. Hasan, R. J. Crawford, and E. P. Ivanova, "Antibacterial surfaces: the quest for a new generation of biomaterials," *Trends in Biotechnology*, vol. 31, no. 5, pp. 295–304, 2013.

[121] C. Tedjo, K. G. Neoh, E. T. Kang, N. Fang, and V. Chan, "Bacteria–surface interaction in the presence of proteins and surface attached poly (ethylene glycol) methacrylate chains," *Journal of Biomedical Materials Research Part A*, vol. 82, no. 2, pp. 479–491, 2007.

[122] I. C. S. Fernández, H. C. van der Mei, M. J. Lochhead, D. W. Grainger, and H. J. Busscher, "The inhibition of the adhesion of clinically isolated bacterial strains on multi-component cross-linked poly(ethylene glycol)-based polymer coatings," *Biomaterials*, vol. 28, no. 28, pp. 4105–4112, 2007.

[123] K. D. Park, Y. S. Kim, D. K. Han et al., "Bacterial adhesion on PEG modified polyurethane surfaces," *Biomaterials*, vol. 19, no. 7–9, pp. 851–859, 1998.

[124] A. Roosjen, H. C. van der Mei, H. J. Busscher, and W. Norde, "Microbial adhesion to poly (ethylene oxide) brushes: influence of polymer chain length and temperature," *Langmuir*, vol. 20, no. 25, pp. 10949–10955, 2004.

[125] G. D. Bixler and B. Bhushan, "Biofouling: lessons from nature, Philosophical Transactions of the Royal Society of London A: Mathematical," *Physical and Engineering Sciences*, vol. 370, no. 1967, pp. 2381–2417, 2012.

[126] E. Celia, T. Darmanin, E. Taffin de Givenchy, S. Amigoni, and F. Guittard, "Recent advances in designing superhydrophobic surfaces," *Journal of Colloid and Interface Science*, vol. 402, pp. 1–18, 2013.

[127] V. A. Ganesh, H. K. Raut, A. S. Nair, and S. Ramakrishna, "A review on self-cleaning coatings," *Journal of Materials Chemistry*, vol. 21, no. 41, pp. 16304–16322, 2011.

[128] R. B. Pernites, C. M. Santos, M. Maldonado, R. R. Ponnapati, D. F. Rodrigues, and R. C. Advincula, "Tunable protein and bacterial cell adsorption on colloidally templated superhydrophobic polythiophene films," *Chemistry of Materials*, vol. 24, no. 5, pp. 870–880, 2012.

[129] K. K. Chung, J. F. Schumacher, E. M. Sampson, R. A. Burne, P. J. Antonelli, and A. B. Brennan, "Impact of engineered surface microtopography on biofilm formation of *Staphylococcus aureus*," *Biointerphases*, vol. 2, no. 2, pp. 89–94, 2007.

[130] M. L. Carman, T. G. Estes, A. W. Feinberg et al., "Engineered antifouling microtopographies—correlating wettability with cell attachment," *Biofouling*, vol. 22, no. 1, pp. 11–21, 2006.

[131] P. Appendini and J. H. Hotchkiss, "Review of antimicrobial food packaging," *Innovative Food Science and Emerging Technologies*, vol. 3, no. 2, pp. 113–126, 2002.

[132] I. Francolini, P. Norris, A. Piozzi, G. Donelli, and P. Stoodley, "Usnic acid, a natural antimicrobial agent able to inhibit bacterial biofilm formation on polymer surfaces," *Antimicrobial Agents and Chemotherapy*, vol. 48, no. 11, pp. 4360–4365, 2004.

[133] M. A. Rojas-Graü, R. Soliva-Fortuny, and O. Martín-Belloso, "Edible coatings to incorporate active ingredients to fresh-cut fruits: a review," *Trends in Food Science and Technology*, vol. 20, no. 10, pp. 438–447, 2009.

[134] J. C. Tiller, C.-J. Liao, K. Lewis, and A. M. Klibanov, "Designing surfaces that kill bacteria on contact," *Proceedings of the*

National Academy of Sciences of the United States of America, vol. 98, no. 11, pp. 5981–5985, 2001.

[135] J. C. J. Webb and R. F. Spencer, "The role of polymethylmethacrylate bone cement in modern orthopaedic surgery," *Journal of Bone and Joint Surgery—Series B*, vol. 89, no. 7, pp. 851–857, 2007.

[136] R. O. Darouiche, "In vivo efficacy of antimicrobial-coated devices," *The Journal of Bone and Joint Surgery*, vol. 90, no. 8, pp. 1785–1786, 2008.

[137] T. Jaeblon, "Polymethylmethacrylate: properties and contemporary uses in orthopaedics," *Journal of the American Academy of Orthopaedic Surgeons*, vol. 18, no. 5, pp. 297–305, 2010.

[138] M. C. B. Ammons, L. S. Ward, and G. A. James, "Anti-biofilm efficacy of a lactoferrin/xylitol wound hydrogel used in combination with silver wound dressings," *International Wound Journal*, vol. 8, no. 3, pp. 268–273, 2011.

[139] A. E. Zeraik and M. Nitschke, "Biosurfactants as agents to reduce adhesion of pathogenic bacteria to polystyrene surfaces: effect of temperature and hydrophobicity," *Current Microbiology*, vol. 61, no. 6, pp. 554–559, 2010.

[140] I. A. Rojas, J. B. Slunt, and D. W. Grainger, "Polyurethane coatings release bioactive antibodies to reduce bacterial adhesion," *Journal of Controlled Release*, vol. 63, no. 1-2, pp. 175–189, 2000.

[141] L. Cegelski, J. S. Pinkner, N. D. Hammer et al., "Small-molecule inhibitors target *Escherichia coli* amyloid biogenesis and biofilm formation," *Nature Chemical Biology*, vol. 5, no. 12, pp. 913–919, 2009.

[142] P. Klemm, V. Hancock, and M. A. Schembri, "Mellowing out: adaptation to commensalism by *Escherichia coli* asymptomatic *bacteriuria strain 83972*," *Infection and Immunity*, vol. 75, no. 8, pp. 3688–3695, 2007.

[143] O. Simonetti, O. Cirioni, R. Ghiselli et al., "RNAIII-inhibiting peptide enhances healing of wounds infected with methicillin-resistant *Staphylococcus aureus*," *Antimicrobial Agents and Chemotherapy*, vol. 52, no. 6, pp. 2205–2211, 2008.

[144] O. Rendueles and J.-M. Ghigo, "Multi-species biofilms: how to avoid unfriendly neighbors," *FEMS Microbiology Reviews*, vol. 36, no. 5, pp. 972–989, 2012.

[145] P. N. Danese, "Antibiofilm approaches: prevention of catheter colonization," *Chemistry and Biology*, vol. 9, no. 8, pp. 873–880, 2002.

[146] K. Vasilev, J. Cook, and H. J. Griesser, "Antibacterial surfaces for biomedical devices," *Expert Review of Medical Devices*, vol. 6, no. 5, pp. 553–567, 2009.

[147] R. Kügler, O. Bouloussa, and F. Rondelez, "Evidence of a charge-density threshold for optimum efficiency of biocidal cationic surfaces," *Microbiology*, vol. 151, no. 5, pp. 1341–1348, 2005.

[148] D. A. Salick, J. K. Kretsinger, D. J. Pochan, and J. P. Schneider, "Inherent antibacterial activity of a peptide-based β-hairpin hydrogel," *Journal of the American Chemical Society*, vol. 129, no. 47, pp. 14793–14799, 2007.

[149] D. F. Williams, "On the mechanisms of biocompatibility," *Biomaterials*, vol. 29, no. 20, pp. 2941–2953, 2008.

[150] J. J. Boelens, J. Dankert, J. L. Murk et al., "Biomaterial-associated persistence of *Staphylococcus epidermidis* in peri-catheter macrophages," *Journal of Infectious Diseases*, vol. 181, no. 4, pp. 1337–1349, 2000.

[151] E. Taylor and T. J. Webster, "Reducing infections through nanotechnology and nanoparticles," *International Journal of Nanomedicine*, vol. 6, pp. 1463–1473, 2011.

[152] P. A. Suci, D. L. Berglund, L. Liepold et al., "High-density targeting of a viral multifunctional nanoplatform to a pathogenic, biofilm-forming bacterium," *Chemistry and Biology*, vol. 14, no. 4, pp. 387–398, 2007.

[153] G. Colon, B. C. Ward, and T. J. Webster, "Increased osteoblast and decreased *Staphylococcus epidermidis* functions on nanophase ZnO and TiO_2," *Journal of Biomedical Materials Research Part A*, vol. 78, no. 3, pp. 595–604, 2006.

[154] N. Jones, B. Ray, K. T. Ranjit, and A. C. Manna, "Antibacterial activity of ZnO nanoparticle suspensions on a broad spectrum of microorganisms," *FEMS Microbiology Letters*, vol. 279, no. 1, pp. 71–76, 2008.

[155] S. D. Puckett, E. Taylor, T. Raimondo, and T. J. Webster, "The relationship between the nanostructure of titanium surfaces and bacterial attachment," *Biomaterials*, vol. 31, no. 4, pp. 706–713, 2010.

[156] M. Salwiczek, Y. Qu, J. Gardiner et al., "Emerging rules for effective antimicrobial coatings," *Trends in Biotechnology*, vol. 32, no. 2, pp. 82–90, 2014.

[157] A. V. Singh, V. Vyas, R. Patil et al., "Quantitative characterization of the influence of the nanoscale morphology of nanostructured surfaces on bacterial adhesion and biofilm formation," *PLoS ONE*, vol. 6, no. 9, Article ID e25029, 2011.

[158] J. V. Loh, S. L. Percival, E. J. Woods, N. J. Williams, and C. A. Cochrane, "Silver resistance in MRSA isolated from wound and nasal sources in humans and animals," *International Wound Journal*, vol. 6, no. 1, pp. 32–38, 2009.

[159] D. Inbakandan, C. Kumar, L. S. Abraham, R. Kirubagaran, R. Venkatesan, and S. A. Khan, "Silver nanoparticles with anti microfouling effect: a study against marine biofilm forming bacteria," *Colloids and Surfaces B: Biointerfaces*, vol. 111, pp. 636–643, 2013.

[160] R. K. Bera, S. M. Mandal, and C. R. Raj, "Antimicrobial activity of fluorescent Ag nanoparticles," *Letters in Applied Microbiology*, vol. 58, no. 6, pp. 520–526, 2014.

[161] R. Sinha, R. Karan, A. Sinha, and S. K. Khare, "Interaction and nanotoxic effect of ZnO and Ag nanoparticles on mesophilic and halophilic bacterial cells," *Bioresource Technology*, vol. 102, no. 2, pp. 1516–1520, 2011.

[162] M. A. Ansari, H. M. Khan, A. A. Khan, S. S. Cameotra, and M. A. Alzohairy, "Anti-biofilm efficacy of silver nanoparticles against MRSA and MRSE isolated from wounds in a tertiary care hospital," *Indian Journal of Medical Microbiology*, vol. 33, no. 1, pp. 101–109, 2015.

[163] K. Naik and M. Kowshik, "Anti-biofilm efficacy of low temperature processed AgCl–TiO_2 nanocomposite coating," *Materials Science and Engineering: C*, vol. 34, no. 1, pp. 62–68, 2014.

[164] V. Kostenko, J. Lyczak, K. Turner, and R. J. Martinuzzi, "Impact of silver-containing wound dressings on bacterial biofilm viability and susceptibility to antibiotics during prolonged treatment," *Antimicrobial Agents and Chemotherapy*, vol. 54, no. 12, pp. 5120–5131, 2010.

[165] J.-H. Lee, Y.-G. Kim, M. H. Cho, and J. Lee, "ZnO nanoparticles inhibit *Pseudomonas aeruginosa* biofilm formation and virulence factor production," *Microbiological Research*, vol. 169, no. 12, pp. 888–896, 2014.

[166] B. M. Geilich and T. J. Webster, "Reduced adhesion of *Staphylococcus aureus* to ZnO/PVC nanocomposites," in *Proceedings of the 39th Annual Northeast Bioengineering Conference (NEBEC '13)*, pp. 7–8, IEEE, Syracuse, NY, USA, April 2013.

[167] W. Zhang, E. S. McLamore, N. T. Garland, J. V. C. Leon, and M. K. Banks, "A simple method for quantifying biomass cell

and polymer distribution in biofilms," *Journal of Microbiological Methods*, vol. 94, no. 3, pp. 367–374, 2013.

[168] F. Haghighi, S. Roudbar Mohammadi, P. Mohammadi, S. Hosseinkhani, and R. Shipour, "Antifungal activity of TiO_2 nanoparticles and EDTA on *Candida albicans* biofilms," *Epidemiology and Medicine*, vol. 1, no. 1, pp. 33–38, 2013.

[169] Y. Ohko, Y. Nagao, K. Okano et al., "Prevention of *Phormidium tenue* biofilm formation by TiO_2 photocatalysis," *Microbes and Environments*, vol. 24, no. 3, pp. 241–245, 2009.

[170] K. Naik, A. Chatterjee, H. Prakash, and M. Kowshik, "Mesoporous TiO_2 nanoparticles containing Ag ion with excellent antimicrobial activity at remarkable low silver concentrations," *Journal of Biomedical Nanotechnology*, vol. 9, no. 4, pp. 664–673, 2013.

[171] G. Ren, D. Hu, E. W. C. Cheng, M. A. Vargas-Reus, P. Reip, and R. P. Allaker, "Characterisation of copper oxide nanoparticles for antimicrobial applications," *International Journal of Antimicrobial Agents*, vol. 33, no. 6, pp. 587–590, 2009.

[172] L. Esteban-Tejeda, F. Malpartida, A. Esteban-Cubillo, C. Pecharromn, and J. S. Moya, "Antibacterial and antifungal activity of a soda-lime glass containing copper nanoparticles," *Nanotechnology*, vol. 20, no. 50, Article ID 505701, 2009.

[173] J. P. Ruparelia, A. K. Chatterjee, S. P. Duttagupta, and S. Mukherji, "Strain specificity in antimicrobial activity of silver and copper nanoparticles," *Acta Biomaterialia*, vol. 4, no. 3, pp. 707–716, 2008.

[174] P. S. Murthy, V. Venugopalan, D. A. Das, S. Dhara, R. Pandiyan, and A. Tyagi, "Antibiofilm activity of nano sized CuO," in *Proceedings of the International Conference on Nanoscience, Engineering and Technology (ICONSET '11)*, pp. 580–583, IEEE, November 2011.

[175] M. Eshed, J. Lellouche, S. Matalon, A. Gedanken, and E. Banin, "Sonochemical coatings of ZnO and CuO nanoparticles inhibit *Streptococcus mutans* biofilm formation on teeth model," *Langmuir*, vol. 28, no. 33, pp. 12288–12295, 2012.

[176] E. N. Taylor, C. P. Toseland, T. K. Attwood, and D. R. Flower, "About novoseek," *International Journal of Nanomedicine*, vol. 4, pp. 145–152, 2009.

[177] M. C. Chifiriuc, A. M. Grumezescu, E. Andronescu et al., "Water dispersible magnetite nanoparticles influence the efficacy of antibiotics against planktonic and biofilm embedded *Enterococcus faecalis* cells," *Anaerobe*, vol. 22, pp. 14–19, 2013.

[178] I. Anghel, C. Limban, A. M. Grumezescu, A. G. Anghel, C. Bleotu, and M. C. Chifiriuc, "In vitro evaluation of antipathogenic surface coating nanofluid, obtained by combining Fe_3O_4/C_{12} nanostructures and 2-((4-ethylphenoxy) methyl)-*N*-(substituted-phenylcarbamothioyl)-benzamides," *Nanoscale Research Letters*, vol. 7, pp. 1–10, 2012.

[179] Q. Yu, J. Li, Y. Zhang, Y. Wang, L. Liu, and M. Li, "Inhibition of gold nanoparticles (AuNPs) on pathogenic biofilm formation and invasion to host cells," *Scientific Reports*, vol. 6, Article ID 26667, 2016.

[180] A. N. Brown, K. Smith, T. A. Samuels, J. Lu, S. O. Obare, and M. E. Scott, "Nanoparticles functionalized with ampicillin destroy multiple-antibiotic-resistant isolates of *Pseudomonas aeruginosa* and *Enterobacter aerogenes* and methicillin-resistant *Staphylococcus aureus*," *Applied and Environmental Microbiology*, vol. 78, no. 8, pp. 2768–2774, 2012.

[181] M. Chamundeeswari, S. S. L. Sobhana, J. P. Jacob et al., "Preparation, characterization and evaluation of a biopolymeric gold nanocomposite with antimicrobial activity," *Biotechnology and Applied Biochemistry*, vol. 55, no. 1, pp. 29–35, 2010.

[182] H. Mu, J. Tang, Q. Liu, C. Sun, T. Wang, and J. Duan, "Potent antibacterial nanoparticles against biofilm and intracellular bacteria," *Scientific Reports*, vol. 6, Article ID 18877, 2016.

[183] W.-Y. Chen, J.-Y. Lin, W.-J. Chen, L. Luo, E. Wei-Guang Diau, and Y.-C. Chen, "Functional gold nanoclusters as antimicrobial agents for antibiotic-resistant bacteria," *Nanomedicine*, vol. 5, no. 5, pp. 755–764, 2010.

[184] J. A. Lichter and M. F. Rubner, "Polyelectrolyte multilayers with intrinsic antimicrobial functionality: the importance of mobile polycations," *Langmuir*, vol. 25, no. 13, pp. 7686–7694, 2009.

[185] B. A. Nevius, Y. P. Chen, J. L. Ferry, and A. W. Decho, "Surface-functionalization effects on uptake of fluorescent polystyrene nanoparticles by model biofilms," *Ecotoxicology*, vol. 21, no. 8, pp. 2205–2213, 2012.

[186] M. A. Hillmyer, "Nanoporous materials from block copolymer precursors," in *Block Copolymers II*, pp. 137–181, Springer, Berlin, Germany, 2005.

[187] W. S. Cheow, M. W. Chang, and K. Hadinoto, "Antibacterial efficacy of inhalable antibiotic-encapsulated biodegradable polymeric nanoparticles against *E. coli* biofilm cells," *Journal of Biomedical Nanotechnology*, vol. 6, no. 4, pp. 391–403, 2010.

[188] X. Li, P. Li, R. Saravanan et al., "Antimicrobial functionalization of silicone surfaces with engineered short peptides having broad spectrum antimicrobial and salt-resistant properties," *Acta Biomaterialia*, vol. 10, no. 1, pp. 258–266, 2014.

[189] S. B. Goodman, Z. Yao, M. Keeney, and F. Yang, "The future of biologic coatings for orthopaedic implants," *Biomaterials*, vol. 34, no. 13, pp. 3174–3183, 2013.

[190] P. J. Nowatzki, R. R. Koepsel, P. Stoodley et al., "Salicylic acid-releasing polyurethane acrylate polymers as anti-biofilm urological catheter coatings," *Acta Biomaterialia*, vol. 8, no. 5, pp. 1869–1880, 2012.

[191] L. G. Harris, S. Tosatti, M. Wieland, M. Textor, and R. G. Richards, "*Staphylococcus aureus* adhesion to titanium oxide surfaces coated with non-functionalized and peptide-functionalized poly(L-lysine)-grafted-poly(ethylene glycol) copolymers," *Biomaterials*, vol. 25, no. 18, pp. 4135–4148, 2004.

[192] P. Kingshott, J. Wei, D. Bagge-Ravn, N. Gadegaard, and L. Gram, "Covalent attachment of poly (ethylene glycol) to surfaces, critical for reducing bacterial adhesion," *Langmuir*, vol. 19, no. 17, pp. 6912–6921, 2003.

[193] K. Bruellhoff, J. Fiedler, M. Möller, J. Groll, and R. E. Brenner, "Surface coating strategies to prevent biofilm formation on implant surfaces," *The International Journal of Artificial Organs*, vol. 33, no. 9, pp. 646–653, 2010.

[194] F. Zhang, Z. Zhang, X. Zhu, E.-T. Kang, and K.-G. Neoh, "Silk-functionalized titanium surfaces for enhancing osteoblast functions and reducing bacterial adhesion," *Biomaterials*, vol. 29, no. 36, pp. 4751–4759, 2008.

[195] E. M. Hetrick, J. H. Shin, N. A. Stasko et al., "Bactericidal efficacy of nitric oxide-releasing silica nanoparticles," *ACS Nano*, vol. 2, no. 2, pp. 235–246, 2008.

[196] L. R. Martinez, G. Han, M. Chacko et al., "Antimicrobial and healing efficacy of sustained release nitric oxide nanoparticles against *Staphylococcus aureus* skin infection," *Journal of Investigative Dermatology*, vol. 129, no. 10, pp. 2463–2469, 2009.

[197] M. R. Mihu, U. Sandkovsky, G. Han, J. M. Friedman, J. D. Nosanchuk, and L. R. Martinez, "The use of nitric oxide releasing nanoparticles as a treatment against *Acinetobacter baumannii* in wound infections," *Virulence*, vol. 1, no. 2, pp. 62–67, 2010.

[198] C. Macherla, D. A. Sanchez, M. S. Ahmadi et al., "Nitric oxide releasing nanoparticles for treatment of *Candida albicans* burn infections," *Frontiers in Microbiology*, vol. 3, article 193, 2012.

[199] D. Depan and R. D. K. Misra, "On the determining role of network structure titania in silicone against bacterial colonization: mechanism and disruption of biofilm," *Materials Science and Engineering: C*, vol. 34, no. 1, pp. 221–228, 2014.

[200] H. Ma, E. T. Darmawan, M. Zhang, L. Zhang, and J. D. Bryers, "Development of a poly (ether urethane) system for the controlled release of two novel anti-biofilm agents based on gallium or zinc and its efficacy to prevent bacterial biofilm formation," *Journal of Controlled Release*, vol. 172, no. 3, pp. 1035–1044, 2013.

[201] K. Ramalingam, N. C. Frohlich, and V. A. Lee, "Effect of nanoemulsion on dental unit waterline biofilm," *Journal of Dental Sciences*, vol. 8, no. 3, pp. 333–336, 2013.

[202] J. Janiszewska, J. Swieton, A. W. Lipkowski, and Z. Urbanczyk-Lipkowska, "Low molecular mass peptide dendrimers that express antimicrobial properties," *Bioorganic and Medicinal Chemistry Letters*, vol. 13, no. 21, pp. 3711–3713, 2003.

[203] E. M. V. Johansson, S. A. Crusz, E. Kolomiets et al., "Inhibition and dispersion of *Pseudomonas aeruginosa* biofilms by glycopeptide dendrimers targeting the fucose-specific lectin LecB," *Chemistry and Biology*, vol. 15, no. 12, pp. 1249–1257, 2008.

[204] A. Gharbi, V. Humblot, F. Turpin, C.-M. Pradier, C. Imbert, and J.-M. Berjeaud, "Elaboration of antibiofilm surfaces functionalized with antifungal-cyclodextrin inclusion complexes," *FEMS Immunology and Medical Microbiology*, vol. 65, no. 2, pp. 257–269, 2012.

[205] C. A. B. Nava-Ortiz, G. Burillo, A. Concheiro et al., "Cyclodextrin-functionalized biomaterials loaded with miconazole prevent *Candida albicans* biofilm formation in vitro," *Acta Biomaterialia*, vol. 6, no. 4, pp. 1398–1404, 2010.

[206] B. Blanco-Fernandez, M. Lopez-Viota, A. Concheiro, and C. Alvarez-Lorenzo, "Synergistic performance of cyclodextrin–agar hydrogels for ciprofloxacin delivery and antimicrobial effect," *Carbohydrate Polymers*, vol. 85, no. 4, pp. 765–774, 2011.

[207] Z. Drulis-Kawa, A. Dorotkiewicz-Jach, J. Gubernator, G. Gula, T. Bocer, and W. Doroszkiewicz, "The interaction between *Pseudomonas aeruginosa* cells and cationic PC: Chol: DOTAP liposomal vesicles versus outer-membrane structure and envelope properties of bacterial cell," *International Journal of Pharmaceutics*, vol. 367, no. 1, pp. 211–219, 2009.

[208] M. Alipour, M. Halwani, A. Omri, and Z. E. Suntres, "Antimicrobial effectiveness of liposomal polymyxin B against resistant Gram-negative bacterial strains," *International Journal of Pharmaceutics*, vol. 355, no. 1-2, pp. 293–298, 2008.

[209] M. Alhariri and A. Omri, "Efficacy of liposomal bismuth-ethanedithiol-loaded tobramycin after intratracheal administration in rats with pulmonary *Pseudomonas aeruginosa* infection," *Antimicrobial Agents and Chemotherapy*, vol. 57, no. 1, pp. 569–578, 2013.

[210] X. F. Wang, S. L. Zhang, L. Y. Zhu et al., "Enhancement of antibacterial activity of tilmicosin against *Staphylococcus aureus* by solid lipid nanoparticles in vitro and in vivo," *The Veterinary Journal*, vol. 191, no. 1, pp. 115–120, 2012.

[211] A. Garg and S. Singh, "Enhancement in antifungal activity of eugenol in immunosuppressed rats through lipid nanocarriers," *Colloids and Surfaces B: Biointerfaces*, vol. 87, no. 2, pp. 280–288, 2011.

[212] I. S. I. Al-Adham, N. D. Al-Hmoud, E. Khalil, M. Kierans, and P. J. Collier, "Microemulsions are highly effective anti-biofilm agents," *Letters in Applied Microbiology*, vol. 36, no. 2, pp. 97–100, 2003.

[213] I. S. I. Al-Adham, H. Ashour, E. Al-Kaissi, E. Khalil, M. Kierans, and P. J. Collier, "Studies on the kinetics of killing and the proposed mechanism of action of microemulsions against fungi," *International Journal of Pharmaceutics*, vol. 454, no. 1, pp. 226–232, 2013.

[214] M.-S. Wong, C.-W. Chen, C.-C. Hsieh, S.-C. Hung, D.-S. Sun, and H.-H. Chang, "Antibacterial property of Ag nanoparticle-impregnated N-doped titania films under visible light," *Scientific Reports*, vol. 5, Article ID 11978, 2015.

[215] J.-H. Lee, Y.-G. Kim, K. Lee, S.-C. Kim, and J. Lee, "Temperature-dependent control of *Staphylococcus aureus* biofilms and virulence by thermoresponsive oligo (N-vinylcaprolactam)," *Biotechnology and Bioengineering*, vol. 112, no. 4, pp. 716–724, 2015.

[216] V. P. Zharov, K. E. Mercer, E. N. Galitovskaya, and M. S. Smeltzer, "Photothermal nanotherapeutics and nanodiagnostics for selective killing of bacteria targeted with gold nanoparticles," *Biophysical Journal*, vol. 90, no. 2, pp. 619–627, 2006.

[217] D. Maity, P. Chandrasekharan, C.-T. Yang et al., "Facile synthesis of water-stable magnetite nanoparticles for clinical MRI and magnetic hyperthermia applications," *Nanomedicine*, vol. 5, no. 10, pp. 1571–1584, 2010.

[218] M. Ramasamy, S. Kim, S. S. Lee, and D. K. Yi, "Recyclable photothermal nano-aggregates of magnetic nanoparticle conjugated gold nanorods for effective pathogenic bacteria lysis," *Journal of Nanoscience and Nanotechnology*, vol. 16, no. 1, pp. 555–561, 2016.

[219] M.-C. Wu, A. R. Deokar, J.-H. Liao, P.-Y. Shih, and Y.-C. Ling, "Graphene-based photothermal agent for rapid and effective killing of bacteria," *ACS Nano*, vol. 7, no. 2, pp. 1281–1290, 2013.

[220] Y. Zhu, M. Ramasamy, and D. K. Yi, "Antibacterial activity of ordered gold nanorod arrays," *ACS Applied Materials and Interfaces*, vol. 6, no. 17, pp. 15078–15085, 2014.

[221] S. S. Lucky, K. C. Soo, and Y. Zhang, "Nanoparticles in photodynamic therapy," *Chemical Reviews*, vol. 115, no. 4, pp. 1990–2042, 2015.

[222] S. Ferro, F. Ricchelli, G. Mancini, G. Tognon, and G. Jori, "Inactivation of methicillin-resistant *Staphylococcus aureus* (MRSA) by liposome-delivered photosensitising agents," *Journal of Photochemistry and Photobiology B: Biology*, vol. 83, no. 2, pp. 98–104, 2006.

[223] S. Khan, F. Alam, A. Azam, and A. U. Khan, "Gold nanoparticles enhance methylene blue-induced photodynamic therapy: a novel therapeutic approach to inhibit *Candida albicans* biofilm," *International Journal of Nanomedicine*, vol. 7, pp. 3245–3257, 2012.

[224] A. Shrestha and A. Kishen, "Antibiofilm efficacy of photosensitizer-functionalized bioactive nanoparticles on multispecies biofilm," *Journal of Endodontics*, vol. 40, no. 10, pp. 1604–1610, 2014.

[225] H. Park, H.-J. Park, J. A. Kim et al., "Inactivation of *Pseudomonas aeruginosa* PA01 biofilms by hyperthermia using superparamagnetic nanoparticles," *Journal of Microbiological Methods*, vol. 84, no. 1, pp. 41–45, 2011.

[226] M.-H. Kim, I. Yamayoshi, S. Mathew, H. Lin, J. Nayfach, and S. I. Simon, "Magnetic nanoparticle targeted hyperthermia of cutaneous *Staphylococcus aureus* infection," *Annals of Biomedical Engineering*, vol. 41, no. 3, pp. 598–609, 2013.

[227] J. R. Morones, J. L. Elechiguerra, A. Camacho et al., "The bactericidal effect of silver nanoparticles," *Nanotechnology*, vol. 16, no. 10, pp. 2346–2353, 2005.

[228] S. Pal, Y. K. Tak, and J. M. Song, "Does the antibacterial activity of silver nanoparticles depend on the shape of the nanoparticle? A study of the gram-negative bacterium *Escherichia coli*," *Applied and Environmental Microbiology*, vol. 73, no. 6, pp. 1712–1720, 2007.

[229] A. M. El Badawy, R. G. Silva, B. Morris, K. G. Scheckel, M. T. Suidan, and T. M. Tolaymat, "Surface charge-dependent toxicity of silver nanoparticles," *Environmental Science and Technology*, vol. 45, no. 1, pp. 283–287, 2011.

[230] M. J. Hajipour, K. M. Fromm, A. Akbar Ashkarran et al., "Antibacterial properties of nanoparticles," *Trends in Biotechnology*, vol. 30, no. 10, pp. 499–511, 2012.

[231] J. A. Lemire, J. J. Harrison, and R. J. Turner, "Antimicrobial activity of metals: mechanisms, molecular targets and applications," *Nature Reviews Microbiology*, vol. 11, no. 6, pp. 371–384, 2013.

[232] R. Y. Pelgrift and A. J. Friedman, "Nanotechnology as a therapeutic tool to combat microbial resistance," *Advanced Drug Delivery Reviews*, vol. 65, no. 13-14, pp. 1803–1815, 2013.

[233] S. L. Warnes, V. Caves, and C. W. Keevil, "Mechanism of copper surface toxicity in *Escherichia coli O157:H7* and *Salmonella* involves immediate membrane depolarization followed by slower rate of DNA destruction which differs from that observed for Gram-positive bacteria," *Environmental Microbiology*, vol. 14, no. 7, pp. 1730–1743, 2012.

[234] H. Yun, J. D. Kim, H. C. Choi, and C. W. Lee, "Antibacterial activity of CNT-Ag and GO-Ag nanocomposites against gram-negative and gram-positive bacteria," *Bulletin of the Korean Chemical Society*, vol. 34, no. 11, pp. 3261–3264, 2013.

[235] G. A. Sotiriou and S. E. Pratsinis, "Antibacterial activity of nanosilver ions and particles," *Environmental Science and Technology*, vol. 44, no. 14, pp. 5649–5654, 2010.

[236] R. Hong, T. Y. Kang, C. A. Michels, and N. Gadura, "Membrane lipid peroxidation in copper alloy-mediated contact killing of *Escherichia coli*," *Applied and Environmental Microbiology*, vol. 78, no. 6, pp. 1776–1784, 2012.

[237] G. Subbiahdoss, S. Sharifi, D. W. Grijpma et al., "Magnetic targeting of surface-modified superparamagnetic iron oxide nanoparticles yields antibacterial efficacy against biofilms of gentamicin-resistant *staphylococci*," *Acta Biomaterialia*, vol. 8, no. 6, pp. 2047–2055, 2012.

[238] C. E. Santo, E. W. Lam, C. G. Elowsky et al., "Bacterial killing by dry metallic copper surfaces," *Applied and Environmental Microbiology*, vol. 77, no. 3, pp. 794–802, 2011.

[239] I. Sondi and B. Salopek-Sondi, "Silver nanoparticles as antimicrobial agent: a case study on *E. coli* as a model for Gram-negative bacteria," *Journal of Colloid and Interface Science*, vol. 275, no. 1, pp. 177–182, 2004.

[240] A. Friedman, K. Blecher, D. Sanchez et al., "Susceptibility of Gram-positive and-negative bacteria to novel nitric oxide-releasing nanoparticle technology," *Virulence*, vol. 2, no. 3, pp. 217–221, 2011.

[241] S. Egger, R. P. Lehmann, M. J. Height, M. J. Loessner, and M. Schuppler, "Antimicrobial properties of a novel silver-silica nanocomposite material," *Applied and Environmental Microbiology*, vol. 75, no. 9, pp. 2973–2976, 2009.

[242] I. Iavicoli, L. Fontana, V. Leso, and A. Bergamaschi, "The effects of nanomaterials as endocrine disruptors," *International Journal of Molecular Sciences*, vol. 14, no. 8, pp. 16732–16801, 2013.

Hindawi Publishing Corporation
BioMed Research International
Volume 2016, Article ID 4034517, 12 pages
http://dx.doi.org/10.1155/2016/4034517

Research Article

Changes in the Expression of Biofilm-Associated Surface Proteins in *Staphylococcus aureus* Food-Environmental Isolates Subjected to Sublethal Concentrations of Disinfectants

Lenka Cincarova,[1] Ondrej Polansky,[2] Vladimir Babak,[1] Pavel Kulich,[3] and Petr Kralik[1]

[1]*Department of Food and Feed Safety, Veterinary Research Institute, Hudcova 70, Brno, Czech Republic*
[2]*Department of Immunology, Veterinary Research Institute, Hudcova 70, Brno, Czech Republic*
[3]*Department of Chemistry and Toxicology, Veterinary Research Institute, Brno, Czech Republic*

Correspondence should be addressed to Lenka Cincarova; lenka.cincarova@gmail.com

Received 14 July 2016; Revised 5 September 2016; Accepted 21 September 2016

Academic Editor: P. Nithyanand

Copyright © 2016 Lenka Cincarova et al. This is an open access article distributed under the Creative Commons Attribution License, which permits unrestricted use, distribution, and reproduction in any medium, provided the original work is properly cited.

Sublethal concentrations (sub-MICs) of certain disinfectants are no longer effective in removing biofilms from abiotic surfaces and can even promote the formation of biofilms. Bacterial cells can probably adapt to these low concentrations of disinfectants and defend themselves by way of biofilm formation. In this paper, we report on three *Staphylococcus aureus* biofilm formers (strong B+++, moderate B++, and weak B+) that were cultivated with sub-MICs of commonly used disinfectants, ethanol or chloramine T, and quantified using Syto9 green fluorogenic nucleic acid stain. We demonstrate that 1.25–2.5% ethanol and 2500 μg/mL chloramine T significantly enhanced *S. aureus* biofilm formation. To visualize differences in biofilm compactness between *S. aureus* biofilms in control medium, 1.25% ethanol, or 2500 μg/mL chloramine T, scanning electron microscopy was used. To describe changes in abundance of surface-exposed proteins in ethanol- or chloramine T-treated biofilms, surface proteins were prepared using a novel trypsin shaving approach and quantified after dimethyl labeling by LC-LTQ/Orbitrap MS. Our data show that some proteins with adhesive functions and others with cell maintenance functions and virulence factor EsxA were significantly upregulated by both treatments. In contrast, immunoglobulin-binding protein A was significantly downregulated for both disinfectants. Significant differences were observed in the effect of the two disinfectants on the expression of surface proteins including some adhesins, foldase protein PrsA, and two virulence factors.

1. Introduction

Staphylococcal food poisoning is considered to be one of the most common foodborne diseases worldwide [1]. Food contamination arises mainly because of inadequately sanitized food-processing equipment and the subsequent formation of biofilms on surfaces [2]. *Staphylococcus aureus* together with *Salmonella* spp., *Campylobacter* spp., enterohemorrhagic *Escherichia coli*, and *Listeria monocytogenes* are the major pathogens that are tested for in the meat industry. Gutiérrez et al., 2012, prepared 442 isolates from food contact surfaces in dairy, meat, or seafood environments and the presence of *S. aureus* was confirmed in 6.1% of samples. The biofilm form of bacteria, in comparison with its free-floating planktonic counterpart, is much more resistant to disinfectants, antibiotics, and phagocytosis [3–5], potentially leading to substantial economic losses and health problems [6]. It was reported that low concentrations (sub-MIC; sub-minimal inhibitory concentration) of residual disinfectants may even provide an opportunity for pathogens to adapt and grow.

A biofilm can be defined as a sessile community of bacterial cells that are embedded in a matrix of extracellular polymeric substance (EPS). Although exopolysaccharides are essential components of the biofilm matrix, recent studies revealed that bacterial surface-exposed proteins probably play a substantial role in biofilm development. Cucarella et al., 2001, studied *S. aureus* adherence and identified a gene, inserted in the SapIbov2 pathogenicity island, which encodes

a surface-exposed protein named Bap (biofilm-associated protein) [7]. The Bap protein is the first of a group of surface-exposed proteins involved in biofilm development to be identified. The *Bap* gene has since been detected in many isolates of staphylococcal species, however, with only low incidence in human isolates. Nevertheless, staphylococcal strains can differ in their pathogenic strategies and may not be dependent on the presence of *Bap* [8]. Cramton et al., 1999, also showed that cell-cell adhesion during biofilm formation is probably mediated via the *ica* locus and, further, that deletion of the *ica* genes (*icaADBC*) eliminates the ability to produce polysaccharide intercellular adhesin (PIA) and to form a biofilm *in vitro* [9]. However, it is now recognized that the accumulation of staphylococci can also be promoted by surface proteins in an *ica*-independent manner (particularly relevant for MRSA strains). These proteins are biofilm-associated proteins Bap [7], ClfB [10], FnBPs [11], SasC [12], SasG [13], and protein A [14]. ClfB, FnBPs, and protein A are widely distributed among strains. When expressed at high levels on the cell surface, FnBPs, protein A, and SasC can promote biofilm formation. However, the mechanisms are not yet clear [11].

Staphylococci are nonmotile and nonspore forming facultative anaerobes. *S. aureus* possesses many adhesion proteins on its surface, but it is not known how they interact with each other to form stable connections with the substrate. Foster et al., 2014, suggested a classification of cell-wall anchored proteins (CWA) based on the presence of motifs that have been defined by structure-function analysis and listed the main group of CWA [15]. The most prevalent group is the Microbial Surface Component Recognizing Adhesive Matrix Molecule (MSCRAMM) family. Many of them are able to bind multiple ligands of the extracellular matrix (ECM) and thus possess extensive substrate plasticity [16]. Expression of surface-exposed proteins can be altered by cultivation conditions: some proteins are expressed mainly in the exponential growth phase [17] and others in the stationary-phase of growth [18].

Cleaning agents containing ethanol are commonly used as disinfectants in food-processing environments. Ethanol is the most popular antibacteriocidal agent, mainly due to its volatile and harmless character; however, alcohols lack sporicidal action and they inadequately penetrate protein-rich materials. For this reason, alcohols are not optimal as single-agent antiseptics for the disposal of biofilms. The bactericidal activity of alcohols is related to their ability to disrupt membrane structures or functions, inhibit protein synthesis [19], interfere with cell division [20], and impair steady-state growth [21]. They also promote variations in fatty acid composition, and alterations in membranes, intracellular pH, and membrane potential [22].

Chloramine T belongs to the group of chlorine-releasing agents (CRAs) and its mechanism of action is not fully known. Chloramine T is bactericidal as well as virucidal [23] and is used in the food industry as an antimicrobial agent [24]. It is commonly used to manage biofilm growth [25]. Growth of a *S. aureus* biofilm can also be enhanced by some processing methods encountered in the food industry, such as suboptimal temperatures or a combination of salt and glucose [26].

The aim of this study was to determine effective concentrations of commonly used food industry disinfectants that can induce biofilm formation and to describe changes in the abundance of surface-exposed proteins during biofilm formation using enzymatic cell surface shaving, dimethyl labeling, and LC-LTQ/Orbitrap analysis.

Enzymatic shaving of intact bacterial cells is a novel, rapid method for identification of surface-exposed peptide epitopes and can be used for protein sorting without the use of, for example, gel separation (2-DE) or 2D-LC coupled with MS/MS [27, 28]. The cell-wall of Gram-positive bacteria is permeable to proteins of approximately 50 kDA and thus trypsin (23 kDa) can diffuse through the cell-wall. Surface-exposed proteins can be integral membrane proteins, lipoproteins, or cell-wall-associated proteins. Cell shaving can result in contamination with cytosolic factors and, thus, the best results have been achieved in Gram-positive bacteria whose thick peptidoglycan cell-walls are more resistant to spontaneous lysis in solution [28]. Tjalsma et al., 2008, also tested trypsin-beads, which are unable to penetrate the bacterial cell-wall and thus probably ensure genuine surface-exposed localization [27]. The trypsin shaving approach has been mainly used thus far in combination with MS analysis for identification of potential vaccine candidates in pathogens such as Streptococcus pyogenes or Bacillus subtilis [29, 30], for characterization of *S. aureus* surfactome interactions with host plasma proteins [31], and for characterization of *S. aureus* adhesins or other surface proteins with adhesive functions [32].

2. Materials and Methods

2.1. Biofilm Cultivation. *Staphylococcus aureus* samples were collected from food contact equipment in meat-processing plants. Sampling was carried out in 2 visits. Samples were taken aseptically from a surface covering approximately 100 cm^2 by using a sterile sampling sponge moistened with LPT Neutralizing Broth and then transported at 4°C to the laboratory for immediate processing. Firstly, the strength of biofilm formation was determined according to Stepanović et al., 2007, [33] and three biofilm forming *S. aureus* isolates (B+++ strong biofilm former, internal collection number: 1275; B++ moderate biofilm former, 1863; B+ weak biofilm former, 1053; all three isolates were collected from knives used in slaughtering) were chosen for assessing the effect of disinfectants on biofilm growth. The *S. aureus* biofilm was grown in TSB (Oxoid Ltd., Hampshire, England) supplemented with 1% NaCl (Penta, Chrudim, Czech Republic) and 1% D-Glucose (Penta, Chrudim, Czech Republic). The *S. aureus* biofilms were cultivated in 96-well polystyrene Nongrowth Enhanced U-Bottomed Tissue Culture Plates (Falcon, NY, USA) with disinfectants (ethanol or chloramine T), which were diluted in supplemented TSB to their respective concentrations (Table 1). A *S. aureus* biofilm cultivated in supplemented TSB without disinfectants was considered as the control. To prepare biofilms, a *S. aureus* inoculum (5 h cultivation in shaking water bath at 37°C) was grown to 1.5×10^9 cfu/mL and then diluted 1 : 100 in TSB and dispensed into 200 μL aliquots in 96-well polystyrene Tissue

Table 1: Tested concentrations of chosen disinfecting agents.

Disinfectant	Characteristic	Range of tested concentrations	Tested concentrations	Concentrations identified as promoting biofilm development (%)
Chloramine T (μg/mL)	Chlorine-releasing agent (CRA)	312–5000	312; 625; 1250; 2500; 5000	Isolates: 1 (B+++): 2500 2 (B++): 2500 3 (B+): 2500
Ethanol (%; v/v)	Alcohol	0.315–20	0.315; 0.63; 1.25; 5; 8; 10; 15; 20	Isolates: 1 (B+++): 0.63; 1.25; 2.5; 5 2 (B++): 0.63; 1.25; 2.5; 5 3 (B+): 1.25

Culture Plates for Syto9 quantification, or into 10 mL aliquots in 6-well polystyrene Flat-Bottomed Nongrowth Enhanced Tissue Culture Plates (Falcon) for surface-exposed protein extraction. Bacteria were incubated in their respective media (control or medium with disinfecting agents) in an incubator (Sanyo, Tokyo, Japan) at 37°C for 48 h. Media were changed after 24 h of cultivation, and biofilms were cultivated for 48 h.

2.2. Biofilm Quantification. *S. aureus* biofilms in 96-well Tissue Culture Plates were quantified after 48 h of growth using Syto9 Green Fluorescent Nucleic Acid Stain (Life Technologies, Eugen, Oregon, USA). After the medium was discarded, biofilms were washed with 200 μL phosphate-buffered saline (PBS; pH = 7.2) at room temperature for 15 min at 250 rpm in a TS-100 thermoshaker (BioSan, Michigan, USA). Syto9 was diluted in PBS (1 : 3600). PBS and diluted Syto9 solution (100 μL of each) were added consecutively per well to the washed biofilms. After 1 h of incubation in a thermoshaker at 37°C at 250 rpm in the dark, fluorescence was measured using a Synergy H1 Hybrid Reader (BioTek, Vermont, USA) (excitation: 478 nm, emission: 510 nm, and gain: 60%).

2.3. Scanning Electron Microscopy (SEM). For SEM, *S. aureus* biofilm former B+ (1053) was grown on plastic cover slips (Falcon) for 48 h as described above. After biofilm cultivation slips were replaced, they were washed three times in PBS, fixed in 3% Millonig phosphate-buffered gluteraldehyde 3x for 10 min (Serva, Germany), postfixed in 2% Millonig osmium tetroxide buffered solution for 1 hour (Serva, Germany), and then washed 3x for 10 min in Millonig phosphate buffer. The samples were subsequently dehydrated in increasing concentrations of acetone (50, 70, 90, and 100%), every step for 20 min, and dried in hexamethyldisilazane (Sigma-Aldrich, Czech Republic) for 3 h in a hood at RT. Then, the samples were placed on carbon tabs attached to an aluminium holder and coated with platinum/palladium (Cressington sputter coater 208 HR, UK). The structure and interaction of biofilm cells were observed under a Hitachi SU 8010 scanning electron microscope (Hitachi High Technologies, Japan) at a magnification of 6000x (at 15 kV, wd 10.9 mm).

2.4. Cell Surface-Exposed Protein Extraction. For the extraction of surface-exposed proteins, *S. aureus* biofilms were cultivated in polystyrene 6-Well Clear Flat Bottom TC-Treated Multiwell Cell Culture Plates (TPP, Trasadingen, Switzerland) and their inoculum in 50 mL tubes (TPP, Trasadingen, Switzerland). The inoculum was used as a control (planktonic cells). The fraction of surface-exposed proteins was prepared by trypsin shaving according to Tjalsma et al., 2008 [27], with minor modifications. Briefly, after medium removal, biofilm cells were resuspended by repeated pipetting in PBS (pH = 7.2), washed twice in PBS, and centrifuged at 14000 ×g for 10 min. Washed biofilm cells were resuspended in 2 mL PBS. The cell number of washed biofilm cells and the inoculum were determined using qPCR. Equal amounts of biofilm cells and inoculum were incubated in a thermoshaker with trypsin to a final concentration of 1 μg/mL at 37°C for 1 h at 550 rpm. After digestion, cells were centrifuged at 14000 ×g for 5 min and supernatants containing shaved proteins were stored. The concentration of "shaved protein" extracts was determined spectrophotometrically (A280) using a NanoDrop™ 2000/2000c (Thermo Scientific, Wilmington, USA). Three independent cultivations and subsequent extractions were carried out. Extracts were reduced, alkylated, and trypsinized prior to mass spectral analysis according to Wiśniewski et al., 2009 [34].

2.5. Protein Labeling for Quantitative Analysis. Protein quantification was based on multiplexed peptide stable isotope dimethyl labeling [35]. Samples (tryptic peptides) were dissolved in 100 mM triethylammonium bicarbonate (TEAB) and 4% formaldehyde CH_2O ("light"). Deuterated formaldehyde CD_2O ("intermediate") or formaldehyde $^{13}CH_2O$ ("heavy") were added followed by 4% sodium cyanoborohydride $NaBH_3CN$ ("light, intermediate") or sodium cyanoborodeuteride $NaBD_3CN$ ("heavy"). The mixtures were incubated for 45 min at room temperature and quenched with 1% NH_3. After addition of 8 μM formic acid, 3 differentially labeled samples were pooled and desalted using Empore™ C18-SD 4 mm/1 mL SPE cartridges (Supelco, Bellefonte, Pennsylvania). Treated biofilm extracts were labeled "heavy," the treated planktonic cell extracts were labeled "intermediate," and inoculum extracts were labeled "light." Labeled extracts were combined as follows: treated biofilm compared to inoculum and treated planktonic cells compared to inoculum. The surfactome of treated biofilm or treated planktonic cells and the inoculum were compared for identification of proteins whose abundance increased in response to cultivation of biofilms with disinfectants. Samples

were analyzed using LC-LTQ/Orbitrap hybrid MS (Thermo Scientific, San Jose, California).

2.6. LC-MS/MS Analysis. LC-MS/MS analysis of tryptic peptides was performed on a Dionex UltiMate 3000 RSLC liquid chromatograph connected to a LTQ-Orbitrap Velos Pro hybrid mass spectrometer (Thermo Scientific). For each analysis, 5 μg of peptide sample was used. Samples were separated on EASY Spray C18 columns (length 50 cm, ID 75 μm, and particles 3 μm) at a flow rate of 200 nL/min and a gradient of 1 hour. The mass spectrometer was operated in MS spectra data-dependent mode (Orbitrap analyzer, 30 000 FWHM resolution, mass range 390–1700 m/z). The ten most abundant peptides were isolated and fragmented using collision-induced dissociation (CID) (normalized collision energy 35) followed by MS/MS scan (LTQ analyzer). Dynamic exclusion was enabled (30 s duration).

2.7. Data Analysis. Raw LC-MS/MS data were analyzed using Proteome Discoverer (v1.4). Tandem mass spectra identification was performed employing the SEQUEST algorithm. For each search, precursor and fragment mass tolerances were 10 ppm and 0.6 Da, respectively. Cysteine carbamidomethylation was set as a fixed modification; methionine oxidation was set as a dynamic modification. Only peptides with false discovery rates of ≤5% were considered.

2.8. Statistical Analysis. Data analysis was performed using the statistical software Statistica 9.1 (StatSoft, Inc., Tulsa, OK, USA) and GraphPad Prism 5.04 (GraphPad Software, Inc., San Diego, CA, USA). Data regarding the fluorescent quantification of biofilms using Syto9 labeling were analyzed by one-factor ANOVA followed by Dunnett's *post hoc* test (treatments versus control).

Evaluation of mass spectrometry quantification data was performed in such a way that medians of folds H/L ("heavy"/"light") and M/L ("intermediate"/"light") of selected proteins for all disinfectants were compared with the value 1.0 using the Wilcoxon signed rank test with null hypothesis: Median = 1.0.

3. Results

3.1. Syto9 Biofilm Quantification. Three chosen isolates of *S. aureus* (B+++ strong biofilm former, internal collection number: 1275; B++ moderate biofilm former, 1863; B+ weak biofilm former, 1053) were cultivated statically in 96-well plates for biofilm with varying concentrations of ethanol or chloramine T (treated cells) or without disinfectant (control cells). After 48 h of cultivation biofilms were quantified using the Syto9 green fluorogenic nucleic acid stain. Syto9 diffuses passively through cellular membranes and binds to DNA. As DNA also forms a substantial part of the extracellular matrix, this dye stains intracellular DNA as well as DNA in the extracellular matrix and thus provides information about total biofilm biomass regardless of whether the cells are alive or dead [35]. To determine sub-MICs of chosen disinfectants that promote biofilm formation, quantities of treated and control biofilms were compared. Statistical analysis revealed that biofilm formation by the biofilm formers was increased after application of disinfection reagents. For isolate B+++ (1275), ethanol, at concentrations from 0.63 to 5% (v/v), approximately equally promoted biofilm formation. Biofilms in treated samples were increased approximately 0.75x compared to the control. Similarly, for isolate B++ (1863), biofilm formation was increased approximately equally (0.66x) to all concentrations of ethanol tested. For the weak biofilm former B+ (1053) the biofilm grew progressively with increasing ethanol concentrations (from 0.63% to 1.25%) and reached a maximum at 1.25% ethanol; biofilm formation then decreased with further increase in ethanol concentration (5% ethanol). With chloramine T treatment, statistically significant biofilm formation by the strong biofilm former B+++ (1275) occurred only at concentrations of 1250 and 2500 μg/mL. At 5000 μg/mL no biofilm formation occurred. Biofilm formation by the moderate biofilm forming isolate B++ (1863) gradually increased with increasing concentrations of chloramine T, and maximum formation was observed at 2500 μg/mL; after application of 5000 μg/mL of chloramine T, biofilm formation decreased. Treatment of the weak biofilm producer B+ (1053) with 623 μg/mL chloramine T did not lead to biofilm formation but this was significantly increased after treatment with 1250, 2500, and 5000 μg/mL chloramine T. Maximum formation of biofilm was measured after treatment with 2500 μg/mL chloramine T ($P > 0.01$; ANOVA, Dunnett's test; Figure 1).

3.2. Enzymatic Extraction of Surface Proteins (Trypsin "Shaving"). The surface proteome was analyzed on *S. aureus* isolate 1053, in which the largest increase in biofilm formation was measured by Syto9 labeling (3.2x with 1.25% ethanol and 2.2x with 2500 μg/mL chloramine T). The biofilm of *S. aureus* isolate 1053 was cultivated for 48 h in 6-well plates with a concentration of ethanol or chloramine T that was observed to promote biofilm formation (1.25% ethanol and 2500 μg/mL chloramine T). Surface-exposed proteins were extracted from biofilms treated with chloramine T and from the inoculum using the trypsin shaving approach. The "harvest" from trypsin shaving was 0.75 mg of cell surface-exposed-protein extract from 1×10^9 nontreated biofilm cells, 0.80 mg from treated biofilm cells, and 0.38 mg of cell surface-exposed protein extract from 1×10^9 inoculum cells.

3.3. Mass Spectrometric Analysis. Extracts from 1.25% ethanol- and 2500 μg/mL chloramine T-treated cells were examined by mass spectrometry and many unique proteins (1162 and 1321, resp.) were identified. Of these, 92 and 128, respectively, of the identified proteins were located in the membrane or cell surface or had an extracellular location.

Our data shows that 6 groups of proteins showed significant up- or downregulation in treated biofilm forming cells compared to the inoculum (Table 2). The following groups of proteins were identified: (1) adhesin proteins involved in surface adherence; (2) proteins involved in cell-wall synthesis and organization; (3) cell maintenance proteins; (4) nascent

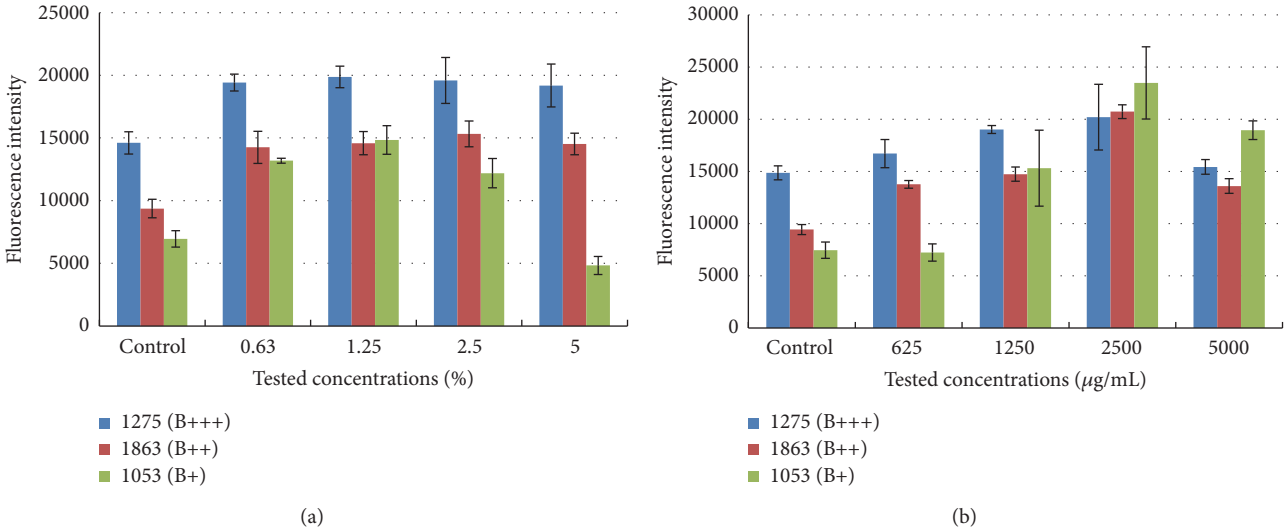

Figure 1: Syto9 quantification of 3 biofilm forming isolates of *S. aureus* treated with different concentrations of ethanol or chloramine T. Strong biofilm former (B+++), moderate biofilm former (B++), and weak biofilm former (B+) were treated with increasing concentrations of ethanol (a) or chloramine T (b) and biofilm quantity was determined by Syto9 labeling. Graphs show biofilm levels in samples cultivated with disinfectants versus controls (samples cultivated without disinfectants). Columns represent mean values of fluorescence and vertical bars represent 95% confidence intervals regarding the means.

transmembrane protein transporters; (5) uncharacterized proteins; (6) virulence factors.

Several proteins were found to be significantly upregulated after treatment: from the adhesins: clumping factor A and extracellular adherence protein Eap; from cell maintenance proteins: large-conductance mechanosensitive channel, uncharacterized lipoprotein SAS2259, and virulence factor EsxA. Immunoglobulin-binding protein A was significantly downregulated with both disinfectants. A statistically significant difference in the effect of tested disinfectants on the expression of surface proteins was measured for adhesins: fibronectin-binding protein A (chloramine T, upregulation; ethanol, downregulation) and iron-regulated surface determinant protein A (ethanol, upregulation; chloramine T, downregulation); nascent transmembrane protein transporters: foldase protein PrsA (ethanol, upregulation; chloramine T, downregulation) and UPF0478 protein SA1560 (chloramine T, upregulation; ethanol, downregulation), and virulence factors: serine-aspartate repeat-containing protein C and staphylococcal secretory antigen ssaA2 (ethanol, upregulation; chloramine T, downregulation).

Significant upregulation of the following proteins was observed only in ethanol-treated biofilm cells compared to the inoculum: clumping factor B, immunoglobulin-binding protein sbi, and virulence factors penicillin-binding protein 1 and phospholipase C. Downregulation was observed for proteins involved in cell-wall synthesis and lipoteichoic acid synthase. Similarly, statistically significant differences were demonstrated only in chloramine T-treatment for the following proteins: from adhesins: fibrinogen-binding protein A (upregulation); from cell-wall synthesis and organization: N-acetylmuramoyl-L-alanine amidase sle1 and probable transglycosylase SceD (downregulation), and from cell maintenance proteins: cold shock protein CspA (downregulation).

3.4. Visualization of S. aureus Control and Treated Biofilms by Scanning Electron Microscopy. Control and 48 h biofilms treated with disinfectants differed not only in quantity, as determined by Syto9 labeling, but also in compactness; this, however, was not clearly captured by Syto9 labeling. For this reason we used scanning electron microscopy (SEM) to visualize the weak biofilm former B+ (1053), which was then used for MS analysis of the surface proteome (Figure 2). It was clearly seen from representative SEM images that biofilms formed after treatment with 1.25% ethanol or 2500 μg/mL chloramine T were more compact in comparison with the control biofilm. In addition, the 2500 μg/mL chloramine T-treated biofilm appeared to be more compact than the biofilm treated with 1.25% ethanol.

4. Discussion

It has been reported that sublethal concentrations (sub-MICs) of certain disinfectants are no longer effective in removing biofilms from abiotic surfaces and can even promote the formation of biofilms. Tolerance of bacterial biofilms to disinfectants increases the risk of cross-contamination of food. Bacterial cells probably react to the presence of disinfectants and defend themselves by way of biofilm formation [36]. As disinfectants diffuse through the biofilm matrix their concentration is lowered and bacterial cells can adapt. For example, biofilm formation of *S. epidermidis* exposed to benzalkonium chloride at 1/16, 1/18, and 1/32 of the MIC was increased from 11.4% to 22.5% without any significant effect on planktonic growth [37].

Our data showed that ethanol and chloramine T, at sub-MICs, are each capable of promoting biofilm formation by *S. aureus*. Different isolates of *S. aureus* from meat-processing environments were tested for biofilm formation

Table 2: Differentially regulated proteins in biofilm samples treated with two disinfectants as determined using LC-LTQ/Orbitrap MS.

	Description	PGA	Ethanol (E)			Chloramine T (C)			Differences between disinfectants[b]
			n	Median[a]	QD	*n*	Median[a]	QD	
Adherence	Clumping factor A	Q6GB45	23	*3.990***	0.119	45	*3.650***	0.648	
	Clumping factor B	Q6G644	6	*2.358***	0.159	11	0.845	0.316	EC**
	Elastin-binding protein EbpS	Q6G983	2	0.879	0.164	8	1.259	0.440	
	Enolase	A7WZT2	88	**0.998***	0.087	83	*1.131***	0.203	
	Extracellular adherence protein Eap	D9RNP1	4	*3.271**	0.379	6	*2.807***	0.144	
	Fibrinogen-binding protein	P68799	2	1.334	0.109	4	*2.114***	0.059	
	Fibronectin-binding protein A	Q6G6H3	4	**0.267***	0.079	8	*1.655***	0.125	EC**
	Immunoglobulin-binding protein A	Q8NYT0	75	**0.091****	0.058	45	**0.018****	0.010	
	Immunoglobulin-binding protein sbi	Q6G6Q3	47	*1.368***	0.263	38	1.088	0.165	EC*
	Iron-regulated surface determinant protein A	A7X148	5	*1.358***	0.058	13	**0.620****	0.040	EC**
Cell wall synthesis and organization	Lipoteichoic acid synthase	Q2FIS2	13	**0.786***	0.322	15	0.407	0.292	
	N-acetylmuramoyl-L-alanine amidase sle1	Q2FJH7	9	0.885	0.361	4	**0.189****	0.008	EC*
	Probable transglycosylase SceD	A7X6T9	2	2.033	0.025	4	**0.305****	0.050	EC*
Physiological proteins	Cold shock protein CspA	Q2FH36	7	0.067	0.335	4	**0.067****	0.009	
	Large-conductance mechanosensitive channel	A7X204	6	*1.527***	0.065	4	*1.306**	0.029	
Transport through membrane	Foldase protein PrsA	A7X3U8	19	*1.287***	0.342	17	**0.668****	0.066	EC**
Uncharacterized proteins	Uncharacterized lipoprotein MW0073	Q8NYU0	1	1.256	0.000	7	0.852	0.072	
	Uncharacterized lipoprotein SAS2259	Q6G6V2	16	*1.461***	0.177	15	*1.259***	0.106	
	UPF0478 protein SA1560	Q7A531	22	**0.862****	0.102	27	*1.245***	0.125	EC**
Virulence factors	Penicillin-binding protein 1	Q8NX37	4	*1.247**	0.041	2	0.323	0.009	
	Phospholipase C	A5IUH1	4	*5.909**	2.231	2	5.252	0.118	
	Secretory antigen SsaA-like protein	A6QEX4	2	5.578	0.106	0			
	Serine-aspartate repeat-containing protein C	Q6GBS6	32	*2.819***	0.404	12	**0.392****	0.054	EC**
	Staphylococcal secretory antigen ssaA2	Q2G2J2	22	*4.088***	2.288	21	**0.469****	0.135	EC**
	Virulence factor EsxA	Q5HJ91	16	*2.002***	0.980	17	*2.261***	1.384	

PGA: protein group accession number; *n*: number of peptides; QD: quartile deviation.
[a]Italic/bold numbers represent statistically significant fold changes in the indicated proteins (upregulated/downregulated) (** $P < 0.01$; * $P < 0.05$; Wilcoxon signed rank test with theoretical median = 1.0).
[b]Statistically significant differences between disinfectants (** $P < 0.01$; * $P < 0.05$; Mann-Whitney test followed by *post hoc* tests).

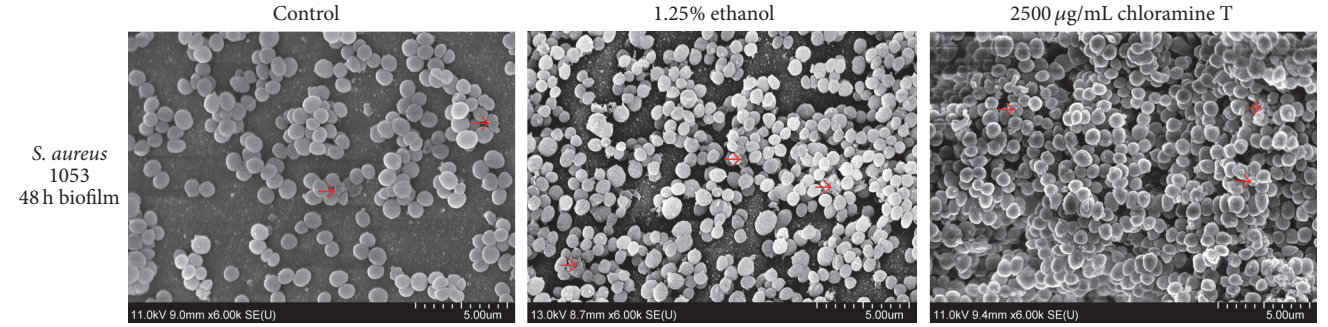

Figure 2: Representative SEM images of 48 h biofilm formed by B+ (1053) isolate in medium (control), 1.25% ethanol, or 2500 μg/mL chloramine T. Arrows: extracellular matrix.

according to the methods of Stepanović et al., 2007 [33]. One representative was a strong biofilm former (B+++), one was a moderate biofilm former (B++), and one was a weak biofilm former. These were chosen to quantify the effects of disinfectants on biofilm formation. The *S. aureus* isolates were cultivated in 96-well plates with different sublethal concentrations of ethanol, or chloramine T, and biofilm formation was quantified using Syto9 Green Fluorescent Nucleic Acid Stain. After application of 1.25% ethanol or 2500 μg/mL chloramine T, not only was there an increase in biofilm formation, as depicted in Figure 1, but also there were changes in the quality of the biofilm compared to the control (the biofilms were firmer and more symmetrically proportioned after application of disinfectants). This qualitative aspect of biofilm formation cannot be fully captured by Syto9 staining, which is why visualization of treated and control biofilms was carried out by scanning electron microscopy (Figure 2).

Statistical analysis showed that 0.63–5% ethanol in case of strong and moderate biofilm formers and 0.63–2.5% ethanol in case of weak biofilm former significantly promoted biofilm formation. The maximum biofilm formation was observed for 2.5% ethanol for moderate and 1.25% ethanol for weak biofilm forming isolates. This finding is in agreement with previous studies [36] where elevated biofilm formation was observed after application of 1-2% ethanol. Ethanol, at 2.4% v/v, enhanced the expression of a number of biofilm-promoting genes in *S. aureus* [38]. It was also demonstrated that application of other alcohols (ethanol, methanol, isopropanol, isoamyl alcohol, and n-butanol) to preformed *S. aureus* biofilms enhanced biofilm growth [39].

The effect of sub-MICs of chloramine T on biofilm formation has not previously been tested. Our data showed a statistically significant increase in biofilm formation in response to 1250 and 2500 μg/mL chloramine T in the strong isolate, 623–5000 μg/mL in the moderate isolate, and 1250–5000 μg/mL in the weak biofilm forming isolate compared to the control (Figure 1). Maximum biofilm formation was observed in all three isolates with 2500 μg/mL of chloramine T.

It was reported that formation of biofilms can be enhanced not only by chemicals, but also by other stress conditions such as temperature [40, 41] or pH [42]. Ciccio et al., 2014, observed that 38 out of 67 tested *S. aureus* strains (57%) grew at 37°C on polystyrene or stainless steel, while, in comparison, only one strain grew at 12°C. They also observed that cell surface hydrophobicity levels increased with temperature.

Ethanol or chloramine T treatments of *S. aureus* biofilms were further analyzed to describe changes in the abundance of surface-exposed proteins after treatment. Enzymatic cell surface shaving, dimethyl labeling, and LC-LTQ/Orbitrap analysis were used to describe changes in the abundance of surface-exposed proteins in treated biofilms and the inoculum. To reduce the number of false positives and to correct for experimental variations, only those proteins with at least two unique peptides in three triplicate experiments were considered significant.

Our data shows that ethanol as well as chloramine T-treated *S. aureus* biofilm cells expressed higher levels of proteins associated with cell attachment than control cells. The observation that biofilm-producing cells overexpress adhesins compared to their planktonic counterparts is in agreement with other studies [43–45]. These proteins belong to the MSCRAMM group of surface-exposed proteins, but their biological importance and their roles in adhesion and virulence of *S. aureus* are not completely known. MSCRAMMs promote adhesion of *S. aureus* to the extracellular matrix, to the surface of host cells, and to biomaterial surfaces that are conditioned, for example, by the deposition of plasma proteins. Four *S. aureus* surface-exposed proteins, clumping factor A (ClfA), fibronectin-binding proteins A and B (FnBPA and FnBPB), and enolase, were found as the main factors involved in the adherence of *S. aureus* to polyurethane membranes of ventricular assist devices [46]. As fibronectin is present on epithelial and endothelial surfaces and is also part of blood clots, fibronectin-binding proteins (Fnbp A/B) and clumping proteins (Clp A and B) help *S. aureus* to invade these tissues [3]. Enolase was identified as a 52 kDa surface receptor of laminins [47] and, thus, may play a critical role in the pathogenesis of *S. aureus* by allowing its adherence to the laminin-containing extracellular matrix. Surface-exposed proteins directly or indirectly interact with integrins and promote the invasion of nonphagocytic host cells. Intercellular bacteria can cause host cell apoptosis or they can enter a nondisruptive semidormant state ("small colony variants"). These surface-exposed proteins probably also play a role in the accumulation of *S. aureus* cells during biofilm formation [11]. Differences between chloramine T and ethanol treatments were recorded for these proteins with adherence function: enolase, fibronectin-binding protein A, and iron-regulated surface determinant protein A (Table 2). The biofilm/inoculum ratios for enolase were approximately 1 for both treatments, which probably means that chloramine T does not lead to upregulation of enolase or ethanol to its downregulation. It is possible that inoculum cells express similar levels of enolase as biofilm cells in order to adhere. Our data show that chloramine T leads to upregulation of fibronectin-binding protein A (fib) and ethanol to its downregulation, despite the fact that fibrinogen-binding protein (fnb) was upregulated after both treatments. The difference between these two proteins is in their substrate plasticity. While fib binds preferentially to fibronectin, fnb protein binds to multiple substrates (Table 3). In contrast, iron-regulated surface determinant protein A (isdA) was downregulated after chloramine T-treatment and upregulated after ethanol treatment. IsdA protein also binds multiple ligands, for example, fibronectin, or contributes to bacterial cell adherence (Table 3). It is questionable whether these data suggest a disinfectant-specific response of *S. aureus*. The remaining identified proteins, on the contrary, might suggest a general stress response. This question would be better answered by a detailed analysis of whole cell extracts and confirmed using RT-PCR transcriptome analysis.

According to our data, proteins involved in cell-wall synthesis were shown to be predominantly downregulated in treated biofilm cells compared to the inoculum. This might have been due to differences in the growth phase between biofilm and inoculum cells: whilst, after 16 h of cultivation,

Table 3: Description of proteins listed in Table 2.

Abbreviation	Description
Clumping factor A (clfA)	Cell surface-associated protein implicated in virulence, promotes bacterial attachment exclusively to the gamma-chain of human fibrinogen, induces formation of bacterial clumps (933 aa)
Clumping factor B (clfB)	Cell surface-associated protein implicated in virulence by promoting bacterial attachment to both alpha- and beta-chains of human fibrinogen and inducing the formation of bacterial clumps (913 aa)
Cold shock protein (cspA)	Involved in cold stress response and in the susceptibility to an antimicrobial peptide of human cathepsin G (CG117-136). Regulates yellowish-orange pigment production through a still unclear SigB-dependent mechanism (66 aa)
Elastin-binding protein (ebpS)	Promotes binding of soluble elastin peptides and tropoelastin to *S. aureus* cells although it is not able to promote bacterial adherence to immobilized elastin and, therefore, is not a Microbial Surface Component Recognizing Adhesive Matrix Molecule (MSCRAMM) (486 aa)
Enolase (eno)	Phosphopyruvate hydratase; catalyzes the reversible conversion of 2-phosphoglycerate into phosphoenolpyruvate; it is essential for the degradation of carbohydrates via glycolysis; binds laminin when expressed on the bacterial cell surface; this probably induces destruction of the extracellular matrix, favoring invasion and dissemination (434 aa)
Extracellular adherence protein (eap)	Adherence and invading of eukaryotic cells (985 aa)
Fibrinogen-binding protein (fib)	Binds to host fibrinogen (165 aa)
Fibronectin-binding protein A (fnb)	Promotes bacterial attachment to multiple substrates, such as fibronectin (Fn), fibrinogen (Fg), elastin peptides, and tropoelastin; this confers to *S. aureus* the ability to invade endothelial cells; promotes adherence to and aggregation of activated platelets (1018 aa)
Foldase protein (prsA)	Export protein; plays a major role in protein secretion by helping the posttranslocational extracellular folding of several secreted proteins (320 aa)
IgG-binding protein SBI (sbi)	Interacts with components of both the adaptive and innate host immune system, thereby protecting the cell against the host immune response (436 aa)
Immunoglobulin G-binding protein A (spA)	Function in pathogenesis (508 aa)
Immunoglobulin G-binding protein Sbi	Interacts with components of both the adaptive and innate host immune system, thereby protecting the cell against the host immune response (436 aa)
Immunoglobulin-binding protein (sbi)	Interacts with components of both the adaptive and innate host immune system, thereby protecting the cell against the host immune response (436 aa)
Iron-regulated surface determinant protein A (isdA)	LPXTG cell-wall surface anchor protein; transfers its hemin to hemin-free IsdC (apo-IsdC) directly probably through the activation of the holo-IsdA-apo-IsdC complex and driven by the higher affinity of apo-IsdC for the cofactor; the reaction is reversible; binds transferrin, lactoferrin, heme, hemoglobin, hemin, fetuin, asialofetuin, protein A; also binds fibronectin and chains B, beta and gamma of fibrinogen, promoting clumping of *S. aureus* with fibrinogen; was also shown to adhere to plastic (350 aa)
Large-conductance mechanosensitive channel (mscL)	Channel that opens in response to stretch forces in the membrane lipid bilayer; may participate in the regulation of osmotic pressure changes within the cell (120 aa)
Lipoteichoic acid synthase (ltaS)	Sulfatase; catalyzes the polymerization of lipoteichoic acid (LTA) polyglycerol phosphate, a reaction that presumably uses phosphatidylglycerol (PG) as substrate is required for staphylococcal growth and cell division process (646 aa)
N-acetylmuramoyl-L-alanine amidase (sle1)	Peptidoglycan hydrolase involved in the splitting of the septum during cell division; binds to both alpha- and beta-chains of human fibrinogen as well as fibronectin, which suggests a role in the colonization of host factor-coated material or host tissue; also exhibits lytic activity against *S. carnosus* and *S. aureus* cells but not against *M. luteus* cells (334 aa)
Penicillin-binding protein 1 (pbp1)	Penicillin-binding protein 1 (744 aa)
Phospholipase C (hlb)	Bacterial hemolysins are exotoxins that attack blood cell membranes and cause cell rupture; beta-hemolysin is a phospholipase C with specific activity toward sphingomyelins; has a high specificity for sphingomyelin and hydrolyzes lysophosphatidylcholine at a much lower rate but has no activity toward phosphatidylcholine, phosphatidylethanolamine, or phosphatidylserine (330 aa)

Table 3: Continued.

Abbreviation	Description
Probable transglycosylase (sceD)	Cleaves peptidoglycan and affects clumping and separation of bacterial cells (231 aa)
Secretory antigen SsA-like protein	Immunogenic protein (267 aa)
Serine-aspartate repeat-containing protein C (sdrC)	sdrC protein; cell surface-associated protein which possibly mediates interactions of *S. aureus* with components of the extracellular matrix of higher eukaryotes; may bind calcium (947 aa)
Staphylococcal secretory antigen Ss aa2 (scaD)	Immunogenic protein (265 aa)
Virulence factor (esxA)	Hypothetical protein; virulence factor that is important for the establishment of infection in the host (97 aa)

source: http://www.string-db.org.

inoculum cells should be in the early stationary-phase of growth, still multiplying and growing, biofilm cells are probably in the late stationary-phase of biofilm formation and differentiation, in which mainly proteins of the extracellular matrix are expressed.

The large-conductance mechanosensitive channel was upregulated after treatment with both disinfectants (Table 2). Probably this protein might participate in regulation of osmotic pressure induced by the presence of chloramine T or ethanol (Table 3). Foldase protein PrsA that participates in transport of secreted proteins through membranes was determined to be downregulated after chloramine T treatment and upregulated after ethanol treatment. Its upregulation may be associated with the fact that ethanol might disrupt the cell membrane or with another metabolic response to ethanol.

Virulence factors of *S. aureus*, such as phospholipase C, iron-regulated surface determinant protein A, staphylococcal secretory antigen ssaA2, and virulence factor EsxA, were also detected. Only virulence factor EsxA was found to be upregulated in the treated biofilm. This is in agreement with the claim that planktonic cells are generally more virulent than their biofilm counterparts [44]. The functions of these proteins are listed in Table 3. Perhaps the most striking differences between the chloramine T and ethanol treatments were measured for two virulence factors of *S. aureus*: serine-aspartate repeat-containing protein C (SdrC) and staphylococcal secretory antigen (ssaA2), which were both upregulated after treatment with ethanol and downregulated by chloramine T treatment. SdrC is a cell surface-associated protein that possibly mediates interactions of *S. aureus* with components of the extracellular matrix of higher eukaryotes. This protein contains the C termini LPXTG motifs and hydrophobic amino acid segments and thus is a characteristic member of surface proteins covalently anchored to peptidoglycan. Staphylococcal secretory antigen ssaA2 is an immunogenic protein of unknown function. It was also observed in other studies that ethanol increased the level of genes considered necessary for production and viability of the biofilm. These included icaAD, sdrDE, pyr, and ure [38]. Generally, exposure to ethanol increases pathogenic traits and induces oxidative-stress responses. This effect of ethanol might be related to the upregulation of sdrC and ssaA2 virulence factors.

The last group of proteins consisted of multiple uncharacterized proteins that could play an important role in biofilm development. Uncharacterized proteins that are upregulated in the biofilm are probably components of metabolic or physiological pathways of biofilm formation and differentiation. Some of these uncharacterized proteins might be stress response factors that could be expressed in response to the presence of disinfectants.

Expression of cell-wall associated proteins in this study, as well as in many other studies, was determined after cultivation in bacterial growth medium. However, when *S. aureus* contaminates, for example, a working table or knives in a food-processing environment, or infects a wound on human skin, the bacterial growth conditions will be quite different from those in medium *in vitro*, and this may affect the expression of surface-exposed proteins. Variable levels of single proteins might also be partly due to biological variation. After binding to the surface, biofilm cells usually become multilayered and differentiated. Growth conditions (supply of oxygen and nutrients) vary greatly among the various layers; this can promote differential growth and physiology and should also result in differences in protein expression.

Analysis of proteomic differences between biofilm and planktonic forms of different bacterial species is currently the subject of much research [48–50]. There are a number of reports on the expression of MSCRAMM adhesins, using one or two basic approaches: studies of surfactome expression at the transcriptome level or studies of surfactome expression at the proteome level. For the first approach, DNA microarray analysis that enables the simultaneous determination of the total transcriptional response is mainly applied [38, 45]. A disadvantage of this approach is that the level of mRNA can differ from the final level of its corresponding protein. For the second, combination of 2D-gel separation and mass spectrometry is generally employed [44, 50–53], or flow cytometry [54]. Enzymatic shaving is a novel and appropriate approach for surface-exposed protein extraction. It is a very simple and fast method and extracts obtained using enzymatic shaving contain minimal levels of cytoplasmic contaminants that could obscure minor amounts of surface-exposed proteins. The simple mixture of dimethyl-labeled samples is also an advantage for mass spectrometric analysis [28].

The major task for the future is to find more effective solutions for biofilm-associated contamination. Bacterial cells are able to adapt to low concentrations of disinfecting substances and form biofilm barriers. During the first step of biofilm formation, adhesive molecules are mainly expressed. They are one of the basic contributors to the survival, pathogenicity, and virulence of bacteria such as *S. aureus* and thus might represent markers for a molecule-targeted approach for the eradication of contaminating biofilms. Surface-exposed proteins are also currently being evaluated as potential antigens in vaccines [55, 56]. These topics require further investigation.

5. Conclusion

In the present work we have demonstrated that treatment of *S. aureus* isolates from a meat-processing environment with 1.25–2.5% ethanol or 2500 μg/mL chloramine T enhanced biofilm formation as determined by Syto9 labeling. The change in compactness of the biofilm after treatment with ethanol or chloramine T was visualized by scanning electron microscopy. Further we demonstrated that trypsin shaving in combination with dimethyl labeling and high-resolution LC-MS/MS analysis serves as a rapid and valuable tool for studying changes in abundance of surface-exposed proteins connected with bacterial biofilm formation. Biofilm cell treated with 1.25% ethanol or 2500 μg/mL chloramine T exhibited elevated expression of proteins that are involved in adhesion and sessile growth of *S. aureus*. The overall control of surface proteins appears to be more or less similar after administration of ethanol or chloramine T. The main differences were in regulation of some adhesins (fibronectin-binding protein A, iron-regulated surface determinant protein A), transport protein foldase protein PrsA, and virulence factors (serine-aspartate repeat-containing protein C; staphylococcal secretory antigen ssaA2). This work confirms results of previous studies where, using classical microbiological methods, some sub-MICs of ethanol and chloramine T were shown to promote *S. aureus* biofilm formation. This is supported by MS proteomic analysis.

Competing Interests

All authors declare no competing interests.

Acknowledgments

This work was supported by the MEYS CZ (COST LD 14015 and NPUI LO1218), EU COST Action CGA FA-1202 BacFoodNet (A European Network for Mitigating Bacterial Colonisation and Persistence on Foods and Food Processing Environments; http://www.bacfoodnet.org/), and MA CZ (RO 0516). The authors thank Andrea Durisova (Veterinary Research Institute, Czech Republic) for technical support. Neysan Donnelly (Max Planck Institute of Biochemistry, Munich, Germany) and Jon Brooker (JK Consulting, Trebon, Czech Republic) are thanked for the grammatical correction of the manuscript.

References

[1] B. Ray and A. K. Bhunia, *Fundamental Food Microbiology*, CRC Press, Taylor & Francis Group, 2008.

[2] D. Gutiérrez, S. Delgado, D. Vázquez-Sánchez et al., "Incidence of staphylococcus aureus and analysis of associated bacterial communities on food industry surfaces," *Applied and Environmental Microbiology*, vol. 78, no. 24, pp. 8547–8554, 2012.

[3] C. R. Arciola, D. Campoccia, S. Gamberini, L. Baldassarri, and L. Montanaro, "Prevalence of cna, fnbA and fnbB adhesin genes among *Staphylococcus aureus* isolates from orthopedic infections associated to different types of implant," *FEMS Microbiology Letters*, vol. 246, no. 1, pp. 81–86, 2005.

[4] T. J. Foster and M. Höök, "Surface protein adhesins of *Staphylococcus aureus*," *Trends in Microbiology*, vol. 6, no. 12, pp. 484–488, 1998.

[5] D. G. Halliman and D. G. Ahearn, "Relative susceptibilities to vancomycin and quinupristin-dalfopristin of adhered and planktonic vancomycin-resistant and vancomycin-susceptible coagulase-negative staphylococci," *Current Microbiology*, vol. 48, no. 3, pp. 214–218, 2004.

[6] A. Bridier, R. Briandet, V. Thomas, and F. Dubois-Brissonnet, "Resistance of bacterial biofilms to disinfectants: a review," *Biofouling*, vol. 27, no. 9, pp. 1017–1032, 2011.

[7] C. Cucarella, C. Solano, J. Valle, B. Amorena, Í. Lasa, and J. R. Penadés, "Bap, a *Staphylococcus aureus* surface protein involved in biofilm formation," *Journal of Bacteriology*, vol. 183, no. 9, pp. 2888–2896, 2001.

[8] C. Latasa, C. Solano, J. R. Penadés, and I. Lasa, "Biofilm-associated proteins," *Comptes Rendus—Biologies*, vol. 329, no. 11, pp. 849–857, 2006.

[9] S. E. Cramton, C. Gerke, N. F. Schnell, W. W. Nichols, and F. Götz, "The intercellular adhesion (ica) locus is present in Staphylococcus aureus and is required for biofilm formation," *Infection and Immunity*, vol. 67, no. 10, pp. 5427–5433, 1999.

[10] N. M. Abraham and K. K. Jefferson, "*Staphylococcus aureus* clumping factor B mediates biofilm formation in the absence of calcium," *Microbiology*, vol. 158, no. 6, pp. 1504–1512, 2012.

[11] J. A. Geoghegan, I. R. Monk, J. P. O'Gara, and T. J. Foster, "Subdomains N2N3 of fibronectin binding protein a mediate *Staphylococcus aureus* biofilm formation and adherence to fibrinogen using distinct mechanisms," *Journal of Bacteriology*, vol. 195, no. 11, pp. 2675–2683, 2013.

[12] K. Schroeder, M. Jularic, S. M. Horsburgh et al., "Molecular characterization of a novel *Staphylococcus aureus* surface protein (SasC) involved in cell aggregation and biofilm accumulation," *PLoS ONE*, vol. 4, no. 10, Article ID e7567, 2009.

[13] J. A. Geoghegan, R. M. Corrigan, D. T. Gruszka et al., "Role of surface protein SasG in biofilm formation by Staphylococcus aureus," *Journal of Bacteriology*, vol. 192, no. 21, pp. 5663–5673, 2010.

[14] N. Merino, A. Toledo-Arana, M. Vergara-Irigaray et al., "Protein A-mediated multicellular behavior in *Staphylococcus aureus*," *Journal of Bacteriology*, vol. 191, no. 3, pp. 832–843, 2009.

[15] T. J. Foster, J. A. Geoghegan, V. K. Ganesh, and M. Höök, "Adhesion, invasion and evasion: the many functions of the surface proteins of Staphylococcus aureus," *Nature Reviews Microbiology*, vol. 12, no. 1, pp. 49–62, 2014.

[16] J. M. Patti, B. L. Allen, M. J. McGavin, and M. Höök, "MSCRAMM-mediated adherence of microorganisms to host tissues," *Annual Review of Microbiology*, vol. 48, pp. 585–617, 1994.

[17] F. M. McAleese, E. J. Walsh, M. Sieprawska, J. Potempa, and T. J. Foster, "Loss of clumping factor B fibrinogen binding activity by *Staphylococcus aureus* involves cessation of transcription, shedding and cleavage by metalloprotease," *The Journal of Biological Chemistry*, vol. 276, no. 32, pp. 29969–29978, 2001.

[18] M. Bischoff, P. Dunman, J. Kormanec et al., "Microarray-based analysis of the Staphylococcus aureus σ^B Regulon," *Journal of Bacteriology*, vol. 186, no. 13, pp. 4085–4099, 2004.

[19] R. Y.-Y. Chiou, R. D. Phillips, P. Zhao, M. P. Doyle, and L. R. Beuchat, "Ethanol-mediated variations in cellular fatty acid composition and protein profiles of two genotypically different strains of *Escherichia coli*O157:H7," *Applied and Environmental Microbiology*, vol. 70, no. 4, pp. 2204–2210, 2004.

[20] M. G. Silveira, M. Baumgärtner, F. M. Rombouts, and T. Abee, "Effect of adaptation to ethanol on cytoplasmic and membrane protein profiles of *Oenococcus oeni*," *Applied and Environmental Microbiology*, vol. 70, no. 5, pp. 2748–2755, 2004.

[21] V. A. Fried and A. Novick, "Organic solvents as probes for the structure and function of the bacterial membrane: effects of ethanol on the wild Type and an ethanol-resistant mutant of *Escherichia coli* K-12," *Journal of Bacteriology*, vol. 114, no. 1, pp. 239–248, 1973.

[22] J. S. Terracciano and E. R. Kashket, "Intracellular conditions required for initiation of solvent production by *Clostridium acetobutylicum*," *Applied and Environmental Microbiology*, vol. 52, no. 1, pp. 86–91, 1986.

[23] T. W. Stief, "The physiology and pharmacology of singlet oxygen," *Medical Hypotheses*, vol. 60, no. 4, pp. 567–572, 2003.

[24] S. L. Rolland, T. E. Carrick, A. W. Walls, and J. F. McCabe, "Dentin decontamination using chloramine T prior to experiments involving bacteria," *Dental Materials*, vol. 23, no. 12, pp. 1468–1472, 2007.

[25] K. C. Bal Krishna, A. Sathasivan, and M. P. Ginige, "Microbial community changes with decaying chloramine residuals in a lab-scale system," *Water Research*, vol. 47, no. 13, pp. 4666–4679, 2013.

[26] T. M. Rode, S. Langsrud, A. Holck, and T. Møretrø, "Different patterns of biofilm formation in *Staphylococcus aureus* under food-related stress conditions," *International Journal of Food Microbiology*, vol. 116, no. 3, pp. 372–383, 2007.

[27] H. Tjalsma, L. Lambooy, P. W. Hermans, and D. W. Swinkels, "Shedding & shaving: disclosure of proteomic expressions on a bacterial face," *Proteomics*, vol. 8, no. 7, pp. 1415–1428, 2008.

[28] N. Solis, M. R. Larsen, and S. J. Cordwell, "Improved accuracy of cell surface shaving proteomics in *Staphylococcus aureus* using a false-positive control," *Proteomics*, vol. 10, no. 10, pp. 2037–2049, 2010.

[29] M. J. Rodríguez-Ortega, N. Norais, G. Bensi et al., "Characterization and identification of vaccine candidate proteins through analysis of the group A *Streptococcus* surface proteome," *Nature Biotechnology*, vol. 24, no. 2, pp. 191–197, 2006.

[30] F. Doro, S. Liberatori, M. J. Rodríguez-Ortega et al., "Surfome analysis as a fast track to vaccine discovery: identification of a novel protective antigen for group B Streptococcus hypervirulent strain COH1," *Molecular and Cellular Proteomics*, vol. 8, no. 7, pp. 1728–1737, 2009.

[31] A. Dreisbach, M. M. van der Kooi-Pol, A. Otto et al., "Surface shaving as a versatile tool to profile global interactions between human serum proteins and the *Staphylococcus aureus* cell surface," *Proteomics*, vol. 11, no. 14, pp. 2921–2930, 2011.

[32] M. Ythier, G. Resch, P. Waridel et al., "Proteomic and transcriptomic profiling of *Staphylococcus aureus* surface LPXTG-proteins: correlation with agr genotypes and adherence phenotypes," *Molecular and Cellular Proteomics*, vol. 11, no. 11, pp. 1123–1139, 2012.

[33] S. Stepanović, D. Vuković, V. Hola et al., "Quantification of biofilm in microtiter plates: overview of testing conditions and practical recommendations for assessment of biofilm production by staphylococci," *APMIS*, vol. 115, no. 8, pp. 891–899, 2007.

[34] J. R. Wiśniewski, A. Zougman, N. Nagaraj, and M. Mann, "Universal sample preparation method for proteome analysis," *Nature Methods*, vol. 6, no. 5, pp. 359–362, 2009.

[35] P. J. Boersema, R. Raijmakers, S. Lemeer, S. Mohammed, and A. J. R. Heck, "Multiplex peptide stable isotope dimethyl labeling for quantitative proteomics," *Nature Protocols*, vol. 4, no. 4, pp. 484–494, 2009.

[36] Y. Tashiro, A. Inagaki, K. Ono et al., "Low concentrations of ethanol stimulate biofilm and pellicle formation in Pseudomonas aeruginosa," *Bioscience, Biotechnology and Biochemistry*, vol. 78, no. 1, pp. 178–181, 2014.

[37] A. Houari and P. Di Martino, "Effect of chlorhexidine and benzalkonium chloride on bacterial biofilm formation," *Letters in Applied Microbiology*, vol. 45, no. 6, pp. 652–656, 2007.

[38] M. Korem, Y. Gov, and M. Rosenberg, "Global gene expression in *Staphylococcus aureus* following exposure to alcohol," *Microbial Pathogenesis*, vol. 48, no. 2, pp. 74–84, 2010.

[39] C. V. Redelman, C. Maduakolam, and G. G. Anderson, "Alcohol treatment enhances *Staphylococcus aureus* biofilm development," *FEMS Immunology & Medical Microbiology*, vol. 66, no. 3, pp. 411–418, 2012.

[40] P. Di Ciccio, A. Vergara, A. R. Festino et al., "Biofilm formation by *Staphylococcus aureus* on food contact surfaces: relationship with temperature and cell surface hydrophobicity," *Food Control*, vol. 50, pp. 930–936, 2015.

[41] Q. G. da Silva Meira, I. de Medeiros Barbosa, A. J. Alves Aguiar Athayde, J. P. de Siqueira-Júnior, and E. L. de Souza, "Influence of temperature and surface kind on biofilm formation by *Staphylococcus aureus* from food-contact surfaces and sensitivity to sanitizers," *Food Control*, vol. 25, no. 2, pp. 469–475, 2012.

[42] T. Zmantar, B. Kouidhi, H. Miladi, K. Mahdouani, and A. Bakhrouf, "A microtiter plate assay for *Staphylococcus aureus* biofilm quantification at various pH levels and hydrogen peroxide supplementation," *New Microbiologica*, vol. 33, no. 2, pp. 137–145, 2010.

[43] D. M. B. Post, J. M. Held, M. R. Ketterer et al., "Comparative analyses of proteins from Haemophilus influenzae biofilm and planktonic populations using metabolic labeling and mass spectrometry," *BMC Microbiology*, vol. 14, no. 1, article 329, 2014.

[44] A. Resch, S. Leicht, M. Saric et al., "Comparative proteome analysis of *Staphylococcus aureus* biofilm and planktonic cells and correlation with transcriptome profiling," *Proteomics*, vol. 6, no. 6, pp. 1867–1877, 2006.

[45] A. Resch, R. Rosenstein, C. Nerz, and F. Götz, "Differential gene expression profiling of Staphylococcus aureus cultivated under biofilm and planktonic conditions," *Applied and Environmental Microbiology*, vol. 71, no. 5, pp. 2663–2676, 2005.

[46] C. Arrecubieta, I. Matsunaga, T. Asai, Y. Naka, M. C. Deng, and F. D. Lowy, "Vaccination with clumping factor A and fibronectin binding protein A to prevent Staphylococcus aureus infection of an aortic patch in mice," *Journal of Infectious Diseases*, vol. 198, no. 4, pp. 571–575, 2008.

[47] C. R. W. Carneiro, E. Postol, R. Nomizo, L. F. L. Reis, and R. R. Brentani, "Identification of enolase as a laminin-binding protein on the surface of *Staphylococcus aureus*," *Microbes and Infection*, vol. 6, no. 6, pp. 604–608, 2004.

[48] D. Seyer, P. Cosette, A. Siroy et al., "Proteomic comparison of outer membrane protein patterns of sessile and planktonic *Pseudomonas aeruginosa* cells," *Biofilms*, vol. 2, no. 1, pp. 27–36, 2005.

[49] Y. Wang, L. Yi, Z. Wu et al., "Comparative proteomic analysis of streptococcus suis biofilms and planktonic cells that identified biofilm infection-related immunogenic proteins," *PLoS ONE*, vol. 7, no. 4, article e33371, 2012.

[50] R. C. Jones, J. Deck, R. D. Edmondson, and M. E. Hart, "Relative quantitative comparisons of the extracellular protein profiles of *Staphylococcus aureus* UAMS-1 and its sarA, agr, and sarA agr regulatory mutants using one-dimensional polyacrylamide gel electrophoresis and nanocapillary liquid chromatography coupled with tandem mass spectrometry," *Journal of Bacteriology*, vol. 190, no. 15, pp. 5265–5278, 2008.

[51] D. Becher, K. Hempel, S. Sievers et al., "A proteomic view of an important human pathogen—towards the quantification of the entire *Staphylococcus aureus* proteome," *PLoS ONE*, vol. 4, no. 12, Article ID e8176, 2009.

[52] S. O. T. Curreem, R. M. Watt, S. K. P. Lau, and P. C. Y. Woo, "Two-dimensional gel electrophoresis in bacterial proteomics," *Protein and Cell*, vol. 3, no. 5, pp. 346–363, 2012.

[53] N. Islam, Y. Kim, J. M. Ross, and M. R. Marten, "Proteomic analysis of Staphylococcus aureus biofilm cells grown under physiologically relevant fluid shear stress conditions," *Proteome Science*, vol. 12, no. 1, article 21, 2014.

[54] N. Mohamed, L. Visai, P. Speziale, and J. M. Ross, "Quantification of Staphylococcus aureus cell surface adhesins using flow cytometry," *Microbial Pathogenesis*, vol. 29, no. 6, pp. 357–361, 2000.

[55] G. Grandi, "Bacterial surface proteins and vaccines," *F1000 Biology Reports*, vol. 2, article 36, 2010.

[56] L. A. Bøhle, T. Riaz, W. Egge-Jacobsen et al., "Identification of surface proteins in Enterococcus faecalis V583," *BMC Genomics*, vol. 12, article 135, 2011.

Hindawi Publishing Corporation
BioMed Research International
Volume 2016, Article ID 1289157, 14 pages
http://dx.doi.org/10.1155/2016/1289157

Research Article

In Vitro and *In Vivo* Biofilm Characterization of Methicillin-Resistant *Staphylococcus aureus* from Patients Associated with Pharyngitis Infection

Shanmugaraj Gowrishankar, Arumugam Kamaladevi, Krishnaswamy Balamurugan, and Shunmugiah Karutha Pandian

Department of Biotechnology, Alagappa University, Science Campus, Karaikudi, Tamil Nadu 630 003, India

Correspondence should be addressed to Shunmugiah Karutha Pandian; sk_pandian@rediffmail.com

Received 19 July 2016; Accepted 15 August 2016

Academic Editor: Carla R. Arciola

Copyright © 2016 Shanmugaraj Gowrishankar et al. This is an open access article distributed under the Creative Commons Attribution License, which permits unrestricted use, distribution, and reproduction in any medium, provided the original work is properly cited.

The present investigation was deliberately aimed at evaluating the biofilm-forming ability of 63 clinical MRSA isolates recovered from pharyngitis patients through different phenotypic assays. The molecular detection of adhesion (*icaA/icaD/icaB/icaC*), adhesins (*fnbA/fnbB*, *clfA*, and *cna*), staphylococcal accessory regulator (*sarA*), and α-toxin (*hla*) genes was done by employing polymerase chain reaction (PCR). Out of 63 isolates, 49 (77.8%) were found slime positive by the Congo red agar (CRA) method and 44 (69.8%) as biofilm positive by the quantitative microtitre plate assays. The results of MATH assay showed that most of the test pathogens are hydrophilic in nature. The molecular investigation of biofilm-associated genes revealed that 84.13% ($n = 53$) of isolates were found positive for *icaADBC* genes. The *fnbA* and *fnbB* genes were present in 49 (77.8%) and 51 (81%) MRSA isolates, respectively. In addition, 58.7% ($n = 37$), 73% ($n = 46$), and 69.8% ($n = 44$) of the isolates harboured the *clfA*, *cna*, and *hla* genes, respectively. Further, nearly 81% ($n = 51$) of the isolates were found positive for the gene *sarA* and all the *ica* negative isolates were also negative for the gene. Furthermore, the results of *in vivo* adherence assay unveiled the factual commonness in the *in vitro* adherence method.

1. Introduction

Globally, myriad of bacterial pathogens inhabiting the environment cause several acute and chronic infections to human through their ability to form dynamic, structurally complex, and multilayered cellular matrix, termed as biofilms [1]. The synthesis of such biofilms by pathogenic bacteria is therefore considered to be a major virulence factor, since the recalcitrant biofilms comprehensively safeguard the pathogens not only from host defence mechanism but also from the targeted action of therapeutic drugs [2]. Methicillin-resistant *Staphylococcus aureus* (MRSA) continues to be the most prominent biofilm-forming human pathogen causing both healthcare-related and community-acquired infections with a substantial increase in morbidity and mortality. Though *S. aureus* can be isolated from various niches of human body, where it exists harmlessly as a commensal, it can also be an opportunistic pathogen in causing diverse array of infections ranging from skin and soft tissue lesions to lethal infections such as osteomyelitis, endocarditis, pneumonia, and septicaemia [3]. This commensal microflora readily colonizes the anterior nares and approximately 30% of healthy people carry this bacterium in their anterior nares [4]. As the nasal and extranasal colonization find chief prominence in the pathogenesis of invasive MRSA infections [5], studies on this pathogen from human throat (a least considered carriage site than the nares) are of dire need.

Besides, *S. aureus* is also widely known for its remarkable ability to infect and damage the indwelling medical prosthetics and other implants usually catheters through the fabrication of biofilm architectures [6, 7]. Another impressive characteristic feature of *S. aureus* in imposing such adverse clinical complications is its metabolic adaptability that facilitates the pathogen to colonize and persist in diverse

environmental conditions. A wide range of virulent factors including extracellular toxins and surface structures in *S. aureus* are influential in the induction and persistence of infectivity within the host [8]. Although the potentials of biofilm assemblage of MRSA isolated from various infection sites of human and even from animals have been well demonstrated, studies on MRSA isolated from human throat are still inadequate. Therefore, the current study was proposed to characterize the biofilm-forming ability among clinical isolates of MRSA recovered from throat swabs pharyngitis patients.

The ability to attach, adhere, and synthesize biofilms has enhanced the virulence in MRSA. The mechanism of biofilm formation in *S. aureus* involves three major stages: initial attachment, maturation of biofilms, and dispersion of bacterial cells [9]. In *S. aureus* biofilm formation, the foremost and fundamental step is initial attachment, that is, adhesion which is being accomplished by the expression of different Microbial Surface Components Recognizing Adhesive Matrix Molecules (MSCRAMMs). These MSCRAMMs have high ability to interact with the host extracellular matrix proteins such as elastin binding protein (*ebpS*), laminin binding protein (*eno*), collagen-binding protein (*cna*), fibronectin-binding proteins A and B (*fnbA* and *fnbB*), fibrinogen binding protein (*fib*), and clumping factors A and B (*clfA* and *clfB*) [10]. Earlier studies on the molecular aspects of growth phase and subsequent establishment of biofilms have shown that *S. aureus* initially adhere to each other and then widen to structurally dynamic and intensely intricate biofilm architectures during the later phases of adherence. The biosynthesis of polysaccharide intercellular adhesin (PIA), a polysaccharide compiled from β-1, 6- linked N-acetyl-D-glucosamines (PNAG), is the hallmark element in the development of actual mature biofilms resulting in notorious multilayered clustering matrix of cells (second stage). PIA is mediated by the intercellular adhesin (*ica*) locus, which comprises four core genes, namely, *icaA*, *icaD*, *icaB*, and *icaC* and a regulatory gene (*icaR*) [6, 11]. The increase in the production of N-acetylglucosaminyl transferase and slime is facilitated by the coexpression of *icaA* and *icaD* genes [12]. While the genes *icaB* and *icaC* encode for extracellular membrane proteins, wherein *icaC* is whispered to have a role as receptor for polysaccharides and the function of *icaB* gene still remains uncover [13]. The accessory gene regulator (*agr*) locus, a well-characterized two-component regulatory system, plays a critical role in the upregulation and downregulation of protease and exotoxins, respectively [14], reflecting the final dispersal stage. In spite of deeper understanding on the biofilm-forming ability of *S. aureus*, it is still essential to extend the research on recently emerging MRSA strains (believed to be evolving from several clonal lineages of methicillin-susceptible *S. aureus* (MSSA) strains) as an attempt to address the complexity of their biofilm formation.

As a response to the above facts, the present study for the first time was focused on assessing the biofilm-forming properties among MRSA isolated from throat swabs of patients associated with pharyngitis through different phenotypic assays like slime synthesis, *in vitro* biofilm formation, and microbial adhesion to hydrocarbons (MATH). Furthermore, polymerase chain reaction (PCR) was performed to detect the adhesion (*icaA*/*icaD*/*icaB*/*icaC*), several adhesins (*fnbA*/*fnbB*, *clfA*, and *cna*), staphylococcal accessory regulator (*sarA*), and α-toxin (*hla*) genes. Finally, the *in vivo* adherence of the phenotypically and genotypically categorized MRSA isolates was assessed using a tropical nematode, *Caenorhabditis elegans,* as an animal model.

2. Materials and Methods

2.1. Bacterial Strains and Culture Conditions. A total of 63 MRSA isolates recovered from GAS associated pharyngitis patients were taken for evaluation of phenotypic and genotypic biofilm characteristics in the current study. The molecular identification and characterization of the MRSA isolates have already been done and reported by the same authors [15]. The MRSA isolates were grown and maintained on Tryptic soy agar/broth (TSA/TSB).

2.2. Phenotypic Assessment of Slime Synthesizing S. aureus Strains Using CRA. The qualitative slime production was assessed on the basis of the colour of *S. aureus* colonies developed on Congo red agar (CRA) plate according to the criteria described previously [16]. Briefly, MRSA clinical isolates were inoculated onto the CRA medium composed of TSB (30 g/L), sucrose (36 g/L), agar powder (18 g/L), and Congo red dye (0.8 g/L) and then cultured for 24 h at 37°C under aerobic conditions. The reference strains MRSA ATCC 33591 (slime producer) and *Staphylococcus epidermidis* ATCC 12228 (non-slime producer) were used as positive and negative controls, respectively.

The results regarding slime production were interpreted as follows: strains producing intensive black, black, and reddish black colonies with a rough, dry, and crystalline consistency were considered to be normal slime producers, whereas red and Bordeaux red with smooth colonies were classified as nonslime producers as reported elsewhere [17].

2.3. In Vitro Adherence Assay on Polystyrene Microtitre Plate (MtP). *In vitro* biofilm formation was spectroscopically quantified by performing polystyrene microtitre plate (MtP) assay, as described previously with slight modifications [21]. Briefly, the test MRSA isolates were inoculated in 2 mL of TSB supplemented with 0.25% glucose and incubated overnight in shaking incubator (80 rpm, orbital shaker; Scigenics Biotech, Orbitek LEBT, India) at 37°C. The overnight culture of the test pathogens (1%) was then used to inoculate 24-well polystyrene MtPs containing 1 mL of fresh TSB supplemented with 0.25% glucose. The plates were incubated for 24 h at 37°C. After incubation, the plates were carefully washed thrice with sterile phosphate buffered saline (7 mM Na_2HPO_4, 3 mM NaH_2PO_4, and 130 mM NaCl at pH 7.4) to remove nonadherent cells and were air-dried in an inverted position before being stained. Adherent cells were stained with 1 mL of 0.4% crystal violet solution (w/v) for 2 min and the excess of dye was poured off. The wells were washed with sterile distilled water and then allowed to air-dry. Finally 1 mL of absolute ethanol was added into each well before being read spectroscopically. The optical density of the adherent biofilm

was determined at OD_{570} nm, using a Multimode Microplate Reader (SpectraMax M3, USA) where the 1 mL of absolute ethanol served as blank. The strain *S. epidermidis* ATCC 12228 was used as the negative control. The adherence ability of tested isolates was classified into four categories based on the obtained OD: strongly adherent ($OD_{570} \geq 3.0$), moderately adherent ($OD_{570} \leq 1.5$–2.0), weakly adherent ($OD_{570} \leq 0.5$–1.0), and nonadherent ($OD_{570} < OD_{570}$ of negative control).

2.4. Confocal Laser Scanning Microscopy (CLSM). In order to visualize the diverse biofilm architecture (on the basis of biofilm-forming potential through phenotypic and genotypic assays) of the four categorized test pathogens GSA-140, GSA-21, GSA-142, and GSA-54, Confocal Laser Scanning Microscopy (CLSM) (model: LSM 710) (Carl Zeiss, Germany) analysis was employed [22].

CLSM analysis was performed for the biofilms formed by the pathogens on glass pieces. The analysis was initiated by dispensing 1% inoculum of overnight cultures grown in TSB supplemented with 0.25% glucose into 24-well MtP containing 1 mL of fresh TSB + 0.25% glucose medium. Plates were statically incubated at 37°C for 24 h. After incubation, the glass pieces were gently washed with PBS and strained with 0.1% acridine orange for 5 min at room temperature in the dark. The stained glass pieces were gently washed thrice with PBS, air-dried, and observed under CLSM. Zen 2009 image software was used for analysis of biofilm images, which allowed for collection of *z*-stacks three-dimensional (3D) reconstruction. Images were acquired from random positions of biofilms formed on the glass slides. COMSTAT software (kind gift from Dr. Claus Sternberg, DTU Systems Biology, Technical University of Denmark) was used for further analysis of the obtained CLSM images (biofilm stack), in which three different parameters such as an average and maximum thickness (μm) of the biofilms and the biovolume (μm^3), which is the volume of bacteria per μm^2 of glass surface used, were analysed [22].

2.5. MATH Assay. Cell surface hydrophobicity of the test pathogens was determined by using MATH (microbial adhesion to hydrocarbons) assay as an evaluation of their affinity towards the hydrophobic hydrocarbon (toluene) following the procedure described previously [23]. Briefly, 1 mL of test bacterial culture ($OD_{530\,nm} = 1.0$) (Abs1) was placed into glass tubes along with 100 μL of toluene. The mixtures were vigorously vortexed for 2 min and incubated for 10 min at room temperature to allow phase separation, and then the $OD_{530\,nm}$ of the aqueous phase was recorded (Abs2). The percentage of hydrophobicity was calculated according to the following formula: % hydrophobicity = $[1 - (Abs2/Abs1)] \times 100$.

2.6. Detection of icaA, icaD, icaB, icaC, fnbA, fnbB, clfA, cna, and hla Genes. The chromosomal DNA of 63 MRSA isolates was extracted using the procedure described previously with minor modification [24] (omission of mutanolysin and hyaluronidase enzymes). The PCR assay for the detection of *icaA*, *icaD*, *icaB*, *icaC*, *sarA*, *fnbA*, *fnbB*, *clfA*, *cna*, and *hla* genes was performed using the primers (forward and reverse) and their respective standardized annealing temperatures as mentioned in Table 1. An aliquot of 2 μL of DNA template (~10 ng) was added to 23 μL of PCR mixture containing 1 × PCR buffer [10 mM Tris–HCl (pH 8.8), 50 mM KCl], 0.2 mM dNTPs, 1.5 mM $MgCl_2$, 50 pM primer, and 1 U Taq polymerase (MBI Fermentas, Germany). Amplified PCR products were analyzed by agarose gel stained with ethidium bromide (0.5 $\mu g\,\mu L^{-1}$) and visualized under ultraviolet transillumination and documented using Gel Doc XR apparatus (Biorad, USA).

2.7. In Vivo Adherence Assay Using C. elegans. A batch of three representative isolates was selected from each of the four categories (classified on the basis of phenotypic and genotypic characterization) for their *in vivo* adherence potential in *C. elegans*. The adherence assay was qualitatively examined by using CLSM as described earlier with slight modifications [25]. Briefly, twenty age-synchronized young adult hermaphrodite nematodes were transferred from a lawn of *E. coli* OP50 to the M9 buffer containing characterized MRSA isolates present in a sterile 24-well culture plate [20% inoculum (0.1 O.D of cells in 660 nm), i.e., 9×10^6 cells m/L of LB medium] and incubated for 24 h at 20°C. After incubation, the nematodes were thoroughly washed and anesthetised by using 0.1 mM sodium azide to avoid expulsion of bacteria from nematodes intestine. Finally, the nematodes were stained with 0.1% acridine orange and visualized under CLSM.

2.8. Colony Forming Unit (CFU) Assay. To further ascertain the CLSM results and to quantify the adherence inside the *C. elegans*, a CFU assay was performed as described previously [25]. Briefly, a batch of ten nematodes were infected with each group of MRSA isolates ($n = 3$) for 24 h and washed thrice with M9 buffer to remove the surface bacteria. The washed nematodes were then transferred to the 1.5 mL microcentrifuge tube and the final volume was made up to 400 μL with M9 buffer. Finally, 400 mg of silicon carbide particles (1.0 mm; Himedia, India) was added to each tube and vortexed at the maximum speed for 2 min. The resulting suspension was serially diluted and plated on Hicrome Aureus agar (Himedia, India) to determine the CFU.

3. Results

3.1. Phenotypic Characterization of S. aureus Slime Production on Congo Red Agar (CRA). The phenotypic determination of slime producing ability in Congo red agar of all the test isolates is shown in Table 2. As it is perceptibly evident from Figures 1 and 2 and Table 2, the different isolates of MRSA were unwaveringly found to be slime producers to varying degrees. Out of 63 MRSA isolates, 18 (28.6%), 23 (36.5%), 8 (12.7%), and 14 (22.2%) were determined to be strong black, black, reddish black, and Bordeaux red colour colony producers, respectively. The reference strains MRSA ATCC 33591 (positive control) and *S. epidermidis* ATCC 12228 (negative control) produced typical black and pink colonies, respectively, after 48 h incubation (Figure 1).

3.2. MATH Assay. The affinity of MRSA isolates towards toluene (nonpolar solvent) was unveiled by MATH assay and

Table 1: Sequences of oligonucleotide primers used for PCR amplification of biofilm-associated genes.

Gene	Nucleotide sequence of primers (5′–3′).		Annealing temperature	Amplicon size (bp)	References
	Forward primer	Reverse primer			
icaA (intercellular adhesion gene)	ACACTTGCTGGCGCAGTCAA	TCTGGAACCAACATCCAACA	53°C	188	[17]
icaD (intercellular adhesion gene)	ATGGTCAAGCCCAGACAGAG	AGTATTTTCAATGTTTAAAGCA	53°C	198	[17]
icaB (intercellular adhesion gene)	CCCAACGCTAAAATCATCGC	ATTGGAGTTCGGAGTGACTGC	53°C	1080	[18]
icaC (intercellular adhesion gene)	CATGAAAATATGGAGGGTGG	TCAAACTGATTTCGCCCACCG	50°C	1000	[18]
fnbA (fibronectin-binding protein A)	ATCAGCAGATGTAGCGGAAG	TTTAGTACCGCTCGTTGTCC	55°C	198	[19]
fnbB (fibronectin-binding protein B)	AAGAAGCACCGAAAACTGTG	TCTCTGCAACTGCTGTAACG	55°C	198	[19]
clfA (clumping factor A)	ATTGGCGTGGCTTCAGTGCT	CGTTTCTTCCGTAGTTGCATTTG	55°C	292	[20]
cna (collagen-binding protein)	AAAGCGTTGCCTAGTGGAGA	AGTGCCTTCCCAAACCTTTT	55°C	192	[12]
sarA (staphylococcal accessory regulatory locus)	CCCAGAAATACAATCACTGTG	AGTGCCATTAGTGCAAAACC	53°C	720	[18]
hla (alpha toxin)	CAACTGATAAAAAAGTAGGCTGGAAAGTGAT	CTGGTGAAAACCCTGAAGATAATAGAG	50°C	200	[17]

Table 2: Relationships among the presence of *icaA*, *icaD*, *icaB, icaC*, *fnbA, fnbB, clfA, cna*, *hla,* and *sarA* genes, slime production, adherence capacity on MtPs, and hydrophobicity index in 63 different clinical MRSA associated with GAS pharyngitis infection.

Strain ID	Biofilm phenotype on CRA	Slime synthesis	*In vitro* adherence (MtP) assay		Hydrophobicity index ± SD	Presence of adhesion genes									
			Adherence OD_{570} nm ± SD	*Adherence ability		*icaA*	*icaB*	*icaC*	*icaD*	*sarA*	*cna*	*clfA*	*fnbA*	*fnbB*	*hla*
GSA-83	Black	Producer	1.42 ± 0.213	++	26.3 ± 0.325	+	+	+	+	+	+	+	+	+	+
GSA-22	Black	Producer	1.79 ± 0.659	++	32.3 ± 0.336	+	+	+	+	+	+	+	+	+	+
GSA-32	Strong black	Producer	3.23 ± 0.986	+++	29.4 ± 0.962	+	+	+	+	+	+	+	+	+	+
GSA-A21	Black	Producer	1.53 ± 0.286	++	40.3 ± 0.560	+	+	+	+	+	+	−	+	−	−
GSA-127	Black	Producer	0.91 ± 0.632	+	32.9 ± 0.123	−	−	−	−	+	−	−	−	+	+
GSA-74	Strong black	Producer	3.21 ± 0.215	+++	41.3 ± 0.963	+	+	+	+	+	+	−	−	−	−
GSA-45	Strong black	Producer	3.09 ± 0.0236	+++	44.2 ± 0.023	+	+	+	+	+	+	+	+	+	+
GSA-150	Reddish black	Nonproducer	0.19 ± 1.023	−	15.3 ± 0.965	−	−	−	−	+	−	+	+	+	+
GSA-99	Reddish black	Nonproducer	1.32 ± 0.963	++	16.4 ± 0.189	+	+	+	+	−	+	−	−	+	+
GSA-103	Bordeaux red	Nonproducer	0.47 ± 0.451	−	21.6 ± 0.651	+	+	+	+	+	+	+	+	+	+
GSA-89	Strong black	Producer	3.41 ± 0.238	+++	29.3 ± 0.359	+	+	+	+	+	+	+	+	+	+
GSA-50	Black	Producer	3.06 ± 0.896	+++	31.2 ± 0.158	+	+	+	+	+	+	+	+	+	+
GSA-A8	Strong black	Producer	2.53 ± 1.639	++	27.9 ± 0.958	+	+	+	+	+	−	+	+	+	+
GSA-44	Strong black	Producer	3.86 ± 0.127	+++	24.6 ± 0.756	+	+	+	+	+	+	+	−	−	−
GSA-46	Bordeaux red	Nonproducer	0.39 ± 0.986	−	24.3 ± 0.286	+	+	+	+	+	+	−	+	+	+
GSA-48	Black	Producer	1.06 ± 1.028	+	20.9 ± 0.396	+	+	+	+	+	+	−	+	+	+
GSA-54	Bordeaux red	Nonproducer	0.49 ± 0.966	−	14.5 ± 0.362	−	−	−	−	+	−	+	−	+	+
GSA-395	Strong black	Producer	3.23 ± 0.523	+++	29.5 ± 0.396	+	+	+	+	+	+	+	+	+	+
GSA-68	Strong black	Producer	3.51 ± 0.889	+++	32.6 ± 0.325	+	+	+	+	+	+	+	+	+	+
GSA-94	Bordeaux red	Nonproducer	0.42 ± 0.365	−	18.6 ± 0.176	−	−	−	−	−	−	−	−	−	−
GSA-104	Black	Producer	1.48 ± 0.632	++	30.9 ± 0.963	−	−	−	−	−	+	+	−	+	+
GSA-140	Strong black	Producer	3.52 ± 0.023	+++	36.2 ± 0.990	+	+	+	+	+	+	−	+	−	−
GSA-145	Strong black	Producer	3.22 ± 0.965	+++	28.9 ± 1.230	+	+	+	+	+	+	−	+	−	−
GSA-142	Reddish black	Nonproducer	0.96 ± 1.036	+	30.6 ± 0.968	−	−	−	−	+	−	−	−	−	−
GSA-70	Bordeaux red	Nonproducer	0.23 ± 0.396	−	13.6 ± 0.869	−	−	−	−	−	−	−	+	+	+
GSA-126	Strong black	Producer	3.62 ± 0.325	+++	43.6 ± 0.310	+	+	+	+	+	+	+	+	+	+
GSA-A4	Black	Producer	2.57 ± 0.635	++	21.5 ± 0.256	+	+	+	+	+	+	+	+	+	+
GSA-92	Reddish black	Nonproducer	0.39 ± 0.961	−	12.9 ± 0.178	+	+	+	+	+	−	−	+	+	+
GSA-365	Black	Producer	1.98 ± 0.362	++	36.5 ± 0.986	+	+	+	+	+	−	+	+	+	−
GSA-A12	Black	Producer	1.59 ± 0.589	++	21.9 ± 0.936	+	+	+	+	+	+	+	+	+	+
GSA-A18	Bordeaux red	Nonproducer	1.09 ± 0.698	+	19.2 ± 0.129	+	+	+	+	+	−	−	+	+	−
GSA-297	Black	Producer	1.96 ± 0.129	++	29.9 ± 0.326	+	+	+	+	+	+	+	+	+	+
GSA-134	Reddish black	Nonproducer	3.12 ± 0.396	+++	13.6 ± 0.349	+	+	+	+	+	+	−	+	+	−
GSA-75	Black	Producer	1.79 ± 0.326	++	30.1 ± 0.559	+	+	+	+	+	+	+	+	+	+
GSA-88	Strong black	Nonproducer	3.09 ± 0.856	+++	24.3 ± 0.552	+	+	+	+	+	+	+	+	+	+
GSA-71	Black	Producer	3.85 ± 0.785	+++	22.3 ± 0.639	+	+	+	+	+	+	+	+	+	+
GSA-A25	Black	Producer	0.85 ± 0.759	+	26.8 ± 1.36	+	+	+	+	+	−	+	+	+	+
GSA-79	Bordeaux red	Nonproducer	0.21 ± 0.856	−	14.9 ± 0.759	−	−	−	−	−	+	−	+	+	−
GSA-52	Black	Producer	3.52 ± 0.996	+++	23.6 ± 0.529	+	+	+	+	+	+	+	−	−	+
GSA-91	Bordeaux red	Nonproducer	0.86 ± 1.236	+	15.9 ± 0.169	+	+	+	+	+	−	+	+	+	+
GSA-84	Strong black	Producer	3.11 ± 1.036	+++	40.1 ± 0.629	+	+	+	+	+	+	−	+	+	+
GSA-53	Bordeaux red	Nonproducer	0.36 ± 0.845	−	19.1 ± 0.785	+	+	+	+	+	−	+	+	+	+

Table 2: Continued.

Strain ID	Biofilm phenotype on CRA	Slime synthesis	*In vitro* adherence (MtP) assay		Hydrophobicity index ± SD	Presence of adhesion genes									
			Adherence OD_{570} nm ± SD	*Adherence ability		*icaA*	*icaB*	*icaC*	*icaD*	*sarA*	*cna*	*clfA*	*fnbA*	*fnbB*	*hla*
GSA-137	Black	Producer	1.56 ± 0.965	++	22.6 ± 0.396	+	+	+	+	+	+	−	+	+	+
GSA-A20	Strong black	Producer	3.51 ± 0.515	+++	42 ± 0.968	+	+	+	+	+	+	−	+	+	+
GSA-291	Black	Producer	1.63 ± 0.689	++	26.9 ± 0.236	+	+	+	+	+	+	−	+	+	+
GSA-98	Black	Producer	1.79 ± 0.632	++	22.6 ± 0.756	+	+	+	+	+	+	−	+	+	+
GSA-73	Strong black	Producer	3.24 ± 0.325	+++	36.2 ± 0.688	+	+	+	+	+	+	−	+	+	+
GSA-A16	Black	Producer	2.06 ± 0.963	++	32.8 ± 0.895	+	+	+	+	−	+	+	+	+	+
GSA-131	Bordeaux red	Nonproducer	1.08 ± 0.896	+	16.3 ± 0.955	+	+	+	+	+	−	−	+	+	−
GSA-410	Strong black	Producer	3.69 ± 0.563	+++	36.8 ± 0.269	+	+	+	+	+	+	+	+	+	+
GSA-377	Bordeaux red	Nonproducer	0.27 ± 1.342	−	17.2 ± 0.745	+	+	+	+	+	+	+	+	+	−
GSA-A1	Black	Producer	3.04 ± 0.506	+++	21.1 ± 0.986	+	+	+	+	+	+	+	−	−	+
GSA-A6	Bordeaux red	Nonproducer	0.79 ± 0.966	+	13.9 ± 0.156	+	+	+	+	+	+	+	+	+	−
GSA-A9	Strong black	Nonproducer	2.89 ± 0.796	++	24.3 ± 0.969	+	+	+	+	+	+	+	+	+	+
GSA-A17	Black	Producer	1.85 ± 0.235	+++	19.9 ± 0.589	+	+	+	+	+	+	+	+	+	+
GSA-28	Bordeaux red	Nonproducer	1.25 ± 0.168	+	19.2 ± 0.129	+	+	+	+	+	+	+	−	+	−
GSA-51	Black	Producer	2.57 ± 0.234	++	21.3 ± 0.345	+	+	+	+	+	+	−	+	+	+
GSA-58	Reddish black	Nonproducer	0.55 ± 0.996	+	18.2 ± 0.569	+	+	+	+	+	+	+	+	+	−
GSA-63	Reddish black	Nonproducer	1.43 ± 0.351	++	11.9 ± 0.266	−	−	−	−	−	−	−	−	−	−
GSA-81	Reddish black	Nonproducer	0.98 ± 0.029	+	19.1 ± 0.192	+	+	+	+	−	−	−	−	−	+
GSA-86	Bordeaux red	Nonproducer	0.49 ± 0.259	−	16.2 ± 0.367	−	−	−	−	−	−	+	−	−	−
GSA-97	Strong black	Nonproducer	3.39 ± 0.125	+++	23.9 ± 0.121	+	+	+	+	+	+	+	+	+	+
GSA-102	Black	Producer	1.08 ± 0.985	+	24.5 ± 0.276	+	+	+	+	+	+	−	+	+	−

∗: Indicating the varied adhering ability of isolates on polystyrene surface, where +++ represents highly adherent (OD570 values of >3.0), ++ represents strongly adherent (OD570 values of >2.0), + represents moderately adherent (OD570 values of >1.0–2.0) and − represents weakly adherent (OD570 values of >0.5–1.0).

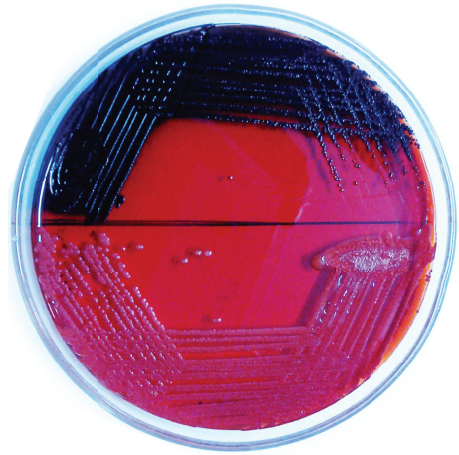

Figure 1: Colony morphologies of reference *Staphylococcus aureus* strains MRSA ATCC 33591 (positive control) and *S. epidermidis* ATCC 12228 (negative control) revealing strong black (upper sector) and pink (lower sector) coloured colonies on Congo red agar medium, respectively.

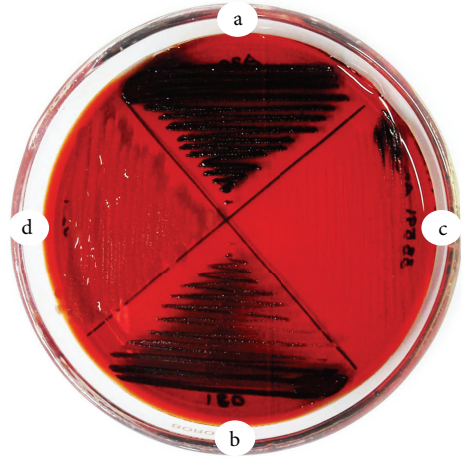

Figure 2: Congo red agar test showing four different slime producing patterns of clinical MRSA isolates: (a) slime positive bacteria with dark shiny black colonies (upper sector); (b) black colonies (bottom sector); (c) weak black colonies (right sector); and (d) slime negative bacteria showing pink coloured colonies (left sector).

the results are summarized in Table 2. From the obtained results, it was found that the majority of the tested MRSA isolates (87.3%) exhibited a hydrophilic character, whereas eight MRSA isolates (12.7%) displayed a relative hydrophobic character.

3.3. In Vitro Adherence Assay on Polystyrene Microtitre Plate (MtP). The quantitative MtP method is the most extensively used gold standard technique for the detection of biofilm formation [26]. Table 2 and Figure 3(a) clearly show that all the MRSA isolates tested were found to be adherent at varying levels on 24-well polystyrene MtPs. Among 63 isolates studied, 21 (33.3%) isolates were highly adherent with OD_{570} values of >3, 5 isolates (7.9%) were strongly adherent with OD_{570} values of >2.0, 19 isolates (30.1%) were moderately adherent with OD_{570} values of >1–2.0, and 18 (28.6%) isolates were weakly adherent with OD_{570} values of <0.5–1. The MRSA ATCC 33591 strain was found to be strongly adherent with an OD_{570} value >2.0, while the *S. epidermidis* ATCC 12228 strain was negatively adherent ($OD_{570} < 0.5$).

3.4. Distribution of Adhesion and Biofilm Loci. As the prime intention of the present study is the genotypic characterization of biofilm responsible genes, PCR assay was employed to detect *icaA*, *icaD*, *icaB*, *icaC*, *fnbA*, *fnbB*, *clfA*, *cna*, *hla*, and *sarA* genes among test MRSA strains. The distributions of these genes in 63 MRSA isolates are summarized in Table 2. As can be seen in Table 2, the majority of MRSA isolates [84.13% ($n = 53$)] were found to be positive for *icaADBC* genes. The prevalence of *sarA*, *fnbA*, *fnbB*, *clfA*, *cna*, and *hla* genes was unswervingly found to be 81, 84.1, 81, 58.7, 90.5, and 70%, respectively (Figure 4). Using the obtained biofilm responsible gene patterns of 63 MRSA isolates, a dendrogram was generated resulting in 5 clusters, namely, A, B,

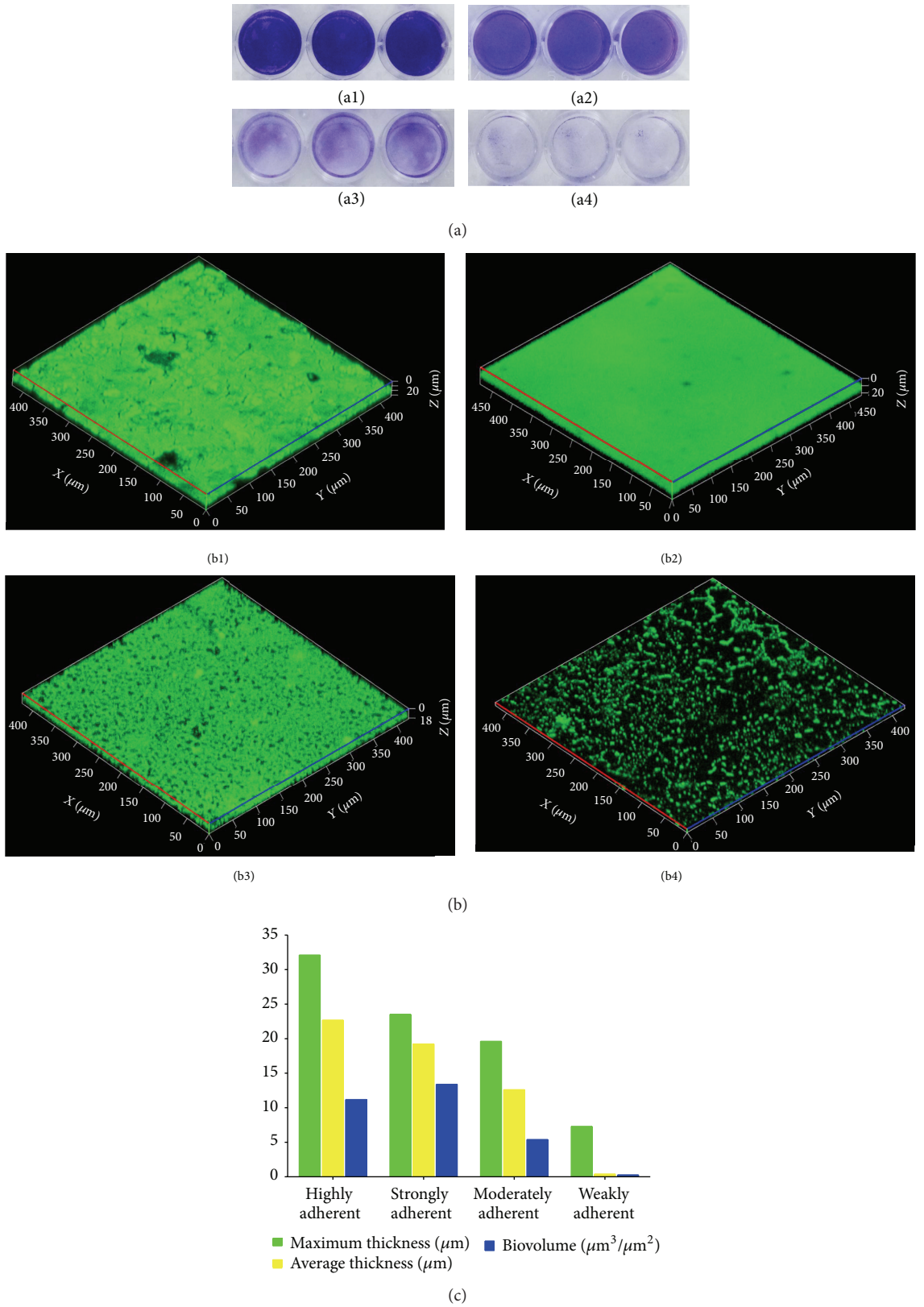

FIGURE 3: Total biofilm formation of different clinical MRSA isolates. (a) The bacterial cells were grown in 24-well Mtps containing TSB supplemented with 0.25% glucose. The cells that adhered to the plate surface after washing with phosphate buffer were visualized by crystal violet staining. The isolates were considered as highly adherent (a1), strongly adherent (a2), moderately adherent (a3), and nonadherent (a4) based upon their absorbance at 570 nm as measured by spectrophotometer. (b) Confocal laser scanning micrographs revealing variable degrees of biofilm production by clinical MRSA isolates on glass surface: (b1) highly adherent; (b2) strongly adherent; (b3) moderately adherent; and (b4) nonadherent isolates. (c) COMSTAT analysis of the obtained CLSM images.

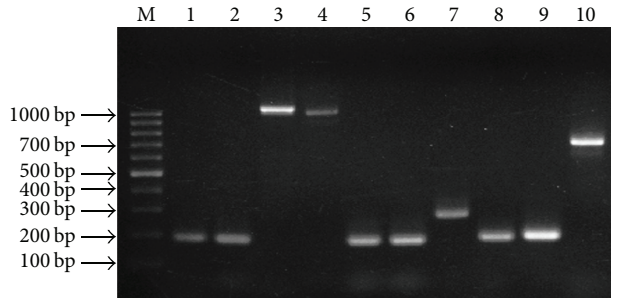

Figure 4: PCR amplification for the detection of genes responsible for biofilm formation in clinical MRSA isolates. Lane 1, 100 bp ladder (MBI Fermentas); lane 1–10, PCR amplicons of *icaA*, *icaD*, *icaB, icaC*, *fnbA*, *fnbB*, *clfA*, *cna*, *hla*, and *sarA* genes amplified from the clinical MRSA isolate GSA-32.

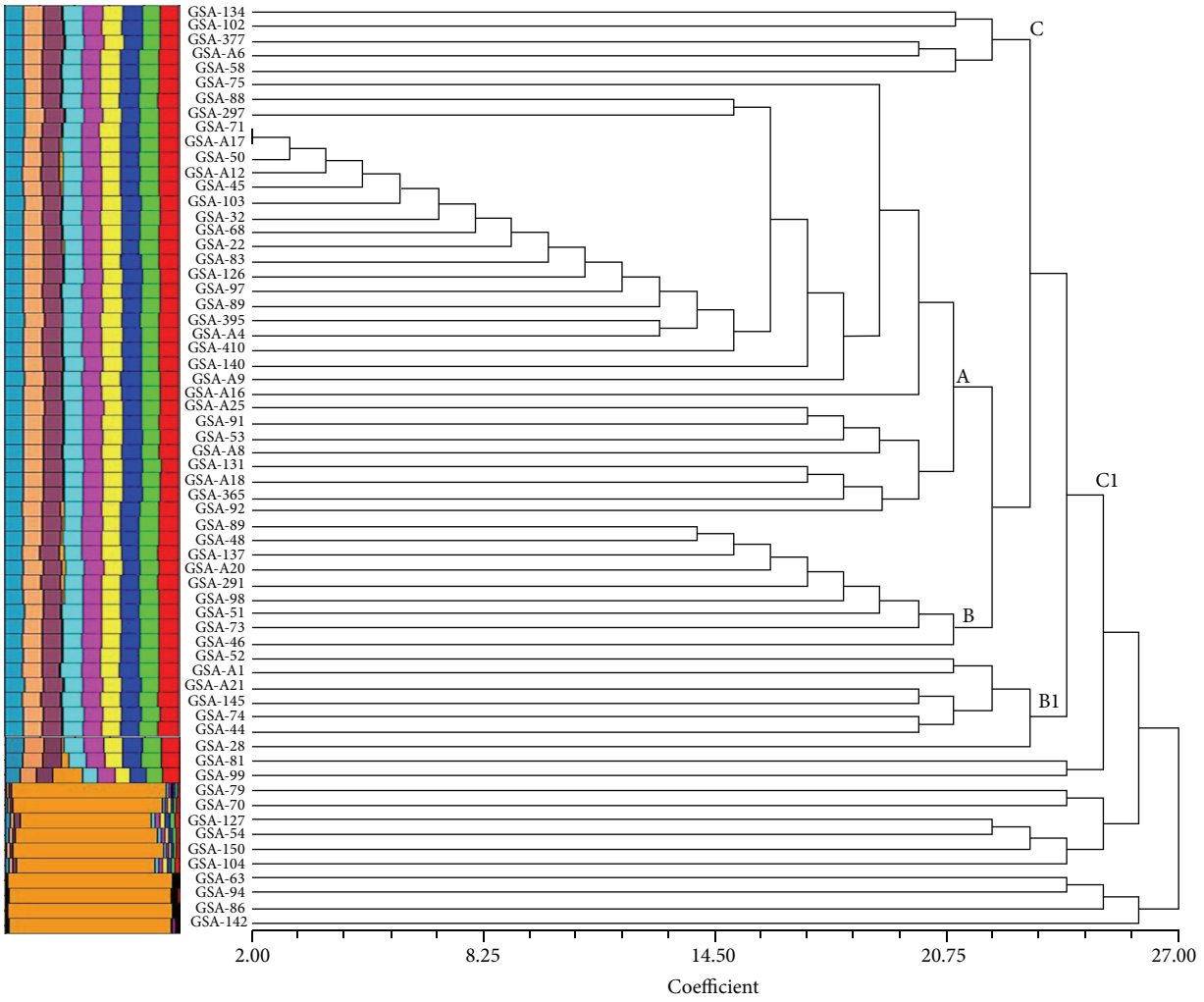

Figure 5: Dendrogram based on the amplification pattern of biofilm responsible genes, demonstrating the genotypic relatedness among the 63 MRSA isolates recovered from GAS pharyngitis patients. Scale represents the distance coefficient.

B1, C, and C1 (Figure 5). The data revealed that most of the strongly and moderately adherent isolates were under clusters B and B1 and around 95% of highly adherent isolates were harboured in cluster A, whereas clusters C and C1 showed the predominance of weak and few moderately adherent isolates.

3.5. In Vivo Adherence and Colonization of MRSA Isolates in C. elegans. In order to study the bioadherence property of four phenotypically and genotypically categorized MRSA isolates (highly, strongly, moderately, and weakly adherent isolates), an *in vivo* assay was performed using *C. elegans*.

For examining the adherence potential of the MRSA isolates, the pathogen-exposed nematodes were examined by CLSM using Zen software. The fluorescence intensity found in the nematodes indicated the density of bacterial load inside the *C. elegans*. As anticipated, the highly and strongly adherent groups showed more intense fluorescence compared to the moderately and weakly adherent groups which showed moderate and very low fluorescence intensities, respectively (Figure 6). Furthermore, the level of CFU in pathogen-exposed nematodes was increased ($152 \pm 17.8 \times 10^4$) in highly adherent groups ($P \leq 0.05$), modest ($32 \pm 4.6 \times 10^4$) in strongly adherent groups ($P \leq 0.05$), and decreased in moderately ($28 \pm 2.6 \times 10^2$) and weakly adherent ($21 \pm 3 \times 10^2$) groups, respectively (Figure 7).

4. Discussion

Beyond being a commensal microflora, *S. aureus* primarily colonizes the anterior nares of human population. In addition, 30% (approximately) of healthy individuals are recognized as the carriers of this bacterium [4]. Though a few reports from the past have depicted that the human throat is less well studied site of carriage than the nares, apart from some isolations accounted, the scientific data obtained during 1940s have reported the throat colonization rate to be 4–63% [27]. Further persistent surveillance studies have reconfirmed the observation that MRSA in throat may be selectively colonized and escape from routine screening process in the infection control programs [28, 29]. Despite the fact that *S. aureus* was incredibly recurrent in causing varied range of human infections (aforementioned), the role of *S. aureus* in causing pharyngitis infection is also becoming noticeable but found less often when compared to the GAS pharyngitis infections [15, 30].

Though plethora of research findings have broadened our knowledge on the biofilm attributes of *S. aureus*, particularly MRSA emerging from various infection sites of human, it was necessarily important to widen our studies on the biofilm characterization of MRSA strains from new sites of infection as well. In our previous study, we demonstrated the possible role of MRSA on its own or in association with GAS in pharyngitis infection [15]. We extend the present study by performing the *in vitro* and *in vivo* biofilm characterization of the MRSA strains ($n = 63$), owing to the fact that the biofilm formation and adhesive ability are the prime virulence traits in *S. aureus*. The current study is the first of its kind to evaluate the biofilm-forming abilities among MRSA isolates recovered from new infection site, that is, throats of pharyngitis patients, which possibly would contribute towards the understanding of infection process. Researchers from the past have demonstrated the significance of MtP, CRA, and/or PCR techniques for the determination of critical virulence factors, particularly the ability of biofilm formation in *Staphylococcus* species [16, 31, 32].

Following the same paradigm, we also assessed 63 MRSA strains for their biofilm-forming capabilities employing three *in vitro* screening procedures (the MtP method, the CRA test, and the PCR technique). It has been well known that *S. aureus* can adhere and build biofilms on the medical implants and/or indwelling medical devices that can be attributed to a characteristic feature known as slime production [33]. This study utilized Congo red agar assay to determine the efficiency of test pathogens for their slime production, considering their high virulence and extreme potency in imposing severe postsurgical infections. Out of 63 MRSA strains tested, 49 (77.8%) were found to exhibit a positive phenotype for slime production by developing strong black or reddish black colonies on CRA plates. This result is in consonance with the previous reports by Kouidhi et al. [17], Arciola et al. [34], and Ammendolia et al. [35], wherein 50, 60.8, and 88.9% of *S. aureus* were found to be positive for slime production, respectively.

Cell surface hydrophobicity (CSH) plays a crucial role in the adherence of staphylococci to the host cells [17, 21]. Several reports from the recent past have reiterated this fact by observing that while there was a decrease in biofilm formation of *S. aureus*, similarly there was also a significant decrease in its cell surface charges like hydrophobicity during the treatment of any antibiofilm or sub-MICs of antibiotic agents [17, 22]. Here, we have determined the hydrophobic index of 63 MRSA isolates by performing MATH assay using toluene. The results summarized in Table 2 indicate that the surface affinity of *S. aureus* towards toluene was low signifying the hydrophilic nature of 87.3% ($n = 54$) of MRSA isolates subjected for this study. However, 12.7% ($n = 8$) of the isolates showed hydrophobicity and have also exhibited a strong biofilm formation on polystyrene MtPs, suggesting the possible interaction between the hydrophobic cells and substrate. The result of this assay is in agreement with the previous reports by Kouidhi et al. [17] and Hamadi et al. [36] portraying the hydrophilic nature of *S. aureus* surface.

Regardless of the actuality that several methods have been described so far to evaluate the accumulation and biofilm formation, MtP-based method was highly employed in most of the studies [37, 38]. The data of quantitative biofilm formation assay using MtPs showed 21 isolates as highly adherent ($OD_{570} > 3$), 5 isolates as strongly adherent ($OD_{570} > 2.0$ but <3), 19 isolates as low grade adherent ($OD_{570} > 2$), and remaining 18 as nonadherent ($OD_{570} < 1$). The result of this assay was validated by the confocal scanning micrographs (Figure 3(b)) followed by the COMSTAT analysis (Figure 3(c)) of the acquired images for single representative isolate from each of the four categories.

Further, the involvement of biofilms in clinical infections has received increasing interest due to the characterization of genes involved in biofilm formation [13]. Multitude of reports has demonstrated the significance of surface components in the biofilm formation of *S. aureus* such as the product of *icaADBC* operon, which encodes proteins for the synthesis of polysaccharide, poly-N-acetyl β-1-6-glucosamine (PNAG) [6, 39]. In addition, few extracellular proteins as well as cell-bound adhesins (also called MSCRAMMs) are considered essential for the pathogenicity of *S. aureus*. Consequently, the MRSA isolates were subjected to genotypic detection of *icaA*, *icaD*, *icaB,* and *icaC* genes and certain adhesin genes like *clfA*, *cna*, *fnbA,* and *fnbB* through PCR. The data of PCR analysis revealed that, except the 10 MRSA isolates, the remaining 53 MRSA isolates (84.13%) were found to harbour

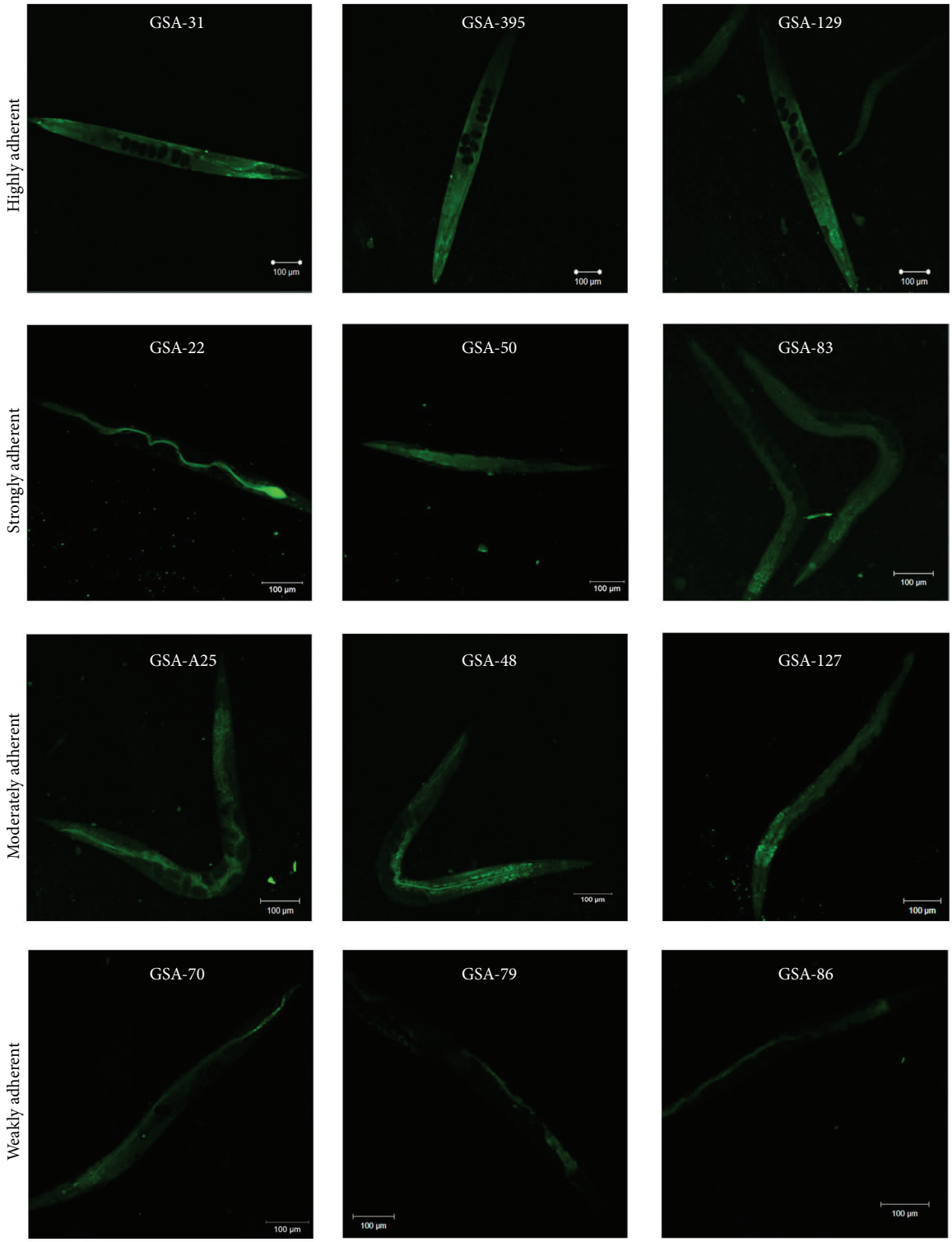

Figure 6: *In vivo* adherence and colonization of *C. elegans* infected with MRSA clinical isolates. Qualitative analysis of colonization in *C. elegans* infected with *S. aureus* clinical isolates using Confocal Laser Scanning Microscopy.

icaADBC genes. Our results were in total agreement with the recent studies stipulating that the percentage of *S. aureus* exhibiting *icaADBC* genotype was 100 [13]. Our findings were collinear with the observations by Atshan et al. [13] and Arciola et al. [12] as there was no difference in the prevalence of *icaADBC* genes in *S. aureus* with high and low virulence; however the only variation is found to be in the phenotypic characterization.

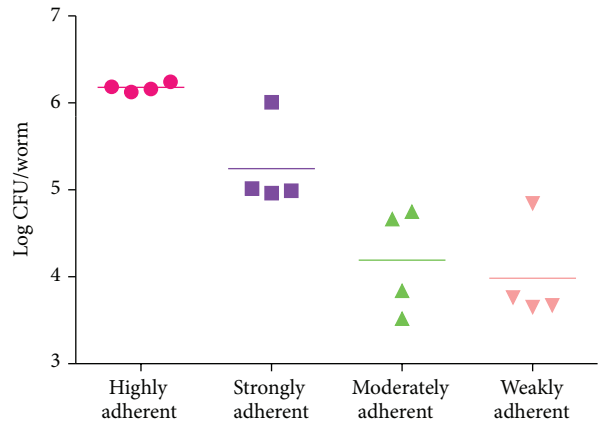

Figure 7: Presence of MRSA inside the *C. elegans*. Quantitative analysis of bacterial load inside the *C. elegans* exposed with MRSA clinical isolates.

Conversely, adhesion to host cells requires genes like *fnb* (*A* and *B*), *clfA*, and *cna* that encode MSCRAMMs unlike the other factors involved in the adhesion to abiotic surfaces. Fibronectin-binding proteins (FnbA and FnbB) are large adhesins that may also function as invasins to modulate the adhesion and internalization of the organisms by different host cells. In addition, it has also been reported that fibronectin-binding facilitates the primary adherence and intercellular accumulation in biofilm assemblies [40]. In the present study, the distribution of *fnbA* and *fnbB* genes has been observed as 77.8% ($n = 49$) and 81% ($n = 51$), respectively, and around 73% ($n = 46$) of the MRSA isolates harboured both *fnbA* and *fnbB* genes (Table 2). A clinical study by Heilmann in 2011 [41] suggested that *S. aureus* strains associated with invasive disease were more likely to encode both *fnbA* and *fnbB* genes. Clumping factor (Clf) A and ClfB encoded by the genes *clfA* and *clfB* are the most important proteins for the binding of *S. aureus* to fibrinogen and fibrin; hence a mutant allele of *clfA* gene failed to clump and thus poorly adheres. In the present study, the *clfA* gene was present in 37 (58.7%) isolates, which was on a par with the previous report by Kohn et al. [42] suggesting that 89% of the test isolates are *clfA* positive. As aforementioned, collagen-binding proteins play an important role in the adhesion and pathogenesis of *S. aureus* [43]. In the current study, the presence of *cna* gene was found in 46 (73%) isolates, which was in agreement with other studies that reported the prevalence of *cna* gene as 46% [1] and 52% [44] in the isolates chosen for their study. However this is highly contrary with a report by Monecke et al. [45] suggesting that *cna* (collagen adhesin) was detected only in some clonal complexes. Staphylococcal alpha-hemolysin is one of the pore-forming toxins encoded by the gene *hla* which plays a major role in the biofilm formation and appears to be primarily required for cell-to-cell interactions. Therefore, a mutant allele of *hla* can initially aid in colonizing a substratum; however, it could not organize into multicellular macrocolonies. The PCR assay for the detection of *hla* gene revealed that 69.8% of ($n = 44$) MRSA strains were positive.

During the process of pathogenesis the chronological expression of several virulence determinants in *S. aureus* has been shown to be under the control of certain genetic loci, namely, *agr* (accessory gene regulator) and *sarA* (staphylococcal accessory regulator) [45]. In the midst, *sarA* is a chief global regulator that is essential for biofilm formation of MRSA and MSSA in both *in vitro* and *in vivo* conditions [46]. Since there has been a mounting evidence to suggest *sarA* as the positive regulator of PNAG-dependent biofilm formation in *S. aureus* [47, 48], in the present study the prevalence of *sarA* gene in MRSA isolates was assayed using PCR. The results revealed that the MRSA isolates harbouring the *icaADBC* genes were also positive for *sarA* gene, whereas the isolates with *icaADBC* negative genotypes were found negative for *sarA*, which is in corroboration with the findings from previous studies [47, 48]. The presence of *sarA* in 90.5% of MRSA strains from pharyngitis patients evidently implies the biofilm-associated pathogenic potential.

Furthermore, bearing in mind that *in vivo* adherence assay would be a better approach to comparatively assess the adhering ability of MRSA isolates with that of the phenotypic assays, three representative isolates from each of the four categories including highly, strongly, moderately, and weakly adherent groups were selected on the basis of their phenotypic and genotypic characteristics. The colonization by MRSA clinical isolates in *C. elegans* was localized using CLSM. The adherence of the pathogen in the host cell may possibly lead to the colonization of the pathogen in the host. As expected, the nematodes infected with highly adherent group showed an extensive intestinal colonization (Figure 6). On the other hand, the strongly adherent group exhibited more intense florescence compared to that of moderately and weakly adherent groups, which displayed very minimal fluorescence intensity. This was further authenticated with the results of CFU assay and therefore it is highly pertinent to state that the outcome of *in vivo* adherence assay clearly portrayed the factual frequency in the results obtained from *in vitro* adherence methods.

5. Conclusion

The data of the current study demonstrated the presence of *ica* genes, several adhesin genes, and the consequent phenotypic

ability to form biofilm by most MRSA isolates. This biofilm-forming potential of MRSA isolates recovered from patients infected with pharyngitis in succession may facilitate and/or aggravate the infection, as such recalcitrant biofilms are 1000-fold more resistant to antibiotics and immune defence which may subsequently alleviate the pathogen to become multidrug resistant or may cause let-down in antibiotic therapy. In addition, the *in vivo* result suggests its good correlation with the findings of quantitative MtP method. Collectively, the outcome of the present study delineates, for the first time, the phenotypic (both *in vivo* and *in vitro*) as well as genotypic biofilm characterization of MRSA isolates recovered from GAS associated pharyngitis, which in turn ameliorates our perception and understanding of the pathogenesis and also its possible impact of causing throat infections.

Competing Interests

All authors declare that they have no competing financial/commercial interests.

Acknowledgments

The authors thankfully acknowledge the Department of Biotechnology, Government of India, for providing Bioinformatics Infrastructure Facility (Grant no. BT/BI/25/012/2012 (BIF)). The instrumentation facility provided by Department of Science and Technology, Government of India, through PURSE [Grant no. SR/S9Z- 415 23/2010/42(G)] and FIST (Grant no. SR-FST/LSI-087/2008) and University Grants Commission, New Delhi, through SAP-DRS1 [Grant no. F.3-28/2011(SAP-II)] is gratefully acknowledged. The authors also acknowledge Dr. Claus Sternberg, DTU Systems Biology, Technical University of Denmark, for providing the COMSTAT software.

References

[1] S. Tsuneda, H. Aikawa, H. Hayashi, A. Yuasa, and A. Hirata, "Extracellular polymeric substances responsible for bacterial adhesion onto solid surface," *FEMS Microbiology Letters*, vol. 223, no. 2, pp. 287–292, 2003.

[2] B. D. Hoyle and J. W. Costerton, "Bacterial resistance to antibiotics: the role of biofilms," *Progress in Drug Research*, vol. 37, pp. 91–105, 1991.

[3] F. D. Lowy, "*Staphylococcus aureus* infections," *The New England Journal of Medicine*, vol. 339, no. 8, pp. 520–532, 1998.

[4] J. A. Kluytmans and H. F. Wertheim, "Nasal carriage of *Staphylococcus aureus* and prevention of nosocomial infections," *Infection*, vol. 33, no. 1, pp. 3–8, 2005.

[5] J. Kluytmans, A. Van Belkum, and H. Verbrugh, "Nasal carriage of *Staphylococcus aureus*: epidemiology, underlying mechanisms, and associated risks," *Clinical Microbiology Reviews*, vol. 10, no. 3, pp. 505–520, 1997.

[6] S. E. Cramton, C. Gerke, N. F. Schnell, W. W. Nichols, and F. Götz, "The intercellular adhesion (ica) locus is present in *Staphylococcus aureus* and is required for biofilm formation," *Infection and Immunity*, vol. 67, no. 10, pp. 5427–5433, 1999.

[7] V. G. Fowler Jr., P. D. Fey, L. B. Reller, A. L. Chamis, G. R. Corey, and M. E. Rupp, "The intercellular adhesin locus ica is present in clinical isolates of *Staphylococcus aureus* from bacteremic patients with infected and uninfected prosthetic joints," *Medical Microbiology and Immunology*, vol. 189, no. 3, pp. 127–131, 2001.

[8] T. J. Foster and M. Höök, "Surface protein adhesins of *Staphylococcus aureus*," *Trends in Microbiology*, vol. 6, no. 12, pp. 484–488, 1998.

[9] M. Otto, "Staphylococcal biofilms," *Current Topics in Microbiology and Immunology*, vol. 322, pp. 207–228, 2008.

[10] Y.-S. Seo, D. Y. Lee, N. Rayamahji, M. L. Kang, and H. S. Yoo, "Biofilm-forming associated genotypic and phenotypic characteristics of *Staphylococcus* spp. isolated from animals and air," *Research in Veterinary Science*, vol. 85, no. 3, pp. 433–438, 2008.

[11] D. McKenney, J. Hübner, E. Muller, Y. Wang, D. A. Goldmann, and G. B. Pier, "The ica locus of *Staphylococcus epidermidis* encodes production of the capsular polysaccharide/adhesin," *Infection and Immunity*, vol. 66, no. 10, pp. 4711–4720, 1998.

[12] C. R. Arciola, D. Campoccia, S. Gamberini, L. Baldassarri, and L. Montanaro, "Prevalence of cna, fnbA and fnbB adhesin genes among *Staphylococcus aureus* isolates from orthopedic infections associated to different types of implant," *FEMS Microbiology Letters*, vol. 246, no. 1, pp. 81–86, 2005.

[13] S. S. Atshan, M. Nor Shamsudin, Z. Sekawi et al., "Prevalence of adhesion and regulation of biofilm-related genes in different clones of *Staphylococcus aureus*," *Journal of Biomedicine and Biotechnology*, vol. 2012, Article ID 976972, 10 pages, 2012.

[14] B. R. Boles and A. R. Horswill, "*agr*-mediated dispersal of *Staphylococcus aureus* biofilms," *PLoS Pathogens*, vol. 4, no. 4, Article ID e1000052, 2008.

[15] S. Gowrishankar, R. Thenmozhi, K. Balaji, and S. K. Pandian, "Emergence of methicillin-resistant, vancomycin-intermediate *Staphylococcus aureus* among patients associated with group A Streptococcal pharyngitis infection in southern India," *Infection, Genetics and Evolution*, vol. 14, no. 1, pp. 383–389, 2013.

[16] D. J. Freeman, F. R. Falkiner, and C. T. Keane, "New method for detecting slime production by coagulase negative staphylococci," *Journal of Clinical Pathology*, vol. 42, no. 8, pp. 872–874, 1989.

[17] B. Kouidhi, T. Zmantar, H. Hentati, and A. Bakhrouf, "Cell surface hydrophobicity, biofilm formation, adhesives properties and molecular detection of adhesins genes in Staphylococcus aureus associated to dental caries," *Microbial Pathogenesis*, vol. 49, no. 1-2, pp. 14–22, 2010.

[18] J.-H. Kim, C.-H. Kim, J. Hacker, W. Ziebuhr, B. K. Lee, and S.-H. Cho, "Molecular characterization of regulatory genes associated with biofilm variation in a *Staphylococcus aureus* strain," *Journal of Microbiology and Biotechnology*, vol. 18, no. 1, pp. 28–34, 2008.

[19] N. M. Abraham and K. K. Jefferson, "A low molecular weight component of serum inhibits biofilm formation in *Staphylococcus aureus*," *Microbial Pathogenesis*, vol. 49, no. 6, pp. 388–391, 2010.

[20] A. Tristan, L. Ying, M. Bes, J. Etienne, F. Vandenesch, and G. Lina, "Use of multiplex PCR to identify *Staphylococcus aureus* adhesins involved in human hematogenous infections," *Journal of Clinical Microbiology*, vol. 41, no. 9, pp. 4465–4467, 2003.

[21] S. Gowrishankar, N. D. Mosioma, and S. K. Pandian, "Coral-associated bacteria as a promising antibiofilm agent against methicillin-resistant and -susceptible *Staphylococcus aureus* biofilms," *Evidence-Based Complementary and Alternative Medicine*, vol. 2012, Article ID 862374, 16 pages, 2012.

[22] S. Gowrishankar, A. Kamaladevi, K. S. Ayyanar, K. Balamurugan, and S. K. Pandian, "*Bacillus amyloliquefaciens*-secreted

cyclic dipeptide—cyclo(l-leucyl-l-prolyl) inhibits biofilm and virulence production in methicillin-resistant *Staphylococcus aureus*," *RSC Advances*, vol. 5, no. 116, pp. 95788–95804, 2015.

[23] H. S. Courtney, I. Ofek, T. Penfound et al., "Relationship between expression of the family of M proteins and lipoteichoic acid to hydrophobicity and biofilm formation in *Streptococcus pyogenes*," *PLoS ONE*, vol. 4, no. 1, Article ID e4166, 2009.

[24] L. Schlegel, F. Grimont, P. A. D. Grimont, and A. Bouvet, "Identification of major streptococcal species by rrn-amplified ribosomal DNA restriction analysis," *Journal of Clinical Microbiology*, vol. 41, no. 2, pp. 657–666, 2003.

[25] A. Kamaladevi and K. Balamurugan, "Role of PMK-1/p38 MAPK defense in *Caenorhabditis elegans* against *Klebsiella pneumoniae* infection during host-pathogen interaction," *Pathogens and Disease*, vol. 73, no. 5, 2015.

[26] G. D. Christensen, W. A. Simpson, J. J. Younger et al., "Adherence of coagulase-negative staphylococci to plastic tissue culture plates: a quantitative model for the adherence of staphylococci to medical devices," *Journal of Clinical Microbiology*, vol. 22, no. 6, pp. 996–1006, 1985.

[27] D. Mertz, R. Frei, B. Jaussi et al., "Throat swabs are necessary to reliably detect carriers of *Staphylococcus aureus*," *Clinical Infectious Diseases*, vol. 45, no. 4, pp. 475–477, 2007.

[28] D. Mertz, R. Frei, N. Periat et al., "Exclusive *Staphylococcus aureus* throat carriage: at-risk populations," *Archives of Internal Medicine*, vol. 169, pp. 172–178, 2009.

[29] A. Hamdan-Partida, T. Sainz-Espuñes, and J. Bustos-Martínez, "Characterization and persistence of *Staphylococcus aureus* strains isolated from the anterior nares and throats of healthy carriers in a Mexican community," *Journal of Clinical Microbiology*, vol. 48, no. 5, pp. 1701–1705, 2010.

[30] C. E. Richmond, M. W. Beyer, B. A. Ferozan, and C. Zipp, "Infectious mononucleosis with *Staphylococcus aureus* pharyngitis coinfection," *Osteopathic Family Physician*, vol. 2, no. 1, pp. 14–17, 2010.

[31] H. Bozkurt, M. G. Kurtoglu, Y. Bayram, R. Keşli, and M. Berktaş, "Correlation of slime production investigated via three different methods in coagulase-negative staphylococci with crystal violet reaction and antimicrobial resistance," *Journal of International Medical Research*, vol. 37, no. 1, pp. 121–128, 2009.

[32] H. A. El-Mahallawy, S. A. Loutfy, M. El-Wakil, A. K. Abd El-Al, and H. Morcos, "Clinical implications of *icaA* and *icaD* genes in coagulase negative Staphylococci and *Staphylococcus aureus* bacteremia in febrile neutropenic pediatric cancer patients," *Pediatric Blood & Cancer*, vol. 52, no. 7, pp. 824–828, 2009.

[33] J. K.-M. Knobloch, K. Bartscht, A. Sabottke, H. Rohde, H.-H. Feucht, and D. Mack, "Biofilm formation by *Staphylococcus epidermidis* depends on functional *RsbU*, an activator of the sigB operon: differential activation mechanisms due to ethanol and salt stress," *Journal of Bacteriology*, vol. 183, no. 8, pp. 2624–2633, 2001.

[34] C. R. Arciola, D. Campoccia, S. Gamberini, M. Cervellati, E. Donati, and L. Montanaro, "Detection of slime production by means of an optimised Congo red agar plate test based on a colourimetric scale in *Staphylococcus epidermidis* clinical isolates genotyped for *ica* locus," *Biomaterials*, vol. 23, no. 21, pp. 4233–4239, 2002.

[35] M. G. Ammendolia, R. Di Rosa, L. Montanaro, C. R. Arciola, and L. Baldassarri, "Slime production and expression of the slime-associated antigen by staphylococcal clinical isolates," *Journal of Clinical Microbiology*, vol. 37, no. 10, pp. 3235–3238, 1999.

[36] F. Hamadi, H. Latrache, M. Mabrrouki et al., "Effect of pH on distribution and adhesion of *Staphylococcus aureus* to glass," *Journal of Adhesion Science and Technology*, vol. 19, no. 1, pp. 73–85, 2005.

[37] J.-O. Cha, Y.-K. Park, Y. S. Lee, and G. T. Chung, "*In vitro* biofilm formation and bactericidal activities of methicillin-resistant *Staphylococcus aureus* clones prevalent in Korea," *Diagnostic Microbiology and Infectious Disease*, vol. 70, no. 1, pp. 112–118, 2011.

[38] H. Kawamura, J. Nishi, N. Imuta et al., "Quantitative analysis of biofilm formation of methicillin-resistant *Staphylococcus aureus* (MRSA) strains from patients with orthopaedic device-related infections," *FEMS Immunology and Medical Microbiology*, vol. 63, no. 1, pp. 10–15, 2011.

[39] T. Maira-Litrán, A. Kropec, C. Abeygunawardana et al., "Immunochemical properties of the Staphylococcal poly-N-acetyl-glucosamine surface polysaccharide," *Infection and Immunity*, vol. 70, no. 8, pp. 4433–4440, 2002.

[40] E. O'Neill, C. Pozzi, P. Houston et al., "A novel *Staphylococcus aureus* biofilm phenotype mediated by the fibronectin-binding proteins, FnBPA and FnBPB," *Journal of Bacteriology*, vol. 190, no. 11, pp. 3835–3850, 2008.

[41] C. Heilmann, "Adhesion mechanisms of staphylococci," in *Bacterial Adhesion: Chemistry, Biology and Physics*, D. Linke and A. Goldman, Eds., vol. 715 of *Advances in Experimental Medicine and Biology*, pp. 105–123, Springer, Berlin, Germany, 2011.

[42] W. G. Kohn, J. A. Harte, D. M. Malvitz, A. S. Collins, J. L. Cleveland, and K. J. Eklund, "Guidelines for infection control in dental health care settings—2003," *The Journal of the American Dental Association*, vol. 135, no. 1, pp. 33–47, 2004.

[43] M. O. Elasri, J. R. Thomas, R. A. Skinner et al., "*Staphylococcus aureus* collagen adhesin contributes to the pathogenesis of osteomyelitis," *Bone*, vol. 30, no. 1, pp. 275–280, 2002.

[44] S. J. Peacock, T. J. Foster, B. J. Cameron, and A. R. Berendt, "Bacterial fibronectin-binding proteins and endothelial cell surface fibronectin mediate adherence of *Staphylococcus aureus* to resting human endothelial cells," *Microbiology*, vol. 145, no. 12, pp. 3477–3486, 1999.

[45] S. Monecke, C. Luedicke, P. Slickers, and R. Ehricht, "Molecular epidemiology of *Staphylococcus aureus* in asymptomatic carriers," *European Journal of Clinical Microbiology α Infectious Diseases*, vol. 28, no. 9, pp. 1159–1165, 2009.

[46] M. P. Trotonda, A. C. Manna, A. L. Cheung, I. Lasa, and J. R. Penadés, "*SarA* positively controls Bap-dependent biofilm formation in *Staphylococcus aureus*," *Journal of Bacteriology*, vol. 187, no. 16, pp. 5790–5798, 2005.

[47] J. Valle, A. Toledo-Arana, C. Berasain et al., "*SarA* and not sigmaB is essential for biofilm development by *Staphylococcus aureus*," *Molecular Microbiology*, vol. 48, no. 4, pp. 1075–1087, 2003.

[48] K. E. Beenken, J. S. Blevins, and M. S. Smeltzer, "Mutation of sarA in *Staphylococcus aureus* limits biofilm formation," *Infection and Immunity*, vol. 71, no. 7, pp. 4206–4211, 2003.

Hindawi Publishing Corporation
BioMed Research International
Volume 2016, Article ID 3671306, 14 pages
http://dx.doi.org/10.1155/2016/3671306

Research Article

Black Currant (*Ribes nigrum* L.) and Bilberry (*Vaccinium myrtillus* L.) Fruit Juices Inhibit Adhesion of *Asaia* spp.

Hubert Antolak, Agata Czyzowska, and Dorota Kregiel

Institute of Fermentation Technology and Microbiology, Lodz University of Technology, Wolczanska 171/173, 90-924 Lodz, Poland

Correspondence should be addressed to Hubert Antolak; hubert.antolak@gmail.com

Received 5 July 2016; Accepted 25 August 2016

Academic Editor: Shunmugiah K. Pandian

Copyright © 2016 Hubert Antolak et al. This is an open access article distributed under the Creative Commons Attribution License, which permits unrestricted use, distribution, and reproduction in any medium, provided the original work is properly cited.

The aim of the study was to evaluate the activity of high-polyphenolic black currant (*Ribes nigrum* L.) and bilberry (*Vaccinium myrtillus* L.) juices against bacterial strains *Asaia lannensis* and *Asaia bogorensis* isolated as spoilage of commercial soft drinks. The composition of fruit juices was evaluated using chromatographic techniques HPLC and LC-MS. The adhesion to glass, polystyrene, and polyethylene terephthalate in two different culture media was evaluated by luminometry and the plate count method. The major anthocyanins in the *V. myrtillus* were petunidin-3-glucoside, malvidin-3-glucoside, cyanidin-3-glucoside, and delphinidin-3-glucoside, while in *R. nigrum* delphinidin-3-rutinoside and cyanidin-3-rutinoside were detected. The LC-MS analysis showed presence of anthocyanins (delphinidin, cyanidin, petunidin, and malvidin derivatives), phenolic acids (chlorogenic and neochlorogenic acids), flavonols (quercetin-3-glucoside, quercetin-3-rutinoside), and flavanols (procyanidin B2 and procyanidin type A2). Additionally, in the bilberry juice A type procyanidin trimer was detected. The adhesion of *Asaia* spp. cells depended on the type of medium, carbon sources, and the type of abiotic surfaces. We noted that the adhesion was significantly stronger in minimal medium containing sucrose. The addition of bilberry and black currant juices notably reduced bacterial growth as well as cell adhesion to polyethylene terephthalate surfaces.

1. Introduction

Nowadays, consumers are increasingly interested in their health and expect the foods, besides possessing the sensory attractiveness, to have health-promoting effects. Numerous studies indicate that a diet rich in berries and their preserves positively affects human health. Regular consumption of fruits may delay ageing processes and reduce the risk of various illnesses, such as cancer, cardiovascular and lung diseases, rheumatoid arthritis, Alzheimer's dementia, or Parkinsonism [1–3]. Fruit berries were identified as sources of phenolic compounds like gallic and ellagic acid with potential cancer chemopreventive activity. The different bioactive phenolic compounds, including flavonoids (flavonols and flavanols), tannins (proanthocyanidins, ellagitannins, and gallotannins), stilbenoids, and phenolic acids, have received considerable interest in bearing possible relations to human health [1]. Besides health-promoting properties, polyphenols may also act as antimicrobials and antiadhesive agents in wide range of pathogens [4]. It was documented that berry extracts or juices showed strong activity against Gram negative bacteria [5, 6]. In the past decade, cranberry extracts were attracting ever-growing attention of microbiologists. It was noted that cranberry polyphenol fraction inhibits growth and adhesion of urinary tract pathogens (*Escherichia coli*, *Proteus vulgaris*), *Helicobacter pylori*, and bacterial etiological factors of oral diseases (*Streptococcus* spp., *Propionibacterium* spp., and *Fusobacterium* spp.) [7–12].

Lately, numerous reports detailed various spoilage microorganisms in soft drinks, for example, acetic acid bacteria belonging to the genus *Asaia* [13–15]. The growth of these microorganisms causes significant changes in both microbiological and organoleptic qualities. *Asaia* spp. cells are able to grow in soft drinks supplemented with different preservatives (benzoate, sorbate, and dimethyl dicarbonate) [15]. What is more, these bacteria show strong adhesive abilities on food-contact technical materials. The biofilm formed by *Asaia* species on solid surfaces of a production line can be a source of secondary contamination of final products [16].

The initial, key step leading to biofilm formation is bacterial adhesion to the surface. This is the complex process, influenced by various physical and chemical properties of microbial cells, media, and abiotic surfaces. Among these factors, modification of media could be changed in order to prevent biofouling in soft drinks technology. New antimicrobial strategy is the use of berry juices to inhibit or reduce bacterial adhesion. The application of native and low-priced fruits with additional potential as health-promoting agents is especially interesting. Therefore, the aim of our study was to investigate antibacterial and antiadhesion activities of juices from bilberries and black currants against *Asaia* spp. cells.

2. Materials and Methods

2.1. Plant Material. The black currant (*R. nigrum* L.) and bilberry (*V. myrtillus* L.) fruits were freshly harvested from the local orchard and forests around Lodz (central Poland). The fruits were washed with sterile water, lightly air-dried, and frozen at −20°C for one month. The fresh juice was squeezed out from defrosted fruits using extractor MES3000 (Bosch, Poland). Cloudy juice was clarified using Whatman qualitative paper-filter and then by 0.45 μm filtration (Filter-Bio). Immediately after preparation, the clear juice was added to the culture media to the final concentration of 10% (v/v).

2.2. Bacterial Strains and Culture Media. The study used the six bacterial strains: *Asaia bogorensis* ISD1 (GenBank KP234014), *A. bogorensis* ISD2 (GenBank KP234015), *A. bogorensis* FFMW (GenBank KC756841), *A. lannensis* IFMW (GenBank KP234011), *A. lannensis* IFCW (GenBank KP234012), and *A. lannensis* FMW1 (GenBank HQ917850) isolated from spoiled flavored mineral water and isotonic drinks. These strains were identified using morphological, physiological, and genetic methods described by Kregiel and coworkers [13, 17]. The obtained nucleotide sequences of 16S rRNA were deposited in GenBank (National Centre of Biotechnology Information) and the bacterial strains were deposited in the Pure Culture Collection of Industrial Microorganisms LOCK 105 at the Institute of Fermentation Technology and Microbiology, Technical University of Lodz (Poland).

The adhesion was investigated in liquid culture media: the rich GC medium (M_1) (0.3% (w/v) peptone, 0.3% (w/v) yeast extract) and the minimal medium (M_2) (0.3% $(NH_4)_2PO_4$ (w/v), 0.3% KH_2PO_4 (w/v), 0.3% $MgSO_4 \times 7H_2O$ (w/v), and 0.05% (w/v) yeast extract). In both media, carbohydrates, glucose, fructose, and sucrose (2% w/v), were used as a carbon source. The sterile media (20 cm^3) were poured aseptically into 25 cm^3 Erlenmeyer flasks covered with a textile cloth in order to ensure aerobic conditions. Sterile carriers were placed vertically in a liquid culture medium in such a way that half of the carrier was immersed in the medium, and the other part was above the liquid.

2.3. Carriers. The bacterial adhesion was carried out to the polystyrene (PS) (Coveris Rigid Poland, Skierniewice) and polyethylene terephthalate (PET) (Coveris Rigid Poland, Skierniewice) slides measuring 76 × 26 mm. These materials are certified by Polish National Institute of Public Health and approved for contact with food. The white glass slides (G) (Knittel Glass, Germany) were used as the reference material. Carriers were sterilized in two-step process. First, the carriers were kept in the 70% ethanol solution for 3 hours. Subsequently, they were placed in a laminar chamber and subjected to UV irradiation for 2 hours.

2.4. Adhesion Analysis. Studies on the *Asaia* spp. attachment and biofilm formation were carried out in two stages. The first stage involved the selection of a culture medium, a carbon source, and an abiotic material where bacteria demonstrated the strongest adhesion abilities. In the second stage, we checked the effect of fruit juices on the growth and adhesion abilities of *Asaia* spp. For this purpose, the culture medium containing selected carbon source, with proper carrier, was supplemented with 10% (v/v) of black currant or bilberry juice.

At the beginning of the experiments culture media were inoculated with standardized bacterial suspensions, to obtain cell concentration $10^5 \div 10^6$ CFU/cm^3. The adhesion ability of the bacterial strains was evaluated according to the method described by Kregiel (2013) [16]. For luminometric tests, the carriers were removed from the culture media, washed with sterile distilled water, and swabbed with pens for ATP sampling (Merck). Measurements were made in relative light units (RLU) using a HY-LiTE® 2 luminometer (Merck). The plate count method was used in order to determine the number of cells attached to the carrier and planktonic cells in the culture medium. The carrier plate was removed from the culture medium, rinsed with sterile distilled water, and swabbed using sterile swabs for surface testing. The bacterial suspensions were vortexed with 0.1% (v/v) Tween 80 and transferred onto GC agar medium supplemented with 0.7% $CaCO_3$ (w/v), and after incubation at 25°C for 92 h the colonies were counted. The number of colony forming units (CFU) per cm^3 (of liquid media) or per cm^2 (of carriers) was calculated. On the basis of the results, the relative adhesion coefficient A (%) was calculated using formula $A\,(\%) = (N_a/N_p) \times 100\%$, where N_a is the number of attached cells to a carrier and N_p is the number of planktonic cells in the culture medium.

2.5. Chemical Constituent's Analysis. The organic acids and carbohydrates profiles of the tested fruit juices were determined using high performance liquid chromatography (HPLC), according to the method described by Gutarowska and Czyżowska (2009) [18]. In addition, the polyphenolic compounds were also characterized using HPLC-DAD method with a diode array detector (Finnigan Surveyor-PDA Plus detector) and a ChromQuest 5.0 chromatography software (Thermo Fisher Scientific Inc., Waltham, MA, USA) as well as using liquid chromatography mass spectrometry (LC-MS; LTQ Velos MS, Thermo Fisher Scientific) following the method described by Antolak et al. (2015) [19].

2.6. Statistics. Means were calculated from the data obtained from three independent experiments, and the standard

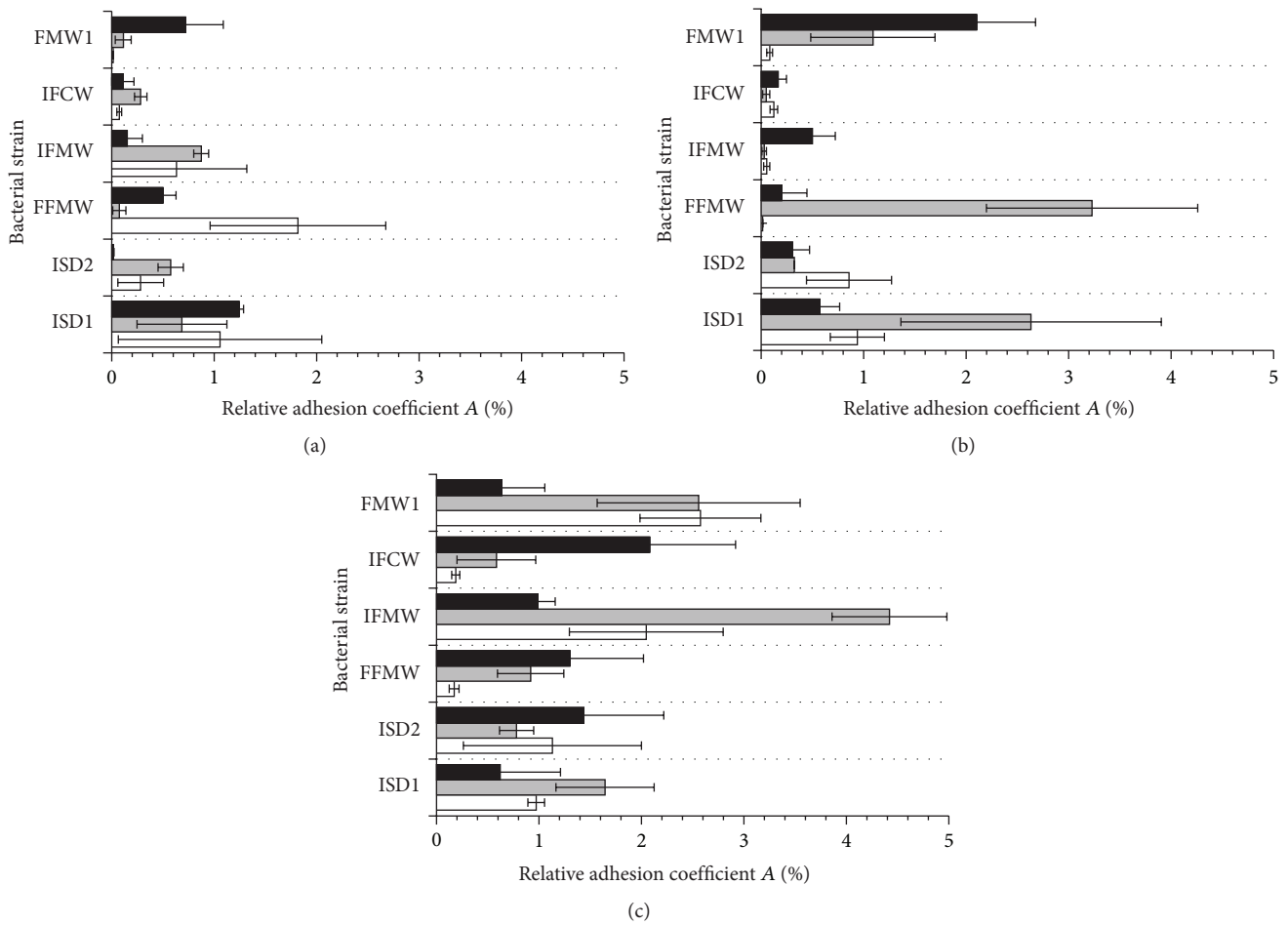

Figure 1: The relative adhesion coefficient A (%) for *A. bogorensis* (ISD1, ISD2, and FFMW) and *A. lannensis* (IFMW, IFCW, and FMW1) strains in M_1 medium with glucose (a), fructose (b), and sucrose (c) to PET (black bars), PS (grey bars), and G (white bars).

deviations (SD) were calculated. The mean values of the adhesion results were compared using one-way repeated measures analysis of variance with Tukey test (ANOVA; OriginPro 8.1, OriginLab Corp., Northampton, MA). Statistical significance was set at the conventional level of 5% ($p < 0.05$).

3. Results and Discussion

3.1. Bacterial Adhesion. To determine the level of bacterial adhesion, two main analytical methods, namely, plate count and luminometry, were used. The evaluation of *Asaia* spp. adhesion to glass, polystyrene, and polyethylene terephthalate surfaces was carried out in rich M_1 and minimal M_2 medium. The influence of the carbon source for bacterial adhesion was tested in culture media supplemented with glucose, fructose, or sucrose as an only carbon source. The results of adhesion studies, expressed as relative adhesion coefficient A (%) for medium M_1 and medium M_2, are presented in Figures 1 and 2, respectively. The biofilm formation of *Asaia* strains significantly increased in culture media supplemented with sucrose ($p < 0.05$) in comparison to media containing glucose or fructose. It was noted that the minimal M_2 medium was a more favorable environment for the *Asaia* spp. adhesion and biofilm formation compared to the rich M_1 medium. The results for adhesion in M_2 medium, with reference to those obtained for the adhesion in M_1 medium, were significantly higher ($p < 0.05$). The average value of A (%) for cells adhesion in M_2 medium with sucrose was $1.72 \pm 0.26\%$, while for the same medium but with fructose and glucose the results were slight lower and equaled $1.10 \pm 0.23\%$ ($p = 0.00001$) and $0.80 \pm 0.19\%$ ($p = 0.00004$), respectively. The highest value of A (%) was noted for *A. lannensis* IFCW strain on PET surface, which was $4.54 \pm 0.37\%$. Figures 3 and 4 present the luminometry results (RLU/cm^2) obtained for bacterial adhesion in M_1 and M_2 media, respectively. The obtained results confirmed that the more favorable environment for biofilm formation is the minimal medium M_2 with sucrose. Average value of the RLU for rich M_1 medium with sucrose (1784 ± 257 RLU/cm^2) was statistically lower ($p = 0.001$) in comparison to minimal medium M_2 with the same carbohydrate (3923 ± 447 RLU/cm^2).

Additionally, to assess the differences between the adhesion abilities of all bacterial strains to all tested carriers in all culture media containing different carbon sources, the mean

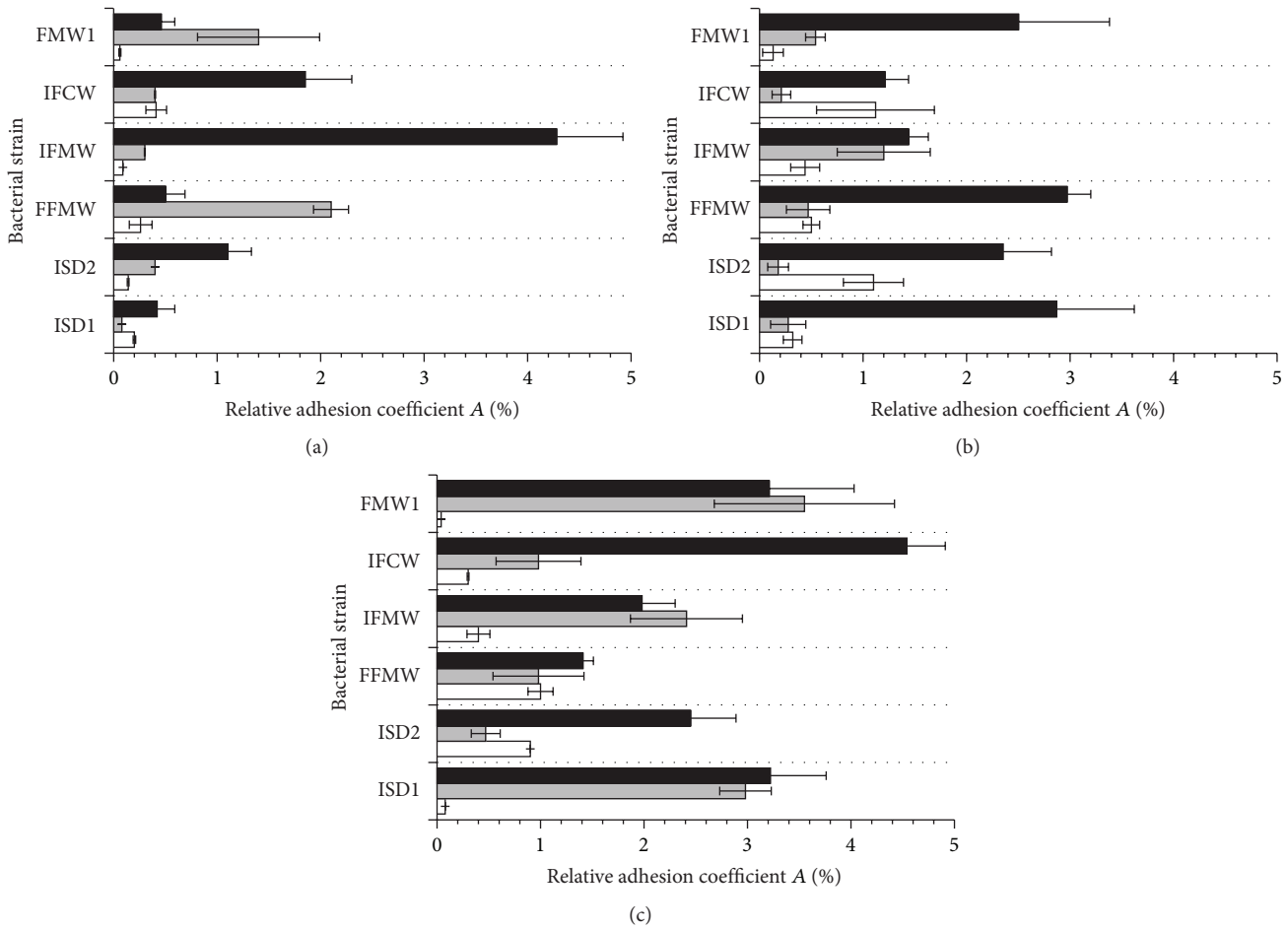

Figure 2: The relative adhesion coefficient A (%) for *A. bogorensis* (ISD1, ISD2, and FFMW) and *A. lannensis* (IFMW, IFCW, and FMW1) strains in M_2 medium with glucose (a), fructose (b), and sucrose (c) to PET (black bars), PS (grey bars), and G (white bars).

values and standard deviations calculated from obtained results of A (%) (Table 1) and the RLU/cm^2 (Table 2) were calculated. It was noted that the adhesion and biofilm formation processes were strain-dependent. *A. lannensis* strains showed slightly stronger adhesion in culture media containing sucrose. The mean A (%) values for *A. lannensis* strains adhesion to PET surface in culture media with sucrose were 1.23 ± 0.61% (M_1) and 3.24 ± 1.05% (M_2) while for the *A. bogorensis* strains 1.12 ± 0.36% ($p = 0.05$) and 2.36 ± 0.74% ($p = 0.02$) were noted, respectively.

A. lannensis and *A. bogorensis* were characterized by stronger adhesion properties to plastic materials in comparison to the glass surface. The average values of the relative adhesion coefficient obtained for the carriers in minimal medium M_2 with sucrose were 0.45 ± 0.05% (G), 1.90 ± 0.23% (PS), and 2.80 ± 0.21% (PET), while for rich M_1 medium 1.18 ± 0.71%, 1.82 ± 1.01%, and 1.17 ± 0.23% were noted, respectively. Performed ANOVA test showed that the results are statistically different. Obtained p values, in comparison to glass, for the M_1 medium were 0.02 (PS) and 0.01 (PET), while the results for M_2 medium were less than 0.01 for both PS and PET. The results of RLU measurement also showed that slightly better surface for biofilm formation in M_2 medium with sucrose is PET.

The similar results for *Asaia* spp. adhesion were obtained by Kregiel (2013) and Kregiel et al. (2014), where, after incubation, the adhesion to plastic materials was several times higher in comparison to the glass surface [16, 17].

Of course, there are different techniques that can be used in the analysis of the microbial adhesion to abiotic surfaces, but neither method is perfect. The plate count technique in particular allows determining culturable microorganisms, while luminometric methods enable estimating total biological material on the abiotic surfaces. This approach is based on bacterial ATP quantification and can be used to evaluate not only the total number of adhering cells, but all biomass: bacteria that are able and unable to grow, extracellular polymeric substances, or adhered organic material from culture media. Thus, comparing the results of the relative coefficient A (%) and RLU/cm^2, the values obtained by these two methods showed differences.

The type of material, its roughness, and hydrophobicity significantly affect bacterial attachment and biofilm development. The plastic materials used in our study were characterized by low surface energy (PET 44 mN/m at 20°C, PS

Table 1: Adhesion of the *Asaia* spp. strains reported as relative coefficient A (%) in M_1 and M_2 media with carbohydrates as a carbon source. The mean values of the adhesion results were compared using one-way repeated measures ANOVA with Tukey test. Two results of p values were obtained: p_1 – p value obtained by the comparison of the A (%) results within a species to the results for M_1 with glucose and glass; p_2 – p value obtained by the comparison of the A (%) between *Asaia bogorensis* and *Asaia lannensis*. Statistical significance was set at the conventional level of 5% ($p < 0.05$).

	Species											
	A. bogorensis						*A. lannensis*					
	Carbon source											
	Glucose		Fructose		Sucrose		Glucose		Fructose		Sucrose	
	Medium											
	M_1	M_2	M_1	M_2	M_1	M_2	M_1	M_2	M_1	M_2	M_1	M_2
Surface												
G	1.05 ± 0.63 $p_2 = 0.11$	0.20 ± 0.05 $p_1 = 0.11$ $p_2 = 0.04$	0.60 ± 0.42 $p_1 = 0.02$ $p_2 = 0.14$	0.64 ± 0.33 $p_1 = 0.03$ $p_2 = 0.14$	0.76 ± 0.42 $p_1 = 0.01$ $p_2 = 0.04$	0.66 ± 0.41 $p_1 = 0.09$ $p_2 = 0.05$	0.24 ± 0.28 $p_2 = 0.11$	0.19 ± 0.16 $p_1 = 0.15$ $p_2 = 0.04$	0.09 ± 0.03 $p_1 = 0.21$ $p_2 = 0.14$	0.56 ± 0.41 $p_1 = 0.14$ $p_2 = 0.14$	1.60 ± 1.03 $p_1 = 0.15$ $p_2 = 0.04$	0.25 ± 0.16 $p_1 = 0.23$ $p_2 = 0.05$
PS	0.44 ± 0.27 $p_1 = 0.04$ $p_2 = 0.11$	0.86 ± 0.89 $p_1 = 0.19$ $p_2 = 0.25$	2.06 ± 1.25 $p_1 = 0.14$ $p_2 = 0.15$	0.31 ± 0.12 $p_1 = 0.12$ $p_2 = 0.09$	1.11 ± 0.38 $p_1 = 0.05$ $p_2 = 0.12$	1.48 ± 1.08 $p_1 = 0.11$ $p_2 = 0.09$	0.42 ± 0.33 $p_1 = 0.26$ $p_2 = 0.11$	0.70 ± 0.50 $p_1 = 0.07$ $p_2 = 0.25$	0.39 ± 0.50 $p_1 = 0.16$ $p_2 = 0.15$	0.65 ± 0.41 $p_1 = 0.20$ $p_2 = 0.09$	2.52 ± 1.57 $p_1 = 0.16$ $p_2 = 0.12$	2.31 ± 1.05 $p_1 = 0.08$ $p_2 = 0.09$
PET	0.59 ± 0.51 $p_1 = 0.13$ $p_2 = 0.15$	0.67 ± 0.30 $p_1 = 0.02$ $p_2 = 0.11$	0.36 ± 0.16 $p_1 = 0.08$ $p_2 = 0.14$	2.73 ± 0.27 $p_1 = 0.02$ $p_2 = 0.02$	1.12 ± 0.36 $p_1 = 0.04$ $p_2 = 0.05$	2.36 ± 0.74 $p_1 = 0.01$ $p_2 = 0.02$	0.33 ± 0.28 $p_1 = 0.09$ $p_2 = 0.15$	2.20 ± 1.58 $p_1 = 0.20$ $p_2 = 0.11$	0.92 ± 0.84 $p_1 = 0.17$ $p_2 = 0.14$	1.72 ± 0.56 $p_1 = 0.03$ $p_2 = 0.02$	1.23 ± 0.61 $p_1 = 0.08$ $p_2 = 0.05$	3.24 ± 1.05 $p_1 = 0.03$ $p_2 = 0.02$

Table 2: Adhesion of the *Asaia* spp. strains, reported in RLU/cm^2, in M_1 and M_2 media with carbohydrates as a carbon source. The mean values of the adhesion results were compared using one-way repeated measures ANOVA with Tukey test. Two results of p values were obtained: p_1 – p value obtained by the comparison of the RLU/cm^2 results within a species to the results for M_1 with glucose and glass; p_2 – p value obtained by the comparison of the RLU/cm^2 between *Asaia bogorensis* and *Asaia lannensis*. Statistical significance was set at the conventional level of 5% ($p < 0.05$).

	Species											
	A. bogorensis						*A. lannensis*					
	Carbon source											
	Glucose		Fructose		Sucrose		Glucose		Fructose		Sucrose	
	Medium											
	M_1	M_2	M_1	M_2	M_1	M_2	M_1	M_2	M_1	M_2	M_1	M_2
Surface												
G	3701 ± 2821 $p_2 = 0.12$	3086 ± 2000 $p_1 = 0.17$ $p_2 = 0.01$	1632 ± 428 $p_1 = 0.12$ $p_2 = 0.09$	504 ± 393 $p_1 = 0.18$ $p_2 = 0.13$	817 ± 894 $p_1 = 0.22$ $p_2 = 0.13$	2010 ± 432 $p_1 = 0.12$ $p_2 = 0.08$	1504 ± 871 $p_2 = 0.12$	2251 ± 1690 $p_1 = 0.16$ $p_2 = 0.01$	1269 ± 1259 $p_1 = 0.16$ $p_2 = 0.09$	376 ± 131 $p_1 = 0.07$ $p_2 = 0.13$	1541 ± 1400 $p_1 = 0.01$ $p_2 = 0.13$	1987 ± 2133 $p_1 = 0.21$ $p_2 = 0.08$
PS	3700 ± 3375 $p_1 = 0.22$ $p_2 = 0.22$	1937 ± 364 $p_1 = 0.13$ $p_2 = 0.01$	340 ± 187 $p_1 = 0.19$ $p_2 = 0.05$	2830 ± 932 $p_1 = 0.05$ $p_2 = 0.13$	308 ± 186 $p_1 = 0.17$ $p_2 = 0.36$	5600 ± 2412 $p_1 = 0.06$ $p_2 = 0.04$	597 ± 259 $p_1 = 0.07$ $p_2 = 0.22$	1783 ± 249 $p_1 = 0.05$ $p_2 = 0.01$	440 ± 71 $p_1 = 0.08$ $p_2 = 0.05$	4640 ± 3503 $p_1 = 0.13$ $p_2 = 0.13$	4120 ± 5289 $p_1 = 0.30$ $p_2 = 0.36$	4633 ± 4082 $p_1 = 0.19$ $p_2 = 0.04$
PET	6247 ± 5177 $p_1 = 0.22$ $p_2 = 0.16$	3463 ± 3539 $p_1 = 0.23$ $p_2 = 0.02$	3223 ± 4227 $p_1 = 0.28$ $p_2 = 0.16$	1487 ± 788 $p_1 = 0.17$ $p_2 = 0.01$	817 ± 130 $p_1 = 0.18$ $p_2 = 0.40$	4252 ± 1591 $p_1 = 0.04$ $p_2 = 0.05$	2433 ± 776 $p_1 = 0.07$ $p_2 = 0.16$	5590 ± 3757 $p_1 = 0.11$ $p_2 = 0.02$	3800 ± 2673 $p_1 = 0.15$ $p_2 = 0.16$	4033 ± 1434 $p_1 = 0.04$ $p_2 = 0.01$	4217 ± 5786 $p_1 = 0.32$ $p_2 = 0.40$	5053 ± 3501 $p_1 = 0.13$ $p_2 = 0.05$

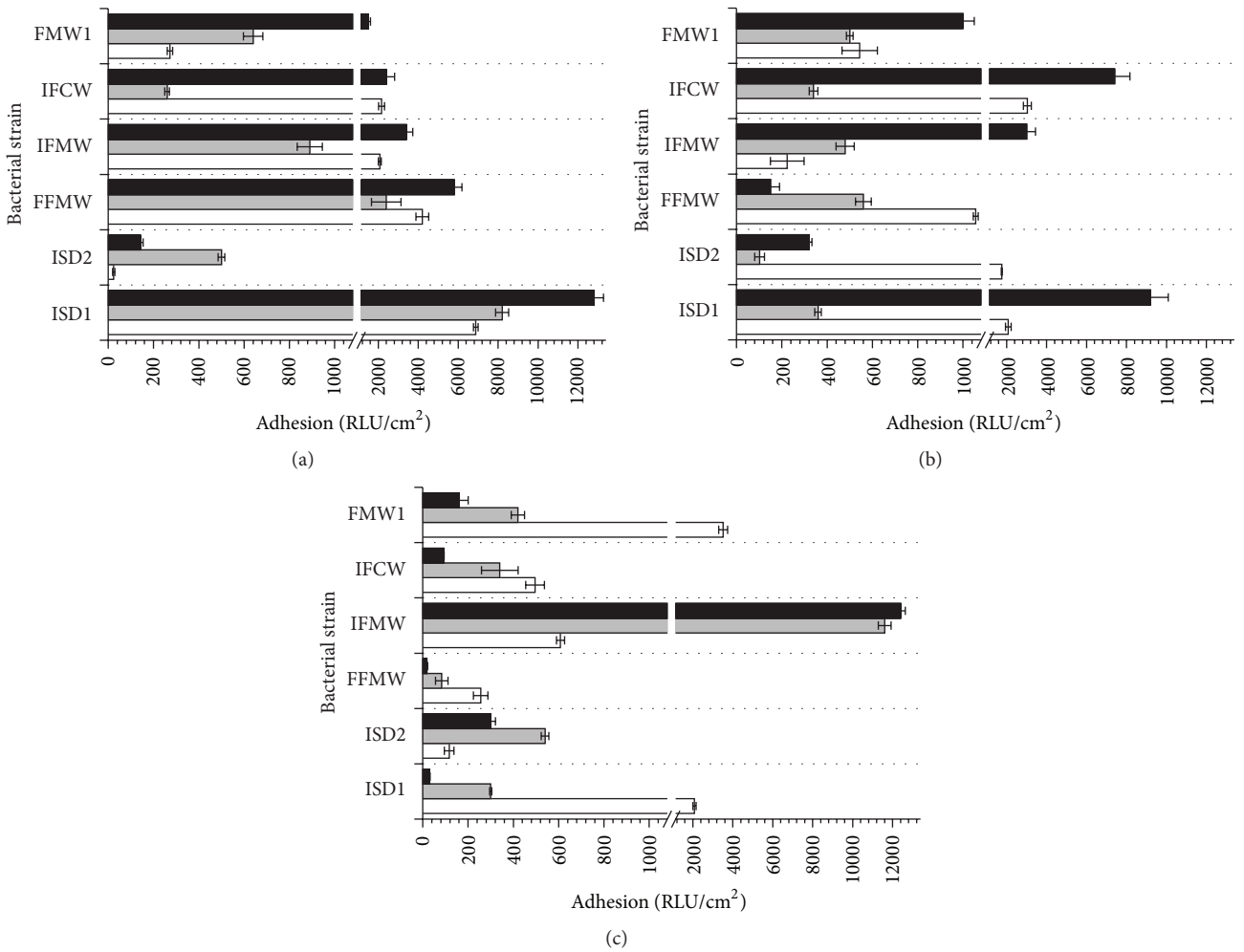

Figure 3: The adhesion (RLU/cm^2) of *A. bogorensis* (ISD1, ISD2, and FFMW) and *A. lannensis* (IFMW, IFCW, and FMW1) strains in M_1 medium with glucose (a), fructose (b), and sucrose (c) to PET (black bars), PS (grey bars), and G (white bars).

40 mN/m at 20°C) in comparison to hydrophilic glass surface (70 mN/m at 20°C) [17, 20]. What is more, studies confirmed that bacterial adhesion is influenced by many physiochemical properties of the environment, the availability and type of carbon source, and type of surface and microorganism abilities [21]. These parameters also determine the cell adhesion in industrial conditions. For example, Møretrø and Langsrud (2004) reported that food-processing environmental factors, including sugars and nutrients, had significant impacts on *Listeria monocytogenes* adhesion and biofilm formation [22]. Therefore, for the next stage of research, involving effect of berries juices on the growth and adhesion of *Asaia* spp., we choose rich M_1 medium with glucose and minimal M_2 medium with sucrose, respectively.

3.2. Chromatographic Analysis of Juices. The carbohydrate profiles of the fruit extracts indicated that the main sugars were glucose and fructose. In the bilberry juice, fructose concentration was 1.94 g/100 mL, while glucose equaled 0.76 g/100 mL. Respectively, for the black currant juice, the values were 0.60 g/100 mL and 0.54 g/100 mL. According to the literature, in the majority of native fruit juices, the content of saccharides is limited only to glucose, fructose, and sucrose. The variability of determined saccharide contents in fruit juices from berries stemmed from differences in variety, stage of ripeness, and climatic conditions [23].

The polyphenolic profiles in fruit juices were determined using HPLC method and the results are presented in Figures 5 and 6. We noted good separation of thirteen anthocyanins in the bilberry juice while for the black currant juice we detected six defined compounds. In the bilberry juice, delphinidin (Dp), cyanidin (Cy), petunidin (Pet), peonidin (Pn), and malvidin (Mal) with galactoside (Gal), glucoside (Glu), and arabinoside (Ara) forms were detected. The results obtained for black currant juice indicate that the material is a source of delphinidin-3-glucoside, delphinidin-3-rutinoside, cyanidin-3-glucoside, and cyanidin-3-rutinoside as well as petunidin-3-glucoside and petunidin-3-rutinoside. The individual anthocyanin contents were determined according to the linear calibration curve (correlation coefficient = 0.989) and expressed as μg of cyanidin-3-glucoside per one mL. The highest concentration of these compounds in the *Vaccinium*

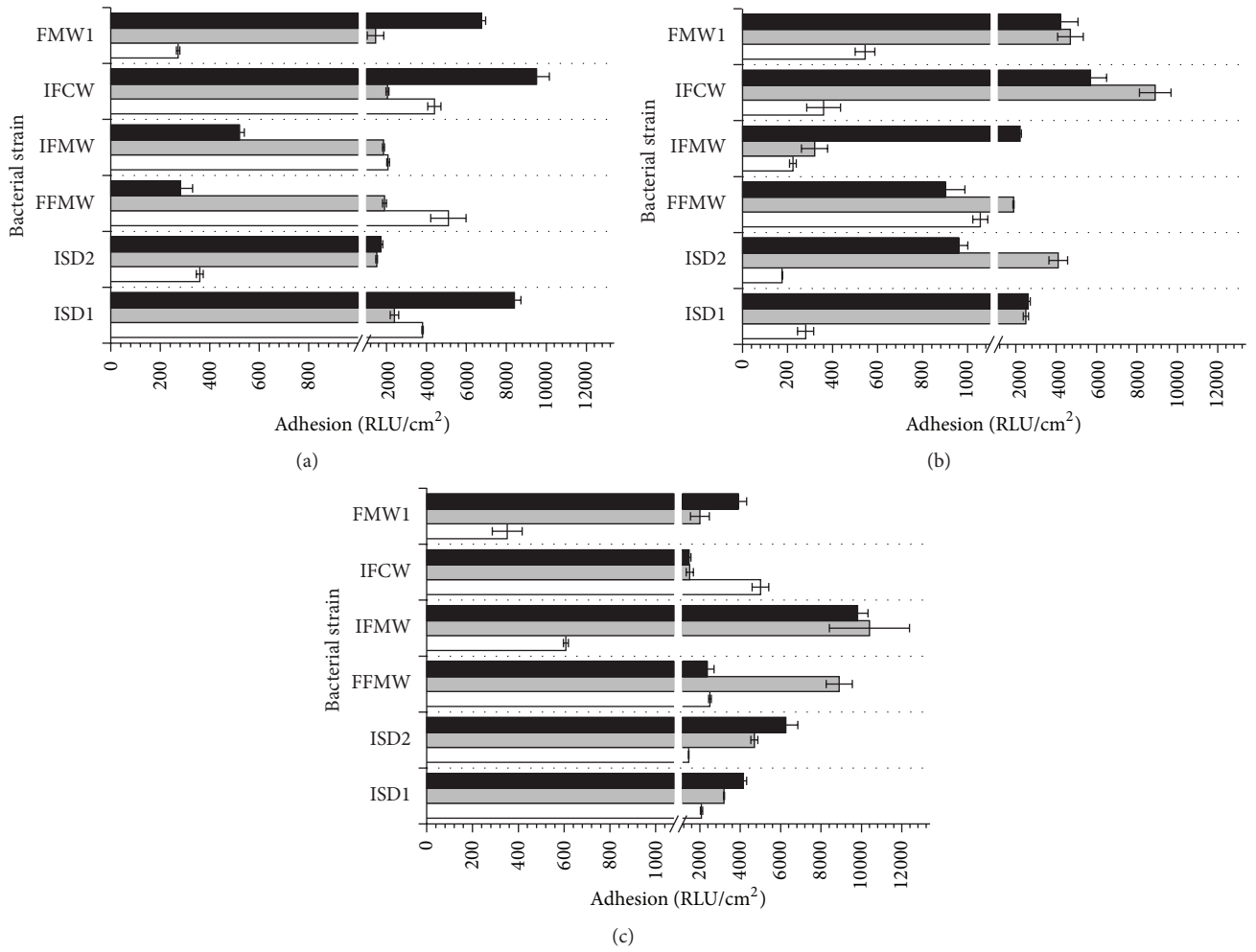

Figure 4: The adhesion (RLU/cm^2) of *A. bogorensis* (ISD1, ISD2, and FFMW) and *A. lannensis* (IFMW, IFCW, and FMW1) strains in M_2 medium with glucose (a), fructose (b), and sucrose (c) to PET (black bars), PS (grey bars), and G (white bars).

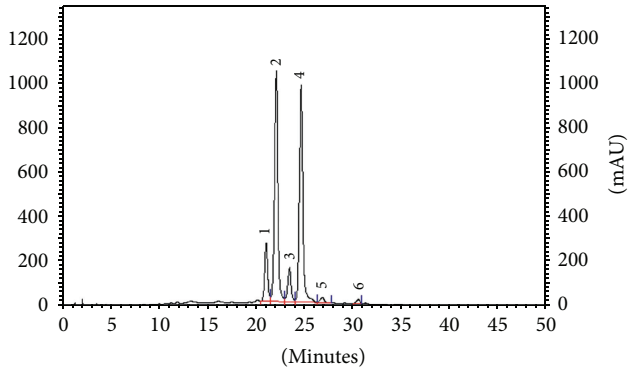

Peak	Conc. (μg/mL)
(1) Dp3Glu	0.48 ± 0.11
(2) Dp3Rut	2.04 ± 0.21
(3) Cy3Glu	0.34 ± 0.04
(4) Cy3Rut	1.99 ± 0.15
(5) Pet3Glu	0.09 ± 0.02
(6) Pet3Rut	0.07 ± 0.01

Figure 5: Anthocyanins profile in the *Ribes nigrum* juice.

myrtillus juice was noted for petunidin-3-glucoside (2.48 μg/mL) and malvidin-3-glucoside (2.41 μg/mL), cyanidin-3-glucoside (1.83 μg/mL), and delphinidin-3-glucoside (1.78 μg/mL). The major anthocyanins in the *Ribes nigrum* juice were delphinidin-3-rutinoside (2.04 μg/mL) and cyanidin-3-rutinoside (1.99 μg/mL). The presence of anthocyanins was also confirmed by LC-MS (Table 3). Twenty-two compounds were detected: seven common for both juices, twelve designated only for bilberry, and three for black currant juice. Besides anthocyanins (delphinidin, cyanidin, petunidin, and malvidin derivatives), phenolic acids (chlorogenic and neochlorogenic) as well as flavonols (quercetin-3-glucoside, quercetin-3-rutinoside) and flavanols (procyanidin B2 and procyanidin type A2) were detected. Numerous studies have reported the composition of phenolic acids, anthocyanins, and flavonols in *Ribes nigrum* [24–26] and *Vaccinium myrtillus* fruits [27–30]. The bilberry fruits are a rich source of delphinidin, cyanidin, petunidin, peonidin, malvidin, and their derivatives. The anthocyanin concentration of bilberry juices ranged from 1610 to 5963 mg/L, with the mean of 3087 mg/L [30] while

Table 3: Bioactive compounds in bilberry and black currant juices.

RT (min)	λ_{max} (nm)	$[M - H]^-$	Fragment ions	Compound	*V. myrtillus*	*R. nigrum*
8.48	244, 323	353	191, 179	Neochlorogenic acid	+	+
9.06	244, 330	355	191	Chlorogenic acid	−	+
9.62	223, 280	463	301	Delphinidin-3-galactoside	+	−
9.73	246, 330	355	179, 163	Caffeoyl hexose	+	+
11.01	522	341	179	Dicaffeic acid	+	−
11.22	278, 521	463	301	Delphinidin-3-glucoside	+	+
11.65	224, 522	609	301, 406	Delphinidin-3-rutinoside	−	+
13.47	280, 520	447	285	Cyanidin-3-glucoside	+	+
15.60	280, 521	477	315	Petunidin-3-galactoside	+	+
15.63	236, 279	577	407	Procyanidin B2	+	−
15.93	236, 280	575	377, 395, 449	Procyanidin A2	+	−
16.04	272, 520	477	315	Petunidin-3-glucoside	+	−
20.78	260, 352	479	317	Myricetin-3-galactoside	−	+
20.84	254, 354	461	301	Quercetin-3-glucoside	+	+
21.20	276, 527	491	329	Malvidin-3-galactoside	+	+
21.47	233, 279	866	577, 451	B-type procyanidin trimer	+	−
25.34	233, 280	863	573, 411	A type procyanidin trimer	+	−
26.45	230, 278	1152	861, 577	A type procyanidin tetramer	+	−
28.59	261, 352	479	317	Myricetin-3-glucoside	+	−
28.68	233, 279	489	285	Cyanidin-6-acetyl-3-glucoside	+	−
30.34	281, 521	505	301	Delphinidin-6-acetyl-3-glucoside	+	−
33.71	258, 354	609	301	Quercetin-3-rutinoside	+	−

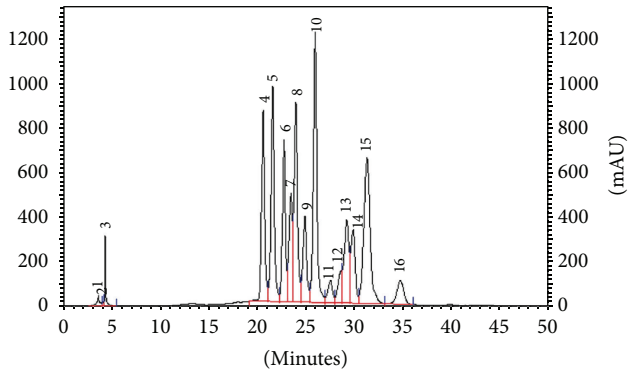

Peak	Conc. (μg/mL)
(1) ND	0.11 ± 0.04
(2) ND	0.05 ± 0.01
(3) ND	0.16 ± 0.03
(4) Dp3Gal	1.59 ± 0.12
(5) Dp3Glu	1.78 ± 0.09
(6) Cy3Gal	1.26 ± 0.08
(7) Dp3Ara	0.96 ± 0.03
(8) Cy3Glu	1.83 ± 0.07
(9) Pet3Gal	0.87 ± 0.05
(10) Pet3Glu	2.48 ± 0.11
(11) Pn3Gal	0.31 ± 0.02
(12) Pet3Ara	0.34 ± 0.02
(13) Pn3Glu	1.08 ± 0.13
(14) Mal3Gal	0.84 ± 0.02
(15) Mal3Glu	2.41 ± 0.06
(16) Mal3Ara	0.47 ± 0.08

Figure 6: Anthocyanins profile in the *Vaccinium myrtillus* juice.

in the case of *R. nigrum* the average content of anthocyanin amounts to 3500 mg/L [31]. In relation to these data, black currant juice used in our study was characterized by much lower content of anthocyanins than bilberry juice, both qualitatively and quantitatively. The variations in anthocyanin profiles may be determined by genotype features of the plants and climatic conditions [28]. Despite the significant differences in the content of polyphenol compounds, juices of black currants and blueberries are rich sources of bioactive compounds that can be used as a remedy in many illnesses. It is well known that these compounds have beneficial effects in preventing cardiovascular and neurological diseases [32, 33] and possess anticancer [34, 35], anti-inflammatory [36, 37], neuroprotective [38], and antidiabetic [39] activities. The antibacterial activities of various fruit extracts on common potential pathogens including antibiotic-resistant strains were also documented [40]. Research suggests that cranberry (*Vaccinium macrocarpon*) juice, in particular, helps in maintaining the health of the urinary tract [41]. The profile of cranberry juice, being rich in A type proanthocyanidins (PACs) in contrast to the B-type PACs, presents in most other fruits [42]. PACs are colorless oligomers and polymers of flavan-3-ols that show especial antiaggregation abilities [43]. The antibacterial activity of cranberry A type proanthocyanidin was demonstrated in vitro on uropathogenic P-fimbriated *Escherichia coli* [44] and other pathogenic bacteria [7, 9]. What is interesting is that our results of LC-MS showed that

bilberry juice is a source of proanthocyanidins type A and procyanidin type 2. Despite the limited literature concerning the data demonstrating the presence of type A proanthocyanidins in cranberry, some research suggests that they may also be present in wild berries. Schmidt et al. (2004) suggest that high molecular weight oligomeric proanthocyanidins from wild *Vaccinium angustifolium* exhibit strong antiproliferation activity against human prostate and mouse liver cancer cell lines [45]. Characterization of proanthocyanidins in wild blackberries was also carried out in the work of Cuevas-Rodríguez et al. (2010) [46]. Generally, the highest contents of all types of proanthocyanidins were determined in blackthorns, chokeberries, saskatoon berries, blueberries, cranberries, and lingonberries [46–52]. Moreover, it was shown that the proanthocyanidins can also be present in the bilberry fruits, chemical composition of which may be similar to that of cranberry fruit [53].

3.3. Growth. Due to the higher A (%) results and quite high RLU values, for the next stage of this study, based on the effect of fruit juices on the growth and adhesion of *Asaia* spp., we chose M_1 medium with glucose for growth analysis and M_2 medium with sucrose with PET carriers for adhesion investigation.

The growth in M_1 medium without fruit juices varied depending on the strain with mean value of $7.02 \pm 2.41 \times 10^9$ CFU/cm^3 (Figure 7). After 14-day incubation, the best growth was noted for *A. bogorensis* ISD2 ($1.08 \pm 0.23 \times 10^{10}$ CFU/cm^3) and *A. bogorensis* ISD1 ($9.97 \pm 1.45 \times 10^9$ CFU/cm^3) while the lowest number of the bacteria was detected for *A. lannensis* FMW1 ($2.67 \pm 1.70 \times 10^9$ CFU/cm^3). The addition of *R. nigrum* and *V. myrtillus* juices caused a slight reduction in the number of viable bacterial cells. The average count in M_1 medium with 10% (v/v) bilberry juice and black currant juice was $2.60 \pm 1.35 \times 10^9$ CFU/cm^3 and $4.37 \pm 2.85 \times 10^9$ CFU/cm^3, respectively. The obtained results suggested that *A. bogorensis* showed higher sensitivity to fruit juices than *A. lannensis* strains.

According to the literature, polyphenols from various fruit demonstrate antibacterial activities, especially against pathogenic strains: *P. aeruginosa*, *Staph. aureus*, *E. coli*, *L. monocytogenes*, and *Salmonella* spp. Polyphenols are able to suppress a number of microbial virulence factors, such as reduction of host ligands adhesion, inhibition of biofilm formation, and neutralization of bacterial toxins, and show synergism with antibiotics [54]. The activity of phenolic compounds includes interaction with microbial enzymes that are responsible for the cell growth or have direct influence on microbial metabolism by inhibition of oxidative phosphorylation [55]. In addition, the cells of Gram negative bacteria are surrounded by an outer membrane, which acts as barrier protecting against many external agents [56]. The permeability of this membrane is regulated by hydrophilic channels which generally exclude the entry of hydrophobic substances to the bacterial cell. However, some agents, including essential oils and terpenoids and other phenolic compounds, affect membrane barriers, which stimulate the penetration of bioactive agents in bacterial cells [57]. It was found that berries

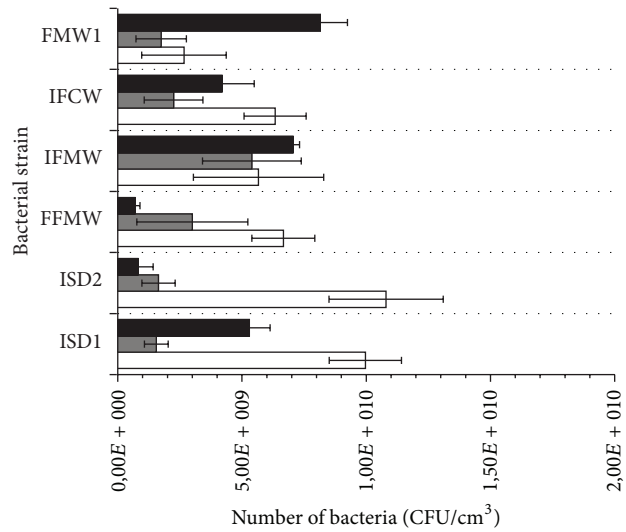

Figure 7: Growth of the *Asaia* spp. strains in M_1 medium with glucose (white bars), supplemented by bilberry (grey bars) and black currant (black bars) juices.

extracts clearly caused higher permeability of *Salmonella* spp. membranes, cell penetration, and reaction with cellular proteins [58]. According to Nohynek et al. (2006), the activity of polyphenolic compounds from berry fruits may be the result of multiple mechanisms and synergies due to the presence of various bioactive compounds [56]. In Puupponen-Pimiä et al. (2001) study, extracts from blueberry and black currant fruits were checked against pathogenic Gram negative and Gram positive bacteria [5]. It was shown that anthocyanins (pelargonidin, cyanidin) as well flavonols (myricetin) showed inhibitory effect against Gram negative cells of *E. coli* and *Salmonella* spp. Phenolic extracts containing tannins and their derivatives showed strong antibacterial effect against *Staph. aureus*, *H. pylori*, *C. perfringens*, *B. cereus*, *Klebsiella* spp., and *Proteus* spp. [56, 58]. However, the knowledge about the effect of fruit phenolics on food spoilage bacteria is still limited.

3.4. Biofouling. It is well known that luminometric measurements in an environment of fruit juices that are rich in polyphenols may carry a margin of error. Luminometry is based on the reaction of enzymatic oxidation of luciferin to oxyluciferin and the presence of antioxidants can influence the final results. It has been documented that polyphenols present in green tea can inhibit the enzymatic activities [59]. Therefore, in the light of that fact, we used two different methods to assess the adhesion of cells to PET surface: luminometry and plate count technique.

The effect of the bilberry and black currant juices on the adhesion properties of *Asaia* spp. was performed during cultivation in M_2 medium with PET carriers. Results, expressed as adhesion relative coefficient A (%) and RLU/cm^2, were presented in Figures 8(a) and 8(b), respectively. The coefficient A (%) calculated for the sixth day of incubation with 10% (v/v) juice showed significant decrease in the adhesion and biofilm

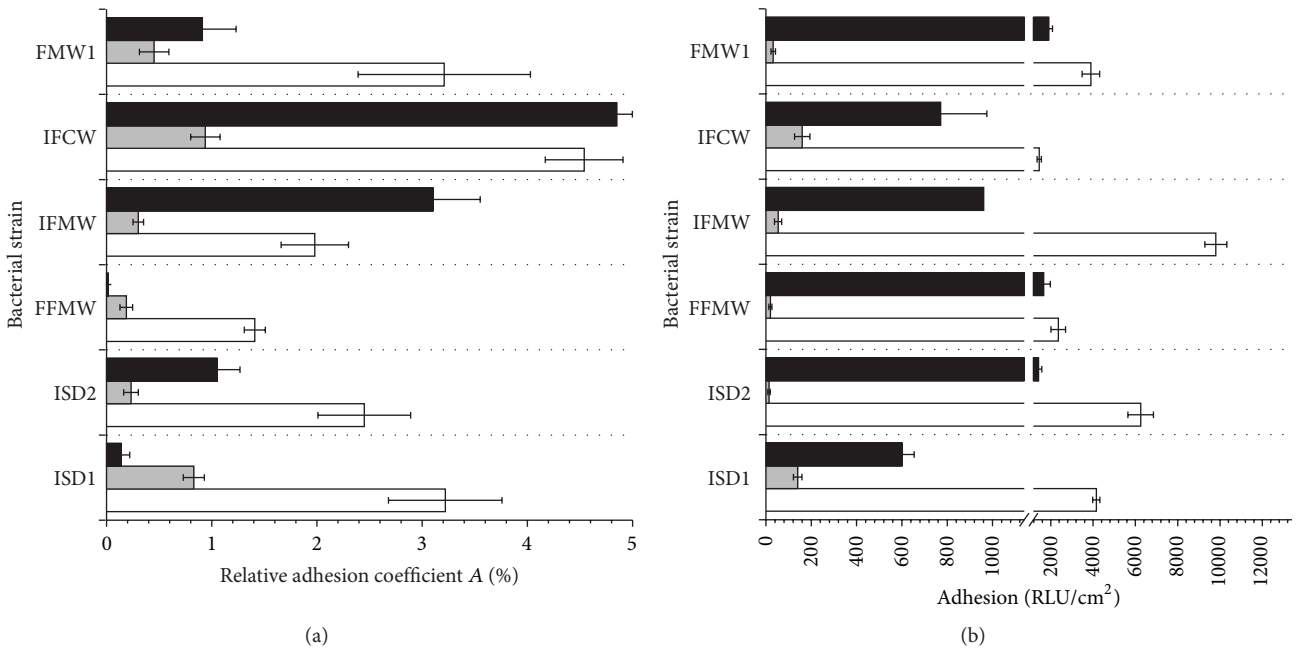

Figure 8: Adhesion of the *Asaia* spp. strains to PET carrier in M_2 medium with sucrose (white bars) supplemented by bilberry (grey bars) and black currant (black bars) juices, evaluated by plate count method (a) and luminometry (b).

formation (Figure 8(a)). This parameter for cell adhesion with bilberry juice ranged from 0.19 ± 0.11% to 0.94 ± 0.59%, while for black currant juice the values were 0.01 ± 0.009% to 4.85 ± 0.41%. The results were 4 ÷ 11 times lower in comparison to the control sample without *V. myrtillus* juice. Luminometric results (RLU/cm^2) also confirmed significant reduction of adhesion (Figure 8(b)). There were statistically significant differences between the control samples and cultures with fruit juices ($p < 0.05$). Additionally, the differences were noted for antiadhesive activities of tested juices. The values ranged from 1460 ± 102 RLU/cm^2 to 9800 ± 520 RLU/cm^2 (Av = 4252 ± 2748 RLU/cm^2) for the control sample and for adhesion in the presence of *V. myrtillus* and *R. nigrum* from 14 ± 5 RLU/cm^2 to 160 ± 34 RLU/cm^2 (Av = 70 ± 58 RLU/cm^2) and from 600 ± 54 RLU/cm^2 to 1900 ± 187 RLU/cm^2, respectively (Av = 1218 ± 474 RLU/cm^2). Thus, bilberry juice inhibited biofouling of all tested *Asaia* spp. bacteria, while in the presence of black currant juice we noted the antiadhesive effect for *A. bogorensis* strains in particular.

The use of fruit juice not only brings antiadhesive effects, but also has other health benefits. The prohealth action of berry juices has been known in folk medicine. However, antiadhesive properties of fruit juices were documented scientifically mainly for cranberry (*Vaccinium macrocarpon*) [17, 41, 54]. The effect of blueberry constituents on the adhesion of *Staph. mutans* was also documented [60]. The recent studies are related to the effect of cranberry juice on the growth and adhesion abilities of bacteria *Asaia* spp. It was documented that, in the presence of cranberry juice, the attachment of *A. bogorensis* cells to plastic surfaces was significantly lower [19]. However, the mechanisms by which cranberry extracts are effective as antiadhesive agent have not been fully established yet. It is believed that there are two main compounds involved in the inhibition of bacterial attachment: fructose blocking bacterial type 1 fimbriae and proanthocyanidins which bind with type P fimbriae, preventing cells adhesion [41, 61]. The chromatographic analysis of the polyphenols in *V. macrocarpon* confirmed the presence of type A proanthocyanidin [19, 62]. Thus, we can assume that type A proanthocyanidins present in berries may show an antiadhesive effect to *Asaia* spp. cells.

4. Conclusions

The results presented in this study suggest that bilberry and black currant juices show high antiadhesive and antibacterial activity against food-spoiled bacteria belonging to the genus *Asaia*. Particularly *V. myrtillus* juice characterized by a higher content of polyphenols including A type proanthocyanidin showed strong antiadhesive and bacteriostatic properties. The high content of bioactive compounds with proven health-promoting properties makes them a valuable supplement of soft drinks, as well as interesting alternative to artificial additives to keep the microbial stability of final products.

Competing Interests

The authors declare that there are no competing interests regarding the publication of this paper.

Acknowledgments

This work was financially supported by the National Science Centre, Poland, Project no. 2015/17/N/NZ9/03635.

References

[1] N. P. Seeram, "Berry fruits for cancer prevention: current status and future prospects," *Journal of Agricultural and Food Chemistry*, vol. 56, no. 3, pp. 630–635, 2008.

[2] A. Szajdek and E. J. Borowska, "Bioactive compounds and health-promoting properties of berry fruits: a review," *Plant Foods for Human Nutrition*, vol. 63, no. 4, pp. 147–156, 2008.

[3] S. Subash, M. M. Essa, S. Al-Adawi, M. A. Memon, T. Manivasagam, and M. Akbar, "Neuroprotective effects of berry fruits on neurodegenerative diseases," *Neural Regeneration Research*, vol. 9, no. 16, pp. 1557–1566, 2014.

[4] O. Paredes-López, M. L. Cervantes-Ceja, M. Vigna-Pérez, and T. Hernández-Pérez, "Berries: improving human health and healthy aging, and promoting quality life—a review," *Plant Foods for Human Nutrition*, vol. 65, no. 3, pp. 299–308, 2010.

[5] R. Puupponen-Pimiä, L. Nohynek, C. Meier et al., "Antimicrobial properties of phenolic compounds from berries," *Journal of Applied Microbiology*, vol. 90, no. 4, pp. 494–507, 2001.

[6] A. Cisowska, D. Wojnicz, and A. B. Hendrich, "Anthocyanins as antimicrobial agents of natural plant origin," *Natural Product Communications*, vol. 6, no. 1, pp. 149–156, 2011.

[7] H. Shmuely, O. Burger, I. Neeman et al., "Susceptibility of *Helicobacter pylori* isolates to the antiadhesion activity of a high-molecular-weight constituent of cranberry," *Diagnostic Microbiology and Infectious Disease*, vol. 50, no. 4, pp. 231–235, 2004.

[8] D. A. Vattem, Y.-T. Lin, R. G. Labbe, and K. Shetty, "Antimicrobial activity against select food-borne pathogens by phenolic antioxidants enriched in cranberry pomace by solid-state bioprocessing using the food grade fungus *Rhizopus oligosporus*," *Process Biochemistry*, vol. 39, no. 12, pp. 1939–1946, 2004.

[9] S. Caillet, J. Côté, J.-F. Sylvain, and M. Lacroix, "Antimicrobial effects of fractions from cranberry products on the growth of seven pathogenic bacteria," *Food Control*, vol. 23, no. 2, pp. 419–428, 2012.

[10] N. Rafsanjany, J. Senker, S. Brandt, U. Dobrindt, and A. Hensel, "*In vivo* consumption of cranberry exerts *ex vivo* antiadhesive activity against FimH-dominated uropathogenic *Escherichia coli*: a combined *in vivo*, *ex vivo*, and *in vitro* study of an extract from *Vaccinium macrocarpon*," *Journal of Agricultural and Food Chemistry*, vol. 63, no. 40, pp. 8804–8818, 2015.

[11] L. Qian, J. Thomas, and J. Taylor, "Antimicrobial effects of cranberry juice against common Gram-negative uropathogens *in vitro*," *American Journal of Clinical Pathology*, vol. 142, article A074, 2014.

[12] B. D. Mathison, L. L. Kimble, K. L. Kaspar, C. Khoo, and B. P. Chew, "Consumption of cranberry beverage improved endogenous antioxidant status and protected against bacteria adhesion in healthy humans: a randomized controlled trial," *Nutrition Research*, vol. 34, no. 5, pp. 420–427, 2014.

[13] D. Kregiel, A. Rygała, Z. Libudzisz, P. Walczak, and E. Ołtuszak-Walczak, "*Asaia lannensis*—the spoilage acetic acid bacteria isolated from strawberry-flavored bottled water in Poland," *Food Control*, vol. 26, no. 1, pp. 147–150, 2012.

[14] J. E. Moore, M. McCalmont, J. Xu, B. C. Millar, and N. Heaney, "*Asaia* sp., an unusual spoilage organism of fruit-flavored bottled water," *Applied and Environmental Microbiology*, vol. 68, no. 8, pp. 4130–4131, 2002.

[15] I. Horsáková, M. Voldřich, M. Čeřovský, P. Sedláčková, P. Šicnerová, and P. Ulbrich, "*Asaia* sp. as a bacterium decaying the packaged still fruit beverages," *Czech Journal of Food Sciences*, vol. 27, pp. S362–S365, 2009.

[16] D. Kregiel, "Attachment of *Asaia lannensis* to materials commonly used in beverage industry," *Food Control*, vol. 32, no. 2, pp. 537–542, 2013.

[17] D. Kregiel, A. Otlewska, and H. Antolak, "Attachment of *Asaia bogorensis* originating in fruit-flavored water to packaging materials," *BioMed Research International*, vol. 2014, Article ID 514190, 6 pages, 2014.

[18] B. Gutarowska and A. Czyżowska, "The ability of filamentous fungi to produce acids on indoor building materials," *Annals of Microbiology*, vol. 59, no. 4, pp. 807–813, 2009.

[19] H. Antolak, D. Kręgiel, and A. Czyżowska, "Adhesion of *Asaia bogorensis* to glass and polystyrene in the presence of cranberry juice," *Journal of Food Protection*, vol. 78, no. 6, pp. 1186–1190, 2015.

[20] J. Lange and Y. Wyser, "Recent innovations in barrier technologies for plastic packaging—a review," *Packaging Technology and Science*, vol. 16, no. 4, pp. 149–158, 2003.

[21] K. Hori and S. Matsumoto, "Bacterial adhesion: from mechanism to control," *Biochemical Engineering Journal*, vol. 48, no. 3, pp. 424–434, 2010.

[22] T. Møretrø and S. Langsrud, "*Listeria monocytogenes*: biofilm formation and persistence in food-processing environments," *Biofilms*, vol. 1, no. 2, pp. 107–121, 2004.

[23] Z. Targoński and A. Stój, "Zafałszowania żywności i metody ich wykrywania," *Żywność: Nauka, Technologia, Jakość*, vol. 4, pp. 30–40, 2005 (Polish).

[24] G. J. McDougall, S. Gordon, R. Brennan, and D. Stewart, "Anthocyanin-flavanol condensation products from black currant (*Ribes nigrum* L.)," *Journal of Agricultural and Food Chemistry*, vol. 53, no. 20, pp. 7878–7885, 2005.

[25] M. J. Anttonen and R. O. Karjalainen, "High-performance liquid chromatography analysis of black currant (*Ribes nigrum* L.) Fruit phenolics grown either conventionally or organically," *Journal of Agricultural and Food Chemistry*, vol. 54, no. 20, pp. 7530–7538, 2006.

[26] V. Gavrilova, M. Kajdžanoska, V. Gjamovski, and M. Stefova, "Separation, characterization and quantification of phenolic compounds in blueberries and red and black currants by HPLC-DAD-ESI-MSn," *Journal of Agricultural and Food Chemistry*, vol. 59, no. 8, pp. 4009–4018, 2011.

[27] K. R. Määttä-Riihinen, M. P. Kähkönen, A. R. Törrönen, and I. M. Heinonen, "Catechins and procyanidins in berries of *Vaccinium* species and their antioxidant activity," *Journal of Agricultural and Food Chemistry*, vol. 53, no. 22, pp. 8485–8491, 2005.

[28] A. K. Lätti, K. R. Riihinen, and P. S. Kainulainen, "Analysis of anthocyanin variation in wild populations of bilberry (*Vaccinium myrtillus* L.) in Finland," *Journal of Agricultural and Food Chemistry*, vol. 56, no. 1, pp. 190–196, 2008.

[29] Š. Može, T. Polak, L. Gašperlin et al., "Phenolics in slovenian bilberries (*Vaccinium myrtillus* L.) and blueberries (*Vaccinium corymbosum* L.)," *Journal of Agricultural and Food Chemistry*, vol. 59, no. 13, pp. 6998–7004, 2011.

[30] D. Müller, M. Schantz, and E. Richling, "High performance liquid chromatography analysis of anthocyanins in bilberries (*Vaccinium myrtillus* L.), blueberries (*Vaccinium corymbosum* L.), and corresponding juices," *Journal of Food Science*, vol. 77, no. 4, pp. C340–C345, 2012.

[31] B. B. Mikkelsen and L. Poll, "Decomposition and transformation of aroma compounds and anthocyanins during black currant (*Ribes nigrum* L.) juice processing," *Journal of Food Science*, vol. 67, no. 9, pp. 3447–3455, 2002.

[32] T. C. Wallace, "Anthocyanins in cardiovascular disease," *Advances in Nutrition*, vol. 2, no. 1, pp. 1–7, 2011.

[33] S. de Pascual-Teresa, "Molecular mechanisms involved in the cardiovascular and neuroprotective effects of anthocyanins," *Archives of Biochemistry and Biophysics*, vol. 559, pp. 68–74, 2014.

[34] F. Aqil, A. Gupta, R. Munagala et al., "Antioxidant and antiproliferative activities of anthocyanin/ellagitannin-enriched extracts from *Syzygium cumini* L. (Jamun, the Indian Blackberry)," *Nutrition and Cancer*, vol. 64, no. 3, pp. 428–438, 2012.

[35] T.-C. Tsai, H.-P. Huang, Y.-C. Chang, and C.-J. Wang, "An anthocyanin-rich extract from *Hibiscus sabdariffa* linnaeus inhibits *N*-nitrosomethylurea-induced leukemia in rats," *Journal of Agricultural and Food Chemistry*, vol. 62, no. 7, pp. 1572–1580, 2014.

[36] I. Edirisinghe, K. Banaszewski, J. Cappozzo et al., "Strawberry anthocyanin and its association with postprandial inflammation and insulin," *British Journal of Nutrition*, vol. 106, no. 6, pp. 913–922, 2011.

[37] D. W. Sohn, W. J. Bae, H. S. Kim, S. W. Kim, and S. W. Kim, "The anti-inflammatory and antifibrosis effects of anthocyanin extracted from black soybean on a peyronie disease rat model," *Urology*, vol. 84, no. 5, pp. 1112–1116, 2014.

[38] K. A. Youdim, B. Shukitt-Hale, and J. A. Joseph, "Flavonoids and the brain: interactions at the blood-brain barrier and their physiological effects on the central nervous system," *Free Radical Biology and Medicine*, vol. 37, no. 11, pp. 1683–1693, 2004.

[39] D. Wang, M. Xia, X. Yan et al., "Gut microbiota metabolism of anthocyanin promotes reverse cholesterol transport in mice via repressing miRNA-10b," *Circulation Research*, vol. 111, no. 8, pp. 967–981, 2012.

[40] Y.-L. Lee, T. Cesario, Y. Wang, E. Shanbrom, and L. Thrupp, "Antibacterial activity of vegetables and juices," *Nutrition*, vol. 19, no. 11-12, pp. 994–996, 2003.

[41] A. B. Howell, "Bioactive compounds in cranberries and their role in prevention of urinary tract infections," *Molecular Nutrition and Food Research*, vol. 51, no. 6, pp. 732–737, 2007.

[42] J. B. Blumberg, T. A. Camesano, A. Cassidy et al., "Cranberries and their bioactive constituents in human health," *Advances in Nutrition*, vol. 4, no. 6, pp. 618–632, 2013.

[43] Y. Wang, A. P. Singh, W. J. Hurst, J. A. Glinski, H. Koo, and N. Vorsa, "Influence of degree-of-polymerization and linkage on the quantification of proanthocyanidins using 4-dimethylaminocinnamaldehyde (DMAC) assay," *Journal of Agricultural and Food Chemistry*, vol. 64, no. 11, pp. 2190–2199, 2016.

[44] L. Y. Foo, Y. Lu, A. B. Howell, and N. Vorsa, "A-type proanthocyanidin trimers from cranberry that inhibit adherence of uropathogenic P-fimbriated *Escherichia coli*," *Journal of Natural Products*, vol. 63, no. 9, pp. 1225–1228, 2000.

[45] B. M. Schmidt, A. B. Howell, B. McEniry et al., "Effective separation of potent antiproliferation and antiadhesion components from wild blueberry (*Vaccinium angustifolium* Ait.) fruits," *Journal of Agricultural and Food Chemistry*, vol. 52, no. 21, pp. 6433–6442, 2004.

[46] E. O. Cuevas-Rodríguez, G. G. Yousef, P. A. García-Saucedo, J. López-Medina, O. Paredes-López, and M. A. Lila, "Characterization of anthocyanins and proanthocyanidins in wild and domesticated mexican blackberries (*Rubus* spp.)," *Journal of Agricultural and Food Chemistry*, vol. 58, no. 12, pp. 7458–7464, 2010.

[47] L. W. Gu, M. A. Kelm, J. F. Hammerstone et al., "Screening of foods containing proanthocyanidins and their structural characterization using LC-MS/MS and thiolytic degradation," *Journal of Agricultural and Food Chemistry*, vol. 51, no. 25, pp. 7513–7521, 2003.

[48] K. R. Määttä-Riihinen, A. Kamal-Eldin, P. H. Mattila, A. M. González-Paramás, and R. Törrönen, "Distribution and contents of phenolic compounds in eighteen scandinavian berry species," *Journal of Agricultural and Food Chemistry*, vol. 52, no. 14, pp. 4477–4486, 2004.

[49] X. Wu, L. Gu, R. L. Prior, and S. McKay, "Characterization of anthocyanins and proanthocyanidins in some cultivars of *Ribes*, *Aronia*, and *Sambucus* and their antioxidant capacity," *Journal of Agricultural and Food Chemistry*, vol. 52, no. 26, pp. 7846–7856, 2004.

[50] B. Buendía, M. I. Gil, J. A. Tudela et al., "HPLC-MS analysis of proanthocyanidin oligomers and other phenolics in 15 strawberry cultivars," *Journal of Agricultural and Food Chemistry*, vol. 58, no. 7, pp. 3916–3926, 2010.

[51] B. L. White, L. R. Howard, and R. L. Prior, "Release of bound procyanidins from cranberry pomace by alkaline hydrolysis," *Journal of Agricultural and Food Chemistry*, vol. 58, no. 13, pp. 7572–7579, 2010.

[52] L. R. Howard, C. Castrodale, C. Brownmiller, and A. Mauromoustakos, "Jam processing and storage effects on blueberry polyphenolics and antioxidant capacity," *Journal of Agricultural and Food Chemistry*, vol. 58, no. 7, pp. 4022–4029, 2010.

[53] D. L. Madhavi, J. Bomser, M. A. L. Smith, and K. Singletary, "Isolation of bioactive constituents from *Vaccinium myrtillus* (bilberry) fruits and cell cultures," *Plant Science*, vol. 131, no. 1, pp. 95–103, 1998.

[54] O. Burger, E. Weiss, N. Sharon, M. Tabak, I. Neeman, and I. Ofek, "Inhibition of *Helicobacter pylori* adhesion to human gastric mucus by a high-molecular-weight constituent of cranberry juice," *Critical Reviews in Food Science and Nutrition*, vol. 42, no. 3, pp. 279–284, 2002.

[55] A. Scalbert, "Antimicrobial properties of tannins," *Phytochemistry*, vol. 30, no. 12, pp. 3875–3883, 1991.

[56] L. J. Nohynek, H.-L. Alakomi, M. P. Kähkönen et al., "Berry phenolics: antimicrobial properties and mechanisms of action against severe human pathogens," *Nutrition and Cancer*, vol. 54, no. 1, pp. 18–32, 2006.

[57] I. M. Helander, H.-L. Alakomi, K. Latva-Kala et al., "Characterization of the action of selected essential oil components on gram-negative bacteria," *Journal of Agricultural and Food Chemistry*, vol. 46, no. 9, pp. 3590–3595, 1998.

[58] R. Puupponen-Pimiä, L. Nohynek, H.-L. Alakomi, and K.-M. Oksman-Caldentey, "Bioactive berry compounds—novel tools against human pathogens," *Applied Microbiology and Biotechnology*, vol. 67, no. 1, pp. 8–18, 2005.

[59] Q. He, Y. Lv, and K. Yao, "Effects of tea polyphenols on the activities of α-amylase, pepsin, trypsin and lipase," *Food Chemistry*, vol. 101, no. 3, pp. 1178–1182, 2006.

[60] E. I. Weiss, R. Lev-Dor, N. Sharon, and I. Ofek, "Inhibitory effect of a high-molecular-weight constituent of cranberry on adhesion of oral bacteria," *Critical Reviews in Food Science and Nutrition*, vol. 42, no. 3, pp. 285–292, 2002.

[61] D. Nicolosi, G. Tempera, C. Genovese, and P. M. Furneri, "Anti-adhesion activity of A2-type proanthocyanidins (a cranberry major component) on uropathogenic *E. coli* and *P. mirabilis* strains," *Antibiotics*, vol. 3, no. 2, pp. 143–154, 2014.

[62] C. G. Krueger, J. D. Reed, R. P. Feliciano, and A. B. Howell, "Quantifying and characterizing proanthocyanidins in cranberries in relation to urinary tract health," *Analytical and Bioanalytical Chemistry*, vol. 405, no. 13, pp. 4385–4395, 2013.

Hindawi Publishing Corporation
BioMed Research International
Volume 2016, Article ID 7461047, 8 pages
http://dx.doi.org/10.1155/2016/7461047

Review Article

Experimental Models of Oral Biofilms Developed on Inert Substrates: A Review of the Literature

Lopez-Nguyen Darrene[1] and Badet Cecile[1,2]

[1] *Université de Bordeaux, 16 Cours de la Marne, 33082 Bordeaux, France*
[2] *ISVV, EA 4577 Unité de Recherche Oenologie, Institut Polytechnique de Bordeaux, Université de Bordeaux, 33140 Villenave d'Ornon, France*

Correspondence should be addressed to Badet Cecile; cecile.badet@u-bordeaux2.fr

Received 3 July 2016; Accepted 14 August 2016

Academic Editor: Aruni Wilson

Copyright © 2016 L.-N. Darrene and B. Cecile. This is an open access article distributed under the Creative Commons Attribution License, which permits unrestricted use, distribution, and reproduction in any medium, provided the original work is properly cited.

The oral ecosystem is a very complex environment where more than 700 different bacterial species can be found. Most of them are organized in biofilm on dental and mucosal surfaces. Studying this community is important because a rupture in stability can lead to the preeminence of pathogenic microorganisms, causing dental decay, gingivitis, or periodontitis. The multitude of species complicates biofilm analysis so its reproduction, collection, and counting are very delicate. The development of experimental models of dental biofilms was therefore essential and multiple *in vitro* designs have emerged, each of them especially adapted to observing biofilm formation of specific bacteria within specific environments. The aim of this review is to analyze oral biofilm models.

1. Introduction

The oral cavity is a complex environment harboring more than 700 bacterial taxa. One major player in this ecosystem is dental plaque which develops naturally on hard and soft tissues of the mouth. Most oral bacteria are found in this biofilm whose complex organization remains relatively stable over time despite regular environmental changes [1–4]. Pathologies such as dental caries or periodontitis may arise when the equilibrium is compromised and when an imbalance occurs among the indigenous bacteria [5].

For many years, the oral ecosystem was studied with a reductionist approach, microbiologists studying bacterial species individually. This strategy made it possible to review and understand all the different components of this ecosystem, but without being able to explain how bacteria can form biofilms or to understand their functioning. The development of experimental models of dental biofilms was therefore essential and multiple *in vitro* models have emerged, each of them especially adapted to observing biofilm formation of specific bacteria within specific environments.

The aim of this review is to present currently available oral biofilm models. Various experimental designs have been developed from simple ones with a single bacterium to more complex multispecies designs.

Interests and limits of each model described below are given in Table 1.

2. Saliva and Medium

2.1. Saliva. Adhesion of bacteria to solid substratum is often mediated by a conditioning film of molecules adsorbed to the surface. In the oral cavity, the dental pellicle needs to be deposited on tooth surfaces for oral biofilm to develop. It is mostly composed of salivary proteins.

In order to mimic this coat, some authors recommend using artificial saliva, the major advantage being that it is reproducible.

Pratten compared various artificial saliva compositions: basic saliva first described by Russell and Coulter [6], hybrid saliva (with modified proportions), modified saliva (without lab-lemco), and complete saliva (with more mucins). Complete saliva seems to be the most reasonable compromise [7]. Basic saliva has also been used in other works that aimed to test the effect of antimicrobial agents on orthodontic bonding materials [8], the effect of manganese

Table 1: Interests and limits of various experimental models of biofilms.

	Interest	Limits
Saliva		
Human	(i) Contains a complex & complete blend of proteins, glycosaminoglycans, and ions that form a pellicle on tooth surface	(i) Quality: need healthy volunteers (ii) Quantity: need many volunteers (iii) Limited reproducibility
Artificial	(i) Reproducibility (ii) Low cost	(i) Less complex blend of molecules (ii) Do not mimic *in vivo* conditions
Substrates		
Glass	(i) Allows a simple and fast screening (ii) Low cost	(i) Direct bacterial adherence: no EAP creation (ii) Scoring could be operator dependent
Dentin/enamel	(i) Study of cariogenic, periodontal, endodontic, and Dentin/Composite interface specific biofilms (ii) Close to *in vivo* condition	Need for human or bovine teeth
Polystyrene (96-well plates)	(i) Can be coated with collagen, saliva, and/or different substances (ii) Allows many simultaneous studies: comparison of different stains, media, and substances in the same array	(i) When not coated: only direct bacterial adherence (ii) Far from *in vivo* conditions
Hydroxyapatite	(i) Best synthetic substrate mimicking human dental tissues (ii) Avoid the search of extracted teeth and their sterilization (iii) Can be coated with collagen, saliva & different substances	(i) Cost (ii) When not coated: only direct bacterial adherence (no EAP creation)
Incubation conditions		
Batch models	(i) Multispecies biofilms (ii) Allows the study of interactions in bacterial communities and the effect of various substances	(i) Far from *in vivo* conditions: does not integrate the changing environmental conditions occurring during biofilm growth
Continuous culture		
Constant depth fermentor	(i) Allows the control of environmental factors: gas flow, real time medium and waste monitoring, biofilm thickness, temperature, and pH (ii) Allows the formation of multispecies biofilms	(i) Cost (ii) Complexity of protocol
Flow cell chamber	(i) Allows the control of environmental factors (ii) Allows real time microscope observation	(iii) No vast simultaneous studies allowed (iv) Can only handle up to 2 experiments at a time
Biofilm collection		
Scrapping	Allows the removal of almost all the biofilm	(i) Operator-dependent
Vortexing & sonification	(i) Reproducibility (ii) Fast and easy	The first (deeper) bacterial layer can remain on the medium
Biofilm analysis		
Cultivation on agar media	(i) Simple (ii) Allows further identification methods (iii) Selection of sustainable strains	(i) Delayed results (ii) Only for culturable species (iii) Time consuming
Gram staining	(i) Low cost (ii) Fast and easy	(i) Limited identification based on colony and bacterial morphology
FISH	(i) Can focus on targeted bacteria in a multispecies biofilm (ii) Possible to combine consecutive FISH with multiple rRNA (iii) Can be combined with CLSM and PCR	(i) Cost (ii) Complexity of protocol (iii) Inability to discriminate live and dead bacteria
CLSM	(i) Allows discriminating between live and dead bacteria (ii) Can determine the distribution of all the different species within the biofilm at different development times (iii) Can be combined with FISH and PCR	(i) Cost (ii) Complexity of protocol (iii) Inability to discriminate stains (only on morphology) (iv) Inability to assess gene expression
SEM	(i) Can determine the distribution of all the different species within the biofilm	(i) Cost (ii) Complexity of protocol (iii) Inability to discriminate live and dead bacteria
PCR	(i) Allows identifying and counting bacterial stains directly (ii) Can be combined with culture on specific media FISH: better results than CFU counts CLSM	(i) Cost (ii) Multispecies biofilms need a cultivation and isolation of every colony prior to PCR (iii) Inability to discriminate live and dead bacteria

on *Streptococcus mutans* biofilm [9], or the effect of various oral rinses on the detachment of an artificial oral biofilm [10]. Wong and Sissons compared two different types of saliva: BMM (Basal Medium Mucin) and DMM (Defined Medium Mucin) [11]. BMM is a complex mucin-containing but chemically undefined medium, while DMM is based on the Shellis artificial saliva [12] and contains various ions, vitamins, amino acids, and growth factors at the same rate as in human saliva. Other authors also supplied their biofilm with DMM in order to test the effect of nutrient variations on the formation of biofilms [12–15].

All these artificial media have a simpler composition than natural human saliva. Particularly, they do not contain the various proteins present in the acquired pellicle (e.g., histatins, proline rich proteins) which play an important role in the mechanisms of bacterial adherence. For this reason, human saliva was used in many other studies in order to be closer to oral conditions [16–18]. Human saliva can be collected from only one or several healthy volunteers [19, 20]. It is obtained by splitting at least 1 hour and a half after eating, drinking, and tooth cleaning. Samples are pooled and centrifuged, and the supernatants are pasteurized and recentrifuged before being stored at −20°C [21].

In order to grow biofilms, media have to reach all the complex nutritional requirements to allow the growth of bacteria. Saliva only or its combination with selective media can be used. Regarding selective media, in case of mono-species biofilms, each bacterium has its preferred medium that eases its growth.

In case of plurispecies biofilms, the Fluid Universal Medium, described by Guggenheim et al. [21], can generally allow the growth of many bacterial species, so it has been used as a support for multispecies biofilms. This FUM went through modifications and created the modified FUM (supplemented with 67 mmol/L Sorensen's buffer, pH 7.2), the enriched FUM (+0.15% sucrose, 0.15% glucose). 50% heat inactivated horse serum can be added to help the growth of certain bacteria, as well as N-acetylmuramic acid for *T. forsythia*, of 0.34 mM hemin for *P. gingivalis* [22].

3. Substrates

3.1. Experimental Oral Biofilms Are Developed on Various Supports

3.1.1. Glass Surfaces. Hamada and Torii described a very simple device for testing biofilm formation on an inert surface [23]. Briefly, an overnight culture was added to a glass tube containing specific medium and sucrose 1%. The cultures were incubated at 37°C with an angle of 30 degrees. Biofilm formation was evaluated after 24 to 48 hours with the Murchison scale from 0 (no adhesion) to 4 (strongly adhesive) [24]. Hasan et al. used this support to study the effect on sucrose-dependent and sucrose-independent adherence of *S. mutans* and the inhibitory effect of a plant extract on these bacteria [25, 26].

This model also enabled the investigation of the adherence capacities of oral lactobacilli for potential probiotic purposes [27] and the antiadherence properties of polyphenolic compounds on oral bacteria [28]. However, this design does not include the formation of the acquired pellicle: the bacteria directly adhere on the glass surface. For the authors, the ability of *S. mutans* cells to colonize various smooth surfaces may be due to the insoluble glucans synthesized from sucrose by the bound glucosyltransferase. Therefore, this experimental model makes it possible to quickly screen the biofilm formation capacity of various strains that possess this enzyme.

3.1.2. Dentin. Most studies carried out on dentin have focused on endodontic infection. Endodontic disease is a biofilm-mediated infection in which *Enterococcus faecalis* is commonly found [29]. The dentin discs used can be of human [30–32] or bovine origin [33–36]. Some other studies have also been performed on human whole teeth [37]. Many studies aimed to evaluate the antimicrobial activity of various solutions and their capacity to eradicate *E. faecalis* biofilm [30, 31, 34, 36]. Unlike the above-mentioned studies, Li et al. worked on the dentin-composite interface subjected to multispecies biofilm [35]. Bovine dentin discs have also been used in a continuous culture model to study the effects of shiitake mushrooms on biofilms composition and cariogenic properties [33].

3.1.3. Enamel. Enamel is mostly used as a substratum for cariogenic biofilm models. Like dentin, it may be of human or bovine origin [38, 39]. The role of sucrose as a cariogenic molecule has been widely investigated using this substratum in batch models [39, 40] or in an artificial mouth [38].

3.1.4. Polystyrene Surfaces. Polystyrene microtiter plates provide a convenient and sterile abiotic surface for studying bacterial biofilm formation. Loo et al. used this support to study *Streptococcus gordonii* biofilm and particularly to identify the genes that code for biofilm phenotypes [41]. Oettinger-Barak et al. as well as Izano et al. used static 96-well plates to investigate the effect of antibiotics on biofilm formation [42, 43]. The biofilms were highlighted with crystal violet staining after a 24-hour incubation. To analyze the effect of the xylitol and ursolic combination or a synthetic peptide, 24-well plates were used to grow biofilms of various *Streptococcus* species [44, 45]. Other species have also been investigated using this medium: for example, *Actinomyces naeslundii* [46] and *E. faecalis* [47]. A comparison between mono-species and duo-species biofilm combining *S. mutans* and *Veillonella parvula* was made by Kara et al. on 96-well plates [48].

In all these studies, bacteria adhered directly on polystyrene surfaces. Other authors have used microtiter plates coated with various substrates. Human saliva was found to allow the growth of mono-species biofilms [49]. Saito et al. inoculated periapical microorganisms on plates coated with collagen to confirm the stimulation of *Fusobacterium nucleatum* biofilm formation by *Porphyromonas gingivalis* [50]. The effect of *Kaempferia pandurata* on multispecies biofilm was investigated by Yanti et al. by coating it on the plates before growing the biofilm [51].

3.1.5. Hydroxyapatite. The use of hydroxyapatite allows studies on synthetic media mimicking dental tissues, thereby avoiding the search for extracted teeth. Many authors have used this medium in form of either beads or discs. Saliva-coated hydroxyapatite beads have been used in various studies. The growth rate and biofilm thickness of a dual biofilm of *S. mutans* and *Streptococcus sobrinus* were studied by Rozen et al. [52]. The adherence properties of bacterial strains as oral probiotic candidates have also been processed on saliva-coated hydroxyapatite beads [53] or discs [27]. Furthermore, hydroxyapatite has been used to investigate the effects of various molecules on *S. mutans* biofilm formation on both beads [50, 54–56] and discs [57–59].

Other authors have investigated dual-species biofilms. Li et al. tested the effect of nicotine on dual-species biofilms of *S. mutans* and *Streptococcus sanguinis* [60]. Ali Mohammed et al. worked on the DNase I and proteinase K treatment of *F. nucleatum* and *P. gingivalis* biofilms [61]. Dual-species biofilms allowed the observation of differences in growth and acid formation between *S. mutans* and *V. parvula* strains [48].

Hydroxyapatite discs were also the medium used in the Zürich model described below [21].

4. Incubation Conditions

Bacterial oral biofilm model systems can be divided into two groups: closed batch culture and open continuous culture models.

4.1. Batch Models. One commonly used model developed by Guggenheim et al. is called the Zürich model [21]. This multispecies model allows the study of interactions in bacterial communities.

The first version of this model contained five different species (*A. naeslundii*, *Veillonella dispar*, *F. nucleatum*, *S. sobrinus*, and *Streptococcus oralis*). Biofilms are developed on hydroxyapatite discs coated with pasteurized human saliva for 64 hours in anaerobic conditions before collection. This model was subsequently improved by adding more bacterial species [62]. Using this more recent model, Ammann et al. demonstrated the importance of nutritional conditions for biofilm development and brought some changes to the culture conditions. The Zürich model has been used extensively to test the effect of various components like plant extracts, polyphenolic compounds, and mouthwashes [28, 59, 63, 64]. Furthermore, it has been used to study the effect of xylitol on a growing biofilm [65]. While various studies have described biofilm formation in static systems, bacteria in the oral cavity are subject to constantly changing environmental conditions (e.g., saliva flow conditions). Static models are not able to simulate these conditions so dynamic models are required.

4.2. Continuous Culture Models

4.2.1. Constant Depth Film Fermenter. The Constant Depth Film Fermenter is a dynamic biofilm model that allows the control of environmental factors such as the substratum, the nutrient source, and the gas flow [66]. Even biofilm thickness can be controlled [67]. Mono-species biofilm can be studied in this apparatus [68], but the principal advantage is to work with multispecies biofilm mimicking *in vivo* conditions as closely as possible. For example, Ready et al. assessed the resistance of a multispecies oral biofilm to tetracycline with this model [69].

The concept consists in a glass cylinder that contains a stainless steel plate linked to an electric motor that allows the plate rotation. Pores at the cylinder summit enable gas and medium to enter and exit. On the plate, wells are dug into which discs or substratum can be dropped. Temperature and gas flow are controlled and medium and saliva are injected with a pump. Excessive medium is absorbed. The Constant Depth Film Fermenter is a complex system allowing only one antimicrobial formula to be tested at a time so it has been improved, and two different treatments can now be performed at the same time [33, 70].

4.2.2. Flow Cell Chamber System. This model consists in a glass slide coated with saliva that is placed in a chamber and is crossed by a continuous flow of medium [71, 72]. Schlafer et al. tested the effect of osteopontin on a multispecies biofilm using this model [73]. Furthermore, by allowing the evaluation of biofilm development under flow and shear conditions, it has been used to assess antibiotics [42]. Periodontal biofilm can also be developed with it [74].

5. Biofilm Collection and Analysis

The methods used to identify different microorganisms in a microcosm biofilm vary according to the models. There are two approaches: cultivation-based and non-cultivation-based.

5.1. Cultivation-Based Methods. This technique needs the biofilm to be collected. Some authors recommend vigorous vortexing to remove cells from the biofilm [64, 75]. Ready et al. add a sonication step after vortexing the biofilm [69]. Wirtanen et al. harvest the biofilm by scratching the surface of the tray with a swab and then immersing it in a dilution medium [76]. In their Zürich model, Guggenheim et al. scratch the surface of the disc with a sterile curette to harvest all the cells of the biofilm, even those that are firmly attached [21]. The collected biofilm is then plated on various selective agar media. The distinct colony morphology and gram staining allow the species to be differentiated. This technique of counting colony forming units makes it possible to investigate the effect of various components on the viability of bacteria both on mono-species biofilms [44, 45, 56] and on plurispecies ones [63, 65, 77, 78]. However, it is a time-consuming method and noncultivable species cannot be included in the biofilm. Moreover, scratching of biofilms on hydroxyapatite surfaces may not be easily reproducible.

5.2. Non-Cultivation-Based Methods. Since oral diseases have a complex etiology and because only around 50% of oral biofilm can be grown at present, culture-independent molecular-based approaches have been developed that give a more comprehensive assessment of the presence of a range of putative pathogens in samples [78]. In studies on

E. faecalis biofilms, dentin specimens were stained with BacLight and observed with a fluorescence microscope [30]. In multispecies models, fluorescence *in situ* hybridization (FISH) in combination with epifluorescence and confocal laser scanning microscopy (CLSM) are other standard methods for the visualization and identification of species.

5.2.1. In Situ Hybridization Fluorescence (FISH). A sequential FISH approach allows multiple populations to be detected in a biofilm sample [79]. Indeed, FISH is a recognized tool for the specific identification of targeted bacteria within multispecies biofilms [62]. Moreover, Thurnheer et al. showed that it is possible to perform several consecutive FISH procedures with multiple rRNA to identify simultaneously many members of biofilms [80]. FISH can also be combined with CLSM [62, 64].

5.2.2. Epifluorescence Microscopy and Confocal Laser Scanning Microscopy (CLSM). The LIVE/DEAD® BacLight™ fluorescence solution can be used to differentiate viable cells from nonviable ones in terms of membrane integrity. Viable cells are stained with SYTO9® which fluoresces green, while the nonviable ones are stained with propidium iodide which fluoresces red. Using BacLight LIVE/DEAD, Standar et al. inspected cells by fluorescence microscopy when they worked on the biofilm behavior of mixed-species cultures with dental and periodontal pathogens [81]. Chávez de Paz also used this technique to assess cell viability within multispecies biofilms in root canals [82].

CLSM has also been widely used to observe biofilms in three dimensions. It allows the systematic collection of high-quality biofilm images suitable for digital image analysis [79]. After 15 mn dark incubation, de Carvalho et al. use an excitation wavelength of 488 nm to collect all light emitted between 500 and 550 nm and over 560 nm by various filters. They use the scan mode time series to take a series of time-lapse scans at intervals of 10 s during 590 s in continuous scanning mode with a 10x objective lens [83]. Hobby et al. incubate the wells for 18 mn before using a Zeiss LSM 510 Meta confocal scanning system [84].

Some models combine non-cultivation-based and cultivation-based methods. According to Blanc et al., it is thus possible to determine the presence of all the species within the biofilm structure, the volume occupied by the bacteria, and the distribution of live and dead cells at the different biofilm development times [85].

5.2.3. Scanning Electron Microscopy (SEM). Standar et al. use SEM to observe their multispecies biofilms models. Biofilms are fixed for 24 hours in a 2.5% glutaraldehyde solution and the supports are rinsed with 0.1 M Na-acetate buffer and dehydrated with a graded ethanol series. Then they are subjected to critical point drying with CO_2, covered with gold (10 nm thickness) and examined with a Zeiss DSM 960 A electron microscope [81]. Howlin et al. also use this technique to visualize biofilms after their removal with an ultrasonically activated water stream [86]. Thurnheer et al. also use SEM to study the role of red complex bacteria in the colonization of gingival epithelia by subgingival biofilms *in vitro* [74].

5.2.4. PCR. Until recently, PCR was mostly used to identify and count bacterial species *in vivo* or in dental plaque samples in connection with oral diseases (caries, periodontitis) [87, 88]. However, in more recent studies, it has also been used to identify species in *in vitro* models either after culture or directly within the biofilm. For example, Zaura et al. used quantitative real-time PCR (qPCR) to observe microbial shifts due to the effect of shiitake mushroom on an *in vitro* caries model [33].

In 2013, Ammann at al. compared a qPCR assay with fluorescence microscopy and colony forming unit counting on selective agars. They found that all ten species included in their *in vitro* biofilm were successfully quantified using qPCR and FISH or immunofluorescence as well as the eight species culturable on selective agar plates. They concluded that CFU counts yielded lower values than the other methods. The same authors also used qPCR combined with CLSM following FISH to compare the quantitative distribution of bacteria and the three-dimensional structure of biofilms either with or without early colonizing species added at a later time point [22]. For a very close purpose, Karched et al. using only qPCR showed that six periodontal species were able to form multispecies biofilm up to eight days *in vitro* without pioneer plaque bacteria [89].

The limitation of qPCR is its inability to discriminate between live and dead cells. Extracellular DNA present in the matrix of the biofilm can also be quantified. To overcome this problem, propidium monoazide has been used in association with qPCR [90, 91]. The results of these studies demonstrated the efficiency of PMA for differentiating viable and dead strains of various species.

6. Conclusion

Because biofilms constitute a privileged way of life for oral bacteria, a clear understanding of the processes involved in their formation, their pathogenicity, and their resistance in various biocides is essential for their control. While several experimental models have been proposed to date, differences in biofilm formation times, growth media, incubation conditions (static or flow, aerobic or anaerobic), and the procedures for collecting and analyzing biofilms make a comparison difficult. Choosing the most suitable procedure depends on the particular objective that is sought and on the laboratory facilities that are available.

Competing Interests

The authors declare that there is no conflict of interests regarding the publication of this paper.

References

[1] P. E. Kolenbrander and J. London, "Adhere today, here tomorrow: oral bacterial adherence," *Journal of Bacteriology*, vol. 175, no. 11, pp. 3247–3252, 1993.

[2] P. D. Marsh and D. J. Bradshaw, "Dental plaque as a biofilm," *Journal of Industrial Microbiology*, vol. 15, no. 3, pp. 169–175, 1995.

[3] J. S. Foster and P. E. Kolenbrander, "Development of a multispecies oral bacterial community in a saliva-conditioned flow cell," *Applied and Environmental Microbiology*, vol. 70, no. 7, pp. 4340–4348, 2004.

[4] P. G. Egland, R. J. Palmer Jr., and P. E. Kolenbrander, "Interspecies communication in Streptococcus gordonii-Veillonella atypica biofilms: signaling in flow conditions requires juxtaposition," *Proceedings of the National Academy of Sciences of the United States of America*, vol. 101, no. 48, pp. 16917–16922, 2004.

[5] W. F. Liljemark and C. Bloomquist, "Human oral microbial ecology and dental caries and periodontal diseases," *Critical Reviews in Oral Biology and Medicine*, vol. 7, no. 2, pp. 180–198, 1996.

[6] C. Russell and W. A. Coulter, "Continuous monitoring of pH and Eh in bacterial plaque grown on a tooth in an artificial mouth," *Applied Microbiology*, vol. 29, no. 2, pp. 141–144, 1975.

[7] J. Pratten, K. Wills, P. Barnett, and M. Wilson, "*In vitro* studies of the effect of antiseptic-containing mouthwashes on the formation and viability of *Streptococcus sanguis* biofilms," *Journal of Applied Microbiology*, vol. 84, no. 6, pp. 1149–1155, 1998.

[8] M. Y. H. Chin, H. J. Busscher, R. Evans, J. Noar, and J. Pratten, "Early biofilm formation and the effects of antimicrobial agents on orthodontic bonding materials in a parallel plate flow chamber," *European Journal of Orthodontics*, vol. 28, no. 1, pp. 1–7, 2006.

[9] P. Arirachakaran, S. Luengpailin, J. A. Banas, J. E. Mazurkiewicz, and E. Benjavongkulchai, "Effects of manganese on streptococcus mutans planktonic and biofilm growth," *Caries Research*, vol. 41, no. 6, pp. 497–502, 2007.

[10] A. S. Landa, H. C. van der Mei, and H. J. Busscher, "Detachment of linking film bacteria from enamel surfaces by oral rinses and penetration of sodium lauryl sulphate through an artificial oral biofilm," *Advances in Dental Research*, vol. 11, no. 4, pp. 528–538, 1997.

[11] L. Wong and C. H. Sissons, "Human dental plaque microcosm biofilms: effect of nutrient variation on calcium phosphate deposition and growth," *Archives of Oral Biology*, vol. 52, no. 3, pp. 280–289, 2007.

[12] R. P. Shellis, "A synthetic saliva for cultural studies of dental plaque," *Archives of Oral Biology*, vol. 23, no. 6, pp. 485–489, 1978.

[13] C. H. Sissons, S. A. Anderson, L. Wong, M. J. Coleman, and D. C. White, "Microbiota of plaque microcosm biofilms: effect of three times daily sucrose pulses in different simulated oral environments," *Caries Research*, vol. 41, no. 5, pp. 413–422, 2007.

[14] L. Wong and C. H. Sissions, "A comparison of human dental plaque microcosm biofilms grown in an undefined medium and a chemically defined artificial saliva," *Archives of Oral Biology*, vol. 46, no. 6, pp. 477–486, 2001.

[15] M.-L. Mei, C.-H. Chu, E.-C. Lo, and L.-P. Samaranayake, "Preventing root caries development under oral biofilm challenge in an artificial mouth," *Medicina Oral, Patología Oral y Cirugia Bucal*, vol. 18, no. 4, pp. e557–e563, 2013.

[16] M. J. Sedlacek and C. Walker, "Antibiotic resistance in an in vitro subgingival biofilm model," *Oral Microbiology and Immunology*, vol. 22, no. 5, pp. 333–339, 2007.

[17] M. J. Verkaik, H. J. Busscher, D. Jager, A. M. Slomp, F. Abbas, and H. C. van der Mei, "Efficacy of natural antimicrobials in toothpaste formulations against oral biofilms *in vitro*," *Journal of Dentistry*, vol. 39, no. 3, pp. 218–224, 2011.

[18] M. J. Verkaik, H. J. Busscher, M. Rustema-Abbing, A. M. Slomp, F. Abbas, and H. C. van der Mei, "Oral biofilm models for mechanical plaque removal," *Clinical Oral Investigations*, vol. 14, no. 4, pp. 403–409, 2010.

[19] S. Shani, M. Friedman, and D. Steinberg, "The anticariogenic effect of amine fluorides on *Streptococcus sobrinus* and glucosyltransferase in biofilms," *Caries Research*, vol. 34, no. 3, pp. 260–267, 2000.

[20] J. Pratten, C. S. Andrews, D. Q. M. Craig, and M. Wilson, "Structural studies of microcosm dental plaques grown under different nutritional conditions," *FEMS Microbiology Letters*, vol. 189, no. 2, pp. 215–218, 2000.

[21] B. Guggenheim, E. Giertsen, P. Schüpbach, and S. Shapiro, "Validation of an in vitro biofilm model of supragingival plaque," *Journal of Dental Research*, vol. 80, no. 1, pp. 363–370, 2001.

[22] T. W. Ammann, G. N. Belibasakis, and T. Thurnheer, "Impact of early colonizers on in vitro subgingival biofilm formation," *PLoS ONE*, vol. 8, no. 12, article 0083090, 2013.

[23] S. Hamada and M. Torii, "Effect of sucrose in culture media on the location of glucosyltransferase of *Streptococcus mutans* and cell adherence to glass surfaces," *Infection and Immunity*, vol. 20, no. 3, pp. 592–599, 1978.

[24] H. Murchison, S. Larrimore, and R. Curtiss III, "Isolation and characterization of *Streptococcus mutans* mutants defective in adherence and aggregation," *Infection and Immunity*, vol. 34, no. 3, pp. 1044–1055, 1981.

[25] S. Hasan, K. Singh, M. Danisuddin, P. K. Verma, and A. U. Khan, "Inhibition of major virulence pathways of *Streptococcus mutans* by Quercitrin and Deoxynojirimycin: a synergistic approach of infection control," *PLoS ONE*, vol. 9, no. 3, Article ID e91736, 2014.

[26] S. Hasan, M. Danishuddin, and A. U. Khan, "Inhibitory effect of zingiber officinale towards Streptococcus mutans virulence and caries development: in vitro and in vivo studies," *BMC Microbiology*, vol. 15, no. 1, article 1, 2015.

[27] J. Samot, J. Lebreton, and C. Badet, "Adherence capacities of oral lactobacilli for potential probiotic purposes," *Anaerobe*, vol. 17, no. 2, pp. 69–72, 2011.

[28] A. Furiga, A. Lonvaud-Funel, G. Dorignac, and C. Badet, "In vitro anti-bacterial and anti-adherence effects of natural polyphenolic compounds on oral bacteria," *Journal of Applied Microbiology*, vol. 105, no. 5, pp. 1470–1476, 2008.

[29] K. Jhajharia, L. Mehta, A. Parolia, and K. Shetty, "Biofilm in endodontics: a review," *Journal of International Society of Preventive & Community Dentistry*, vol. 5, no. 1, pp. 1–12, 2015.

[30] A. Kishen, C.-P. Sum, S. Mathew, and C.-T. Lim, "Influence of irrigation regimens on the adherence of enterococcus faecalis to root canal dentin," *Journal of Endodontics*, vol. 34, no. 7, pp. 850–854, 2008.

[31] P. Baca, P. Junco, M. T. Arias-Moliz, M. P. González-Rodríguez, and C. M. Ferrer-Luque, "Residual and antimicrobial activity of final irrigation protocols on *Enterococcus faecalis* biofilm in dentin," *Journal of Endodontics*, vol. 37, no. 3, pp. 363–366, 2011.

[32] M. T. Arias-Moliz, R. Ordinola-Zapata, P. Baca et al., "Antimicrobial activity of chlorhexidine, peracetic acid and sodium hypochlorite/etidronate irrigant solutions against *Enterococcus faecalis* biofilms," *International Endodontic Journal*, vol. 48, no. 12, pp. 1188–1193, 2015.

[33] E. Zaura, M. J. Buijs, M. A. Hoogenkamp et al., "The effects of fractions from shiitake mushroom on composition and

cariogenicity of dental plaque microcosms in an *in vitro* caries model," *Journal of Biomedicine and Biotechnology*, vol. 2011, Article ID 135034, 10 pages, 2011.

[34] T. Du, Q. Shi, Y. Shen et al., "Effect of modified nonequilibrium plasma with chlorhexidine digluconate against endodontic biofilms in vitro," *Journal of Endodontics*, vol. 39, no. 11, pp. 1438–1443, 2013.

[35] Y. Li, C. Carrera, R. Chen et al., "Degradation in the dentin-composite interface subjected to multi-species biofilm challenges," *Acta Biomaterialia*, vol. 10, no. 1, pp. 375–383, 2014.

[36] C. A. Nascimento, M. Tanomaru-Filho, N. B. Faria-Junior, G. Faria, J. M. Guerreiro-Tanomaru, and S. G. Patil, "Antimicrobial activity of root canal irrigants associated with cetrimide against biofilm and planktonic *Enterococcus faecalis*," *The Journal of Contemporary Dental Practice*, vol. 15, no. 5, pp. 603–607, 2014.

[37] C. Estrela, G. B. Sydney, J. A. P. Figueiredo, and C. R. De Araújo Estrela, "A model system to study antimicrobial strategies in endodontic biofilms," *Journal of Applied Oral Science*, vol. 17, no. 2, pp. 87–91, 2009.

[38] R. A. Arthur, E. K. Kohara, R. A. Waeiss, G. J. Eckert, D. Zero, and M. Ando, "Enamel carious lesion development in response to sucrose and fluoride concentrations and to time of biofilm formation: an artificial-mouth Study," *Journal of Oral Diseases*, vol. 2014, Article ID 348032, 8 pages, 2014.

[39] F. H. van de Sande, M. S. Azevedo, R. G. Lund, M. C. D. N. J. M. Huysmans, and M. S. Cenci, "An in vitro biofilm model for enamel demineralization and antimicrobial dose-response studies," *Biofouling*, vol. 27, no. 9, pp. 1057–1063, 2011.

[40] C. C. Ribeirom, R. A. Ccahuana-Vásquez, C. D. Carmo et al., "The effect of iron on Streptococcus mutans biofilm and on enamel demineralization," *Brazilian Oral Research*, vol. 26, no. 4, pp. 300–305, 2012.

[41] C. Y. Loo, D. A. Corliss, and N. Ganeshkumar, "*Streptococcus gordonii* biofilm formation: identification of genes that code for biofilm phenotypes," *Journal of Bacteriology*, vol. 182, no. 5, pp. 1374–1382, 2000.

[42] O. Oettinger-Barak, S. G. Dashper, D. V. Catmull et al., "Antibiotic susceptibility of aggregatibacter actinomycetemcomitans JP2 in a biofilm," *Journal of Oral Microbiology*, vol. 5, Article ID 20320, pp. 1–8, 2013.

[43] E. A. Izano, H. Wang, C. Ragunath, N. Ramasubbu, and J. B. Kaplan, "Detachment and killing of *Aggregatibacter actinomycetemcomitans* biofilms by dispersin B and SDS," *Journal of Dental Research*, vol. 86, no. 7, pp. 618–622, 2007.

[44] B. R. da Silva, V. A. A. de Freitas, V. A. Carneiro et al., "Antimicrobial activity of the synthetic peptide Lys-a1 against oral streptococci," *Peptides*, vol. 42, pp. 78–83, 2013.

[45] Y. Zou, Y. Lee, J. Huh, and J. Park, "Synergistic effect of xylitol and ursolic acid combination on oral biofilms," *Restorative Dentistry & Endodontics*, vol. 39, no. 4, pp. 288–295, 2014.

[46] S. Yoneda, T. Kawarai, N. Narisawa et al., "Effects of short-chain fatty acids on *Actinomyces naeslundii* biofilm formation," *Molecular Oral Microbiology*, vol. 28, no. 5, pp. 354–365, 2013.

[47] J. M. Duggan and C. M. Sedgley, "Biofilm formation of oral and endodontic *Enterococcus faecalis*," *Journal of Endodontics*, vol. 33, no. 7, pp. 815–818, 2007.

[48] D. Kara, S. B. I. Luppens, and J. M. T. Cate, "Differences between single- and dual-species biofilms of *Streptococcus mutans* and *Veillonella parvula* in growth, acidogenicity and susceptibility to chlorhexidine," *European Journal of Oral Sciences*, vol. 114, no. 1, pp. 58–63, 2006.

[49] M. R. T. R. Oliveira, M. H. Napimoga, K. Cogo et al., "Inhibition of bacterial adherence to saliva-coated through plant lectins," *Journal of Oral Science*, vol. 49, no. 2, pp. 141–145, 2007.

[50] Y. Saito, R. Fujii, K.-I. Nakagawa, H. K. Kuramitsu, K. Okuda, and K. Ishihara, "Stimulation of *Fusobacterium nucleatum* biofilm formation by *Porphyromonas gingivalis*," *Oral Microbiology and Immunology*, vol. 23, no. 1, pp. 1–6, 2008.

[51] Yanti, Y. Rukayadi, K.-H. Lee, and J.-K. Hwang, "Activity of panduratin A isolated from *Kaempferia pandurata* Roxb. against multi-species oral biofilms *in vitro*," *Journal of Oral Science*, vol. 51, no. 1, pp. 87–95, 2009.

[52] R. Rozen, G. Bachrach, B. Zachs, and D. Steinberg, "Growth rate and biofilm thickness of *Streptococcus sobrinus* and *Streptococcus mutans* on hydroxapatite," *Acta Pathologica, Microbiologica, et Immunologica Scandinavica*, vol. 109, no. 2, pp. 155–160, 2001.

[53] E. M. Comelli, B. Guggenheim, F. Stingele, and J.-R. Neeser, "Selection of dairy bacterial strains as probiotics for oral health," *European Journal of Oral Sciences*, vol. 110, no. 3, pp. 218–224, 2002.

[54] S. B. Ekenbäck, L. E. Linder, M.-L. Sund, and H. Lönnies, "Effect of fluoride on glucose incorporation and metabolism in biofilm cells of *Streptococcus mutans*," *European Journal of Oral Sciences*, vol. 109, no. 3, pp. 182–186, 2001.

[55] A. Yamanaka, R. Kimizuka, T. Kato, and K. Okuda, "Inhibitory effects of cranberry juice on attachment of oral streptococci and biofilm formation," *Oral Microbiology and Immunology*, vol. 19, no. 3, pp. 150–154, 2004.

[56] A. Yano, S. Kikuchi, T. Takahashi, K. Kohama, and Y. Yoshida, "Inhibitory effects of the phenolic fraction from the pomace of Vitis coignetiae on biofilm formation by Streptococcus mutans," *Archives of Oral Biology*, vol. 57, no. 6, pp. 711–719, 2012.

[57] H. Koo, M. F. Hayacibara, B. D. Schobel et al., "Inhibition of Streptococcus mutans biofilm accumulation and polysaccharide production by apigenin and tt-farnesol," *Journal of Antimicrobial Chemotherapy*, vol. 52, no. 5, pp. 782–789, 2003.

[58] P. T. M. Nguyen, M. L. Falsetta, G. Hwang, M. Gonzalez-Begne, and H. Koo, "α-Mangostin disrupts the development of *Streptococcus mutans* biofilms and facilitates its mechanical removal," *PLoS ONE*, vol. 9, no. 10, Article ID e111312, 2014.

[59] M. Barnabé, C. H. C. Saraceni, M. Dutra-Correa, and I. B. Suffredini, "The influence of Brazilian plant extracts on *Streptococcus mutans* biofilm," *Journal of Applied Oral Science*, vol. 22, no. 5, pp. 366–372, 2014.

[60] M. Li, R. Huang, X. Zhou, K. Zhang, X. Zheng, and R. L. Gregory, "Effect of nicotine on dual-species biofilms of Streptococcus mutans and Streptococcus sanguinis," *FEMS Microbiology Letters*, vol. 350, no. 2, pp. 125–132, 2014.

[61] M. M. Ali Mohammed, A. H. Nerland, M. Al-Haroni, and V. Bakken, "Characterization of extracellular polymeric matrix, and treatment of *Fusobacterium nucleatum* and *Porphyromonas gingivalis* biofilms with DNase I and proteinase K," *Journal of Oral Microbiology*, vol. 5, article 10, 2013.

[62] T. W. Ammann, R. Gmür, and T. Thurnheer, "Advancement of the 10-species subgingival Zurich Biofilm model by examining different nutritional conditions and defining the structure of the *in vitro* biofilms," *BMC Microbiology*, vol. 12, article 227, 2012.

[63] A. Furiga, C. Roques, and C. Badet, "Preventive effects of an original combination of grape seed polyphenols with amine fluoride on dental biofilm formation and oxidative damage by oral bacteria," *Journal of Applied Microbiology*, vol. 116, no. 4, pp. 761–771, 2014.

[64] S. Shapiro, E. Giertsen, and B. Guggenheim, "An in vitro oral biofilm model for comparing the efficacy of antimicrobial mouthrinses," *Caries Research*, vol. 36, no. 2, pp. 93–100, 2002.

[65] C. Badet, A. Furiga, and N. Thébaud, "Effect of xylitol on an in vitro model of oral biofilm," *Oral Health & Preventive Dentistry*, vol. 6, no. 4, pp. 337–341, 2008.

[66] J. Pratten, "Growing oral biofilms in a constant depth film fermentor (CDFF)," in *Current Protocols in Microbiology*, chapter 1, Unit 1B.5, 2007.

[67] A. J. McBain, "Chapter 4 in vitro biofilm models. An overview," *Advances in Applied Microbiology*, vol. 69, pp. 99–132, 2009.

[68] S. P. Valappil, G. J. Owens, E. J. Miles et al., "Effect of gallium on growth of *Streptococcus mutans* NCTC 10449 and dental tissues," *Caries Research*, vol. 48, no. 2, pp. 137–146, 2014.

[69] D. Ready, A. P. Roberts, J. Pratten, D. A. Spratt, M. Wilson, and P. Mullany, "Composition and antibiotic resistance profile of microcosm dental plaques before and after exposure to tetracycline," *The Journal of Antimicrobial Chemotherapy*, vol. 49, no. 5, pp. 769–775, 2002.

[70] D. M. Deng, C. van Loveren, and J. M. ten Cate, "Caries-preventive agents induce remineralization of dentin in a biofilm model," *Caries Research*, vol. 39, no. 3, pp. 216–223, 2005.

[71] S. Periasamy and P. E. Kolenbrander, "Mutualistic biofilm communities develop with Porphyromonas gingivalis and initial, early, and late colonizers of enamel," *Journal of Bacteriology*, vol. 191, no. 22, pp. 6804–6811, 2009.

[72] S. Periasamy and P. E. Kolenbrander, "Central role of the early colonizer *Veillonella* sp. in establishing multispecies biofilm communities with initial, middle, and late colonizers of enamel," *Journal of Bacteriology*, vol. 192, no. 12, pp. 2965–2972, 2010.

[73] S. Schlafer, M. K. Raarup, P. L. Wejse et al., "Osteopontin reduces biofilm formation in a multi-species model of dental biofilm," *PLoS ONE*, vol. 7, no. 8, Article ID e41534, 2012.

[74] T. Thurnheer, G. N. Belibasakis, and N. Bostanci, "Colonisation of gingival epithelia by subgingival biofilms in vitro: role of 'red complex' bacteria," *Archives of Oral Biology*, vol. 59, no. 9, pp. 977–986, 2014.

[75] J. Pratten, A. W. Smith, and M. Wilson, "Response of single species biofilms and microcosm dental plaques to pulsing with chlorhexidine," *The Journal of Antimicrobial Chemotherapy*, vol. 42, no. 4, pp. 453–459, 1998.

[76] G. Wirtanen, S. Salo, I. M. Helander, and T. Mattila-Sandholm, "Microbiological methods for testing disinfectant efficiency on *Pseudomonas* biofilm," *Colloids and Surfaces B: Biointerfaces*, vol. 20, no. 1, pp. 37–50, 2001.

[77] B. Guggenheim and A. Meier, "In vitro effect of chlorhexidine mouth rinses on polyspecies biofilms," *Schweizer Monatsschrift für Zahnmedizin*, vol. 121, no. 5, pp. 432–441, 2011.

[78] T. Do, D. Devine, and P. D. Marsh, "Oral biofilms: molecular analysis, challenges, and future prospects in dental diagnostics," *Clinical, Cosmetic and Investigational Dentistry*, vol. 5, pp. 11–19, 2013.

[79] R. Almstrand, H. Daims, F. Persson, F. Sörensson, and M. Hermansson, "New methods for analysis of spatial distribution and coaggregation of microbial populations in complex biofilms," *Applied and Environmental Microbiology*, vol. 79, no. 19, pp. 5978–5987, 2013.

[80] T. Thurnheer, R. Gmür, and B. Guggenheim, "Multiplex FISH analysis of a six-species bacterial biofilm," *Journal of Microbiological Methods*, vol. 56, no. 1, pp. 37–47, 2004.

[81] K. Standar, B. Kreikemeyer, S. Redanz, W. L. Münter, M. Laue, and A. Podbielski, "Setup of an in vitro test system for basic studies on biofilm behavior of mixed-species cultures with dental and periodontal pathogens," *PLoS ONE*, vol. 5, no. 10, article e13135, 2010.

[82] L. E. Chávez de Paz, "Development of a multispecies biofilm community by four root canal bacteria," *Journal of Endodontics*, vol. 38, no. 3, pp. 318–323, 2012.

[83] F. G. de Carvalho, R. M. Puppin-Rontani, S. B. P. de Fúcio, T. de Cássia Negrini, H. L. Carlo, and F. Garcia-Godoy, "Analysis by confocal laser scanning microscopy of the MDPB bactericidal effect on *S. mutans* biofilm CLSM analysis of MDPB bactericidal effect on biofilm," *Journal of Applied Oral Science*, vol. 20, no. 5, pp. 568–575, 2012.

[84] G. H. Hobby, C. L. Quave, K. Nelson, C. M. Compadre, K. E. Beenken, and M. S. Smeltzer, "*Quercus cerris* extracts limit *Staphylococcus aureus* biofilm formation," *Journal of Ethnopharmacology*, vol. 144, no. 3, pp. 812–815, 2012.

[85] V. Blanc, S. Isabal, M. C. Sánchez et al., "Characterization and application of a flow system for in vitro multispecies oral biofilm formation," *Journal of Periodontal Research*, vol. 49, no. 3, pp. 323–332, 2014.

[86] R. P. Howlin, S. Fabbri, D. G. Offin et al., "Removal of dental biofilms with an ultrasonically activated water stream," *Journal of Dental Research*, vol. 94, no. 9, pp. 1303–1309, 2015.

[87] Y. Abiko, T. Sato, G. Mayanagi, and N. Takahashi, "Profiling of subgingival plaque biofilm microflora from periodontally healthy subjects and from subjects with periodontitis using quantitative real-time PCR," *Journal of Periodontal Research*, vol. 45, no. 3, pp. 389–395, 2010.

[88] P. Liu, Y. Liu, J. Wang, Y. Guo, Y. Zhang, and S. Xiao, "Detection of *Fusobacterium nucleatum* and *fadA* adhesin gene in patients with orthodontic gingivitis and non-orthodontic periodontal inflammation," *PLoS ONE*, vol. 9, no. 1, Article ID e85280, 2014.

[89] M. Karched, R. G. Bhardwaj, A. Inbamani, and S. Asikainen, "Quantitation of biofilm and planktonic life forms of coexisting periodontal species," *Anaerobe*, vol. 35, pp. 13–20, 2015.

[90] G. Àlvarez, M. González, S. Isabal, V. Blanc, and R. León, "Method to quantify live and dead cells in multi-species oral biofilm by real-time PCR with propidium monoazide," *AMB Express*, vol. 3, pp. 1–8, 2013.

[91] M. C. Sánchez, M. J. Marín, E. Figuero et al., "Quantitative real-time PCR combined with propidium monoazide for the selective quantification of viable periodontal pathogens in an in vitro subgingival biofilm model," *Journal of Periodontal Research*, vol. 49, no. 1, pp. 20–28, 2014.